WILD SOYBEAN (*GLYCINE SOJA*) AS A SOURCE OF RESISTANCE TO SOYBEAN CYST NEMATODE AND STRESS

by

Melissa Hatley

A dissertation submitted to the faculty of
The University of North Carolina at Charlotte
in partial fulfillment of the requirements
for the degree of Doctor of Philosophy in
Biology

Charlotte

2026

Approved by:

_____
Dr. Bao-Hua Song

_____
Dr. Morgan Carter

_____
Dr. Denis Jacob Machado

_____
Dr. Kenneth Piller

_____
Dr. Adam M. Reitzel

ABSTRACT

MELISSA HATLEY. Wild Soybean (*Glycine soja*) as a Source of Resistance to Soybean Cyst Nematode and Stress. (Under the direction of DR. BAO-HUA SONG)

Crop wild relatives (CWRs) such as wild soybean (*Glycine soja*) are critical and underutilized sources of genetic diversity with the potential to improve stress resilience of crops in modern agriculture. Wild soybean, the wild progenitor of cultivated soybean (*Glycine max*), is a reservoir of genetic and phenotypic variation that was previously lost through domestication. The genetic diversity of wild soybean provides an opportunity to identify novel mechanisms of resistance and stress tolerance that may contribute to the development of more durable crops.

This dissertation investigates *G. soja* as a source of resistance to the soybean cyst nematode (SCN; *Heterodera glycines*), the most damaging pathogen to soybean yields that is increasing in virulence worldwide. Wild soybean is used as a model to elucidate how resistance is shaped by genetic architecture, pathogen diversity, and environmental stress. First, quantitative trait loci (QTL) mapping in a recombinant inbred population identified two new resistance-associated loci, located in chromosomes19 (QTL-19) and 13 (QTL-13). Additionally, epistatic interactions involving these QTLs indicate that resistance is also affected by interactions among loci. Interestingly, QTL-19 represents a genomic region distinct from those commonly identified in cultivated soybean.

Second, a diverse panel of wild soybean accessions was screened against two SCN types (HG 0 and HG 1.2.5.7) to evaluate resistance breadth. Resistance levels varied among different accessions and across pathogen types, indicating strong host-pathogen specificity. Excitingly, accessions S54 and S55 exhibited broad-spectrum resistance. Root architectural traits, particularly root length as a function of perimeter (RLP), were associated with SCN reproduction in a population-dependent manner. These findings suggest that phenotypic responses to SCN infection are affected both by host accession and pathogen virulence profile.

Finally, the stability of SCN resistance was evaluated under combined stress conditions, SCN infection with water deficit. While no overall treatment effect was detected, accession-specific responses revealed variable shifts in SCN reproduction and plant performance. Integration of SCN reproduction and growth performance identified accessions with potentially stable resistance across environmental conditions. Multivariate modeling of physiological and spectral traits demonstrated that SCN reproductive success is influenced by multiple, modest-effect associations, including plant health, photosynthetic efficiency, and resource allocation, rather than a single dominant driver.

In summary, these findings demonstrate that SCN resistance in *G. soja* is a multidimensional, context-dependent trait governed by interacting genetic, physiological, and environmental factors. This work highlights the value of wild soybean as a crop wild relative with an important role in future soybean improvement. It establishes a framework for integrating diverse resistance sources, phenotypic traits, and environmental conditions into soybean breeding strategies aimed at improving resistance durability.

DEDICATION

"Hence, a traveller should be a botanist, for in all views plants form the chief embellishment."

—Charles Darwin, *The Voyage of the Beagle* (1839)

For all the girls who read outside, dig in the dirt, and wonder how the world works.

ACKNOWLEDGEMENTS

"After five years' work I allowed myself to speculate on the subject, and drew up some short notes; these I enlarged in 1844 into a sketch of the conclusions which then seemed to me probable: from that period to the present day I have steadily pursued the same object."

—Charles Darwin, *On the Origin of Species* (1859)

Foremost, I would like to express my sincere gratitude to my advisor, Dr. Bao-Hua Song. Her insight, encouragement, and patience have played an essential role in shaping this work and my growth as a scientist.

I am also indebted to the members of my dissertation committee—Dr. Morgan Carter, Dr. Kenneth Piller, Dr. Adam Reitzel, and Dr. Denis Jacob Machado—for their feedback and encouragement throughout my time as a graduate researcher. Their perspectives strengthened this work and broadened my understanding of genetics, plant pathology, and evolutionary biology. I am especially grateful to Dr. Jacob Machado for his support, generosity with his time, and thoughtful advice, all of which were invaluable in bringing this dissertation to completion. I would also like to thank Dr. Larry Leamy for his collaboration and insight; his contributions to the analyses in chapters 2 and 4 are greatly appreciated.

This work was made possible by the support of the UNC Charlotte Department of Biological Sciences, whose faculty, staff, and resources provided an excellent research and learning environment. My colleagues in Song Lab were always willing to lend a hand, and I appreciate their help. I'm also grateful to Dr. Jeff Gillman and the Botanical Gardens greenhouse staff for their hard work, logistical support, and advice. Dr. Michelle Pass and Dr. Judith Krauss acted as teaching mentors, and I am very grateful for their guidance and kindness. They provided me with opportunities to teach subjects I love, and were generous sources of advice and encouragement. They made my first teaching experiences a delight, while also pushing me to do my best for my students.

I am thankful for my fellow graduate researchers and friends who provided support and advice throughout this journey. They are joyful sources of laughter and scientific insight for which I will always be grateful. Dr. Kareen Pestana and Dr. Farida Yasmin also provided long-distance support after finishing their own PhDs. You ladies are the best friends a scientist could ask for.

I cannot fully express the depth of my gratitude to my family for their unconditional support. My parents and parents-in-law, as well as the rest of the family, have been steadfast in their encouragement. I am especially grateful to my husband, Shannon Craven, whose love, support, and the occasional (metaphorical) kick in the pants made this dissertation possible. I love you all very much.

TABLE OF CONTENTS

LIST OF TABLES

LIST OF FIGURES

LIST OF ABBREVIATIONS

ANOVA	Analysis of variance
CWR	Crop wild relative
FI	Female index
G. max	*Glycine max*; domesticated soybean
G. soja	*Glycine soja*; wild soybean
HG type	*Heterodera glycines* type
LOD	Logarithm of odds
PI	Plant introduction
PVE	Phenotypic variance explained
QTL	Quantitative trait loci
Rhg1	Major soybean cyst nematode locus on chromosome 18
Rhg4	Major soybean cyst nematode locus on chromosome 8
SCN	Soybean cyst nematode (*Heterodera glycines*)
SNP	Single-nucleotide polymorphism

CHAPTER 1: INTRODUCTION

Agricultural & Economic Importance of Soybean

Soybean (*Glycine max*) is one of the most important crop species in the global food system. It is one of the richest sources of plant-derived protein and oil, with seeds containing approximately 35-55% protein and 17-25% oil by dry weight. In addition, soybean contains a wide variety of vitamins, minerals, and other beneficial bioactive compounds. Soybean is not only a key component of human food systems, but also is widely used as livestock feed and has varied industrial applications (Dilawari et al., 2022; I-S Kim et al., 2021; Kholmurodova et al., 2023; Kumari et al., 2025). Global soybean production currently exceeds 350 million metric tons annually, and is concentrated in a small number of nations, including Brazil, the United States, Argentina, China, and Paraguay. These countries produced over 85% of global soybean production in 2025 (U.S. Department of Agriculture, Foreign Agricultural Service, n.d). As a legume capable of biological nitrogen fixation, soybean also reduces the need for nitrogen fertilizers, benefiting subsequent crops in rotation (Du et al., 2019). The domestication of this crop wild relative (CWR) fundamentally shaped the genetic diversity and agronomic traits of modern soybean.

Domestication of *Glycine max* from *Glycine soja*

Cultivated soybean originated in East Asia approximately 9,000 years ago, originating in the Huang He Valley region of China. Over time, sustained artificial selection for agronomic and nutritional traits reduced its genetic diversity as producers retained seeds from preferred plants. The domestication process was accompanied by substantial phenotypic changes, including the transformation of a small plant with vine-like growth to a larger, erect crop plant with larger leaves and roots, increased seed size and nutritional composition (Kofsky et al., 2018; Zhou et al., 2022).

The genetic architecture of soybean has been dramatically shaped by several historical genetic bottlenecks associated with domestication and modern breeding. Genetic changes associated with domestication altered the vine growth habit of wild soybeans, resulting in erect architecture, larger seeds, and reduced pod shattering typical of cultivated soybeans. However, the domestication of *G. soja* and subsequent breeding of modern cultivars were accompanied by the loss of many rare alleles, altering allelic combinations and contributing to the loss of important traits. The main genetic bottlenecks in soybean include the initial domestication of *G. soja* in Asia, the introduction of a limited germplasm base into North America, and intensive breeding efforts over the past century. In particular, North American cultivars reflect a much narrower genetic base, retaining only a portion of the allelic diversity present in Asian landraces. Although elite cultivars retain a proportion of genetic diversity found in landraces, they retain far less of the original genetic diversity of their wild progenitors (Hyten et al., 2006; Kofsky et al., 2018; Sedivy et al., 2017).

Value of Wild Soybean for Stress Resilience

Wild soybean (*Glycine soja*) represents a critical reservoir of genetic variation for soybean improvement traits because it has retained substantially greater genetic diversity than its cultivated descendant, including alleles lost during domestication and subsequent modern breeding. Artificial selection during domestication and later breeding programs favored uniform agronomic performance, causing major genetic bottlenecks that reduced allelic diversity across the genome, constraining the adaptive potential of modern soybean germplasm, particularly for complex traits such as resistance to disease and tolerance to abiotic stress.

In contrast, wild populations of *G. soja* persist across a broad geographic range – from eastern Siberia, throughout China, to the Korean peninsula and Japan – where they occupy heterogeneous habitats including riverbanks, field margins, and variable moisture regimes. Long-term exposure to fluctuations in climatic and environmental conditions has promoted local adaptation and the maintenance of rare alleles associated with tolerance to

drought, extreme temperatures, pathogens, and nutrient stress. As a result, wild soybeans harbor diverse genetic variation with the potential to enhance soybean resilience to both abiotic and biotic stressors.

Wild germplasm has historically contributed to valuable resistance loci and quantitative trait variation for cultivated soybeans, particularly resistance to disease and pests. Beyond single major disease resistance loci, *G. soja* is also a source of novel allelic variation underlying quantitative stress tolerance. Introgression of wild alleles can expand the adaptive capacity of elite breeding pools, the top performing genetic lines were developed to provide superior resistance to disease, consistent yields, and other important agronomic traits. The combination of wild alleles within these lines will increase phenotypic plasticity and maintain, or even improve, yields under stress conditions (Zhu et al., 2025; Zhuang et al., 2022). With approximately 80% more rare alleles (with a minor allele frequency of less than 1%) than domesticated lines, wild soybean represents a substantial genetic resource for soybean improvement (Liu et al., 2025). Additionally, wild soybean germplasm has been used to improve stress tolerance in other crops, highlighting the broader utility of CWRs in agricultural systems (Duan et al., 2025; Hu et al., 2014; W. Kim et al., 2023; Sun et al., 2025).

Practical considerations make *G. soja* invaluable in the development of improved soybean cultivars. Differences in genomic sequence and phenotype generally separate them as species, though they are closely related (Joshi et al., 2013). *G. soja* and *G. max* share the same chromosome number (2n = 40) and are fully cross-compatible, enabling efficient gene flow between wild and cultivated backgrounds. This compatibility facilitates pre-breeding and introgression strategies aimed at broadening the genetic base of cultivated soybeans. Although linkage drag and undesirable wild traits may accompany introgression, advances in genomic tools, marker-assisted selection (MAS), and genomic prediction have improved the precision with which beneficial genes can be identified and incorporated into elite cultivars (Hyten, 2012; X. Wu et al., 2025).

Global agriculture faces increasing pressure from drought, pathogen virulence, and environmental instability. Therefore, the strategic use of wild soybean germplasm offers a sustainable pathway to enhance stress resilience and sustain productivity in cultivated soybean systems. The genetic diversity of wild soybeans is important because major stressors, both biotic and abiotic, threaten soybean production. Among the most significant biotic stressors threatening soybean production worldwide is the soybean cyst nematode (*Heterodera glycines*, SCN), a pathogen that has driven extensive efforts to identify new sources of host resistance.

Biology and Agricultural Significance of Soybean Cyst Nematode

The soybean cyst nematode (*Heterodera glycines*, SCN) is the most economically damaging pathogen affecting soybean production worldwide. SCN is an obligate, sedentary plant-parasitic nematode that infects soybean roots, disrupting normal plant function through the formation of specialized feeding structures known as syncytia. These feeding sites divert host nutrients toward nematode development, reducing plant vigor and ultimately lowering yield. Damaged soybean roots can also lead to secondary pathogen infections and increased susceptibility to damaging environmental conditions, further reducing yields. Between 2015 and 2019, SCN caused greater yield loss than any other soybean disease in North America, with annual losses estimated at up to $1.5 billion dollars annually (Bradley et al., 2021; Telenko et al., 2025).

SCN completes a short life cycle (approximately 28 days) beginning with the egg state. Host root exudates and internal cues stimulate egg hatch, which releases the infective second-stage juvenile (J2). After penetrating the root epidermis, it migrates inward toward the vascular cylinder. After choosing an initial syncytial cell, the juvenile nematode injects effector proteins from its esophageal glands to initiate the formation of a specialized feeding site, the syncytium. Effector-driven remodeling converts approximately 200 individual root cells into a large, multinucleate feeding structure that sustains nematode development. After death, the body of nematode females hardens, forming a protective cyst containing up to 500

eggs. SCN populations can thus persist in the soil for over a decade (Inagaki & Tsutsumi, 1971; H. Wu et al., 2019).

The short generation time of SCN and durable survival stage allow SCN to accumulate rapidly and persist in fields for years following initial infestation. The biological characteristics of SCN, including its short life cycle and high reproductive potential, also contribute to the rapid evolution of virulent populations capable of overcoming existing host resistance.

Diversity and Virulence of SCN Populations

Field populations of the soybean cyst nematode are genetically heterogeneous and vary in their capability to reproduce on different sources of host resistance. This variation, commonly described as virulence, reflects the presence of diverse genotypes among and within SCN populations. Because SCN reproduces sexually, and populations can contain substantial genetic variation, shifts in virulence have occurred when specific resistance sources are extensively deployed in agricultural systems. Widespread and repeated use of SCN resistance sources, most notably those derived from PI 88788, has imposed directional selection on SCN populations towards virulence on such cultivars. Distinct populations of SCN may be able to overcome the same host resistance sources using different mechanisms, indicating high genetic diversity within and among SCN populations (Masonbrink et al., 2019). Though some sources of host resistance have been remarkably effective in reducing SCN infection, their continued usage has led to populations increasingly capable of reproducing on formerly resistant cultivars, leading to greater virulence. This process has led to the erosion of formerly resilient resistance loci and altered the composition of SCN communities within fields and across soybean growing regions.

Formerly, SCN populations were categorized using a "race" classification system based on differential reproduction on a limited set of soybean indicator lines. Though initially useful, the system lacked resolution and did not fully capture the complexity and variability present within field populations. To create a more standardized system and reflect

virulence diversity, the HG type classification system was developed. The system uses seven indicator lines representing different SCN resistance sources to determine whether an SCN population can successfully reproduce. This framework provides a more precise assessment of virulence phenotypes.

The HG system also allows shifts in virulence to be tracked over time as different sources of resistance are deployed. SCN heterogeneity, differences in cultivar deployment history and resistance source usage, and local agronomic practices, including the use of nematicides, create distinct selection pressures across cropping systems. As a result, one SCN population type may become predominant within a region, while nearby fields, counties, or states, may harbor populations with different virulence profiles.

The dynamic nature of SCN population structure presents a significant challenge for durable resistance breeding. Effective SCN management requires not only the identification of novel resistance sources, including those derived from wild soybean, but also an understanding of how resistance deployment shapes pathogen population evolution. As such, sustained efficacy of resistance depends on integrating knowledge of SCN virulence and its diversity with strategic resistance deployment and breeding practices.

Global Distribution of SCN

Soybean cyst nematode occurs in most soybean-producing regions across temperate and subtropical climates. It was first reported in Japan in the 1880s, and it is now a persistent constraint in major soybean-producing countries, including China, the United States, Brazil, Argentina, and India. In the United States, SCN was first reported in 1954 in North Carolina, and has since spread throughout most soybean growing regions of the country. Its ability to survive in a semi-desiccated state facilitates its spread through the movement of infested soil and plant material. SCN development is favored within a broad temperature range (15–33° C), and its ability to complete multiple generations per growing season, makes it difficult for producers to control its spread (St-Mareseille et al., 2018).

Genetic Resistance to SCN and Other Stressors

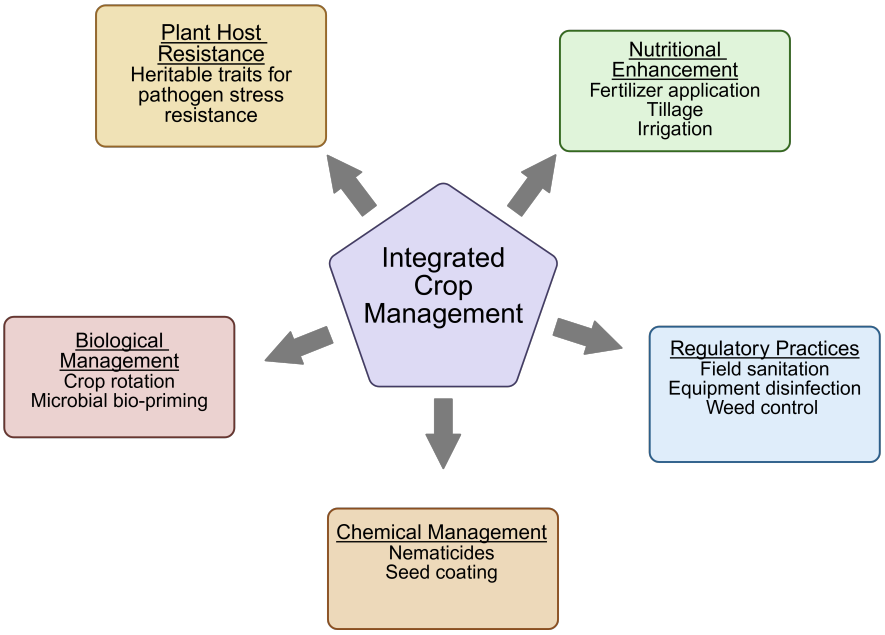

Figure 1.1: Integrated crop management practices include a wide variety of strategies aimed at improving crop productivity by maximizing host vigor and minimizing the harmful effects of environmental stressors, including pathogens such as soybean cyst nematode.

Host resistance represents the most effective and economically sustainable strategy for SCN management in agricultural systems. Although crop rotation, nematicides, and other management strategies can help enhance soybean vigor and therefore suppress SCN populations, host resistance remains the primary tool used by producers to reduce SCN reproduction and minimize yield losses (Figure 1.1). Host resistance, on the other hand, provides self-contained mechanisms that reduce pathogen load without significant metabolic trade offs, allowing plants to allocate resources toward growth and reproduction rather than to defense against pathogens and environmental stressors (Shaibu et al., 2020).

Host resistance generally occurs in the form of quantitative, or polygenic, traits. These are measurable phenotypes that continuously vary within a population and are determined by the combined effects of multiple genetic loci and environmental conditions. The inheritance of quantitative traits is less predictable than simple Mendelian traits. They often approximate a normal distribution and can be conceptualized as:

$$Phenotype = Genotype + Environment + G \times E \; (Genotype \times Environment)$$

Because many loci contribute small effects, the expression of these traits is frequently sensitive to environmental fluctuations, and a broad range of phenotypes is produced, rather than discrete categories of a trait. In crop plants, quantitative traits include yield, seed composition (e.g. protein and oil content), and many forms of disease response and stress tolerance. As a result, plant improvement programs rely on quantitative genetic and statistical frameworks to analyze, predict, and select these complex phenotypes.

Quantitative traits contrast with qualitative traits (monogenic), which are typically controlled by one or a few main resistance (R) genes. Qualitative resistance traits in plants often follow the gene-for-gene model by which a plant host R gene product detects a matching pathogen avirulence (avr) factor. Recognition of this factor triggers a localized hypersensitive response and infection containment (Hammond-Kosack & Jones, 1997). Although highly effective, the strong response triggered by this type of qualitative resistance can be rapidly overcome, making it less stable over time. This adaptation to qualitative resistance by pathogen populations results in "boom and bust" dynamics between pathogens and their hosts (Delmotte et al., 2016; McGee et al., 2025; Mundt, 2014).

Quantitative resistance often provides partial or incomplete protection; frequently this protection is broader in effectiveness and more durable. This durability occurs due to the partial nature of this protection; quantitative resistance imposes more diffuse selection pressure on pathogen populations (Corwin & Kliebenstein, 2017; Michel et al., 2023). In many systems, quantitative resistance gradually erodes rather than abruptly collapses as pathogens require multiple genetic adaptations to substantially reduce the effectiveness of host protections (Cowger & Brown, 2019). However, quantitative resistance can still exhibit population-specific effects depending on host pathogen interactions.

Because environmental conditions strongly influence the expression of polygenic traits, crop performance reflects both inherited potential and environmental reality. In applied crop breeding, both genetic factors and environmental conditions and inputs (e.g., climate and weather, soil management, nutrition, irrigation) are managed to maximize

yields. Increasingly, plant breeders use high-density molecular markers and genome-wide data to select favorable combinations of alleles associated with improved performance. Genomic tools, including dense SNP (single-nucleotide polymorphism) datasets and predictive models, enable more efficient identification and deployment of beneficial haplotypes, accelerating genetic gains relative to conventional breeding practices.

Major SCN Resistance Loci

Among characterized sources of resistance to soybean cyst nematode, the *Rhg1* locus represents one of the most widely deployed and mechanistically understood forms of soybean defense. Developed from Plant Introduction (PI) 88788, resistance at the *Rhg1* locus results from copy number variation of a gene complex in which higher copy number generally corresponds with stronger resistance. This locus contains a set of genes including an amino acid transporter, an -SNAP (soluble N-ethylmaleimide-sensitive factor (NSF) attachment protein, and a wound inducible protein. Resistant soybeans carry an atypical form of the -SNAP. In normal function of this protein, -SNAP supports vesicle trafficking through the disassembly of SNARE complexes, the SCN-resistant -SNAP disrupts vesicle trafficking in the syncytium and induces cytotoxicity, limiting the nematode's ability to maintain its feeding site (Bayless et al., 2016).

Rhg4 is another key locus contributing to population-specific resistance. Cultivars with 'Peking' and 'Forrest' resistance backgrounds contain this locus, the *Rhg4* locus enhances the efficacy of the *Rhg1* locus. *Rhg4* has been linked to a gene encoding a serine hydroxymethyltransferase (SHMT), which restricts syncytium development (Kandoth et al., 2017; Yuan et al., 2012). The widespread distribution of soybean cyst nematode has driven overreliance on these limited forms of host resistance. Both PI-88788 and Peking-type resistance have been effective forms of SCN resistance when deployed appropriately. This effectiveness has led to overuse, especially in the case of PI 88788. For the past 30 years in the United States, over 95% of soybean cultivars with SCN resistance are descended from sources with PI 88788-type resistance; for the past 20 years, other sources of SCN resistance

have come from Peking-type resistance (Tylka, 2022). This intensive use of *Rhg1* and *Rhg4* loci to combat SCN has contributed to the selection for SCN populations with increased virulence on these forms of host resistance, complicating SCN management (Kwon et al., 2024; Nissan et al., 2022). These trends highlight the need to identify additional sources of resistance, particularly through the exploration of genetically diverse germplasm such as wild soybean.

Other Stressors for Soybean

Plants in agricultural systems are exposed simultaneously to environmental and biological stressors that influence growth, development, and productivity. These interactions are commonly conceptualized as a disease triangle, which describes the dynamic relationship among host genotype and vigor, environmental conditions, and pathogen pressure over time (Pokhrel, 2021). In soybean production systems, these abiotic (nonliving) and biotic (living) factors frequently occur together, and can enhance one another while simultaneously weakening crop plants (Figure 1.2). Early exposure to one stress factor can increase vulnerability to subsequent challenges throughout the growing season (Choudharry Senthil-Kumar, 2024; Mahecha-Garnica et al., 2022; Martin-Cardoso San Segundo, 2025).

Among abiotic stressors, access to sufficient water is one of the most significant factors limiting soybean productivity worldwide. Water deficit affects soybean growth across developmental stages by reducing photosynthetic efficiency, limiting leaf expansion, altering carbon allocation, and modifying root architecture (Du et al., 2024; X. Wang et al., 2022). Water deficit tolerance is associated with genetic traits that improve water acquisition or conservation, including increased root depth, altered development and resource allocation towards root growth, and improved water use efficiency (Ku et al., 2013; Valliyodan et al., 2017). When soybean encounters water deficit early in the growing season, plant growth can be substantially reduced, and may alter nitrogen fixation via effects on root nodulation; both of these outcomes can have lasting effects on crop performance over the course of the growing season, causing significant loss in crop quality and yields (Ergin et al., 2025;

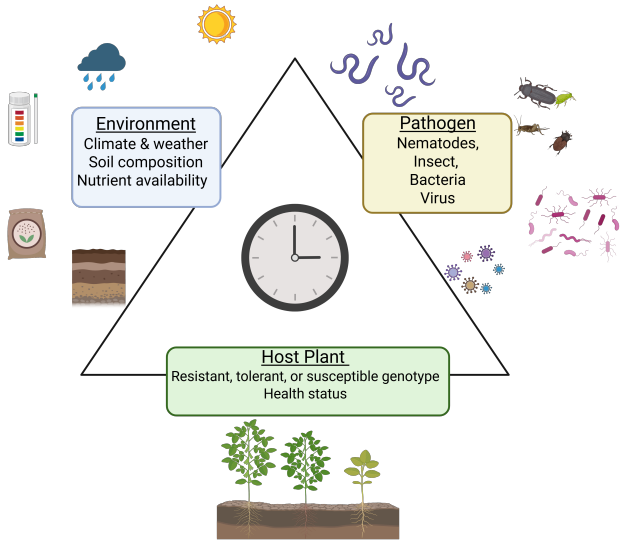

Figure 1.2: The plant-disease triangle illustrates how plants encounter a variety of abiotic and biotic conditions over the course of a growing season that influence host plant development.

Ferreira et al., 2024; Lumactud et al., 2022). However, plant performance in agricultural systems rarely reflects responses to a single stressor.

Combined Stress in Soybean

Although SCN and water deficit responses in soybean are often studied independently, crops rarely encounter a single stress factor. Combined stresses can produce non-additive effects on growth and physiology, complicating prediction of host responses and reducing productivity (Zandalinas Mittler, 2022). The interaction between soybean, SCN, and water deficit is particularly important as both the pathogen and the environmental condition have strong effects on host root function and nutrient uptake. Soybean cyst nematode damages roots, alters root structure, and diverts nutrient allocation. Water deficit can also affect root growth and limit water availability for the rest of the plant. Together, these processes can intensify reductions in water and nutrient uptake, resulting in compounded impacts on growth and yield.

In this way, combined SCN and water deficit constitute a distinct, complex state

that cannot be predicted by studying each stressor in isolation. The combination of abiotic and biotic stressors often induces distinct transcriptomic and physiological responses due to complex signaling crosstalk of phytohormones and reactive oxygen species. The result of these interactions is often unpredictable. One stressor may induce protective responses, leading to host resilience to subsequent stress conditions (antagonist response). However, the joint effect of multiple stressors can produce a more severe impact than the sum of the individual effects. This synergistic response occurs because multiple stressors can produce unique damage pathways and decrease the host's ability to cope with multiple threats, stunting plant development, and reducing fitness (Chojak-Koźniewska et al., 2018; Nejat & Mantri, 2017).

Early exposure to these stressors can be especially consequential as soybean seedlings prioritize root establishment and vegetative development during initial growth stages. Since SCN juveniles become infectious as soon as it is able to perceive host root exudates (i.e., soon after germination), and early water deficiency can cause the reallocation of resources normally utilized for energy production, understanding how soybean responds to simultaneous SCN infection and water deficit is crucial for the development of cultivars with durable resistance and stress tolerance (Narayana et al., 2024; Wrather Anand, 1988). Despite the importance of these interactions, relatively few studies have examined how SCN infection and water deficit stress combine to influence plant resistance and physiological performance, particularly in wild soybean.

Investigating Wild Soybean

The narrow genetic base of cultivated soybean makes it more susceptible to increasing severity of stressors such as soybean cyst nematode and water deficit, and its global importance makes revitalizing its genetic base crucial in the face of global climate change and a growing population. The overuse of SCN resistance derived from PI 88788 and Peking has contributed to the continued selection of SCN populations with increasing virulence, complicated by the potential effects of water deficit conditions that cannot be precisely pre-

dicted. Agricultural land use demands are also increasing, along with increased demand for animal products, so that producers must make the most use possible of existing croplands (Alexander et al., 2015; Ray et al., 2013; Yang et al., 2024).

The evolutionary history of modern elite cultivars has favored traits beneficial to growers, such as large biomass, high seed number, and uniform growth, which enable consistent performance under managed, relatively favorable conditions. However, this specialization can also make them more vulnerable to marginal environments and stronger pathogens. Since crops such as soybean have limited ability to defend themselves and adapt to existing conditions, new mechanisms of plant defense must be found to maintain, or even exceed, current crop yields.

Discovering traits of crop wild relatives (CWR) such as wild soybean is critically important for modern agriculture and enables the identification of valuable traits to improve existing crops. Phenotyping CWR traits faces significant bottlenecks due to high costs and the resource-intensive nature of analyzing a range of wild traits in diverse environmental conditions. High-performing automated phenotyping systems are expensive and less accessible, and rapid screening of large diverse populations remains difficult. There is increasing demand for high-throughput, low cost methods to analyze CWRs for disease resistance and abiotic stress tolerance (Einspanier et al., 2024; Rangan et al., 2023; Rosenqvist et al., 2019). The study of combined stress phenomics has received even less attention due to the complexity of untangling the effects of multiple harmful environmental conditions in crop plants. (Priya et al., 2023)However, linking measurable plant traits to genomics and environmental responses will allow researchers to accelerate plant breeding for higher yields, stress tolerance, and resource efficiency. In this way, genetic resources can be characterized more efficiently for future crop development and provide a strong basis of our understanding of crop plant development that will allow us to better predict agronomic needs, improving agricultural sustainability. Bridging the gap between genotypic potential and phenotypic expression is necessary to develop soybean varieties that maintain high

yields under environmental stress (Jiang Zhu, 2024; Kaya, 2025).

Wild soybeans provide potential solutions to the simultaneous pressures of changing abiotic and biotic conditions, including year-to-year climatic variability and evolving pathogen populations. Wild soybean is an important genetic resource for crop improvement against both SCN and water deficit conditions, among other crop-reducing stressors. Their extensive genetic diversity has demonstrated tolerance to stress and resistance to disease that will be useful for soybean breeding programs. Although *G. max's* responses to SCN and water deficit have been well characterized individually, relatively little is known about the combined effects of these stressors in *G. soja*. Similarly to cultivated soybeans, studies of wild soybean response to water deficit have occurred primarily only under that single stress. Identification of important resistance to SCN and tolerance to water deficits is essential for soybean production.

Knowledge Gaps

Although soybean is widely cultivated and researched, much less is known about its wild progenitor. Some important accessions have been studied for important traits such as SCN resistance and tolerance to water deficit, but the systematic screening of wild soybean germplasm on a scale is not currently complete. The USDA's soybean germplasm repository contains hundreds of *Glycine soja* accessions, the second largest repository of wild soybean germplasm in the world. However, systematic screening for important pathogen-related traits takes time and resources, and new accessions are added every year. Our understanding of broad resistance to SCN, especially in wild soybean, is limited by the use of single population types in most studies. Many studies evaluate resistance using a single SCN population, and so resistance to a large number of SCN HG types and its durability is still poorly characterized. Identifying and elucidating the mechanisms of wild soybean resistance are crucial due to potential effects of overuse and selection that can lead to increased SCN virulence, as studied in PI 88788 and PI 437654 respectively (Gardner et al., 2017).

The genetic architecture of SCN resistance, water deficit tolerance, and other important traits of wild soybeans is only partially elucidated. A few novel QTL and SNPs have been identified, though fewer have been integrated into the soybean genome (Meinhardt et al., 2021). Plant response to stressors can include both general stress responses and responses specific to the pathogen or environmental stressor it encounters, producing protective compounds, adjusting morphological traits, and repressing growth (Y. Zhang et al, 2023). Identifying and characterizing novel resistance loci, as well as phenotypic and physiological traits in wild soybean can help to expand the genetic toolkit for soybean breeding.

In agricultural systems, crops experience multiple stressors simultaneously. Most resistance studies examine single pathogens under optimal environmental conditions, while the interaction between the response to abiotic and biotic stress remains underinvestigated. Multiple stressors often produce non-additive effects because signaling pathways which regulate the abiotic and biotic stress response interact, creating a unique response compared to that of a single stress, and leading to transcriptional and physiological changes that differ from those observed under individual stressors (Saijo Loo, 2019; Zandalinas Mittler, 2022). Addressing these knowledge gaps requires integrated investigation of wild soybean genetic diversity, resistance to diverse SCN populations, and plant responses to combined abiotic and biotic stress.

Dissertation Overview

Despite extensive research on the evolutionary history, pathogen resistance, and response profiles to individual stressors of cultivated soybean, significant knowledge gaps remain regarding the genetic and physiological basis of stress resilience in wild soybean (Glycine soja). In particular, the interaction between host genetic architecture, pathogen population diversity, and environmental stress has not been comprehensively evaluated in wild soybean germplasm. Cultivated soybean has been intensively studied for resistance to soybean cyst nematode (SCN) and for water deficit tolerance independently, yet the

genetic resources and phenotypic responses found in wild soybean remain underexplored, particularly under multifactorial stress conditions.

As a reservoir of allelic diversity that will contribute to novel mechanisms of resistance or tolerance to both biotic and abiotic stressors, wild soybean must be more thoroughly investigated so that these important traits may be deployed. Knowledge of the genetic architecture underlying SCN resistance in wild soybean is essential to understand the mechanisms of novel SCN resistance loci. Furthermore, given the heterogeneity of the SCN populations and their high capacity for virulence changes under strong selection pressure, it is critical to evaluate accessions of wild soybeans against diverse SCN populations to fully understand the breadth and durability of resistance. Soybean production increasingly occurs under variable and often water-limited conditions, in addition to pathogen pressure. Because water deficit and SCN both interfere with root function and resource acquisition, their combined effects may be synergistic rather than additive. However, little is known about the physiological response of wild soybeans to simultaneous exposure to SCN infection and water deficit. Integrating SCN reproduction, plant growth parameters, and physiological indicators assessment proves a more comprehensive understanding of stress resilience than only a single trait-evaluation.

This study investigates the genetic and phenotypic underpinnings of wild soybean responses to SCN. This important resource is examined in the context of both SCN infection and water deficit in order to identify germplasm accessions and traits of agricultural importance. The phenotyping of wild germplasm is still essential because the identification of loci associated with resistance and tolerance is dependent on precise phenotyping. This is especially true in the case of combined stresses, as the effects of multiple sources of stress are nonadditive and can vary by pathogen and abiotic stress type. This research advances our understanding of stress resilience in wild soybeans and provides a foundation for future breeding efforts. This dissertation addresses knowledge gaps through three complementary studies of wild soybean that examine the genetic basis of SCN resistance, the breadth

of resistance across diverse SCN populations, and the stability of SCN resistance under combined biotic and abiotic stress.

Dissertation Chapters

Chapter 2 characterizes the genetic architecture of wild soybean resistance to soybean cyst nematode through quantitative mapping of the trait locus (QTL) and epistatic analysis. This study identifies novel loci conferring SCN resistance in wild soybean independent of those found in widely utilized and well-characterized loci such as *Rhg1*.

Chapter 3 investigates the response of wild soybean germplasm to various populations of soybean cyst nematode with differential virulence and identifies sources of broad-spectrum and population-specific resistance to SCN.

Chapter 4 evaluates the performance of wild soybean resistance under combined biotic and abiotic stress, and identifies physiological and phenotypic traits associated with resistance.

Chapter 5 synthesizes the findings of the previous chapters and discusses their implications for soybean breeding, stress resilience, and future research directions.

References

Alexander, P., Rounsevell, M. D., Dislich, C., Dodson, J. R., Engström, K., & Moran, D. (2015). Drivers for global agricultural land use change: The nexus of diet, population, yield and bioenergy. *Global Environmental Change*, 35, 138–147. https://doi.org/10.1016/j.gloenvcha.2015.08.011

Bayless, A. M., Smith, J. M., Song, J., McMinn, P. H., Teillet, A., August, B. K., & Bent, A. F. (2016). Disease resistance through impairment of -SNAP–NSF interaction and vesicular trafficking by soybean *Rhg1*. *Proceedings of the National Academy of Sciences*, 113(47), E7375–E7382. https://doi.org/10.1073/pnas.1610150113

Chojak-Koźniewska, J., Kuźniak, E., & Zimny, J. (2018). The Effects of Combined Abiotic and Pathogen Stress in Plants: Insights From Salinity and *Pseudomonas syringae pv lachrymans* Interaction in Cucumber. *Frontiers in Plant Science*, 9, 1691. https://doi.org/10.3389/fpls.2018.01691

Cowger, C., & Brown, J. K. (2019). Durability of quantitative resistance in crops: greater than we know? *Annual Review of Phytopathology*, 57(1), 253–277. https://doi.org/10.1146/annurev-phyto-082718-100016

Delmotte, F., Bourguet, D., Franck, P., Guillemaud, T., Reboud, X., Vacher, C., & Walker, A. (2016). Combining selective pressures to enhance the durability of disease resistance genes. *Frontiers in Plant Science*, 7, 1916. https://doi.org/10.3389/fpls.2016.01916

Dilawari, R., Kaur, N., Priyadarshi, N., Prakash, I., Patra, A., Mehta, S., Singh, B., Jain, P., & Islam, M. A. (2022). Soybean: A Key Player for Global Food Security. In Soybean Improvement (pp. 1–46). https://doi.org/10.1007/978-3-031-12232-3_1

Du, Q., Zhou, L., Chen, P., Liu, X., Song, C., Yang, F., Wang, X., Liu, W., Sun, X., Du, J., Liu, J., Shu, K., Yang, W., & Yong, T. (2019). Relay-intercropping soybean with maize maintains soil fertility and increases nitrogen recovery efficiency by reducing nitrogen input. *The Crop Journal*, 8(1), 140–152. https://doi.org/10.1016/j.cj.2019.06.010

Einspanier, S., Tominello-Ramirez, C., Hasler, M., Barbacci, A., Raffaele, S., & Stam, R. (2024). High-resolution Disease Phenotyping Reveals Distinct Resistance Mechanisms of Tomato Crop Wild Relatives against *Sclerotinia sclerotiorum*. *Plant Phenomics*, 6, 0214. https://doi.org/10.34133/plantphenomics.0214

Ferreira, R. C., Sibaldelli, R. N. R., Crusiol, L. G. T., Neumaier, N., & Farias, J. R. B. (2024). Soybean Yield Losses Related to Drought Events in Brazil: Spatial–Temporal Trends over Five Decades and Management Strategies. *Agriculture*, 14(12), 2144. https://doi.org/10.3390/agriculture14122144

Gardner, M., Heinz, R., Wang, J., & Mitchum, M. G. (2017). Genetics and adaptation of soybean cyst nematode to broad spectrum soybean resistance. *G3 Genes Genomes Genetics*, 7(3), 835–841. https://doi.org/10.1534/g3.116.035964

Hammond-Kosack, K. E., & Jones, J. D. G. (1997). Plant Disease Resistance Genes. *Annual Review of Plant Physiology and Plant Molecular Biology*, 48(1), 575–607. https://doi.org/10.1146/annurev.arplant.48.1.575

Hu, Z., Zhang, D., Zhang, G., Kan, G., Hong, D., & Yu, D. (2014). Association mapping of yield-related traits and SSR markers in wild soybean (*Glycine soja* Sieb. and Zucc.). *Breeding Science*, 63(5), 441–449. https://doi.org/10.1270/jsbbs.63.441

Hyten, D. L. (2012). Advances in genome sequencing and genotyping technology for soybean diversity analysis. In Elsevier eBooks (pp. 45–52). https://doi.org/10.1016/b978-0-9830791-0-1.50007-8

Hyten, D. L., Song, Q., Zhu, Y., Choi, I., Nelson, R. L., Costa, J. M., Specht, J. E., Shoemaker, R. C., & Cregan, P. B. (2006). Impacts of genetic bottlenecks on soybean genome diversity. *Proceedings of the National Academy of Sciences*, 103(45), 16666–16671. https://doi.org/10.1073/pnas.0604379103

Inagaki, H., & Tsutsumi, M. (1971). Survival of the soybean cyst nematode, *Heterodera glycines* Ichinohe (Tylenchida: Heteroderidae) under certain storing conditions. *Applied Entomology and Zoology*, 6:156-162.

Jiang, N., & Zhu, X. (2024). Modern phenomics to empower holistic crop science, agronomy, and breeding research. *Journal of Genetics and Genomics*, 51(8), 790–800. https://doi.org/10.1016/j.jgg.2024.04.016

Joshi, T., Valliyodan, B., Wu, J., Lee, S., Xu, D., & Nguyen, H. T. (2013). Genomic differences between cultivated soybean, *G. max* and its wild relative *G. soja*. *BMC Genomics*, 14(S1), S5. https://doi.org/10.1186/1471-2164-14-s1-s5

Kandoth, P. K., Liu, S., Prenger, E., Ludwig, A., Lakhssassi, N., Heinz, R., Zhou, Z., Howland, A., Gunther, J., Eidson, S., Dhroso, A., LaFayette, P., Tucker, D., Johnson, S., Anderson, J., Alaswad, A., Cianzio, S. R., Parrott, W. A., Korkin, D.. . . Mitchum, M. G. (2017). Systematic mutagenesis of serine hydroxymethyltransferase reveals an essential role in nematode resistance. *Plant Physiology*, 175(3), 1370–1380. https://doi.org/10.1104/pp.17.00553

Kaya, C. (2025). Optimizing crop production with plant phenomics through High-throughput Phenotyping and AI in controlled environments. *Food and Energy Security*, 14(1). https://doi.org/10.1002/fes3.70050

Kholmurodova, G., Tangirova, G., Rakhmankulov, M., & Yuldasheva, R. (2023). Analysis of protein and oil content in seeds of soybean collection varieties. *E3S Web of Conferences*, 377, 03016. https://doi.org/10.1051/e3sconf/202337703016

Kim, I., Kim, C., & Yang, W. (2021). Physiologically Active Molecules and Functional Properties of Soybeans in Human Health—A Current Perspective. *International Journal of Molecular Sciences*, 22(8), 4054. https://doi.org/10.3390/ijms22084054

Kim, W. J., Kang, B. H., Moon, C. Y., Kang, S., Shin, S., Chowdhury, S., Jeong, S., Choi, M., Park, S., Moon, J., & Ha, B. (2023). Genome-Wide Association Study for Agronomic Traits in Wild Soybean (*Glycine soja*). *Agronomy*, 13(3), 739. https://doi.org/10.3390/agronomy13030739

Kofsky, J., Zhang, H., & Song, B. (2018). The Untapped Genetic Reservoir: The Past, Current, and Future Applications of the Wild Soybean (*Glycine soja*). *Frontiers in*

Plant Science, 9, 949. https://doi.org/10.3389/fpls.2018.00949.

Kumari, S., Dambale, A. S., Samantara, R., Jincy, M., & Bains, G. (2025). Introduction, History, Geographical Distribution, Importance, and Uses of Soybean (*Glycine max* L.). In Soybean Production Technology (pp. 1–17). https://doi.org/10.1007/978-981-97-8677-0_1

Kwon, K. M., Masonbrink, R. E., Maier, T. R., Gardner, M. N., Severin, A. J., Baum, T. J., & Mitchum, M. G. (2024). Comparative Transcriptomic Analysis of Soybean Cyst Nematode Inbred Populations Non-adapted or Adapted on Soybean *Rhg1*-a/*Rhg4*-Mediated Resistance. *Phytopathology*, 114(10), 2341–2350. https://doi.org/10.1094/phyto-03-24-0095-r

Liu, Z., Shi, X., Yang, Q., Li, Y., Yang, C., Zhang, M., An, Y. C., Nguyen, H. T., Yan, L., & Song, Q. (2025). Landscape of rare-allele variants in cultivated and wild soybean genomes. *The Plant Genome*, 18(2), e70020. https://doi.org/10.1002/tpg2.70020

Masonbrink, R., Maier, T. R., Muppirala, U., Seetharam, A. S., Lord, E., Juvale, P. S., Schmutz, J., Johnson, N. T., Korkin, D., Mitchum, M. G., Mimee, B., Akker, S. E. D., Hudson, M., Severin, A. J., & Baum, T. J. (2019). The genome of the soybean cyst nematode (*Heterodera glycines*) reveals complex patterns of duplications involved in the evolution of parasitism genes. *BMC Genomics*, 20(1), 119. https://doi.org/10.1186/s12864-019-5485-8

McGee, R., Zaleski-Cox, M., Jayawardana, M. A., Tillman, B. L., Wally, O., Esquivel-Garcia, L., Fernando, W. G. D., Raman, H., Bariana, H. S., Copley, T., Carter, A. H., & Hoyos-Villegas, V. (2025). Breeding for quantitative disease resistance: Case studies, emerging approaches, and exploiting pathogen variation. *Crop Science*, 65(6). https://doi.org/10.1002/csc2.70202

Meinhardt, C., Howland, A., Ellersieck, M., Scaboo, A., Diers, B., & Mitchum, M. G. (2021). Resistance gene pyramiding and rotation to combat widespread soybean cyst nematode virulence. *Plant Disease*, 105(10), 3238–3243. https://doi.org/10.

1094/pdis-12-20-2556-re

Michel, S., Löschenberger, F., Ametz, C., & Bürstmayr, H. (2023). Toward combining qualitative race-specific and quantitative race-nonspecific disease resistance by genomic selection. *Theoretical and Applied Genetics*, 136(4), 79. https://doi.org/10.1007/s00122-023-04312-2

Mundt, C. C. (2014). Durable resistance: A key to sustainable management of pathogens and pests. *Infection Genetics and Evolution*, 27, 446–455. https://doi.org/10.1016/j.meegid.2014.01.011

Narayana, N. K., Wijewardana, C., Alsajri, F. A., Reddy, K. R., Stetina, S. R., & Bheemanahalli, R. (2024). Resilience of soybean genotypes to drought stress during the early vegetative stage. *Scientific Reports*, 14(1), 17365. https://doi.org/10.1038/s41598-024-67930-w

Nejat, N., & Mantri, N. (2017). Plant immune system: Crosstalk between responses to biotic and abiotic stresses the missing link in understanding plant defence. *Current Issues in Molecular Biology*, 23, 1–16. https://doi.org/10.21775/cimb.023.001

Nissan, N., Mimee, B., Cober, E. R., Golshani, A., Smith, M., & Samanfar, B. (2022b). A broad review of soybean research on the ongoing race to overcome soybean cyst nematode. *Biology*, 11(2), 211. https://doi.org/10.3390/biology11020211

Priya, P., Patil, M., Pandey, P., Singh, A., Babu, V. S., & Senthil-Kumar, M. (2023). Stress combinations and their interactions in plants database: a one-stop resource on combined stress responses in plants. *The Plant Journal*, 116(4), 1097–1117. https://doi.org/10.1111/tpj.16497

Rangan, P., Pradheep, K., Archak, S., Smýkal, P., & Henry, R. (2023). Editorial: Genomics and phenomics of crop wild relatives (CWRs) for crop improvement. *Frontiers in Plant Science*, 14, 1221601. https://doi.org/10.3389/fpls.2023.1221601

Ray, D. K., Mueller, N. D., West, P. C., & Foley, J. A. (2013). Yield trends are insufficient to double global crop production by 2050. *PLoS ONE*, 8(6), e66428.

https://doi.org/10.1371/journal.pone.0066428

Rosenqvist, E., Grobkinsky, D. K., Ottosen, C., & Van De Zedde, R. (2019). The Phenotyping Dilemma—The challenges of a diversified Phenotyping Community. *Frontiers in Plant Science*, 10, 163. https://doi.org/10.3389/fpls.2019.00163

Saijo, Y., & Loo, E. P. (2019). Plant immunity in signal integration between biotic and abiotic stress responses. *New Phytologist*, 225(1), 87–104. https://doi.org/10.1111/nph.15989

Sedivy, E. J., Wu, F., & Hanzawa, Y. (2017b). Soybean domestication: the origin, genetic architecture and molecular bases. *New Phytologist*, 214(2), 539–553. https://doi.org/10.1111/nph.14418

Shaibu, A. S., Li, B., Zhang, S., & Sun, J. (2020). Soybean cyst nematode-resistance: Gene identification and breeding strategies. *The Crop Journal*, 8(6), 892–904. https://doi.org/10.1016/j.cj.2020.03.001

St-Marseille, A. G., Lord, E., Véronneau, P., Brodeur, J., & Mimee, B. (2018). Genome scans reveal homogenization and local adaptations in populations of the soybean cyst nematode. *Frontiers in Plant Science*, 9, 987. https://doi.org/10.3389/fpls.2018.00987

Sun, Y., Chen, L., Jin, Y., Wang, S., Ma, S., Yu, L., Tang, C., Ye, Y., Li, M., Zhou, W., Chen, E., Kong, X., Fu, J., Wang, J., Chen, Q., & Yang, M. (2025). Identification of key Waterlogging-Tolerance genes in cultivated and wild soybeans via integrated QTL–Transcriptome analysis. *Agronomy*, 15(8), 1916. https://doi.org/10.3390/agronomy15081916

Tylka, G. More soybean varieties with Peking SCN resistance for 2023, but more needed. (2022.). *Integrated Crop Management*. https://crops.extension.iastate.edu/cropnews/2022/11/more-soybean-varieties-peking-scn-resistance-2023-more-needed

U.S. Department of Agriculture, Foreign Agricultural Service. (n.d.). Soybeans: Production data. https://www.fas.usda.gov/data/production/2222000

Wrather, J. A., & Anand, S. C. (1988). Relationship Between Time of Infection with *Heterodera glycines* and Soybean Yield. *PubMed*, 20(3), 439–442. https://pubmed.ncbi.nlm.nih.gov/19290235

Wu, H. Y., Luo, M., Zhang, L. Y., & Zhou, X. B. (2019). Nematicidal Activity of Fosthiazate Against Soybean Cyst Nematode *Heterodera glycines*. *Journal of Nematology*, 51(1), 1–9. https://doi.org/10.21307/jofnem-2019-021

Wu, X., Feng, Q., Zhang, Z., Zhang, X., Liu, Z., Yang, Q., Shi, X., Zhang, M., & Yan, L. (2025). Analysis of genetic diversity among wild soybean (*Glycine soja*) from Hengshui Lake in Hebei Province, China. *BMC Genomic Data*, 26(1), 84. https://doi.org/10.1186/s12863-025-01332-3

Yang, Y., Tilman, D., Jin, Z., Smith, P., Barrett, C. B., Zhu, Y., Burney, J., D'Odorico, P., Fantke, P., Fargione, J., Finlay, J. C., Rulli, M. C., Sloat, L., Van Groenigen, K. J., West, P. C., Ziska, L., Michalak, A. M., Team, T. C., Lobell, D. B., . . . Zhuang, M. (2024). Climate change exacerbates the environmental impacts of agriculture. *Science*, 385(6713), eadn3747. https://doi.org/10.1126/science.adn3747

Yuan, C., Li, Y., Liu, Z., Guan, R., Chang, R., & Qiu, L. (2012). DNA sequence polymorphism of the *Rhg4* candidate gene conferring resistance to soybean cyst nematode in Chinese domesticated and wild soybeans. *Molecular Breeding*, 30(2), 1155–1162. https://doi.org/10.1007/s11032-012-9703-1

Zandalinas, S. I., & Mittler, R. (2022). Plant responses to multifactorial stress combination. *New Phytologist*, 234(4), 1161–1167. https://doi.org/10.1111/nph.18087

Zhang, Y., Xu, J., Li, R., Li, R., Ge, Y., Li, Y., Li, R., & Li, R. (2023). Plants' response to abiotic stress: Mechanisms and strategies. *International Journal of Molecular Sciences*, 24(13), 10915. https://doi.org/10.3390/ijms241310915

Zhu, Z., Wang, Y., Liu, S., Wang, S., Li, J., Fang, C., Liu, Y., Yang, X., Tian, D., Song, S., & Tian, Z. (2025). Genomic atlas of 8,105 accessions reveals stepwise domestication, global dissemination, and improvement trajectories in soybean. *Cell*, 188(23),

6519-6535.e15. https://doi.org/10.1016/j.cell.2025.09.007

Zhou, X., Wang, D., Mao, Y., Zhou, Y., Zhao, L., Zhang, C., Liu, Y., & Chen, J. (2022). The organ size and morphological change during the domestication process of soybean. *Frontiers in Plant Science*, 13, 913238. https://doi.org/10.3389/fpls.2022.913238

Zhuang, Y., Li, X., Hu, J., Xu, R., & Zhang, D. (2022). Expanding the gene pool for soybean improvement with its wild relatives. *aBIOTECH*, 3(2), 115–125. https://doi.org/10.1007/s42994-022-00072-7

CHAPTER 2: GENETIC ARCHITECTURE OF SCN RESISTANCE IN WILD SOYBEAN (*GLYCINE SOJA*)

2.1 Introduction

Soybean (*Glycine max*) is one of the most important crops in the world. However, soybean crops are devastated by the soil-borne soybean cyst nematode (SCN, *Heterodera glycines*). SCN is a widespread pathogen that can survive harsh conditions inside protective cysts, allowing pathogen populations to persist in soil for years and infect host plants, reducing yields. During parasite establishment, the pathogen remodels root cells into a multinucleate feeding cell (syncytium), leading to stunted roots, reduced nodulation and nitrogen fixation, and reduced yields (Akinrinlola et al., 2024; Wendimu, 2022). SCN alone causes more than 30% of soy yield losses annually, at a cost of approximately $1.5 billion annually in North America alone (Kim et al., 2016; Tylka & Marett, 2021).

To combat this threat, growers use an integrated pest management approach, combining host genetic resistance, crop rotation, and nematicides for maximum efficacy (Roth et al., 2020). Host genetic resistance remains the primary approach to control SCN. Most host resistance is facilitated through the use of either PI 88788 and 'Peking' (PI 548402). However, the overuse of these genetic lines has reduced their long-term effectiveness. The rapid life cycle of SCN, its spread to uninfected soil, and its resilience in the face of harsh conditions allow populations to adapt to commonly deployed resistance strategies, particularly those derived from PI 88788 (Faghihi et al., 2018; Nissan et al., 2022; You et al., 2024).

Currently, most host genetic resistance is based on two main resistance mechanisms of two soybean strains: PI 88788-type resistance and Peking-type resistance. PI 88788 is a major source of resistance and has been used to develop up to 95% of SCN-resistant

cultivars. However, recent overuse of these, especially PI 88788, has led to the selection of SCN biotypes such as the SCN HG Type 1.2.5.7, which are capable of overcoming the resistance mechanisms of its host (Critchfield et al., 2023; Torabi et al., 2023; Yan & Baidoo, 2018).

In contrast, wild soybean *Glycine soja* has greater genetic diversity that suggests untapped potential for pathogen resistance which will improve crop yields and the sustainability of crop production (Kofsky et al., 2018). During the domestication process of *G. max* from its progenitor, *G. soja*, genetic diversity was lost due to selection for agronomically beneficial traits such as increased oil and protein (Sedivy et al., 2017). Consequently, domesticated soybean has a narrower genetic base compared to wild soybean. The genetic diversity of wild soybeans was the result of adaptation in a wide range of geographic and environmental conditions. Wild soybeans are a rich source of potential genetic resistance to this devastating pathogen (Anderson et al., 2019). Based on this premise, we initiated a quantitative trait locus (QTL) study to explore potentially novel genomic regions of *G. soja* "S54". S54 is a wild soybean accession that has previously been shown to exhibit resistance to SCN (H. Zhang et al., 2017-a). The F4 generation of a cross between *G. soja* 'S54' and *G. max* cultivar 'NC-Raleigh' was challenged with SCN H. G. type 1.2.5.7 (previously 'Race 2') to identify novel loci and candidate genes for soybean cyst nematode resistance. The goal of this study was to elucidate the genetic architecture of resistance to SCN in wild soybean by identifying novel loci and candidate genes associated with resistance.

2.2 Materials & Methods

Plant Materials

The single-seed descent method was used to create a recombinant inbred line population from a cross between cultivated soybean 'NC-Raleigh' and wild soybean'S54' (PI 424093) at the Central Crops Research Station (CCRS), Clayton, North Carolina, USA. 'NC-Raleigh was chosen as the SCN susceptible *G. max* parent, as its flowering period overlaps with that of the *G. soja* donor parent, 'S54' (Burton et al., 2006). S54 is a plant

introduction (PI) of *G. soja* originally from Chungcheongbuk-do Province, South Korea. It has previously demonstrated resistance to SCN HG type 2.5.7 (H. Zhang et al., 2016).The F1 seeds were grown in the USDA-ARS Tropical Agricultural Research Station, Isabela, Puerto Rico, USA. The F2 generation, and subsequent generations, were grown at CCRS via single-seed descent until the F4 generation, from which a sample size of 185 was utilized. All wild soybean plant material was obtained from USDA germplasm and complied with relevant institutional, national, and international guidelines.

SCN Bioassay, DNA Extraction, Genotyping

SCN Bioassay was conducted in the greenhouse at the University of North Carolina at Charlotte using previously established methods. (Niblack et al. 2002; Niblack et al. 2009; H. Zhang et al., 2017-a). The SCN HG type 1.2.5. used in this study was an inbred and near homozygous population maintained on susceptible soybean stocks for over 30 generations in the University of North Carolina at Charlotte research greenhouse. Confirmation of the SCN population type was performed by inoculation of HG testing indicator lines ('Peking', PI 88788, PI 90763, PI 437654, PI 209332, PI 89772, and PI 548316). The parental lines "S54" and "NC-Raleigh", and susceptible control "Williams 82" were inoculated along with the F4 mapping population. Seeds were sterilized with 0.5% sodium hypochlorite solution, scarified, and germinated on sterile filter paper in petri dishes for 5 days. Germinated seeds were transplanted into plastic cones (Stuewe Sons, Tangent, Oregon, USA) containing sterilized sand. Two days after transplanting, SCN eggs were harvested and purified by sucrose flotation, and each plant was inoculated with approximately 2000 SCN eggs (Matthews et al., 2003). All plants were grown for one life cycle of *Heterodera glycines* under greenhouse conditions (27℃, 16/8 hour day/night cycle). Seedlings were watered twice daily to maintain healthy plant growth conditions. Thirty days after SCN infection, cysts produced by the nematodes were extracted from RIL, indicator, parental, and susceptible check lines and caught in a 250 μm sieve stacked on a 25 μm sieve (Fisherbrand) and counted under a 10X microscope (Fisher Scientific). Female

index (FI), a standardized measure of SCN reproduction, was used as the phenotype. FI calculates the number of SCN cysts formed on a test line relative to a susceptible check, calculated per Niblack et al., 2002:

$$FI = \left(\frac{\bar{x}_{\text{test}}}{\bar{x}_{\text{susceptible}}} \right) \times 100$$

where $\bar{x}_{\text{test line}}$ represents the mean cyst count on the test line and $\bar{x}_{\text{susceptible check}}$ represents the mean cyst count on the susceptible control (Niblack et al., 2002).

Leaf tissue was collected, freeze dried, and shredded by the Taliercio lab at North Carolina State University. DNA extraction was performed by the University of Minnesota Genomics Center using the QiagenKit. Genome-wide genotyping with BARCSoySNP6K assay was performed. (Q. Song et al., 2020) and 6000 SNPs were identified. Genome Studio was used to assess and remove low-quality reads, after which homozygous SNPs were removed, leaving only high-quality reads for analysis (Illumina 2014).

QTL & Epistatic Analysis

BARCSoySNP6K genotyping for each plant was performed, identifying 6000 SNPs. In order to utilize the most informative single nucleotide polymorphisms, quality control was done to remove SNPs that were identical for both parental lines and a few low quality reads. After quality control, 3085 SNPs (51.4%) distributed over 20 chromosomes remained for quantitative trait locus mapping. QTL analysis was performed using inclusive composite interval mapping with QTL Icimapping software. The scanning step parameter was 1 cM with a set P-value of 0.001. The standard LOD value of 3 was set as the significance threshold for QTL analysis (Kumar et al., 2023; Meng et al, 2015; Wang et al 2014). Additionally, a permutation test was performed to control the genome-wide error rate. Phenotypic data were shuffled randomly 1,000 times to determine against the genotypic data to establish a genomic wide significance threshold for Type I errors at =0.05. This empirical threshold holds for multiple testing and the specific genetic architecture of the mapping population. Linkage maps were constructed using IciMapping software, with the LOD threshold of 3.0

(Figure A1A and A1B). A linkage map was constructed, spanning 1735.1 cM across 20 chromosomes (Chr), and varying among chromosomes from 76.1 cM (chromosome 19) 89 cM (chromosome 2).

We also tested any SNP markers identified as potential QTL in the mapping scan to see if they epistatically interacted with each other or with any other markers throughout the genome. To accomplish this, we used SAS software (SAS Institute, Inc., Cary, NC, USA) to calculate a simple linear model for each SNP pair, with a significant interaction suggesting epistasis. An LOD score of 3 as the threshold for significance was used as it signifies significant evidence that two loci are physically linked on a chromosome (Balestre De Souza, 2016; Nyholt, 2000).

Allele Effect Analysis

To further investigate the phenotypic effects of detected QTL, allele effects were evaluated at the peak marker with the strongest statistical signal; in this case, the right marker for both QTL. Recombinant inbred lines of the mapping population were grouped according to genotype at each marker, and the distribution of female index values among genotype classes was visualized using violin plots with overlaid boxplots and individual observations. Differences in FI among genotype classes were evaluated using the Kruskal-Wallis test, a non-parametric alternative to analysis of variance that does not assume normally distributed results. When significant differences were detected among groups, Dunn's post-hoc test was used to perform pairwise comparisons among genotype classes; p-values were adjusted using the Benjamini-Hochberg false discovery rate correction to account for multiple comparisons.

To evaluate the contribution of multiple loci to SCN resistance, allele stacking analysis was performed using the peak markers representing QTL-19 and QTL-13. The resistance allele at each locus was defined as the allele associated with reduced SCN reproduction (i.e. low female index) in the peak marker analysis. For each RIL, the total number of resistance alleles present across both loci was calculated (range: 0-4).

Lines were then grouped according to this cumulative allele count and the distribution of FI values among allele stacking groups was visualized using violin plots and box plots. Statistical differences in FI among allele stacking groups were evaluated using the Kruskal-Wallis test, followed by Dunn's pairwise comparisons with Benjamini-Hochberg adjustment (Benjamini Hochberg, 1995; Dunn, 1964; Kruskal Wallis, 1952). Additionally, the relationship between FI and the number of resistance alleles was evaluated using linear regression to quantify the overall trend in SCN reproduction across allele stacking groups. FI distributions were assessed with Spearman rank correlation to determine if there was a monotonic relation between the resistance allele number and FI. Non-parametic tests such as Kruskal-Wallis, Dunn's, and Spearman's correlation analysis are widely used because they are robust to non-normal phenotype distributions and unequal genotype genotype group sizes (Blanca et al., 2017; Broman, 2003; Qi et al., 2014; Spearman, 1904). Because the resistance allele number represents an ordered variable, the Jonckheere-Terpstra test was used to evaluate whether FI decreased progressively with increasing numbers of resistance alleles (Manning et al., 2023). All statistical analysis and figure generation for allele effects were conducted in R (R Core Team, 2024).

2.3 Results

Phenotypic Variation and Genetic Linkage Analysis

The FI values showed a large variation between the F4 progeny, ranging from 0 to 130.9 with a mean of 44.1. Some skewness (γ_1= 0.275) and flattening of the phenotype were observed in this experiment; however, the distribution of these values (Figure 2.1, Table A1) was normal (Shapiro-Wilk w = 0.972, p > 0.05). Per Niblack et al 2009, The HG type test was used to confirm the degree to which a set of seven standard soybean cultivars are able to resist SCN infection. Using these standards, the biotype of SCN was confirmed to be HG type 1.2.5.7 (Table A2).

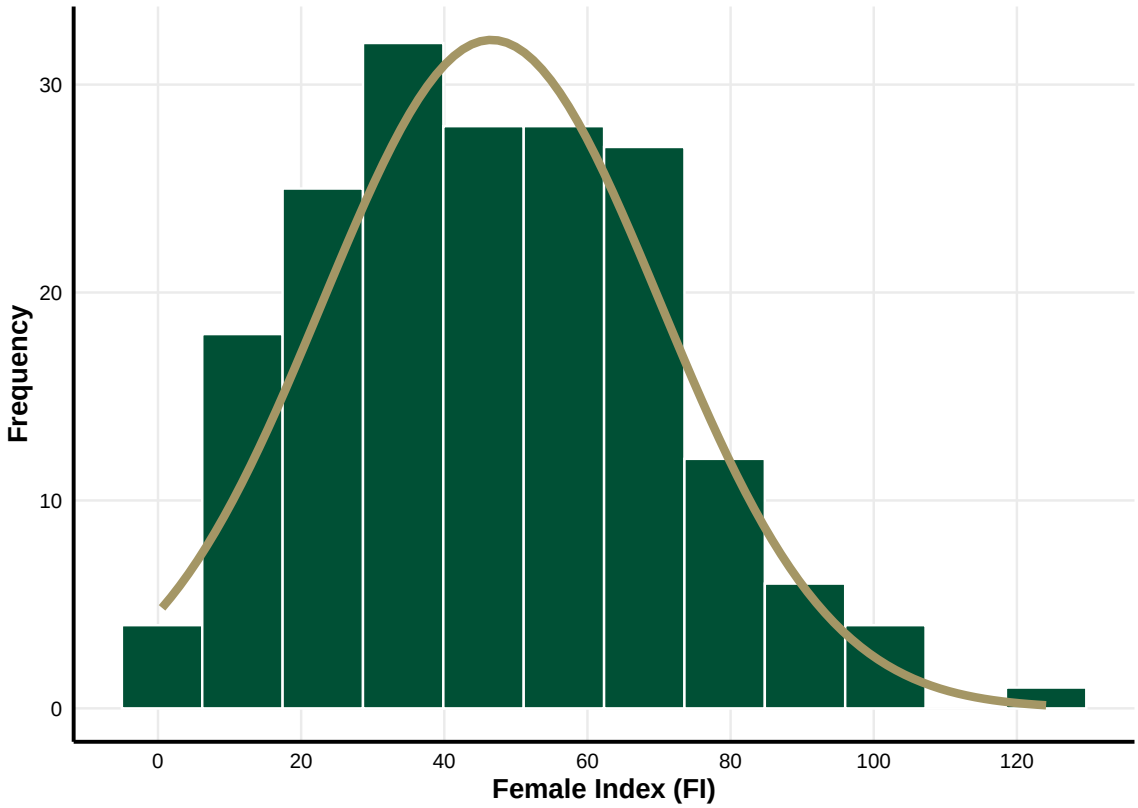

Figure 2.1: Frequency distribution of Female Index (F) scores across the S54 x NC-Raleigh mapping population when challenged with SCN HG type 1.2.5.7. The distribution exhibits positive skew (γ_1= 0.275)

QTL for SCN-Resistance and Epistatic Analysis

In the genomic scan, two large-effect QTLs associated with resistance to SCN HG type 1.2.5.7 were detected (Table 2.1). The largest effect QTL was mapped to chromosome 19 (linkage group, LG, L, designated QTL-19) with a LOD score = 8.84, Its additive effect, the value of the effect of the presence of the resistance allele, was -6.17 and explained 22.2% of total phenotypic variation (PVE). The second major QTL, mapped to chromosome 13 (LG F, designated QTL-13), had an additive effect of -10.1254 and explained 8.23% of the total phenotypic variation (QTL-13). Basic chromosomal linkage maps were created and a genome-wide scan showing significant LOD was visualized (Figures A1 and A2 respectively). genome-wide LOD profiles of SCN resistance were visualized with a Manhattan plot (Figure 2.2). The Manhattan plot illustrates the distribution of LOD scores across 20

soybean chromosomes highlighting candidate QTL regions (M. Li. et al 2024).

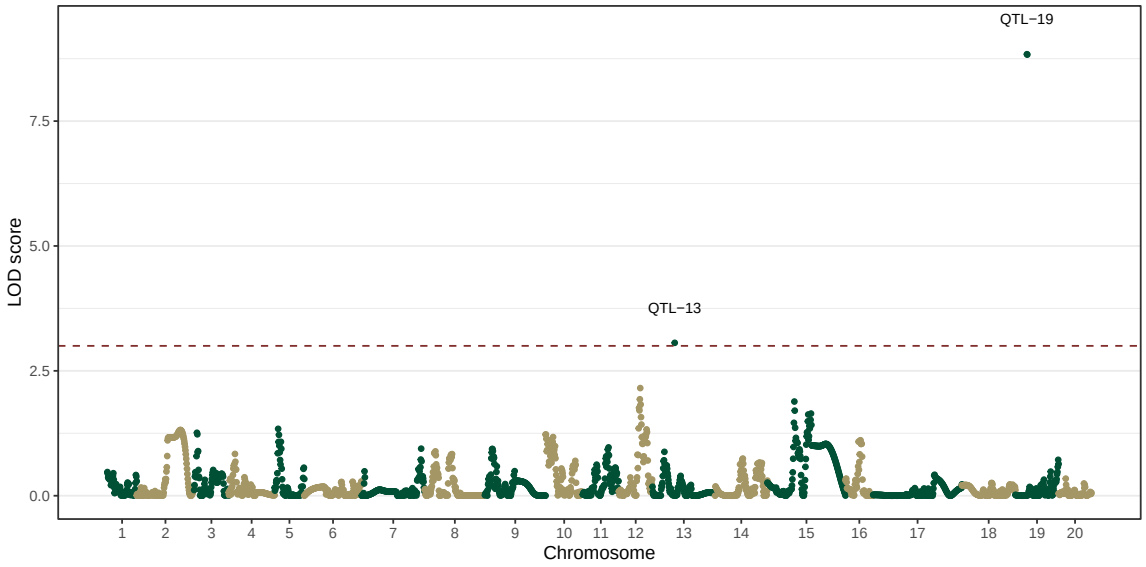

Figure 2.2: Manhattan plot illustrating quantitative trait loci (QTL) associated with SCN resistance. The x-axis represents the 20 chromosomes of the soybean genome arranged by cumulative position; the y-axis represents the logarithm of odds (LOD) score. The red dashed line denoted the primary significance threshold (LOD = 3.0). Specifically identified loci, QTL-13 and QTL-19 are highlighted to indicate regions of significant genomic association with SCN resistance.

Table 2.1: LOD scores, additive effects, and percentage of total variation explained for significant SNP markers singly or interactively affecting FI values.

Locus	Left Marker	Right Marker	LOD	PVE (%)	Additive Effect
QTL-13	Gm27373181-GA	Gm27302662-CT	3.06	8.23	−6.17
QTL-19	Gm48378286-AG	Gm48433644-AG	8.84	22.20	−10.13

Both QTLs also interacted epistatically with other regions of the genome. QTL-13 was found to interact with a SNP locus on chromosome 11 (designated Epi-11), and QTL-19 with a SNP locus on chromosome13 (Epi-13). In addition, the QTL-19 and QTL-13 combination also exhibited a three-way interaction with a SNP locus on chromosome 2 (Epi-2) (Table 2.2). To show these two interactions graphically, the SNP nucleotide bases

were plotted in Excel based on the SAS analysis; slope between the lines indicates epistatic interaction (Figure A3).

Table 2.2: Epistatic interactions between QTL associated with SCN resistance.

Interacting QTL	Epistatic Locus	Epistatic Marker	LOD	F-value	Probability
QTL-19	Epi-13	Gm32875289-CA	3.12	11.90	0.0008
QTL-13	Epi-11	Gm11615530-TC	3.93	15.81	0.0001
QTL-19 × QTL-13	Epi-02	Gm14508130-CT	3.47	14.54	0.0002

Results of permutation testing confirmed the presence of QTL-19, with an LOD of 8.83 and was calculated to explain 18.999% of phenotypic variation. A second peak was identified at QTL-13 with LOD= 3.06, representing 6.341% of phenotypic variation. However, the second peak did not reach the 5% genome-wide significance level established by the permutation test and is therefore reported as a suggestive locus (Table A3). Over 3000 markers were distributed across the 20 chromosomes of the soy genome. The average genetic distance between markers was 0.52 cM, with a range from 0.40 to 89.8 cM Though there was some clustering of markers, the distribution provided sufficient coverage of the entire soybean genome (Table A4).

To further characterize the phenotypic effects of the identified quantitative trait loci, FI values were examined across genotype classes at the peak markers within each QTL interval. Significant differences in FI distributions were detected among genotype classes at both the right and left markers for QTL-19 and QTL-13 (Kruskal-Wallis, $p < 0.001$), as summarized in Table A5.

At QTL-19, RILs carrying the GG allele exhibited substantially lower FI values than those carrying the AA allele (Dunn's with Benjamini-Hochberg correction: $p < 0.001$ for both right and left markers); heterozygous lines displayed intermediate responses. Differences between heterozygous and homozygous genotypes were not significant, potentially indicating an additive pattern in which the resistance allele was associated with reduced

SCN reproduction. QTL-13 exhibited a similar effect. At marker 13Gm27373181-AG, AA genotypes had significantly higher FI values than both AG and GG genotypes ($p < 0.05$ and $p < 0.001$, respectively). Marker 13Gm27302662-CT displayed significantly higher FI for the TT genotype than either CC or CT ($p < 0.001$ and $p < 0.05$, respectively); however CT and CC genotypes did not differ significantly from one another. The strongest statistical signal was found in the right markers, displayed in Figure 2.3; left markers are displayed in Figure A4. In both QTL regions, FI distributions showed substantial overlap among genotype classes.

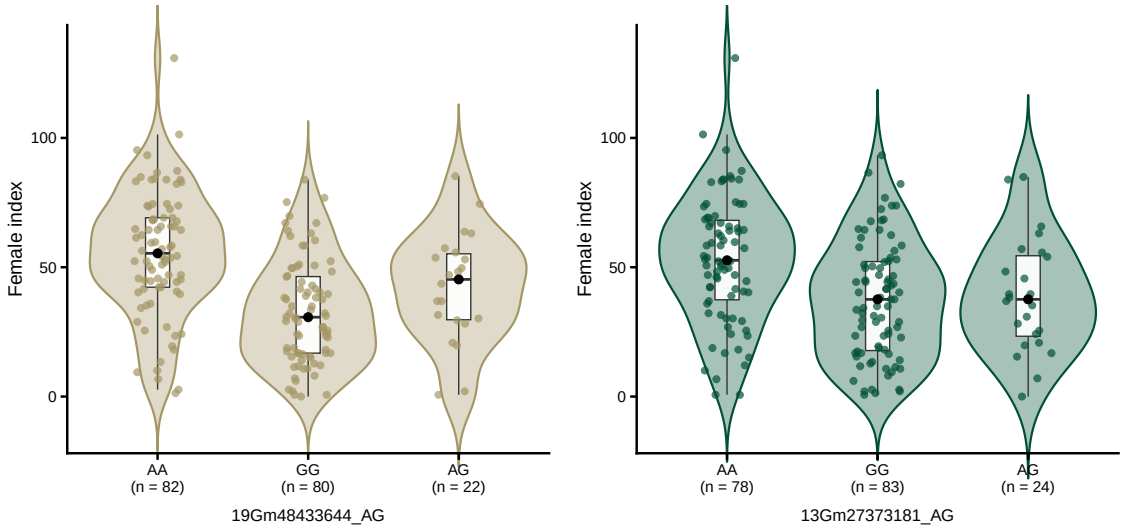

Figure 2.3: Violin plots illustrating the distribution of female index (FI) values among recombinant inbred lines (RIL) grouped by genotype at the peak right markers for QTL-19 (left; 19Gm48433644-AG) and QTL-13 (right; 13Gm27373181-AG). Violin plots show the distribution of FI values for each genotype class with overlaid box plots indicating the median and interquartile range. Individual points represent FI values for individual RIL lines of the mapping population, and sample sizes for each genotype class are indicated on the x-axis. Lower FI values correspond to reduced SCN reproduction and increased resistance. Differences among genotype classes were evaluated using Kruskal-Wallis tests followed by Dunn's pairwise comparisons with Benjamini-Hochberg correction for multiple testing.

To evaluate the combined effects of QTL-19 and QTL-13, the RIL mapping lines were grouped according to the total number of resistance alleles present across both loci, where the G allele at each right marker was associated with reduced SCN reproduction,

and was therefore considered the resistance allele. As visualized in Figure 2.4, female index differed significantly among the allele-stacked groups (Kruskal–Wallis $\chi^2 = 50.52$, $p < 0.001$). Post-hoc comparisons indicated that lines carrying 3 or 4 resistance alleles exhibited significantly lower FI values than lines carrying 0 or 1 allele. Linear regression analysis revealed a significant negative relationship between FI and the number of resistance alleles ($p < 0.001$, $R = 0.247$; Figure A5); each additional resistance allele reduced FI by approximately 8.9. Consistent with this pattern, both Spearman correlation ($\rho = 0.50$, $p < 0.001$) and the Jonckheere-Terpstra trend test ($p < 0.001$) supported a significant ordered decrease in nematode reproduction as resistance alleles accumulated across loci (Table A6).

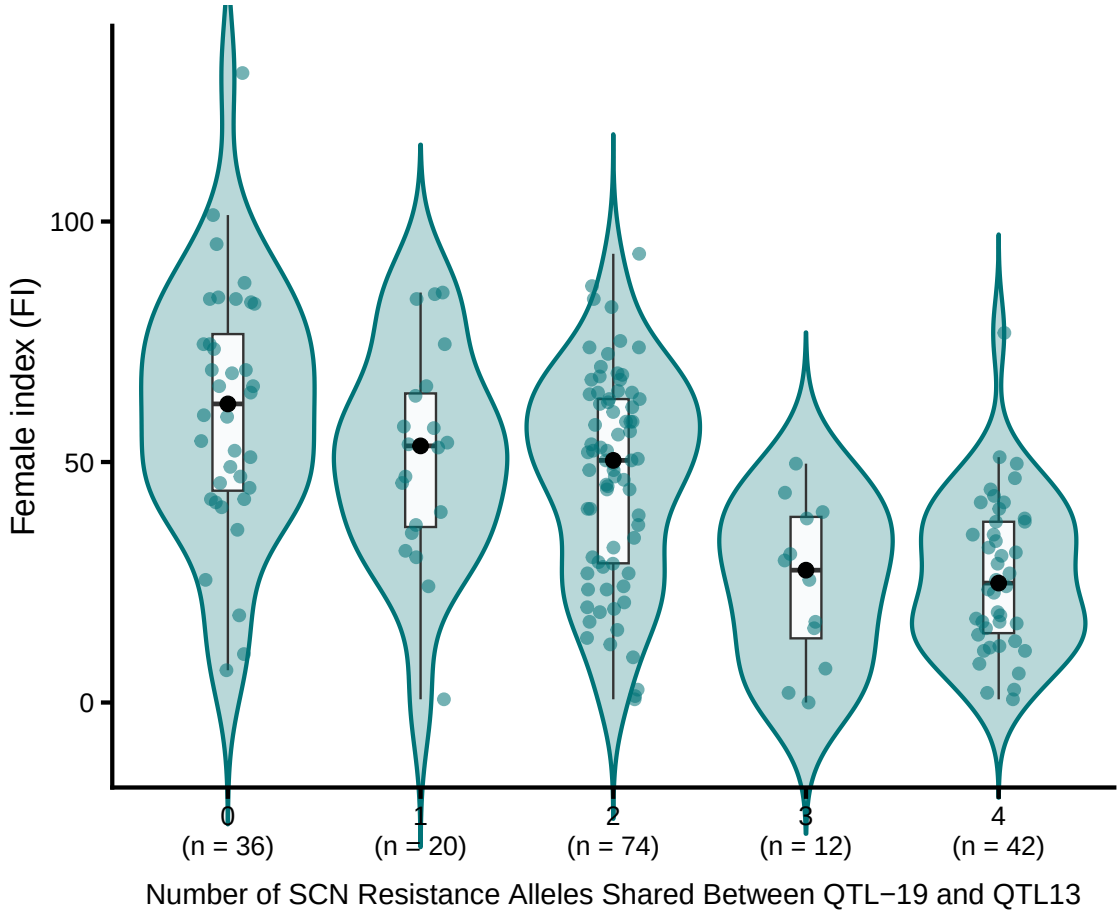

Figure 2.4: Allele stacking effect of QTL-19 and QTL13 on soybean cyst nematode reproduction. Female index (FI) of the recombinant inbred line (RIL) mapping populations grouped by the total number of resistance alleles present across QTL-19 and QTL-13. The G allele at each peak marker was associated with reduced SCN reproduction and was therefore considered the resistance allele. Groups represent the cumulative number of resistance alleles across both loci (0-4). Violin plots illustrate the distribution of FI values within each group, with overlaid boxplots indicating the interquartile range and the median. Points represent individual recombinant inbred lines. FI differed significantly among the allele stacking groups (Kruskal-Wallis $p < 0.001$); FI decreased progressively as resistance alleles accumulated, consistent with additive effects of QTL-19 and QTL-13 on SCN resistance.

Candidate Genes From Detected QTL

A total of 138 candidate genes were identified within the major QTL regions as well as those containing epistatic interactions (Table A7). Based on soybase.org Williams 82 Assembly version 6, (glyma.Wm82.gnm6), 36 candidate genes were located within the major QTL region on chromosome 19 (QTL-19). Epistatically interacting with this QTL,

a single nucleotide polymorphism (SNP) was identified on chromosome 13, noted as Epi-13. The second major QTL, on chromosome 13, (denoted QTL-13) was identified. A SNP on chromosome 11 (denoted Epi-11) was found to epistatically interact with QTL-13. An interaction was also found between QTL-19, QTL-13, and a marker region on chromosome 2, denoted Epi-02. Candidate genes were distributed across these QTL and epistatic regions. The functional annotations of all 138 candidate genes were obtained from Soybase (https://www.soybase.org, Brown et al., 2021). Within all of these genomic regions, 16 genes were labeled as uncharacterized, hypothetical, unnamed, or unknown proteins in soybean. These genes are listed in full in Table A7.

2.4 Discussion

Novel QTLs identified in wild soybean Two major QTLs were identified in the experimental population produced by crossing the wild soybean parent with SCN-resistance, 'S54', and the SCN-susceptible Glycine max parent, 'NC-Raleigh'. Loci associated with SCN resistance was identified on chromosomes 19 and 13 (QTL-19 and QTL-13 respectively). While defense genes were previously noted in these regions, our study identifies novel markers associated with SCN defenses in *Glycine soja* when challenged with HG 1.2.5.7. Of the 138 candidate genes identified in this study, 26 show promise for resistance to SCN due to their utilization in plant stress responses. The summaries of the annotated candidate genes with potential applications in resistance to SCN are found in Table 2.3.

Table 2.3: Candidate genes identified within the QTL-19 and QTL-13 intervals and their interacting epistatic regions (Epi-13, Epi-11, and Epi-02), including gene identifiers for candidate genes with potential for SCN resistance.

Locus	Chromosome	No. of Genes	Notable Candidate Genes
QTL-19	Chr19	36	F-box proteins; NAC domain TF; Rho GTPase activating protein
QTL-13	Chr13	25	Glutathione S-transferase; lipid-transfer protein; F-box proteins
Epi-13	Chr13	29	F-box/LRR proteins; protein kinase; methionine sulfoxide reductase
Epi-11	Chr11	21	RING/U-box zinc finger protein; auxin response factor
Epi-02	Chr02	11	Carboxylesterases; calcium/calmodulin kinase

QTL-19: Promising SCN Resistance

QTL-19 (LOD = 8.84) in wild soybean was associated with the 48,378,286 - 48,433,644 bp region of *Glycine soja*. This score exceeds the genome-wide significance threshold determined by permutation testing. QTL-19 could represent a major new source of resistance to SCN in wild soybeans, an important discovery in soybean breeding. This study identified a total of 36 candidate genes within the QTL-19 region. Many of these genes fall into functional categories commonly associated with plant defense responses, including transcriptional regulation, protein turnover, and cellular signaling.

Transcription factors involved in plant immunity represent one important category of genes within this region. A NAC transcription factor was identified within QTL-19 and has previously been reported to be upregulated in wild soybean during defense responses

to SCN HG type 2.5.7 (Dong et al., 2024; H. Zhang et al., 2017-a). A basic leucine zipper (bZIP) gene (Glyma.19G194500) was also found; theser may contribute to stress response signaling (Collin et al., 2021).

A second functional group includes ubiquitin-mediated protein degradation and regulatory genes of the immune response. Several F-box and F-box/LRR (Leucine rich repeats) proteins were identified within QTL-19 and the associated epistatic regions (Glyma.19G194600, Glyma.19G194964, and Glyma.19G196400). These proteins target specific proteins for degradation; these influence plant immunity and the programmed cell death response during pathogen infection, including during pathogenic nematode infection (Sá et al., 2012; C. Zhang et al., 2018).

Genes associated with cellular signaling and stress response pathways were also present in this region. a Rho GTPase-activating protein gene (Glyma.19G194992) was identified; these have been found to regulate molecular switches that control downstream defense signaling cascades (Feiguelman et al., 2017). Glyma.19G196000 is another signaling gene in the QTL-19 region; it encodes a tetratricopeptide repeat domain protein. These proteins function in plant hormone signaling pathways and in protein-protein interactions; interestingly, they were previously found in common bean (*Phaseolus vulgaris* L.) to be associated with SCN resistance (Jain et al., 2019; Schapire et al., 2006). Previous work has also reported defense related genes on chromosome 19 of wild soybean. In a genome-wide association study (GWAS), where *G. soja* was challenged with HG type 2.5.7, SNPs associated with genes encoding a multidrug and toxic compound extrusion (MATE) transporter and an MYB transcription factor. MATE transporters have been implicated in abscisic acid transport and secondary metabolite movement during stress responses (Mathew et al., 2024; H. Zhang et al. 2017-a). MYB TFs are widely known regulators of plant response to biotic stress; they have been specifically associated with disruption of nematode induced syncytia and activation of SCN resistance pathways (Biswas et al., 2023; Qu et al., 2025; Wiśniewska et al., 2021). Similarly, Vuong et al (2015) have identified multiple LRR pro-

teins, F-box proteins, and serine-threonine protein kinases associated with SCN resistance responses. The presence of these gene families across different studies suggests that wild soybean may harness the power of diverse signaling and regulatory pathways to contribute to SCN resistance.

QTL-13: Important Minor Effects

The second QTL identified in this study, QTL-13, contained twenty-five candidate genes. Similarly to QTL-19, many of these fall into functional groups associated with plant defenses and stress responses.

One major category of these include detoxification and oxidative stress response enzymes. Glyma.13G154000 encodes a glutathione S-transferase (GST); this enzyme may protect cells from cellular damage during stress conditions, including nematode infection and abiotic stress in *G. soja* (Gullner et al., 2018; Ji et al., 2010; Sá et al., 2012).

A second category of defense in the QTL-13 region includes defense related proteins involved in systemic acquired resistance and cell wall defense maintenance. A candidate for lipid transfer (Glyma.13G154100) can contribute to acquired systemic resistance (Li et al., 2022; Niraula et al., 2020). Another gene in this region, Glyma.13G155800, encodes a glycosyl hydrolase family protein that contains a chitinase insertion domain and may participate in jasmonic acid-mediated defense responses. These may enhance other plant defense pathways following pathogen attack (Nissan et al., 2023; Vaghela et al., 2022).

As in QTL-19, the QTL-13 region also contains genes associated with protein turnover and signaling regulation. These include an F-box protein (Glyma.13G154400). These play an important role in the regulation of immune responses through selective post-translational modification of proteins by the ubiquitination of regulatory proteins.

Previous work has also reported minor-effect resistance loci on chromosome 13. In 2023, Jiang et al. identified an increased expression of resistance genes in cultivated soybeans; these include serine-threonine protein kinases and acyl-activating enzymes. Similarly, Glyma.13G13173300, an O-methyltransferase gene involved in the methylation of

secondary metabolites associated with plant defense, has been shown to increase expression during SCN infection (Mittal, 2021). Previously, SCN resistance genes induced by SCN HG type 2.5.7 infection have been identified near QTL-13 in a different accession of wild soybean, NRS100, though not within the same genomic region. These genes, Glyma.13G109800 and Glyma.13G370100 were found at 22,363,971-22, 366,280 and 45,564,565-45,566732, respectively, by Kofsky et al (2021). Of these, the first is a gene in the jasmonic acid biosynthesis pathway, oxophytodienoate reductase 3 (DDE1/OPR3), while the second is a gene in the WRKY transcription factor family that Kofsky et al. 2021 noted was highly induced in both S54 and NRS100 during SCN infection. Both genes act in defense signaling, although the genes did not overlap with the genomic region in our recent findings using donor parent S54 (Kerschbaumer et al., 2024; Yang et al., 2017). Together, these findings suggest that QTL-13 may represent a quantitative modification locus that contributes to resistance to SCN in combination with other genetic regions.

QTL-13, found in this study at the interval 27,373,181 -27,302,662 bp, had an slightly exceeded the LOD threshold of 3 (LOD = 3.06). This QTL may represent a quantitative modifier to SCN resistance. With a PVE of more than 18%, its effect may be minor, but vital for the response of wild soybeans to the pathogenic nematode, especially in the context of its epistatic interactions.

Candidate Genes In Epistatic Regions Understanding the epistatic influence of genes is an important component of the genetic architecture of traits such as resistance to disease. These molecular level gene interactions are important factors that should be considered when attempting to adopt new traits for crop improvement (Holland, 2010). Several candidate genes located within epistatic regions (Epi-11, Epi-13, and Epi-02) also belong to functional categories commonly associated with plant defense signaling. Both QTL were found to interact epistatically with separate regions of the wild soybean genome, as well as interacting together with a third region. These interactions were illustrated in Figure 2.5 (Gu, 2014).

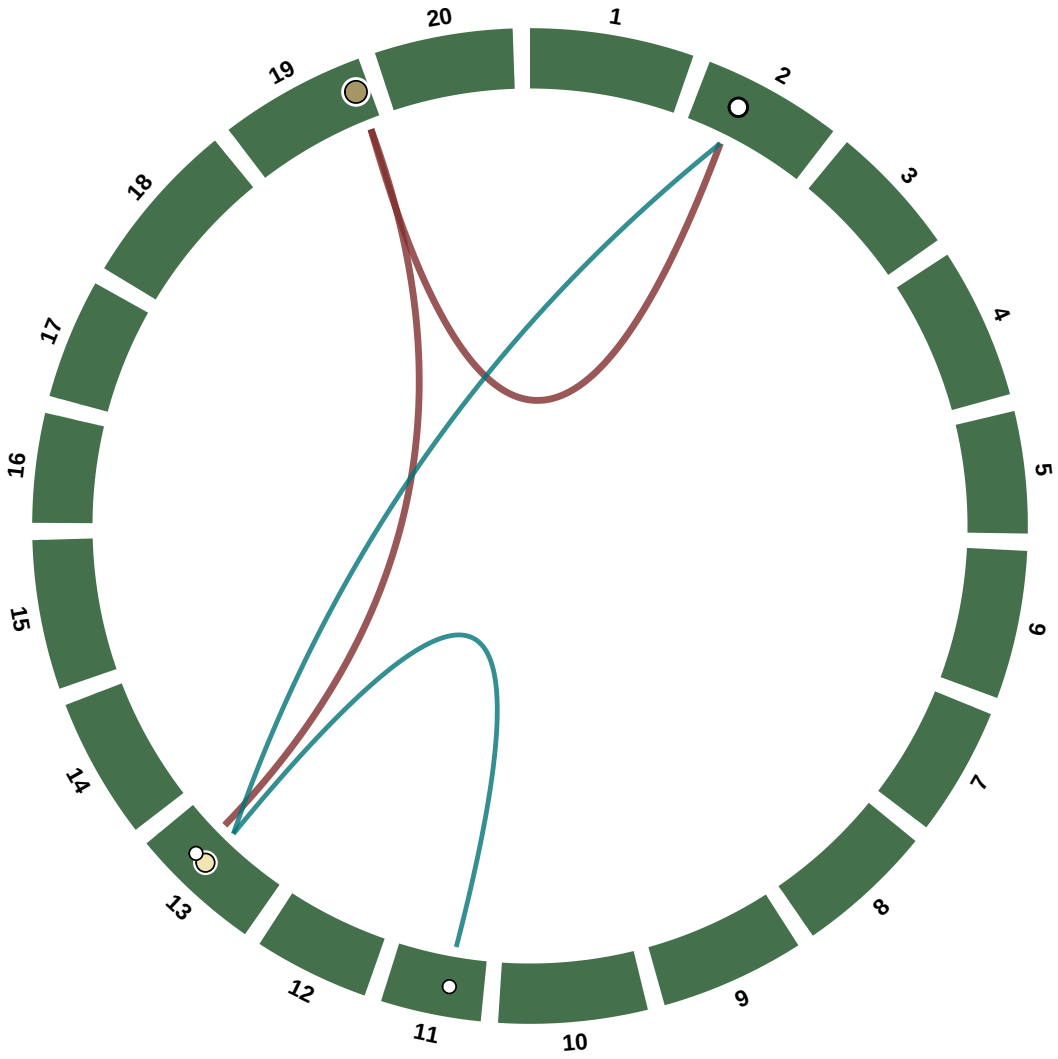

Figure 2.5: Circos genomic visualization illustrating the genetic architecture of SCN resistance in *Glycine soja*. Primary QTL (QTL-19 and QTL-13) are shown as highlighted markers, whereas epistatic loci are depicted with white circles. QTL-19 (LOD= 8.84) forms strong interactions with loci on chromosomes 13 and 2 (red lines). QTL-13 (blue lines) interacts with loci on chromosomes 11 and 2. Epistatic loci Epi-02 may act as a shared downstream interaction hub. Chromosome segments are scaled to physical length based on the W82.a2.v1 reference G. max genome. The network architecture suggests partial convergence of independent major and minor QTL (QTL-19 and QTL-13, respectively) onto a common epistatic node, consistent with a coordinated genetic mechanism underlying SCN resistance.

QTL-19 was found to interact epistatically with a SNP on chromosome 13 (Epi-13). Within the Epi-13 region, genes involved in protein turnover and signaling regulation were

again identified, including two F-box or F-box/LRR protein genes (Glyma.13G211000 and Glyma.13G11600. These are involved in ubiquitination pathways and have been associated with responses to abiotic and biotic stress, including SCN infection (C. Zhang et al., 2018; X. Zhang et al., 2019.

Genes associated with polyamine biosynthesis and protection against oxidative stress were present in the Epi-13 region. Glyma.13G211700 encodes an adenosylmethionine decarboxylase involved in the biosynthesis of spermidine and spermine. Polyamines are known regulators of plant stress responses, and have been reported to be upregulated in SCN-resistant *G. soja* accessions (Kofsky et al., 2021). Other genes in this region are associated with repairing oxidative damage during stress responses (Bent, 2022; Medina et al., 2018; Rathinam et al., 2025).

The Epi-13 region contains additional genes involved in the production of secondary metabolites and transcriptional regulation, including Glyma.13G213500, which participates in terpenoid biosynthesis. Terpenoids are widely distributed plant secondary metabolites that contribute to pathogen defense responses across many plant species and pathogen types (C. Li et al., 2023; Wittsock and Gershenzon, 2002). A RING?FYVEPHD zinc finger protein gene (Glyma.1313600 was found in this epistatic region; these have been reported to function as regulators of downstream transcriptional responses during the resistance response of soybean cyst nematode (W. Song et al., 2019).

QTL-13 interacted epistatically with an SNP on chromosome 11 (Epi-11); candidate genes in this region included additional defense signaling and hormone response protein genes. In this study genes similar to those identified in GWAS studies of SCN resistance were found. Interestingly, these GWAS investigations utilized HG types 0 and 2.5.7 studies. Their utility across a spectrum of SCN virulence types may indicate a broad-spectrum approach to SCN resistance for these genes, rather than a population specific defense response (Tran et al., 2019). Other plant proctective genes found in this region includde genes involved in salicyclic acid signaling, previously shown to successfully reduce SCN

paraistism (J. Lin et al., 2024; Mindrebo et al., 2016).

QTL-19 and QTL-13 were both found to interact with a single epistatic region, Epi-02, on chromosome 2. Several genes associated with plant immunity signaling were found in this region. Among these were multiple carboxylesterase genes (Glyma.02G133800, Glyma.02G133900, Glyma.02G13400, Glyma.02G134100, and Glyma.02G134200). These participate in hypersensitive response signaling and defense cascades triggered by pathogen infection (Lee et al., 2024; Melillo et al., 1989). Carboxylesterases have been found to accumulate in multiple host species during pathogen infection; they can contribute to lignification and incompatible defense responses during soybean cyst nematode infection (Andres et al., 2001; Huang et al., 2022).

Additional signaling proteins were identified in this region. Proteins containing nucleotide-binding and leucine rich repeat domains (NBS-LRRs) act as classical resistance (R) genes across many plant species. They detect pathogen effector proteins and activate immune responses (Arya & Acharya, 2017). Similar proteins have been identified in common beans when infected with SCN HG type 2.5.7, and these genes are widely distributed throughout the soybean genome (Kang et al., 2012; Shi et al., 2025). Another signaling gene, Glyma.02134600, encodes calcium/calmodulin-dependent protein kinases (CDPK). These function as key components of signal integration during stress responses. They sense calcium influx triggered by cell damage and activate downstream defense pathways, including salicylic acid-mediated systemic acquired resistance (Kang et al., 2012; Torabi et al., 2023).

Epistasis occurs when the effect of one locus depends on the presence of a specific set of alleles or another locus. In this case, the major locus, QTL-19 may be modulated by the other identified loci. QTL-13 may function as part of a coordinated defense pathway with QTL-19 and the epistatic regions. In particular, the interaction of QTL-19 and QTL-13 with Epi-02 suggests that the region may function as a downstream signaling hub; therefore, resistance may depend not only on additive effects, but also on coordinated

epistatic interactions between large and minor-effect loci.

Candidate genes located near these QTL and epistatic regions were identified to better understand the potential molecular interactions underlying SCN resistance in the S54 accession. Several defense related genes identified within the Epi-02 region further support the potential importance of this locus in resistance mechanisms. Interestingly, transcripts for chitin receptor kinase molecules, jasmonic acid methyltransferases, and the salicylic acid signaling enzyme GmSAMT1 were previously shown to be upregulated in S54 when challenged with HG 2.5.7. These genes are associated with pathogen defense signaling pathways; overexpression of GmSAMT1 in transgenic soybean has demonstrated potential for broad-spectrum resistance to SCN (J. Lin et al., 2016; H. Zhang et al., 2017-a). Together, these observations suggest that the Epi-02 region may contribute to downstream defense signaling pathways associated with the broad-spectrum resistance observed in S54.

Allele Effects at Peak Markers

QTL-19 showed a clear additive relationship between genotype and nematode reproduction: lines carrying the GG allele exhibited substantially lower female index values than those carrying the AA allele, while the heterozygous allele (AG) displayed intermediate SCN reproduction. This pattern suggests that resistance at this locus acts in a largely additive fashion, with each copy of the resistance allele contributing to reduced SCN reproduction. Additive effects for SCN resistance have been previously reported for several SCN loci, including the widely prevalent *Rhg1* locus. The additive nature of QTL-19 suggests that the locus may contribute incrementally to resistance when combined with other resistance loci; this has been successfully demonstrated using wild soybean resistance loci and presents a source of resistance variation needed to enhance the durability of SCN resistance (Cook et al., 2012; Meinhardt et al., 2021).

A similar, if weaker, trend was observed for QTL-13, consistent with the smaller phenotypic variance (PVE) explained by this locus. At this marker, heterozygous genotypes were not significantly different from one of the homozygous classes, suggesting the

possibility of a partial dominance effect or a reduced additive contribution to SCN resistance. Overlap of the distribution of FI is expected for quantitative resistance traits, where phenotypic variation reflects the combined influence of multiple loci and environmental factors.

When the effects of both loci were evaluated together through allele stacking analysis, FI declined progressively as the number of resistance alleles increased. This pattern indicates that QTL-19 and QTL-13 resistance is additive, supporting a polygenic architecture in which multiple loci collectively influence resistance to soybean cyst nematode. Such additive resistance is particularly valuable for breeding because the accumulation of moderate effect loci can enhance the durability of resistance and reduce the likelihood that SCN populations will overcome a single resistance source.

Wild Soybean S54 Potential for Soybean Breeders

Resistance to soybean cyst nematode can fluctuate in response to various environmental factors, making important resistance genes difficult to pinpoint. With the overuse of some cultivars for SCN resistance, efforts to discover new SCN resistance genes are crucial (Bradley et al., 2021; Mitchum, 2016). In this investigation, wild soybean (*Glycine soja*) was utilized to find novel genes for SCN-resistance. The wild soybean utilized in this study ('S54') demonstrated full resistance (FI < 10) to multiple SCN types, including HG 1.2.5.7, HG 0, and HG 2.5.7 (formerly Races 2, 3, and 5, respectively; unpublished data). Its high resistance to some of the most common types of SCN make it a promising contender in the development of soybean cultivars with broad-spectrum SCN-resistance.

The wild relatives of crops have long shown promise for crop improvement and have already proven their utility in a variety of important crops and differing traits, including resistance to disease (Rajpal et al., 2023; Zhang et al., 2017-b). The stacking of soybean cyst nematode resistance genes from wild and domestic sources has conferred resistance to multiple types of SCN (Brzostowski & Diers, 2017; Meinhardt et al., 2021), providing more durable resistance, an especially important factor with fields infected by diverse SCN

populations (Howland et al., 2018; You et al., 2024).

Methodological Considerations in QTL Detection

In this study, quantitative trait mapping was used to determine loci associated with resistance to SCN population HG 1.2.5.7. The program QTL IciMapping was used for this due to its ability to build high density linkage maps and utilize inclusive composite interval (CI) mapping to identify important loci. In this way, we were able to find two significant QTL associated with SCN resistance with a F4 recombinant inbred line RIL mapping population. QTL detection can be more precise when analyzing a larger population, as well as when using an F5 or later generation, since this is when lines begin to stabilize. However, the use of an RIL increases the number of recombination events, providing finer mapping of QTLs than for other population types, which may require larger population sizes (Jeon et al., 2023; X. Li et al., 2006; Takuno et al., 2012). CI mapping is one of the most commonly used statistical methods, but does not always control for background noise; inclusive composite interval mapping imrpoves upon this (Akond et al., 2019; Meng et al., 2015).

The Logarithm of Odds (LOD) score is a statistical measure of evidence for linkage between markers and traits of interest (Akond et al., 2019). Higher LOD scores represent a higher probability of association with a trait of interest. Thus, the observed marker-trait association has a higher likelihood of being due to genetic linkage rather than stochastic variation (random chance).

Lander and Bostein and others argued that an LOD threshold of 2.4 to 3.0 is necessary to maintain a genome-wide significance level of () of 0.05 (Lander and Bostein, 1989; Zou & Zeng, 2008), making QTL-19's LOD of 8.84 a strong case for its strong association with SCN resistance. Similarly, QTL-13's LOD of 3.06 may indicate a genomic region containing important minor effects genes. Although QTL-13's LOD exceeded the accepted threshold of 3.0 for significance, it was not supported by permutation testing and is still low compared to that of QTL-19. However, its association with Epi-11 and Epi-02 indicates

that the association with SCN resistance was not created by chance and provided minor effects, rather than the larger resistance effect of QTL-19.

Lander and Kruglyak (1995) proposed the term "suggestive linkage" to allow for the publication of results that are not significant but point to some level of association between markers and traits. In 1999, van Ooijen proposed that suggestive linkage should be applied to RIL-derived loci when LOD = 2.1. In this case, QTL-13 meets the significance threshold. Since QTL-13 was not confirmed by permutation analysis but was associated with epistatic interactions, suggestive linkage may be appropriate in this case. Further analysis via fine mapping may better reveal loci associated with SCN resistance.

For the most accurate analysis, over 3000 quality markers for QTL identification (Song et al 2020) were used. Reversed marker orders were observed in some regions, including in some regions of chromosomes 13 and 19. This type of deviation has been noted in previous studies (Guo-a et al., 2005; Wu et al., 2009). This could be due to population size and type and mapping methods (Concibido et al., 2004). QTL detection and the estimation of their positions also depends on how many molecular markers are utilized and their distribution across the genome. While some gaps were observed, most molecular markers were successfully mapped on the 20 chromosomes of the soybean genome (Table A4).

Many QTL studies of SCN resistance ignore epistasis. This is due to the type of mapping populations used, or the inability of the software utilized to detect epistasis. However, modification of gene expression by the interactions of multiple genes plays a central role in the development of complex traits such as resistance to disease. Epistatic effects help to explain genetic effects, and thus are able to identify traits that are not immediately detected by QTL analysis alone. Lack of epistatic analysis may also lead to an overestimation of the effects of individual QTLs, and an underestimation of genetic variance, which is an important aspect of a trait's phenotype. Including epistatic analysis provides potential for increase in genetic response to marker assisted selection (P Liu et

al., 2004; Wu et al., 2009). It is important to note that the more loci that are involved with an interaction, the more challenging it is to detect epistatic effects; they require robust phenotypic data and large mapping populations (Dwivedi et al., 2024). With 185 progeny, our mapping population was able to detect 3 significant interactions between the detected QTL and other loci, including a three-way interaction between QTL-19, QTL-13, and the epistatic loci Epi-02. Although the effect of the main QTL plays an important role in the resistance of S54-type to SCN, epistatic interactions may amplify the resistant reaction (Dwivedi et al., 2024), making elucidating these interactions an important step to provide robust and diversified forms of resistance to pathogens.

Variation in cyst counts was observed between replicates within the mapping population. Variation is expected in quantitative trait analysis by its very nature. The segregation of multiple resistance loci which may provide incomplete resistance occurs across the mapping population; this becoming more fixed generation by generation. An F4 generation of a recombinant inbred line is still useful for mapping, and reduces resources required to produce later generation populations, variance may still occur at the early F4 stage, as each line can be described as a mosaic of homozygous segments from either parent.(Kearsey Farquhar, 1998; Takuno et al., 2012; Young, 1996).

Variance may also be influenced by biological stochasticity produced by egg inoculation and the use of sand as growth media. Egg inoculation is common in nematology and QTL studies of resistance to *H. glycines*. It mimics the natural hatching process, wherein eggs may hatch over the course of days, rather than the immediate penetration of stage 2 juveniles . Environmental variance, including the use of sand as growth media, can increase SCN reproduction. Even in controlled conditions such as greenhouse assays, high environmental sensitivity can influence plant growth and pathogen success so that higher variance is observed. This variance does not bias QTL location, but can reduce statistical power (Wang Zu, 2019).

Soybean provides a classic model for the complex genetic architecture of quantitative

resistance. The two most important and widely utilized sources of SCN resistance, *Rhg1* and *Rhg4* work in concert to provide protection against *H. glycines*. In many resistant varieties like Peking, the interaction of *Rhg1* and *Rhg4* is necessary for SCN resistance (Concibido et al., 2004; S. Liu et al., 2012; Patil et al 2019). Minor QTLs have been found in many varieties of soybean, and have an especially important role in the development of cultivars used for broad-spectrum SCN resistance. (Guo-b et al., 2006; Jiang et al 2023).

Impacts and Future Research

This study illustrates the value of crop wild relatives in the discovery of novel genetic loci for pathogen resistance. Using the*G. soja* accession S54, we were able to map QTL associated with SCN resistance and determine that these loci interacted with other loci in the *G. soja* genome. With higher genetic diversity, crop wild relatives have demonstrated their potential for crop improvement across the spectrum of major crops, including soybean, maize, and rice. Traits for improvement include both biotic and abiotic stress resistance, as well as other crop improvement traits. Wild soybean genes, in combination with rhg1-a/Rhg4 and rhg1-b alleles, along with rotation of resistance sources have demonstrated effectiveness not only in reducing SCN population density, but also in minimizing SCN adaptation to their host (Song 2017-b; Meinhardt et al., 2021).

The *Rhg1* locus on chromosome 18 has been found to confer the strongest form of *G. max*-derived SCN resistance. Obtained from domesticated cultivars developed from PI 88788, the rhg1-b haplotype provides the most common form of SCN resistance in soybean. This form of resistance relies on a defective α-SNAP (soluble N-diethylmaleimide-sensitive factor attachment protein) protein to protect the host from SCN, with stronger resistance associated with higher copy number variation (Lee et al., 2015). Peking-type resistance occurs through the epistatic interaction of *Rhg1*, utilizing an rhg1-a haplotype and the *Rhg4* locus found on chromosome 8 to encode GmSHMT. This serine hydroxymethyltransferase gene family restricts syncytium development, halting SCN development (Bent, 2022; Patil et al., 2019).

This study provides another source of SCN resistance distinct from those already in use. SCN populations are increasingly adapting to the main sources of host resistance, PI 88788 and Peking-type resistance (Bent, 2022). Phylogenetic analysis of whole-genome SNP signatures of *G. soja* accessions with SCN resistance show S54/PI 424093 is distinct from *Rhg1*-type resistance. A small number of *G. soja* accessions contain multiple copies of the rhg1 allele, sharing structural similarities with *G. max* haplotypes. However, S54-type resistance has been demonstrated to be distinct from this sort of SCN resistance, highlighting probable mechanistic differences in providing SCN protection ((**?**)). Fine-mapping of both QTL and epistatic regions identified in this study could further refine regions associated with resistance to SCN to pinpoint defense-related genes. Functional validation of these genes will elucidate the mechanisms of this resistance, providing further insight into this novel form of SCN defense. By providing a potential source for novel resistance mechanisms, both traditional plant breeding and modern biotechnologies such as CRISPR may be utilized to develop SCN resistance cultivars of soybean.

To provide better resistance to SCN in commercially grown soybeans, plant breeders need new genetic resources for the introduction of existing cultivars and the development of completely new soybean lines. *Glycine soja*, the wild crop relative of soybeans, is a rich source of new genes for important crop traits for existing and emerging soybean stressors. In this study, we used a new source of soybean genetic diversity, the wild soybean denoted as 'S54', to discover exciting QTL associated with SCN resistance. To maximize our understanding of the genetic architecture of resistance to SCN in wild soybeans, we additionally performed an analysis of epistatic interactions between these QTL. These results suggest candidate genes within these loci, especially the novel QTL on chromosome 19, which will be useful genetic resources to improve future resistance to soybean cyst nematodes and improve soybean crop yields and quality.

References

Akinrinlola, R. J., Kelly, H. M., Sinclair, T. R., & Shekoofa, A. (2024). *Heterodera glycines* HG type 1.2.5.7 causes a decrease in soybean (*Glycine max* [L.] Merr.) nitrogen fixation and growth variables. *Journal of Crop Improvement*, 299–316.

Akond, Z., Alam, M. J., Hasan, M. N., Uddin, M. S., Alam, M., & Mollah, N. H. (2019). A comparison on some interval mapping approaches for QTL detection. *Bioinformation*, 15(2), 90–94. https://doi.org/10.6026/97320630015090

Anderson, E. J., Ali, M. L., Beavis, W. D., Chen, P., Clemente, T. E., Diers, B. W., Graef, G. L., Grassini, P., Hyten, D. L., McHale, L. K., Nelson, R. L., Parrott, W. A., Patil, G. B., Stupar, R. M., & Tilmon, K. J. (2019). Soybean [Glycine max (L.) Merr.] Breeding: History, Improvement, Production and Future Opportunities. *Advances in Plant Breeding Strategies: Legumes*, 431–516.

Andres, M. F., Melilo, M. T., Delibes, A., Romera, M. D., Bleve-Zacheo, T. (2001). Changes in wheat root enzymes correlated with resistance to cereal cyst nematodes. *New Phytologist*, 152(2), 343-354. https://doi.org/10.1111/j.0028-646X.2001.00258.x.

Arya, P., & Acharya, V. (2017). Plant STAND P-loop NTPases: a current perspective of genome distribution, evolution, and function. *Molecular Genetics and Genomics*, 293(1), 17–31.

Balestre, M., & De Souza, C. L. (2016). Bayesian reversible-jump for epistasis analysis in genomic studies. *BMC Genomics*, 17(1). https://doi.org/10.1186/s12864-016-3342-6

Bassetti, N., Caarls, L., Bukovinszkine'Kiss, G., El-Soda, M., Van Veen, J., Bouwmeester, K., Zwaan, B. J., Schranz, M. E., Bonnema, G., & Fatouros, N. E. (2022). Genetic analysis reveals three novel QTLs underpinning a butterfly egg-induced hypersensitive response-like cell death in *Brassica rapa*. *BMC Plant Biology*, 22(1), 140. https://doi.org/10.1186/s12870-022-03522-y

Benjamini, Y., & Hochberg, Y. (1995). Controlling the false discovery Rate: A practical

and powerful approach to multiple testing. *Journal of the Royal Statistical Society Series B (Statistical Methodology)*, 57(1), 289–300. https://doi.org/10.1111/j.2517-6161.1995.tb02031.x

Bent, A. F., (2022). Exploring Soybean Resistance to Soybean Cyst Nematode. *Annual Review of Phytopathology*, 60(1), 379-409.

Biswas, D., Gain, H., & Mandal, A. (2023). MYB transcription factor: A new weapon for biotic stress tolerance in plants. *Plant Stress*, 10, 100252.

https://doi.org/10.1016/j.stress.2023.100252

Blanca, M., Alarcón, R., Arnau, J., Bono, R., & Bendayan, R. (2017). Non-normal data: Is ANOVA still a valid option? *Psicothema*, 4(29), 552–557.

https://doi.org/10.7334/psicothema2016.383

Bradley, C. A., Allen, T. W., Sisson, A. J., Bergstrom, G. C., Bissonnette, K. M., Bond, J., Byamukama, E., Chilvers, M. I., Collins, A. A., Damicone, J. P., Dorrance, A. E., Dufault, N. S., Esker, P. D., Faske, T. R., Fiorellino, N. M., Giesler, L. J., Hartman, G. L., Hollier, C. A., Isakeit, T., . . . Wise, K. A. (2021). Soybean Yield Loss Estimates Due to Diseases in the United States and Ontario, Canada, from 2015 to 2019. *Plant Health Progress*. https://doi.org/10.1094/PHP-01-21-0013-RS

Broman, K. W. (2003). Mapping quantitative trait LOCI in the case of a spike in the phenotype distribution. *Genetics*, 163(3), 1169–1175. https://doi.org/10.1093/genetics/163.3.1169

Brown AV, Conners SI, Huang W, Wilkey AP, Grant D, Weeks NT, Cannon SB, Graham MA, Nelson RT. A new decade and new data at SoyBase, the USDA-ARS soybean genetics and genomics database. *Nucleic Acids Res*. 2021 Jan 8;49(D1):D1496-D1501. doi: 10.1093/nar/gkaa1107.

Brzostowski, L. F., & Diers, B. W. (2017). Pyramiding of Alleles from Multiple Sources Increases the Resistance of Soybean to Highly Virulent Soybean Cyst Nematode Isolates. *Crop Science*, 57(6), 2932–2941.

Burton, J. W., Carter, T. E., Fountain, M. O., & Bowman, D. T. (2006). Registration of "NC-Raleigh" Soybean. *Crop Science*, 46(6), 2710–2711.

Chang, W., Dong, L., Wang, Z., Hu, H., Han, Y., Teng, W., Zhang, H., Guo, M., & Li, W. (2011). QTL underlying resistance to two HG types of *Heterodera glycines* found in soybean cultivar "L-10." *BMC Genomics*, 12(1), 233. https://doi.org/10.1186/1471-2164-12-233

Collin, A., Daszkowska-Golec, A., & Szarejko, I. (2021). Updates on the Role of ABSCISIC ACID INSENSITIVE 5 (ABI5) and ABSCISIC ACID-RESPONSIVE ELEMENT BINDING FACTORs (ABFs) in ABA Signaling in Different Developmental Stages in Plants. *Cells*, 10(8), 1996.

Concibido, V. C., Diers, B. W., & Arelli, P. R. (2004). A Decade of QTL Mapping for Cyst Nematode Resistance in Soybean. *Crop Science*, 44(4), 1121–1131.

Cook, D. E., Lee, T. G., Guo, X., Melito, S., Wang, K., Bayless, A. M., Wang, J., Hughes, T. J., Willis, D. K., Clemente, T. E., Diers, B. W., Jiang, J., Hudson, M. E., & Bent, A. F. (2012). Copy number variation of multiple genes at *Rhg1* mediates nematode resistance in soybean. *Science*, 338(6111), 1206–1209. https://doi.org/10.1126/science.1228746

Critchfield, R., King, J., Bonkowski, J., Telenko, D., Creswell, T., & Zhang, L. (2023). Characterization of Virulence Phenotypes during 2020 in Indiana. *Journal of Nematology*, 55(1). https://sciendo.com/pdf/10.2478/jofnem-2023-0039

Dong, B., Liu, Y., Huang, G., Song, A., Chen, S., Jiang, J., Chen, F., & Fang, W. (2024). Plant NAC transcription factors in the battle against pathogens. *BMC Plant Biology*, 24(1), 1–13.

Dunn, O. J. (1964). Multiple comparisons using rank sums. *Technometrics*, 6(3), 241–252. https://doi.org/10.1080/00401706.1964.10490181

Dwivedi, S. L., Heslop-Harrison, P., Amas, J., Ortiz, R., Edwards, D. (2024). Epistasis and pleiotropy-induced variation for plant breeding. *Plant Biotechnology Journal*,

22(10), 2788-2807.

Faghihi, J., Donald, P. A., Noel, G., Welacky, T. W., & Ferris, V. R. (2018). Soybean Resistance to Field Populations of Heterodera glycines in Selected Geographic Areas. *Plant Health Progress*. https://doi.org/10.1094/PHP-2010-0426-01-RS

Feiguelman, G., Fu, Y., & Yalovsky, S. (2017). ROP GTPases Structure-Function and Signaling Pathways. *Plant Physiology*, 176(1), 57–79.

Grunwald, D. J., Zapotocny, R. W., Ozer, S., Diers, B. W., Bent, A. F. (2021). Detection of rare nematode resistance rhg1 haplotypes in *Glycine soja* and a novel rhg1 -SNAP. *The Plant Genome*, 15(1).

Gullner, G., Komives, T., Király, L., & Schröder, P. (2018). Glutathione S-Transferase Enzymes in Plant-Pathogen Interactions. *Frontiers in Plant Science*, 9, 427485.

Gu, Z. (2014) circlize implements and enhances circular visualization in R. *Bioinformatics*.

Guo-a, B., Sleper, D. A., Arelli, P. R., Shannon, J. G., & Nguyen, H. T. (2005). Identification of QTLs associated with resistance to soybean cyst nematode races 2, 3 and 5 in soybean PI 90763. *TAG. Theoretical and Applied Genetics. Theoretische Und Angewandte Genetik*, 111(5), 965–971.

Guo-b, B., Sleper, D. A., Nguyen, H. T., Arelli, P. R., & Shannon, J. G. (2006). Quantitative Trait Loci underlying Resistance to Three Soybean Cyst Nematode Populations in Soybean PI 404198A. *Crop Science*, 46(1), 224–233. https://doi.org/10.2135/cropsci2004.0757

Holland, J. B. (2010). Epistasis and Plant Breeding. In *Plant Breeding Reviews* (pp. 27–92). John Wiley & Sons, Ltd.

Howland, A., Monnig, N., Mathesius, J., Nathan, M., & Mitchum, M. G. (2018). Survey of *Heterodera glycines* Population Densities and Virulence Phenotypes During 2015–2016 in Missouri. *Plant Disease*. https://doi.org/10.1094/PDIS-04-18-0650-SR

Huang, M., Jiang, Y., Qin, R., Jiang, D., Chang, D., Tian, Z., Li, C., Wang, C. (2022). Full-

length transcriptional analysis of the same soybean genotype with compatible and incompatible reactions to *Heterodera glycines* reveals nematode infection activating plant defense response. *Frontiers in Plant Science*, 13. https://doi.org/10.3389/fpls.2022.866322.

Illumina. (2014). Infinium genotyping data analysis - Illumina. *Infinium Genotyping Data Analysis*. https://www.illumina.com/documents/products/technotes/technote_infinium_genotyping

Jain, S., Poromarto, S., Osorno, J. M., McClean, P. E., & Nelson, B. D. (2019). Genome wide association study discovers genomic regions involved in resistance to soybean cyst nematode (*Heterodera glycines*) in common bean. *PLOS ONE*, 14(2), e0212140.

Jeon, D., Kang, Y., Lee, S., Choi, S., Sung, Y., Lee, T., & Kim, C. (2023). Digitalizing breeding in plants: A new trend of next-generation breeding based on genomic prediction. *Frontiers in Plant Science*, 14, 1092584. https://doi.org/10.3389/fpls.2023.1092584

Ji, W., Zhu, Y., Li, Y., Yang, L., Zhao, X., Cai, H., & Bai, X. (2010). Over-expression of a glutathione S-transferase gene, GsGST, from wild soybean (*Glycine soja*) enhances drought and salt tolerance in transgenic tobacco. *Biotechnology Letters*, 32(8), 1173–1179.

Jiang, H., Lv, S., Zhou, C., Qu, S., Liu, F., Sun, H., Zhao, X., Han, Y. (2023). Identification of QTL, QTL-by-environment interactions, and their candidate genes for resistance HG type 0 and HG type 1.2.3.5.7 in soybean using 3VmrMLM. *Frontiers in Plant Science*, 14. https://doi.org/10.3389/fpls.2023.1177345.

Kang, Y. J., Kim, K. H., Shim, S., Yoon, M. Y., Sun, S., Kim, M. Y., Van, K., & Lee, S.-H. (2012). Genome-wide mapping of NBS-LRR genes and their association with disease resistance in soybean. *BMC Plant Biology*, 12(1), 1–13.

Karikari, B., Wang, Z., Zhou, Y., Yan, W., Feng, J., & Zhao, T. (2020). Identification of quantitative trait nucleotides and candidate genes for soybean seed weight by

multiple models of genome-wide association study. *BMC Plant Biology*, 20(1), 404. https://doi.org/10.1186/s12870-020-02604-z

Kaur, J., Kaur, J., Dhillon, G. S., Kaur, H., Singh, J., Bala, R., Srivastava, P., Kaur, S., Sharma, A., & Chhuneja, P. (2021). Characterization and Mapping of Spot Blotch in *Triticum durum–Aegilops speltoides* Introgression Lines Using SNP Markers. *Frontiers in Plant Science*, 12, 650400. https://doi.org/10.3389/fpls.2021.650400

Kearsey, M. J., & Farquhar, A. G. L. (1998). QTL analysis in plants; where are we now? *Heredity*, 80(2), 137–142. https://doi.org/10.1038/sj.hdy.6885001

Kerschbaumer, B., Macheroux, P., & Bijelic, A. (2024). Analysis of homodimer formation in 12-oxophytodienoate reductase 3 in solution and crystallo challenges the physiological role of the dimer. *Scientific Reports*, 14(1), 1–12.

Kim, K.-S., Vuong, T. D., Qiu, D., Robbins, R. T., Grover Shannon, J., Li, Z., & Nguyen, H. T. (2016). Advancements in breeding, genetics, and genomics for resistance to three nematode species in soybean. *TAG. Theoretical and Applied Genetics. Theoretische Und Angewandte Genetik*, 129(12), 2295–2311.

Kofsky, J., Zhang, H., & Song, B.-H. (2018). The Untapped Genetic Reservoir: The Past, Current, and Future Applications of the Wild Soybean (*Glycine soja*). *Frontiers in Plant Science*, 9, 949.

Kofsky, J., Zhang, H., & Song, BH. Novel resistance strategies to soybean cyst nematode (SCN) in wild soybean. *Scientific Reports*, 11, 7967. https://doi.org/10.1038/s41598-021-86793-z

Kruskal, W. H., & Wallis, W. A. (1952). Use of ranks in One-Criterion variance analysis. *Journal of the American Statistical Association*, 47(260), 583–621. https://doi.org/10.1080/01621459.1952.10483441

Kumar, R., Saini, M., Taku, M., Debbarma, P., Mahto, R. K., Ramlal, A., Sharma, D., Rajendran, A., Pandey, R., Gaikwad, K., Lal, S. K., Taludar, A. (2023). Identification of quantitative trait loci (QTLs) and candidate genes for seed shape and

100-seed weight in soybean [*Glycine max* (L.) Merr. *Frontiers in Plant Science*, (13), https://doi.org/10.3389/fpls.2022.1074245

Lakhssassi, N., Liu, S., Bekal, S., Zhou, Z., Colantonio, V., Lambert, K., Barakat, A., & Meksem, K. (2017). Characterization of the Soluble NSF Attachment Protein gene family identifies two members involved in additive resistance to a plant pathogen. *Scientific Reports*, 7(1), 1–11.

Lander, E. S., & Botstein, D. (1989). Mapping mendelian factors underlying quantitative traits using RFLP linkage maps. *Genetics*, 121(1), 185–199.

https://doi.org/10.1093/genetics/121.1.185

Lander, E., & Kruglyak, L. (1995). Genetic dissection of complex traits: guidelines for interpreting and reporting linkage results. *Nature Genetics*, 11(3), 241–247. https://doi.org/10.1038/ng1195-241

Lee, S.-K., Liao, P.-Z., Lin, C.-Y., Chen, H.-W., Hsieh, M.-S., Lin, Y.-P., Chen, Y.-J., Hong, J.-H., Chiang, Y.-L., Cheng, C.-P., Chen, P.-C. J., Lee, C.-R., Yang, J.-I., & Ting, H.-M. (2024). Wild mungbean resistance to the nematode Meloidogyneenterolobii involves the induction of phenylpropanoid metabolism and lignification. *Physiologia Plantarum*, 176(5), e14533.

Lee, T. G., Kumar, I., Diers, B. W., Hudson, M. E.. (2015). Evolution and selection of *Rhg1*, a copy number variant nematode resistance locus. *Molecular Ecology*, 24(8), 1774-1791.

Li, C., Zha, W., Li, W., Wang, J., & You, A. (2023). Advances in the Biosynthesis of Terpenoids and Their Ecological Functions in Plant Resistance. *International Journal of Molecular Sciences*, 24(14), 11561.

Li, X., Tang, Y., Wang, L., Chang, Y., Wu, J., & Wang, S. (2022). QTL mapping and identification of genes associated with the resistance to *Acanthoscelides obtectus* in cultivated common bean using a high-density genetic linkage map. *BMC Plant Biology*, 22(1), 1–15.

Li, M., Song, Z., Gurinovich, A., Schork, N., Sebastiani, P., & Monti, S. (2024). yQTL Pipeline: A structured computational workflow for large scale quantitative trait loci discovery and downstream visualization. *PloS ONE*, 19(6), e0298501. https://doi.org/10.1371/journal.pone.0298501

Li, X., Quigg, R. J., Zhou, J., Xu, S., Masinde, G., Mohan, S., & Baylink, D. J. (2006). A critical evaluation of the effect of population size and phenotypic measurement on QTL detection and localization using a large F2 murine mapping population. *Genetics and Molecular Biology*, 29(1), 166–173. https://doi.org/10.1590/s1415-47572006000100030

Lin, J., Mazarei, M., Zhao, N., Hatcher, C. N., Wuddineh, W. A., Rudis, M., Tschaplinski, T. J., Pantalone, V. R., Arelli, P. R., Hewezi, T., Chen, F., & Stewart, C. N. (2016). Transgenic soybean overexpressing GmSAMT1 exhibits resistance to multiple-HG types of soybean cyst nematode Heterodera glycines. *Plant Biotechnology Journal*, 14(11), 2100–2109. https://doi.org/10.1111/pbi.12566

Lin, J., Wang, W., Mazarei, M., Zhao, N., Chen, X., Pantalone, V. R., Hewezi, T., Stewart, C. N., & Chen, F. (2024). GmSABP2-1 encodes methyl salicylate esterase and functions in soybean defense against soybean cyst nematode. *Plant Cell Reports*, 43(6), 1–11.

Liu, P., Zhu, J., & Lu, Y. (2004). Marker-assisted selection in segregating generations of self-fertilizing crops. *TAG. Theoretical and Applied Genetics. Theoretische Und Angewandte Genetik*, 109(2), 370–376.

Liu, S., Kandoth, P. K., Warren, S. D., Yeckel, G., Heinz, R., Alden, J., Yang, C., Jamai, A., El-Mellouki, T., Juvale, P. S., Hill, J., Baum, T. J., Cianzio, S., Whitham, S. A., Korkin, D., Mitchum, M. G., & Meksem, K. (2012). A soybean cyst nematode resistance gene points to a new mechanism of plant resistance to pathogens. *Nature*, 492(7428), 256–260. https://doi.org/10.1038/nature11651

Mahmood, A., Bilyeu, K. D., Škrabišová, M., Biová, J., De Meyer, E. J., Meinhardt, C. G.,

Usovsky, M., Song, Q., Lorenz, A. J., Mitchum, M. G., Shannon, G., & Scaboo, A. M. (2023). Cataloging SCN resistance loci in North American public soybean breeding programs. *Frontiers in Plant Science*, 14, 1270546.

Mathew, D., Valsalan, R., & Shijili, M. (2024). Genome-wide mining and characterization of MATE transporters in Coriandrum sativum L. *PubMed*, 13(3), 155–164. https://doi.org/10.22099/mbrc.2024.49840.1954

Matthews, B. F., Macdonald, M. H., Thai, V. K., & Tucker, M. L. (2003). Molecular Characterization of Arginine Kinases in the Soybean Cyst Nematode (*Heterodera glycines*). *Journal of Nematology*, 35(3), 252–258.

Medina, C., da Rocha, M., Magliano, M., Raptopoulo, A., Marteu, N., Lebrigand, K., Abad, P., Favery, B., & Jaubert-Possamai, S. (2018). Characterization of siRNAs clusters in *Arabidopsis thaliana* galls induced by the root-knot nematode *Meloidogyne incognita*. *BMC Genomics*, 19(1), 1–16.

Meinhardt, C., Howland, A., Ellersieck, M., Scaboo, A., Diers, B., & Mitchum, M. G. (2021). Resistance Gene Pyramiding and Rotation to Combat Widespread Soybean Cyst Nematode Virulence. *Plant Disease*. https://doi.org/10.1094/PDIS-12-20-2556-RE

Melillo, M. T., Bleve-Zacheo, T., Zacheo, G., & Gahan, P. B. (1989). Histochemical localisation of carboxylesterases in roots of *Lycopersicon esculentum* in response to *Meloidogyne incognita* infection. *Annals of Applied Biology*, 114(2), 325–330.

Meng, L., Li, H., Zhang, L., Wang, J. (2015). QTL IciMapping: Integrated Software for Genetic Linkage Map Construction and Quantitative Trait Locus Mapping In Biparental Populations. *The Crop Journal*, 3(3), 269-283. https://doi.org/10.1016/j.cj.2015.01.001

Mindrebo, J. T., Nartey, C. M., Seto, Y., Burkart, M. D., & Noel, J. P. (2016). Unveiling the functional diversity of the alpha/beta hydrolase superfamily in the plant kingdom. *Current Opinion in Structural Biology*, 41, 233–246. https://doi.org/10.1016/j.sbi.2016.08.005

Mitchum, M. G. (2016). Soybean Resistance to the Soybean Cyst Nematode *Heterodera glycines*: An Update. *Phytopathology*. https://doi.org/10.1094/PHYTO-06-16-0227-RVW

Niblack, T. L., Arelli, P. R., Noel, G. R., Opperman, C. H., Orf, J. H., Schmitt, D. P., Shannon, J. G., & Tylka, G. L. (2002). A Revised Classification Scheme for Genetically Diverse Populations of Heterodera glycines. *Journal of Nematology*, 34(4), 279–288.

Manning, S. E., Ku, H., Dluzen, D. F., Xing, C., & Zhou, Z. (2023). A nonparametric alternative to the Cochran-Armitage trend test in genetic case-control association studies: The Jonckheere-Terpstra trend test. *PloS ONE*, 18(2), e0280809. https://doi.org/10.1371/journal.pone.0280809

Mittal, N. (2021) Genetic and Metabolic Characterization of Wild Soybean in Response to Soybean Cyst Nematode (Heterodera glycine). Doctoral Dissertation. University of North Carolina at Charlotte. https://ninercommons.charlotte.edu/record/1002?ln=en&v=pdf

Niblack, T. L. (2005). Soybean Cyst nematode management reconsidered. *Plant Disease*, 89(10), 1020–1026. https://doi.org/10.1094/pd-89-1020

Niblack, T., Tylka, G. L., Arelli, P., Bond J., Diers, B., Donald, P., Faghili, J., Ferris, V. R., Gallo, K., Heinz, R. D., Lopez-Nicora, H., Von Qualen, R., Welacky, T., Wilcox, J. (2009). A standard greenhouse method for assessing soybean cyst nematode resistance in soybean: SCE08 (standardized cyst evaluation 2008). Online. *Plant Health Progress*. https://doi.org/10.1094/PHP-2009-0513-01-RV

Niraula, P. M., Sharma, K., McNeece, B. T., Troell, H. A., Darwish, O., Alkharouf, N. W., Lawrence, K. S., & Klink, V. P. (2020). Mitogen activated protein kinase (MAPK)-regulated genes with predicted signal peptides function in the Glycine max defense response to the root pathogenic nematode *Heterodera glycines*. *PLOS ONE*, 15(11), e0241678.

Nissan, N., Hooker, J., Arezza, E., Dick, K., Golshani, A., Mimee, B., Cober, E., Green, J., & Samanfar, B. (2023). Large-scale data mining pipeline for identifying novel soybean genes involved in resistance against the soybean cyst nematode. *Frontiers in Bioinformatics*, 3, 1199675.

Nissan, N., Mimee, B., Cober, E. R., Golshani, A., Smith, M., & Samanfar, B. (2022). A Broad Review of Soybean Research on the Ongoing Race to Overcome Soybean Cyst Nematode. *Biology*, 11(2), 211.

Nyholt, D. R. (2000). All LODs Are Not Created Equal. *The American Journal of Human Genetics*, 67(2), 282–288. https://doi.org/10.1086/303029

Patil, G. B., Lakhssassi, N., Wan, J. Song, L., Zhou, Z., Klepadlo, M., Vuong, T. D., Stec, A. O., Kahil, S., S., Colantionio, V., Valliyodan, B., Rice, J. H., Piya, S., Hewezi, T., Stupar, R. M., Meksem, K., Nguyen, H. T. (2019) Whole-genome re-sequencings reveals the impact of the interaction of copy number variants of the *Rhg1* and *Rhg4* loci on broad-based resistance to soybean cyst nematode. *Plant Biotechnology Journal*, 17(8), 1595-1611.

PI 424093 GRIN-Global. (n.d.). Retrieved May 28, 2025, from https://npgsweb.ars-grin.gov/gringlobal/accessiondetail?id=1319366

Qi, J., Asl, H. F., Björkegren, J., & Michoel, T. (2014). kruX: matrix-based non-parametric eQTL discovery. *BMC Bioinformatics*, 15(1), 11. https://doi.org/10.1186/1471-2105-15-11

Qu, S., Hu, S., Song, G., Zhang, M., Han, Y., Teng, W., Li, Y., Wang, H., Li, H., & Zhao, X. (2025). Transcription Factor GmMYB29 Activates GmPP2C-37like Expression to Mediate Soybean Defense Against *Heterodera glycines* Race 3. *Plants*, 14(23), 3612. https://doi.org/10.3390/plants14233612

Pundir, S., Sharma, R., Kumar, D., Singh, V. K., Chaturvedi, D., Kanwar, R. S., Röder, M. S., Börner, A., Ganal, M. W., Gupta, P. K., Sharma, S., & Sharma, S. (2022). QTL mapping for resistance against cereal cyst nematode (*Heterodera avenae* Woll.) in

wheat (Triticum aestivum L.). *Scientific Reports*, 12(1), 9586. https://doi.org/10.1038/s41598-022-12988-7

R Core Team. (2024). R: A language and environment for statistical computing. *R Foundation for Statistical Computing*, Vienna, Austria. https://www.R-project.org/

Rajpal, V. R., Singh, A., Kathpalia, R., Thakur, R. K., Khan, M. K., Pandey, A., Hamurcu, M., & Raina, S. N. (2023). The Prospects of gene introgression from crop wild relatives into cultivated lentil for climate change mitigation. *Frontiers in Plant Science*, 14, 1127239.

Rathinam, M., Dokka, N., Senthil, M. K., Mahawar, M. S., Tyagi, S., Rengarajan, M. D., Vijayaraghavareddy, P., Iyyappan, M. Y., Basavaraj, Y. B., Reddy, M. S., Vinutha, T., Rama, P. G., Sinha, S. K., Dash, P. K., Sreeman, S., Majee, M., & Sreevathsa, R. (2025). Cellular Responses in the Pigeonpea Wild Relative Cajanus platycarpus to Helicoverpa armigera Herbivory: The Role of Methionine Sulfoxide Reductase B1 (CpMSRB1) in Enhanced Defense. https://doi.org/10.1094/MPMI-11-24-0149-R

Roth, M. G., Webster, R. W., Mueller, D. S., Chilvers, M. I., Faske, T. R., Mathew, F. M., Bradley, C. A., Damicone, J. P., Kabbage, M., & Smith, D. L. (2020). Integrated management of important soybean pathogens of the United States in changing climate. *Journal of Integrated Pest Management*, 11(1). https://doi.org/10.1093/jipm/pmaa013

Sá, M. E. L. de, Lopes, M. J. C., Campos, M. de A., Paiva, L. V., Amorim, R. M. S. de, Beneventi, M. A., Firmino, A. A. P., & Sá, M. F. G. de. (2012). Transcriptome analysis of resistant soybean roots infected by Meloidogyne javanica. *Genetics and Molecular Biology*, 35(1), 272–282.

Schapire, A. L., Valpuesta, V., & Botella, M. A. (2006). TPR Proteins in Plant Hormone Signaling. *Plant Signaling & Behavior*, 229–230.

Sedivy, E. J., Wu, F., & Hanzawa, Y. (2017). Soybean domestication: the origin, genetic architecture and molecular bases. *The New Phytologist*, 214(2), 539–553.

Shaibu, A. S., Li, B., Zhang, S., Sun, J. (2020). Soybean cyst nematode resistance: Gene identification and breeding strategies. *The Crop Journal*, 8(6), 892-904.

Shi, A., Xiong, H., Michaels, T. E., & Chen, S. (2025). Genome and GWAS analyses for soybean cyst nematode resistance in USDA world-wide common bean (*Phaseolus vulgaris*) germplasm. *Frontiers in Plant Science*, 16, 1520087.

Song, Q., Yan, L., Quigley, C., Fickus, E., Wei, H., Chen, L., Dong, F., Araya, S., Liu, J., Hyten, D., Pantalone, V., & Nelson, R. L. (2020). Soybean BARCSoySNP6K: An assay for soybean genetics and breeding research. *The Plant Journal: For Cell and Molecular Biology*, 104(3), 800–811.

Song, W., Qi, N., Liang, C., Duan, F., & Zhao, H. (2019). Soybean root transcriptome profiling reveals a nonhost resistant response during *Heterodera glycines* infection. *PloS One*, 14(5), e0217130.

Spearman, C. (1904). The Proof and Measurement of Association between Two Things. *The American Journal of Psychology*, 15(1), 72. https://doi.org/10.2307/1412159

Takuno, S., Terauchi, R., & Innan, H. (2012). The Power of QTL Mapping with RILs. *PLoS ONE*, 7(10), e46545. https://doi.org/10.1371/journal.pone.0046545

Torabi, S., Seifi, S., Geddes-McAlister, J., Tenuta, A., Wally, O., Torkamaneh, D., & Eskandari, M. (2023). Soybean–SCN Battle: Novel Insight into Soybean's Defense Strategies against Heterodera glycines. *International Journal of Molecular Sciences*, 24(22), 16232.

Tran, D. T., Steketee, C. J., Boehm, J. D., Noe, J., & Li, Z. (2019). Genome-Wide Association Analysis Pinpoints Additional Major Genomic Regions Conferring Resistance to Soybean Cyst Nematode (*Heterodera glycines* Ichinohe). *Frontiers in Plant Science*, 10, 433137.

Tylka, G. L., & Marett, C. C. (2021). Known Distribution of the Soybean Cyst Nematode, *Heterodera glycines*, in the United States and Canada in 2020. *Plant Health Progress*. https://doi.org/10.1094/PHP-10-20-0094-BR

Usovsky, M., Gamage, V. A., Meinhardt, C. G., Dietz, N., Triller, M., Basnet, P., Gillman, J. D., Bilyeu, K. D., Song, Q., Dhital, B., Nguyen, A., Mitchum, M. G., & Scaboo, A. M. (2023). Loss-of-function of an -SNAP gene confers resistance to soybean cyst nematode. *Nature Communications*, 14(1), 1–14.

Vaghela, B., Vashi, R., Rajput, K., Joshi, R. (2022). Plant chitinases and Their Role in Plant Defense: A Comprehensive Review. *Enzyme and Microbial Technology*, 159, 110055. https://doi.org/10.1016/j.enzmictec.2022.110055.

Van Ooijen, J. W. (1999). LOD significance thresholds for QTL analysis in experimental populations of diploid species. *Heredity*, 83(5), 613–624. https://doi.org/10.1038/sj.hdy.6886230

Vuong, T. D., Sonah, H., Meinhardt, C. G., Deshmukh, R., Kadam, S., Nelson, R. L., Shannon, J. G., & Nguyen, H. T. (2015). Genetic architecture of cyst nematode resistance revealed by genome-wide association study in soybean. *BMC Genomics*, 16(1), 593. https://doi.org/10.1186/s12864-015-1811-y

Wang, M., & Xu, S. (2019). Statistical power in genome-wide association studies and quantitative trait locus mapping. *Heredity*, 123(3), 287–306. https://doi.org/10.1038/s41437-019-0205-3

Wendimu, G. Y. (2022). Cyst Nematode (*Heterodera glycines*) Problems in Soybean (*Glycine max* L.) Crops and Its Management. *Advances in Agriculture*, 2022(1), 7816951.

Wittstock, U., & Gershenzon, J. (2002). Constitutive plant toxins and their role in defense against herbivores and pathogens. *Current Opinion in Plant Biology*, 5(4), 300–307. https://doi.org/10.1016/s1369-5266(02)00264-9

Wiśniewska, A., Wojszko, K., Różańska, E., Lenarczyk, K., Kuczerski, K., & Sobczak, M. (2021). Arabidopsis thaliana Myb59 Gene Is Involved in the Response to *Heterodera schachtii* Infestation, and Its Overexpression Disturbs Regular Development of Nematode-Induced Syncytia. *International Journal of Molecular Sciences*,

22(12), 6450.

Wu, X., Blake, S., Sleper, D. A., Shannon, J. G., Cregan, P., & Nguyen, H. T. (2009). QTL, additive and epistatic effects for SCN resistance in PI 437654. *Theoretical and Applied Genetics.*, 118(6), 1093–1105.

Yan, G., & Baidoo, R. (2018). Current Research Status of *Heterodera glycines* Resistance and Its Implication on Soybean Breeding. *Proceedings of the Estonian Academy of Sciences: Engineering*, 4(4), 534–541.

Yang, Y., Zhou, Y., Chi, Y., Fan, B., & Chen, Z. (2017). Characterization of Soybean WRKY Gene Family and Identification of Soybean WRKY Genes that Promote Resistance to Soybean Cyst Nematode. *Scientific Reports*, 7(1), 1–13.

You, J., Wang, J., Tian, R., Wang, S., Yu, Y., Xu, L., Zhou, C., Pan, F., Chen, J., Sui, Y., & Hu, Y. (2024). Survey of *Heterodera glycines* Population Abundance and Virulence Phenotypes During 2021 to 2022 in Heilongjiang Province. *Plant Disease*. https://doi.org/10.1094/PDIS-02-24-0442-SR

Young, N. D. (1996). QTL MAPPING AND QUANTITATIVE DISEASE RESISTANCE IN PLANTS. *Annual Review of Phytopathology*, 34(1), 479–501. https://doi.org/10.1146/annurev.phyto.34.1.479

Zhang, C., Song, L., Choudhary, M. K., Zhou, B., Sun, G., Broderick, K., Giesler, L., & Zeng, L. (2018). Genome-wide analysis of genes encoding core components of the ubiquitin system in soybean (Glycine max) reveals a potential role for ubiquitination in host immunity against soybean cyst nematode. *BMC Plant Biology*, 18(1), 1–20.

Zhang, H., Kjemtrup-Lovelace, S., Li, C., Luo, Y., Chen, L. P., & Song, B.-H. (2017-a). Comparative RNA-Seq Analysis Uncovers a Complex Regulatory Network for Soybean Cyst Nematode Resistance in Wild Soybean (*Glycine soja*). *Scientific Reports*, 7, 9699.

Zhang, H., Li, C., Davis, E. L., Wang, J., Griffin, J. D., Kofsky, J., & Song, B.-H. (2016). Genome-Wide Association Study of Resistance to Soybean Cyst Nematode

(*Heterodera glycines*) HG Type 2.5.7 in Wild Soybean (*Glycine soja*). *Frontiers in Plant Science*, 7, 215632.

Zhang, H., Mittal, N., Leamy, L. J., Barazani, O., & Song, B.-H. (2017-b). Back into the wild—Apply untapped genetic diversity of wild relatives for crop improvement. *Evolutionary Applications*, 10(1), 5–24.

Zhang, X., Gonzalez-Carranza, Z. H., Zhang, S., Miao, Y., Liu, C.-J., & Roberts, J. A. (2019). F-Box Proteins in Plants. In *Annual Plant Reviews online* (pp. 307–328). John Wiley & Sons, Ltd.

CHAPTER 3: SCREENING WILD SOYBEAN (*GLYCINE SOJA*) FOR RESISTANCE TO *HETERODERA GLYCINES*

3.1 Introduction

Cultivated soybean (*Glycine max*) was domesticated from its wild progenitor, *Glycine soja* in East Asia, undergoing repeated genetic bottlenecks that have reduced its genetic diversity. In contrast, wild soybean has retained extensive allelic variation shaped by natural selection across heterogeneous climates, soils, and pathogen pressures, including *Heterodera glycines*, the most damaging soybean pathogen (Hyten et al., 2006; Leamy et al., 2016; F. Li et al., 2024; L. Li et al., 2024; Sedivy et al., 2017).

SCN populations are genetically diverse and capable of rapid adaptation to host resistance, enabling populations to undergo shifts in virulence in response to selection pressures imposed by resistant soybean cultivars (Niblack et al., 1993; Tylka & Marett, 2021; H-M. Wang et al., 2015). Previous classification systems described SCN populations using a pathogen race system based on reproduction on fewer host lines. However, this system was unable to adequately capture the genetic diversity of SCN resistance between populations, and its use led to a ballooning of potential population types. The HG type classification system was developed to address this limitation by evaluating SCN reproduction on seven indicator soybean lines (Niblack et al., 2002). HG types describe phenotypic virulence patterns, not genetic identity; therefore populations with the same HG designation may still differ genetically. HG typing provides a practical framework for evaluating the effectiveness of soybean resistance sources against different SCN populations. HG type 0 populations are widespread; however, they are unable to overcome host resistance on seven standard soybean cultivars (Table 3.1). Higher designations indicate the ability to reproduce on specific lines (Niblack et al., 2002). SCN virulence is dynamic, able to rapidly adapt to

deployed resistance sources and change over time as host resistance sources are rotated. This has been documented extensively in field surveys within the United States and other countries. For example, in Indiana, USA, SCN populations were dominated by HG type 0. Over time, these have shifted to HG types 2.5.7 and 1.2.5.7, reflecting adaptation to the widespread use of PI 88788- and Peking-type resistance (Critchfield et al., 2023).

Table 3.1 summarizes the *G. max* standard soybean lines used in the HG classification scheme as devised by Niblack et al., 2002, as well as the virulence profiles of two SCN populations evaluated in this study. An SCN population able to infect an accession becomes part of the HG classification: thus, HG type 0 populations cannot overcome the resistance of any of the HG standard soybeans. Resistant host plants are still able to be infected and maintain SCN through its life cycle, if at lower numbers than susceptible plant host lines. In this study, a SCN population previously classified "race 2" is able to infect the two major sources SCN resistance used in soybean production today, PI 548402 (also called 'Peking') and PI 88788, as well as PI 209332, and PI 548316/'Cloud'. The HG convention provides a more detailed description of SCN pathogenicity commonly deployed resistance sources. By characterizing SCN populations in this way, growers are better able to choose host resistance sources.

Table 3.1: Virulence classification of *Heterodera glycines* populations on standard HG type indicator lines. V = virulent (female index ≥ 10%), A = avirulent (female index < 10%).

Indicator Line	HG Type 0	HG Type 1.2.5.7	HG Type 2.5.7
PI 548402 (Peking)	A	V	A
PI 88788	A	V	V
PI 90763	A	A	A
PI 437654	A	A	A
PI 209332	A	V	V
PI 89772	A	A	A
PI 548316	A	V	V

The wild relatives of crops (CWRs) are widely recognized as reservoirs of greater genetic diversity than their domesticated counterparts. Despite this potential, they remain underutilized due to the challenges of linkage drag, genetic compatibility constraints, and limited characterization of their responses to diverse environmental stresses (Ford-Lloyd et al., 2011; Ortiz et al., 2024; H. Zhang et al., 2016-b). Screening large panels of wild accessions for a small number of traits requires substantial resources, often with uncertain immediate return of actionable data (Migcovsky & Myles, 2017). Nevertheless, systematic evaluation of wild germplasm provides the foundational knowledge necessary to identify and deploy novel alleles to strengthen soybean crop resilience under evolving biotic and abiotic pressures. Due to its similarities to domesticated soybean, genetic diversity, and adaptability, wild soybean is a promising source of genetic resistance diversity for its cultivated descendants.

The screening of traits of interest has promoted the discovery and utilization of a wide range of traits from CWRs to improve soybeans and other important agricultural products. The CWR germplasm has improved a wide range of agronomically important traits. Included are yield traits such as seed size and composition, as well as indirect crop

enhancement through the improvement of disease resistance and tolerance to abiotic stress (Bronzynska et al., 2016; H. Zhang et al., 2016-b).

Although evaluations of many distinct traits of soybeans have been performed extensively, these investigations usually focused on domesticated accessions. This focus on cultivars and landraces is due to uniformity of phenotypes and direct usability in breeding programs with reduced or non-existent linkage drag problems and other plant breeding challenges (Acharya & Yan, 2021; Hua et al., 2018). Although wild relatives of the crop introduce greater variability in phenotype, this variability is valuable for the discovery of new traits and the improvement of soybean cultivars.

Identification of durable resistance to SCN begins with the discovery of resistance sources. Previously, this work has focused on *Glycine max* cultivars (USDA-ARS 2023; Lian et al., 2023; K-S. Kim et al., 2016). Numerous cultivars have been tested, most SCN resistance in *G. max* has been found to be based on variation at a limited number of major loci, particularly *Rhg1* and *Rhg4*. The repeated and widespread use of these resistance sources has contributed to the selection of increasingly virulent SCN populations capable of reproducing in formerly effective cultivars (Arelli et al., 2015; Lian et al., 2023; Project: USDA ARS, 2023).

In contrast, wild soybean has been underutilized as a source of resistance to SCN. Wild soybean evaluations have focused on traits more directly related to yield, such as 100-seed weight, protein content, and maturity timing, or other pathogens, rather than resistance to SCN (Jacquet et al., 2023; La et al., 2019). Research specifically examining SCN resistance in wild soybean have largely concentrated on a limited number of accessions, including PI 468916, PI 464925B, and PI 578345 (designated NRS100) (Kofsky et al., 2021; Winter et al., 2007; Yu & Diers, 2017).

More distantly related species, namely *Glycine tomentella*, have been tested for resistance to SCN. *G. tomentella* is one of many genetically diverse *Glycine* species studied for agronomically important traits. However, with genetic distance come complications in

effective cross breeding, including differences in ploidy and maturity, making them less desirable for the introduction of beneficial traits (Blower et al., 2025; Brozynska et al., 2016; Dempewolf et al., 2017; Herman et al., 2020; Hwang et al., 2019; Wen et al., 2017). Although modern breeding practices are widely used in the accurate and rapid development of new crop cultivars, conventional practices still in use rely on the ability to effectively cross species for trait selection (Anand et al., 2023; Lamichhane & Thapa, 2022). More beneficial for soybean breeders, *Glycine soja* readily hybridizes with *G. max*, shortening the time needed to develop introgression lines for study and plant breeding (Singh & Hymowitz, 1988) and making it a more practical source of novel resistance alleles.

Given the dynamic nature of SCN virulence, identifying additional resistance mechanisms, particularly those effective against heterogeneous SCN populations, is essential for maintaining long-term resistance durability against this damaging pathogen. By using a closely related species like *Glycine soja* to discover agronomically important traits, the timeline of trait discovery to SCN-resistant cultivar development may be shortened (Zhuang et al., 2022).

Foundation for Present Study

Previous work utilized a large number of *Glycine soja* accessions to identify single nucleotide polymorphisms associated with resistance to SCN HG type 2.5.7 as part of a genome-wide association study (GWAS) aimed at identifying SNPs associated with SCN resistance. Although the primary goal of that study was genetic mapping rather than germplasm evaluation, it effectively functioned as a large-scale pre-screen for resistance phenotypes within wild soybean germplasm.

Of the accessions studied in the GWAS, 43 were found to have full resistance (FI <10) or moderate resistance (FI 10–30) (H. Zhang et al., 2016-a), providing a biologically enriched subset of accessions exhibiting resistance associated phenotypes. Two additional accessions with FI slightly above the "moderately resistant" threshold were included in this study to avoid excluding potentially important resistance phenotypes due to categorical

boundary effects. These resistant accessions formed the basis of the screening panel used in the present study, allowing evaluation of whether resistance identified against HG 2.5.7 also extends to additional SCN populations.

The present study builds directly upon that foundation. Rather than sampling *G. soja* based on geographic stratification, the panel evaluated in this work was selected from those previously identified with potential for resistance to an economically important subset of *Heterodera glycines* (HG 2.5.7). This strategy allowed for targeted evaluation of whether resistance observed under one virulence context would be maintained across additional SCN populations of economic importance. Although accession selection was based on prior resistance-associated performance, rather than geographic origin, the resulting panel represents diverse regions across East Asia (Figure 3.1), providing descriptive context for the genetic diversity represented within the study while maintaining a biologically-focused selection framework. The objective of this study was to determine whether wild soybean accessions previously identified as resistant to HG type 2.5.7 also exhibit resistance to other economically important SCN populations (HG 0 and HG 1.2.5.7), thereby identifying wild accessions with potential broad-spectrum resistance to this damaging pathogen. Identifying wild soybean accessions that maintain resistance across contrasting SCN populations represents an important step toward expanding the genetic base of SCN resistance in domesticated soybean and improving the durability of future soybean cultivars.

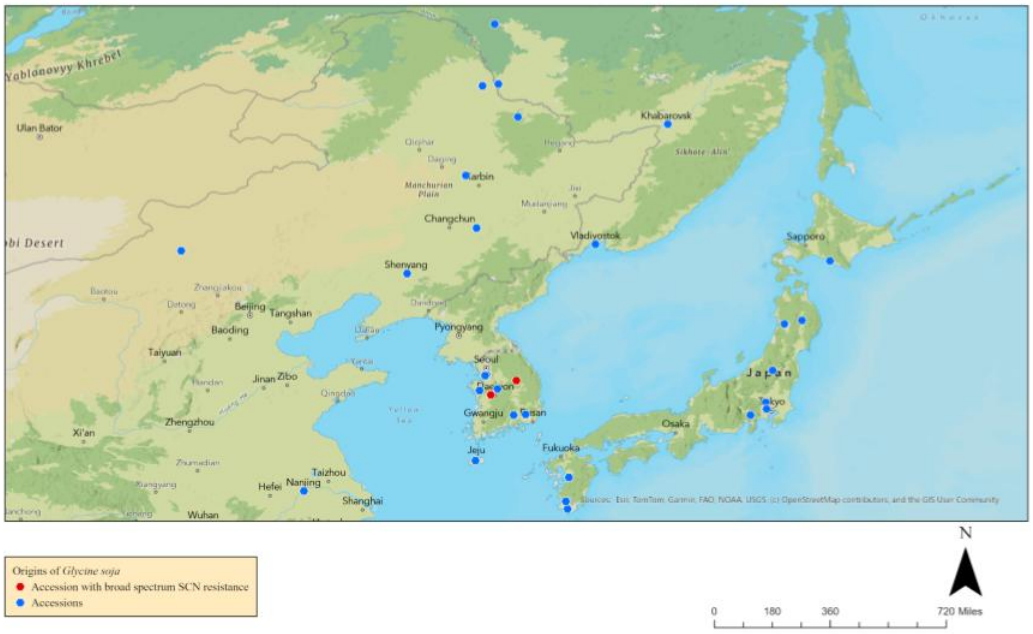

Figure 3.1: Geographic origins of *Glycine soja* accessions evaluated in this study. Accessions were selected based on prior resistance-associated performance against *Heterodera glycines* HG 2.5.7 rather than geographic stratification. Markers represent screened wild soybean accessions, and red markers indicate accessions representing broad-spectrum resistance to both HG 0 and HG 1.2.5.7 in the present study.

3.2 Materials & Methods

Plant Materials and SCN Bioassay

Previously, Zhang et al 2016 used 235 accessions of *Glycine soja* to perform a genome-wide association study for resistance to SCN HG type 2.5.7 (formerly "race 5"). Plant accessions previously identified as resistant or moderately resistant were utilized as a pre-screened panel to evaluate whether resistance to HG type 2.5.7 extended to additional SCN populations. Forty-three wild soybean accessions were used in this study (Table B1). All accessions were sourced from the USDA National Plant Germplasm System (USDA, 2026). Seed coats were sterilized with 0.5% sodium hypochlorite solution and scarified for uniform germination. Seeds were germinated in petri dishes with sterilized water and filter paper, which were replaced daily to reduce microbial growth. After five days of germination, healthy seedlings were planted in sterilized sand in plastic cones (Greenhouse

Megastore, Danville IL, USA). *G. max* cultivars Williams 82 and Lee 74 were grown as susceptible check lines to calculate the phenotype of interest, female index (FI). Each plant was inoculated with approximately 2500 eggs to allow the pathogen to fully infect the plants and align with previous SCN infection standards (Zhang et al., 2016).

The HG type of each SCN population was confirmed by also infecting plants of the HG typing indicator lines (respectively: PI 548402 ('Peking'), PI 88788, PI 90763, PI 437654, PI 209332, PI 548316) (Table 1). Plants were grown in a randomized block design in a greenhouse maintained at 27℃ under a 16 hours light/8 hours dark system.

Previous to this study, soybean cyst nematode populations were maintained on susceptible *G. max* cultivar Williams 82 for over 50 generations. SCN cysts were removed from the roots of these plants and eggs purified by sucrose flotation (Jenkins, 1964). Plants were grown for one SCN life cycle, approximately 30 days. After 30 days, cysts were extracted from roots. Cysts were counted and the phenotype was calculated.

In addition to cyst counts,measurements of the roots were taken using the CI-202 Portable Laser Leaf Area Meter (LAM) (CID Bio-Science, Camas, WA, USA). Measurements included: root length, width, area, perimeter, and aspect ratio. Per manufacturer's instructions, a second, more reliable measurement of root length was obtained by calculating the root length as a function of the root perimeter (CI Bio-Science, 2020). Portable leaf area meters such as the CI-202 have been used in plant growth studies to quantify not only leaf area, but also root size traits following harvest and cleaning using scan-based workflows analogous to leaf measurement. Portable leaf area meters have been widely used to quantify root morphological traits for a wide array of purposes, including parasitic nematode infection. They provide reliable estimates comparable to traditional root measurement approaches (Bauhaus & Messier, 1999; CI BioScience, 2020; Comas, et al., 2002; Costa et al., 2002; Willig et al., 2023).

Statistical Analysis

The standard method of assessing SCN virulence on soybean, the calculation of the

female index (FI) was calculated using the formula:

$$\text{FI} = \left(\frac{\bar{x}_{\text{test line}}}{\bar{x}_{\text{susceptible check}}} \right) \times 100 \tag{3.1}$$

The female index was calculated using two susceptible soybean check lines, Williams 82 (W82) and Lee 74 to improve reliability of susceptibility estimates. Lee 74 is a standard susceptible check for SCN infection and Williams 82 is also widely used (Niblack et al., 2009). Under the greenhouse conditions of this study, Williams 82 exhibited more consistent germination and was retained as the primary check for subsequent FI calculations. The female index (FI) was initially calculated using both check lines. Williams 82 produced lower average cyst counts than Lee 74, and was therefore used for subsequent FI calculations to provide conservative estimates of SCN reproduction. The validation of susceptibility by the use of Williams 82 and Lee 74 confirmed assay conditions and strengthened confidence in the categorization of female index calculations, especially those near threshold values between resistant, moderately resistant, moderately susceptible, and susceptible responses(R, MR, MS, and S, respectively).

Cyst count data were analyzed independently from root measurement data to identify *Glycine soja* accessions exhibiting differential SCN reproduction when challenged with different SCN populations. Since cyst counts are typically skewed, and to maintain assumptions of normality and variance required for modeling, raw cyst counts (x) were transformed via $\log_{10}(\text{cyst} + 1)$ prior to analysis to account for variance and non-normal data, as well as to allow the inclusion of replicates where x = 0 (McCarville et al., 2017; Mengistu et al 2024; Niblack et al 2002; Taylor, 1961).

A two-way analysis of variance (ANOVA) was performed to evaluate the fixed effects of the 45 wild soybean accessions, the two populations of soybean cyst nematode, and their interaction with respect to the log-transformed cyst counts. The majority of the evaluated accessions were represented by a minimum of 3 biological replicates. However, in some cases, unreliable germination and the effect of SCN infection on some replicate

plants (i.e., plant death) before the end of a full life cycle of SCN led to uneven sample numbers among accession-pathogen combinations. Numbers varied among accession-pathogen combinations (n = 1-7), so ANOVA Type III sums of squares were used to account for the unbalanced experimental design (Acharya & Yan, 2021; Arantes Tihoood, 1998; Shaw & Mitchell-Olds, 1993). Because cyst counts represent discrete infection counts that may exhibit over-dispersion, an additional generalized linear modeling approach appropriate for count data was also used to confirm patterns observed in the ANOVA.

The analyzes were repeated with the complete dataset and with a minimum of three replicates. The consistency of significant effects across both iterations of analysis validates the identified trends, particularly the accession x pathogen interaction; these may be interpreted as more robustly representative of broader accession-pathogen responses and not artifacts of limited sampling in specific lines. To focus on host-pathogen effects with biological meaning (rather than comparing every accession-pathogen pair), a simple effects analysis was performed following ANOVA to focus on targeted contrasts of SCN virulence (*Fixing the Bridge Between Biologists and Statisticians*, 2026; Pogorelko et al., 2020; Schabenberger et al., 2000; Xiang et al., 2025).

Since cyst counts represent discrete count data and can deviate from normality even after transformation, cyst reproduction was analyzed with a negative binomial generalized linear model (NB-GLM). These models are appropriate for overdispersed count data commonly observed in plant-pathogen infection assays (Pérez-Hernández et al., 2019). The model included accession, SCN population (HG 0 or HG 1.2.5.7), and the accession x population interaction as fixed effects. The significance of the model terms was evaluated using likelihood ratio tests with Type III analysis of deviance. To identify accessions with differential responses between SCN populations, pairwise contrasts comparing HG 0 and HG 1.2.5.7 within each accession were performed and adjusted for multiple tests using the Benjamini-Hochberg false discovery rate (FDR) correction (Benjamini & Yekutieli, 2001). Cyst counts estimated by the model were determined to visualize differences in nematode

reproduction between host accessions and pathogen populations.

To validate categorical resistance ratings (R, MR, MS and S), Spearman's Rank Correlation was conducted between raw cyst counts and assigned ordinal ranks (R=1 to S = 4)(Spearman, 1904).

Root Trait Analysis

Subsequent analysis combined cyst counts and root phenotype measurements to determine whether variation in root system architecture was associated with nematode reproduction. Seven root traits were evaluated: root area, root perimeter, total root length, root width, aspect ratio, and root length as a function of perimeter (denoted RLP), and manually measured root length. RLP was calculated according to the manufacturer's recommendation for the CI-202 Portable Leaf Area Meter:

$$\text{RLP} = \frac{\text{Perimeter}}{2} \tag{3.2}$$

per CID Bio-Science (2020). This metric provides an estimate of functional root length that accounts for branching of the root system. All traits were analyzed to avoid bias towards a single morphological metric. Measurements were log transformed to account for non-normality.

To evaluate accession effects, pathogen effects, and accession x pathogen interactions on each root trait, a two-way factorial ANOVA using type III Sum of Squares was performed (Shaw & Mitchell-Olds, 1993). A simple effects analysis was performed for each trait to determine if differences exist between a accession's response to HG 0 and HG 1.2.5.7. Additionally Spearman's rank correlation coefficient (ρ) was calculated between individual plant cyst counts and each root trait. Spearman's correlation was selected due to its robustness to non-normally distributed data and ability to assess non-linear monotonic relationships (Spearman, 1904). Analyses were performed using both the full data set and a filtered dataset including only accession x pathogen combinations with three or more replicates ($n \geq 3$) to ensure robustness of conclusions.

To further evaluate relationships among root traits and their association with SNC reproduction, exploratory diagnostics were conducted prior to multivariate modeling. Distributions of cyst counts and root traits were examined using histograms and box plots to assess skewed distributions and potential outliers. Cyst counts are typically right-skewed, and were thus transformed using $\log_{10}(\text{cyst} + 1)$ prior to analysis to stabilize variance while retaining observations with zero cyst counts (Taylor, 1961). Pairwise relationships between root traits and cyst counts were evaluated using Pearson (r) correlation coefficients and Spearman rank correlations (ρ). Pearson correlations were used to evaluate linear relationships among root traits, while Spearman correlations were used to assess monotonic relationships between root morphology and cyst counts due to the non-normal distribution of SCN reproduction data.

Principal component analysis (PCA) was conducted to identify major axes of variation in root morphology. The seven traits are those included above, namely: root area, root perimeter, root length, root width, aspect ratio, root length calculated from perimeter (RLP) and manually measured root length. Sampling adequacy for PCA was measured using Kaiser-Meyer-Olkin (KMO) statistics to assess whether variables share sufficient common variance to justify dimensionality reduction. Principal component (PC) scores were calculated for each plant, and the proportion of variance explained by each component was evaluated using scree plots. Relationships between PC scores and cyst counts were further evaluated using Pearson correlation to determine whether major axes of root morphological variation were associated with SCN reproduction.

All analyses were performed in R (version 4.5.2) using RStudio (Posit Software, Boston, MA). Susceptible *G. max* cultivars and HG standard lines were included in this study to characterize overall variation in SCN reproduction and confirm each SCN populations' HG classification. However, cyst and root trait-cyst association analyses were restricted to wild soybean (*Glycine soja*) accessions. This avoided potential bias introduced by *G. max* cultivars with more extensive root systems and a separate evolutionary history. Since *G.*

max cultivars are not representative of the genetic variation of wild soybean under study, they were excluded from analysis (Prince et al., 2015; K. Kim et al., 2021).

3.3 Results

Confirmation of Susceptible Checks

Both Williams 82 and Lee 74 were utilized to calculate and categorize the resistance of the selected *G. soja* accessions. When challenged with HG 0, Lee 74 maintained an average 559.4 SCN cysts, and Williams 82 maintained 433.3 cysts. When challenged by the HG 1.2.5.7 population of SCN, Lee 74 and Williams 82 had averages of 313.6 and 312.3, respectively. There was no significant difference in cyst counts between these susceptible checks for either treatment group. Categorization of HG 0 susceptibility for accessions H01, H25, and S91 varied depending on the check line used. These were resistant to Lee 74, but only moderately resistant to Williams 82.

Similarly, when challenged with HG 0, accessions H23, H27, S76, S85, and S88 were categorized as moderately resistant using Lee 74, and moderately susceptible when calculating female index with Williams 82. In the case of the HG 1.2.5.7 SCN population, only S05 was categorized differently with Lee 74 and Williams 82; it was calculated to be moderately susceptible on Lee 74, and susceptible on Williams 82. Therefore, Williams 82 was used for subsequent analysis of the Female Index for the most conservative evaluation of SCN virulence on the selected test lines.

Confirmation of SCN Populations

The virulence phenotype of the SCN populations utilized in this study was determined by assessing the reproduction of the population on standard Glycine max cultivars and calculating the female index. These cultivars include PI 548402 (Peking), PI 88788, PI 90763, PI 437654, PI 209332, PI89772, and PI 548316. Both Williams 82 and Lee 74 were used to determine SCN virulence on these standard test lines (Niblack et al., 2009). Soybean cyst nematode population type HG 0 was determined with all 7 test lines having a FI <10 using both Williams 82 and Lee 74. HG 1.2.5.7 was found when calculated with

both the Williams 82 and Lee 74 cyst averages (Table B2). The two soybean cyst nematode populations were found to be significantly different in their overall virulence across the *G. soja* test line accessions (p<0.0001,value F=88.3), and their FI values as calculated with Williams 82 as the susceptible check are visualized in Figure 3.2.

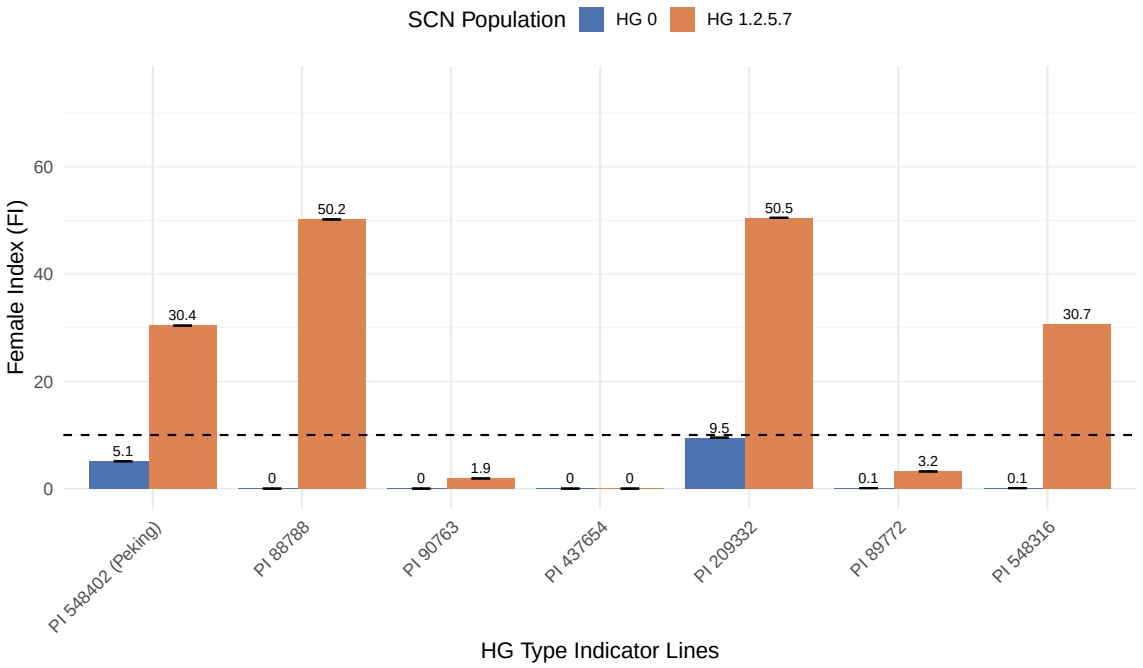

Figure 3.2: Female index values for two soybean cyst nematode (SCN) populations across HG type indicator lines using Williams 82 as the susceptible check. Numeric labels above each bar show the female index (FI) for that HG type indicator line and SCN population. The dashed line at FI = 10 denotes the threshold for classify resistance. Bars are grouped by SCN population, with HG 0 represented by blue and HG 1.2.5.7 by orange.

Glycine soja Resistance to SCN Populations HG 0 and HG 1.2.5.7

Resistance of the selected *Glycine soja* accessions to two populations of *H. glycines* (HG 0 and HG 1.2.5.7) was evaluated based on the Female Index (FI). Resistance was classified into four categories: resistant (R = FI < 10), moderate resistance (MR = FI 10-30), moderate susceptibility (MS = FI 30-60), and susceptible (S = FI > 60). A heatmap illustrating the FI values for each accession-pathogen combination was used to illustrate each accession's level of resistance to the two pathogen populations (Figure 3.3). A highly significant accession-by-population interaction was observed in the two-way ANOVA

analysis using Type III Sum of Squares ($p < 0.0001$, $F = 3.24$), demonstrating that nematode development was dependent upon the specific combination of host and SCN HG type. A simple effects analysis was performed to better understand the different responses of each accession to each SCN population. Statistical analyses were restricted to accession-pathogen combinations with at least three biological replicates ($n \geq 3$). Overall, highly significant differences in SCN reproduction were observed among the wild soybean test accessions and check lines (Table B3).

Among the evaluated accessions, only two plant accessions exhibited consistent resistance across both SCN populations. S54 and S55 exhibited full resistance to HG 0 (FI = 6.2 and FI = 3.0, respectively), as well as to HG 1.2.5.7 (FI = 8.1 and FI = 8.6, respectively). These two accessions suppressed SCN reproduction to minimal levels across each of the SCN populations. There was no significant difference in S54 cyst numbers between SCN HG 0 treatment and SCN HG 1.2.5.7 treatment ($p = 0.465$). Likewise, S55 did not exhibit a significant difference in cyst numbers between the two SCN populations ($p = 0.232$).

Two accessions, H05 and S100, were fully resistant to HG 0, but only had moderate resistance to HG 1.2.5.7. H05 was observed to have a significantly higher number of cysts on HG 1.2.5.7 than on HG0 ($p < 0.01$). S100, on the other hand, did not exhibit a significant difference between the two SCN populations. In a similar vein, six of the tested wild soybean accessions were categorized as fully resistant (R) to HG 0, but moderately susceptible (MS) to HG 1.2.5.7. Two accessions, H33 and S14 were observed to have a significant difference in the number of cysts between the two nematode groups ($p < 0.001$); additionally H21, S74 and S39 also exhibited a significant difference in cyst counts between the SCN populations ($p < 0.05$). H34 did not exhibit a significant difference between SCN treatments.

Moderate resistance to both soybean cyst nematode populations was shared by accessions S11, S32, H03, H14, H20, H24, and H26), and there was no significant difference between the two SCN populations for these seven accessions.

Seventeen accessions shared moderate resistance to HG 0, but were moderately susceptible to HG 1.2.5.7. Of these, 6 exhibited a significantly different cyst counts ($p<0.05$) to HG 0 and HG 1.2.5.7: H01, H15, H25, H28, S03, and S96. The other 11 (H02, H22, H29, H30, H35, S01, S04, S32, S89, S91, and S92) did not demonstrate a significant difference in cyst counts between the SCN populations.

The remaining 8 *G. soja* accessions (H27, S83, S88, S85, H23, S05, S57, and H31) were moderately susceptible to HG 0 and moderately susceptible or fully susceptible to HG 1.2.5.7, with no significant differences between the cyst counts for the two treatments. Two G. max cultivars, NC-Raleigh and NC-Dunphy were fully susceptible to both SCN population types, with no significant differences between the averages of those cultivars under HG 0 and HG 1.2.5.7 treatment.

Due to low germination numbers and plant death before the end of the SCN life cycle, two *G. soja* test lines had insufficient replicate numbers for either the HG 0 population (S86) or the HG 1.2.5.7 population (S76). They were included in the heatmap for completeness and clarity; they are marked with an asterisk (†) and colored with grey to indicate that they are not reliable indications of their response to the SCN populations in this study (Figure 3.3).

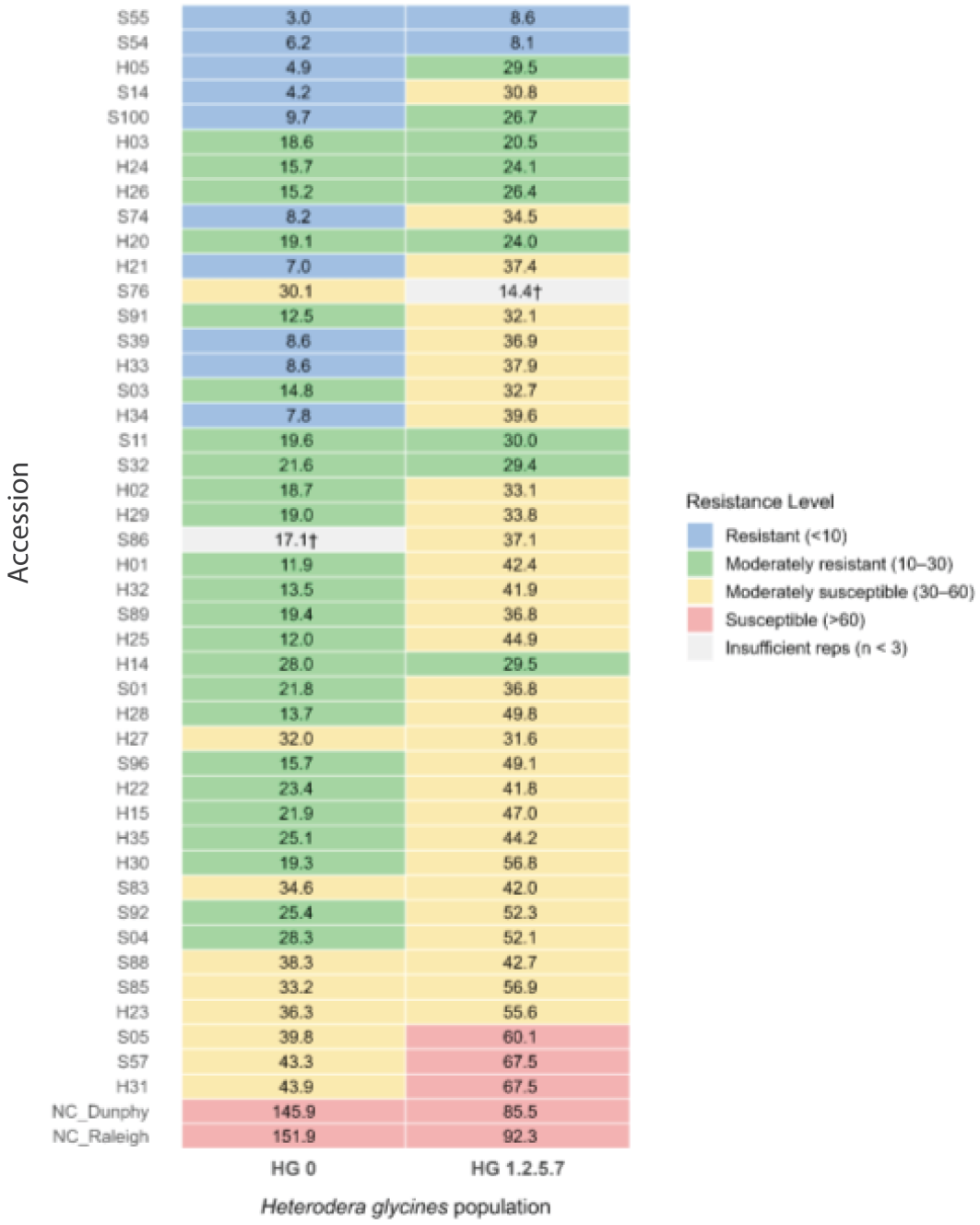

Figure 3.3: Heatmap of Female Index (FI) of selected *Glycine soja* accessions following infection with different *Heterodera glycines* populations (HG 0 and HG 1.2.5.7). Accessions are ordered by increasing FI across both SCN populations. Cells are colored according to resistance classification: resistant (FI <10, blue), moderately resistant (FI 10–30, green), moderately susceptible (FI 30–60, yellow), and susceptible (FI >60, red). Values represent mean FI per accession; daggers (†) and grey cells indicate accessions where FI was calculated with fewer than three biological replicates.

Spearman Rank Correlation analysis was performed to validate the relationship between categorical resistance classifications (female index) and quantitative SCN reproduction. A strong positive correlation was observed (ρ = 0.75, p < 0.001) (Figure 3.4, Table B4). Analysis included 46 degrees of freedom for accession, 1 degree of freedom for pathogen population type, and 434 residual degree of freedom, despite the presence of lines with low replicate numbers (Arantes & Tihohood, 1998; Acharya & Yan, 2021; Steel & Torrie, 1980).

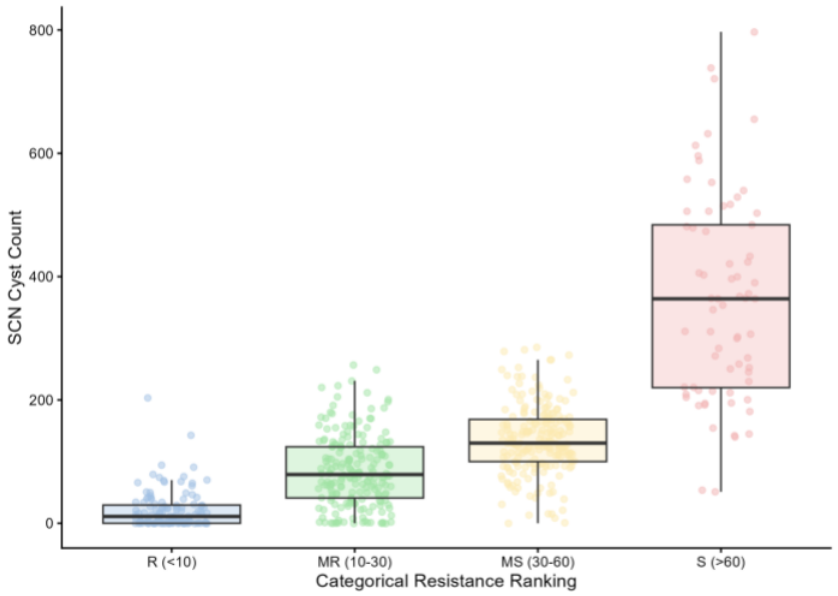

Figure 3.4: Spearman rank correlation between Female Index (FI) resistance category and SCN cyst count. Resistance categories were defined as R (Resistant, <10), MR (Moderately resistant, 10–30), MS (Moderately susceptible, 30–60), and S (Susceptible, >60). Cyst counts increased with increasing susceptibility category (ρ = 0.749, p < 0.001).

Root Length as a Function of Perimeter (RLP) - A Primary Root Trait Associated with Accession and Pathogen Effects

All measured root traits were initially analyzed to determine which best captured biologically significant differences between *accessions of G. soja* and treatments with SCN pathogens using a two-way factorial ANOVA (Type III Sum of Squares). Among the seven traits evaluated, the length of the root as a function of the perimeter, RLP, showed the

strongest and most consistent statistical signals in the analyzes in the filtered dataset ($n \geq 3$ replicates per combination of accession x pathogen).

RLP differed significantly among accessions ($p < 0.001$, $F = 2.35$). A significant effect of the pathogen population was also detected ($p<0.001$, $F = 21.91$). A significant interaction between the accession and the pathogen was observed ($p < 0.001$, $F = 4.12$), indicating that the root architecture of *G. soja* responded differentially to HG 0 compared to HG 1.2.5.7 depending on the accession (Table B5).

To evaluate whether root morphology traits were associated with soybean cyst nematode reproduction, a Spearman rank correlation analysis was conducted between individual plant cyst counts and RLP. A moderately positive correlation ($\rho = 0.407$, $p < 0.001$) was detected.

Secondary Traits Associated with Plant Accession and Pathogen Effects

Other root traits exhibited significant accession-pathogen interaction effects, though were more variable when analyzed by accession or by pathogen HG type. The root area showed significant differences between the accessions ($p < 0.001$, $F = 3.52$), as well as between the interactions between the accession and the pathogen ($p < 0.001$, $F = 3.54$). However, there was no significant difference between the pathogen groups for this trait. The perimeter trait also displayed this pattern: significant differences between accession-pathogen interactions ($p < 0.001$, $F = 3.87$) and between accessions ($p < 0.001$, $F = 3.84$), but no significant differences between pathogen populations. Results of Spearman correlation analysis indicated root area and perimeter both show moderate positive correlations between each of these and cyst count ($\rho = 0.358$, and $p < 0.001$, and $\rho = 0.339$ and $p < 0.001$, respectively). These patterns were similar to the association of RLP with cyst count, though a lower association (ρ) than RLP (Table B6).

In contrast, root width, aspect ratio, and manually measured root length did not demonstrate as strong an association with SCN reproduction as RLP. These three traits showed limited or inconsistent accession effects (Table B6). Based on these results, RLP

was selected as the primary root phenotype for subsequent interpretation; root area and root perimeter were retained as secondary supporting traits reflecting overall root system size. Although multiple size-related traits exhibited similar patterns, RLP demonstrated the strongest and most consistent statistical signal across accession, interaction, and correlation analyses.

Root Phenotypes Are Associated with Pathogen Population and SCN Reproduction

Functional root length (RLP) was significantly influenced by *G. soja* accession ($p < 0.001$, $F = 5.10$), pathogen population ($p<0.001$, $F = 20.72$), and the host-pathogen interaction ($p < 0.001$, $F=3.73$) in the filtered dataset. These data indicate that root system architecture varied among accessions and that the magnitude of pathogen-induced root responses differed across genetic backgrounds. Across every accession but one RLP was greater under HG 1.2.5.7 relative to HG 0 ($p < 0.05$). The exception, S14, still indicated higher RLP under HG 1.2.5.7 than HG 0, but the difference was not significant. Spearman rank correlation analysis further demonstrated a positive association between RLP and cyst count ($\rho = 0.303$, $p < 0.001$), indicating larger functional root systems were associated with increased nematode reproduction.

Significant accession x pathogen interactions were detected for RLP ($p < 0.001$). Simple effects analysis compared HG 0 and HG 1.2.5.7 within each accession, revealing all but one wild soybean accession with significant differences in RLP between pathogen populations ($p < 0.05$). In all significant cases, RLP was greater under HG 1.2.5.7 than HG 0. The magnitude of the difference varied among accessions, but the direction of effect was consistent.

A linear model including RLP, SCN populations, and their interaction revealed a significant interaction ($p < 0.001$), indicating that the association between this root architecture trait and SCN reproduction differed between HG types. Under HG 0, RLP was positively associated with nematode reproduction ($\beta \approx 0.088$), whereas the relationship was negligible when under HG 1.2.5.7 challenge ($\beta \approx 0.001$). The full model explained

36.7% of the variation in log-transformed cyst counts (R^2 = 0.367; n =471) (Figure 3.5).

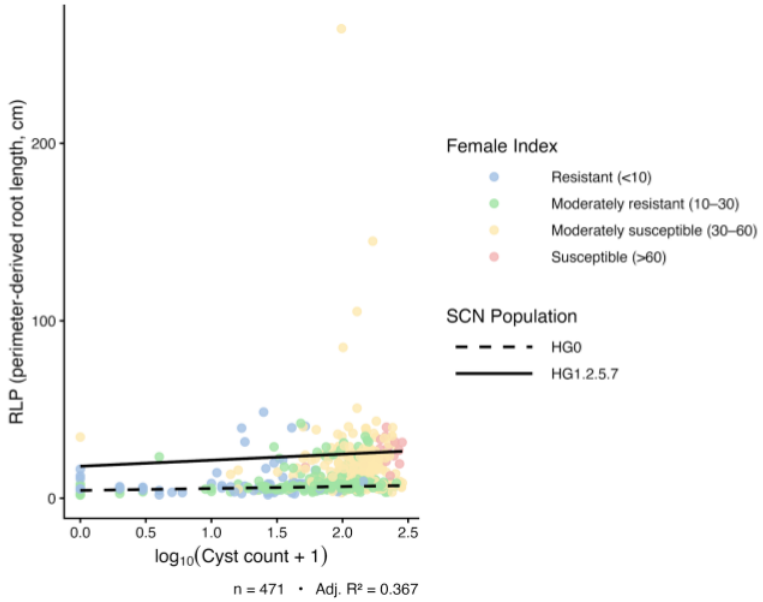

Figure 3.5: Relationship between functional root length (RLP; perimeter derived root length) and soybean cyst nematode reproduction in *Glycine soja* accessions. Points are colored according to Female Index category (blue = resistant, green = moderately resistant, yellow = moderately susceptible, and red = susceptible). Lines represent the linear regressions fitted separately for HG 0 (dashed) and HG 1.2.5.7 (solid) populations of SCN. A Significant interactions between RLP and SCN population was observed ($p < 0.001$), indicating the association between RLP and SCn reproduction differs between pathogen populations (Adj. R^2 = 0.367).

As secondary root traits, root perimeter and root area showed similar, though less consistent patterns. Significant accession-pathogen interactions were also detected for root perimeter. Simple effects analysis revealed 12 accessions ($p < 0.05$) that exhibited significant differences in perimeter measurements between SCN populations HG 0 and HG 1.2.5.7. Among these, 10 showed greater root perimeter under HG 1.2.5.7, whereas 2 exhibited greater perimeter under HG 0. Simple effects analysis for root area revealed 8 accessions that exhibited significant differences between HG 0 and HG 1.2.5.7 infection ($p < 0.05$). All of these showed higher root area under HG 1.2.5.7 infection than under HG 0.

Multivariate Structure of Root Traits

Pairwise trait-correlation diagnostics further indicated several root size traits cap-

tured overlapping dimensions of root morphology. Pearson correlation analysis showed moderate positive associations between log-transformed cyst counts and root area, root length, manually measured root length, (r = 0.36 - 0.41). Associations with perimeter and RLP were smaller (r = 0.27 and r = 0.21, respectively). In contrast, root width (r = 0.10) and aspect ratio (r = 0.05) showed little relationship with cyst counts. Among root traits, perimeter and RLP were strongly correlated (r = 0.86); similarly, root length and manually measured root length were also strongly correlated (r = 0.80).

Principal component analysis (PCA) was performed to characterize the multivariate structure of the seven measured root traits among wild soybean accessions. Sampling adequacy for dimensionality reduction was moderate (KMO = 0.68). The first two components explained the majority of variation in root morphology (PC1 = 46.4%, PC2 =25.9%), together accounting for 72.3% total variance (Figure B1). Loadings indicated that PC1 primarily represented overall root system size, with the strongest contributions from root perimeter, root area, and root length traits (root length as measured with CI-202, root length derived from perimeter, RLP, and manually measured root length). On the other hand, PC2 reflected variation in root architecture, with the largest contributions from root width and aspect ratio (Figure 6, Table 2). Visualization of the PCA biplot showed that traits associated with root system size clustered closely along the PC1 axis, whereas root width and aspect ratio were separated along PC2, independent from overall root size. PCA scores for plants infected with HG 0 and HG 1.2.5.7 overlapped extensively (Figure 3.6). Correlation analysis further revealed a moderate positive association between the root size axis (PC1) and log-transformed cyst counts (r = 0.40, $p < 0.001$).

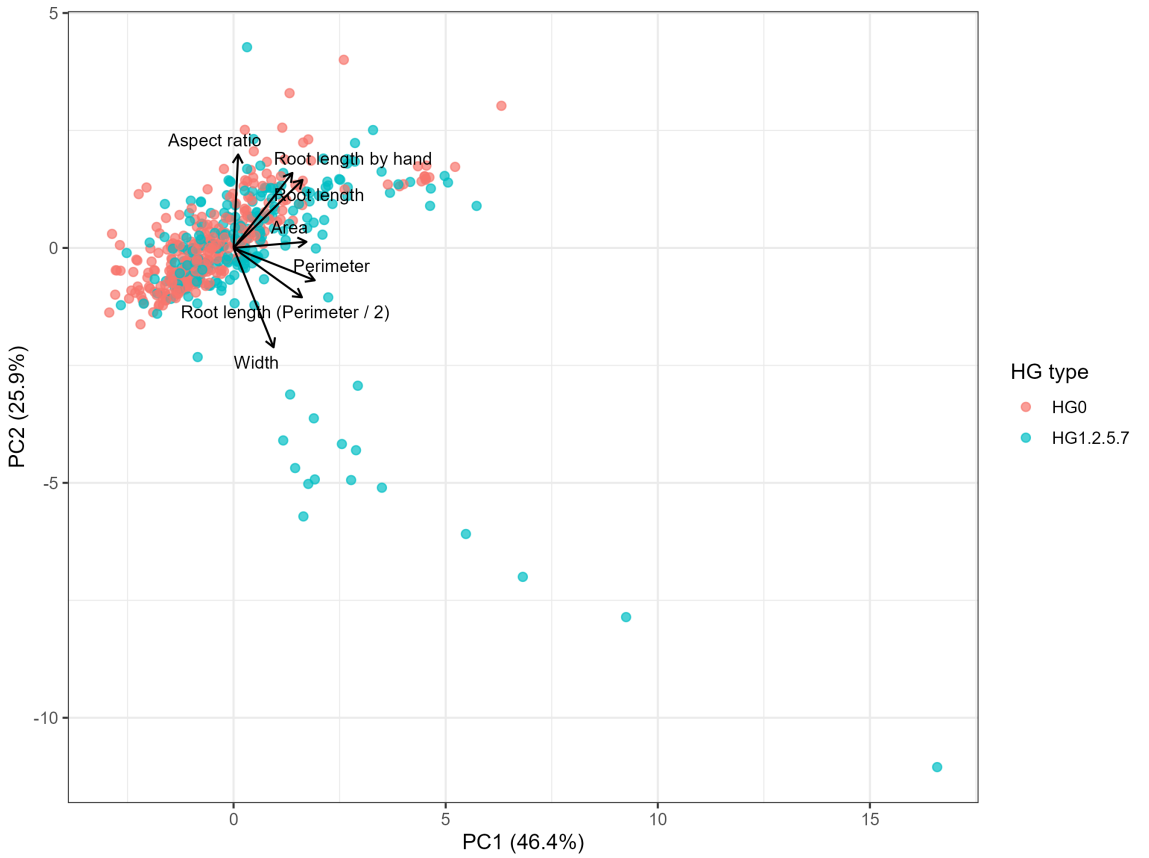

Figure 3.6: Principal component analysis (PCA) biplot of seven root morphological traits measured in wild soybean accessions. Points represent individual plants and are colored according to the SCN population used for infection (HG 0 in pink and HG 1.2.5.7 in blue). Arrows indicate trait loadings on the first two principal components (PC). PC1 represents overall root system size, with strong contributions from perimeter area, total root length, root length derived from perimeter (RLP) and manually measured root length. PC2 reflects variation in root architecture, primarily driven by root width and aspect ratio.

To confirm the robustness of the observed accession responses using a model appropriate for count data, cyst counts were further analyzed using a negative binomial generalized linear model. Plant accession had a significant effect on SCN reproduction (χ^2 = 169.07, df = 43, P < 0.001), indicating variation in resistance among *Glycine soja* accessions. SCN population also had a significant effect (χ^2 = 4.49, df = 1, P < 0.05), showing that HG 0 and HG 1.2.5.7 differed in their average reproductive success across host accessions. However, the accession x population interaction was not significant (χ^2 = 48.13, df = 43, P = 0.23), showing similar accession response to the two SCN populations.

Contrasts comparing HG 0 and HG 1.2.5.7 within each accession were evaluated and adjusted for multiple testing using the Benjamini-Hochberg false discovery rate correction. Model estimated cyst counts derived from the negative binomial GL model illustrate the variation in nematode reproduction among the selected *G. soja* accessions when infected with the two SCN populations (Figure 3.7). A single accession, H21, exhibited significantly different SCN reproduction between the two populations (FDR < 0.05) as summarized in Table B7. This plant accession changes from resistant to moderately susceptible (R $\rightarrow$ MS) between HG 0 and HG 1.2.5.7. Resistance breadth across SCN populations was summarized using female index values for each accession (Table B8). Only two accessions, S54 and S55 maintained resistance to both populations, while other accessions (excepting H21) exhibited mostly small shifts of increased susceptibility from HG 0 to HG 1.2.5.7. These findings highlight the diverse resistance responses and root phenotypes present within *G. soja* and provide a framework for understanding how host accession and root architecture may influence SCN reproduction across pathogen populations.

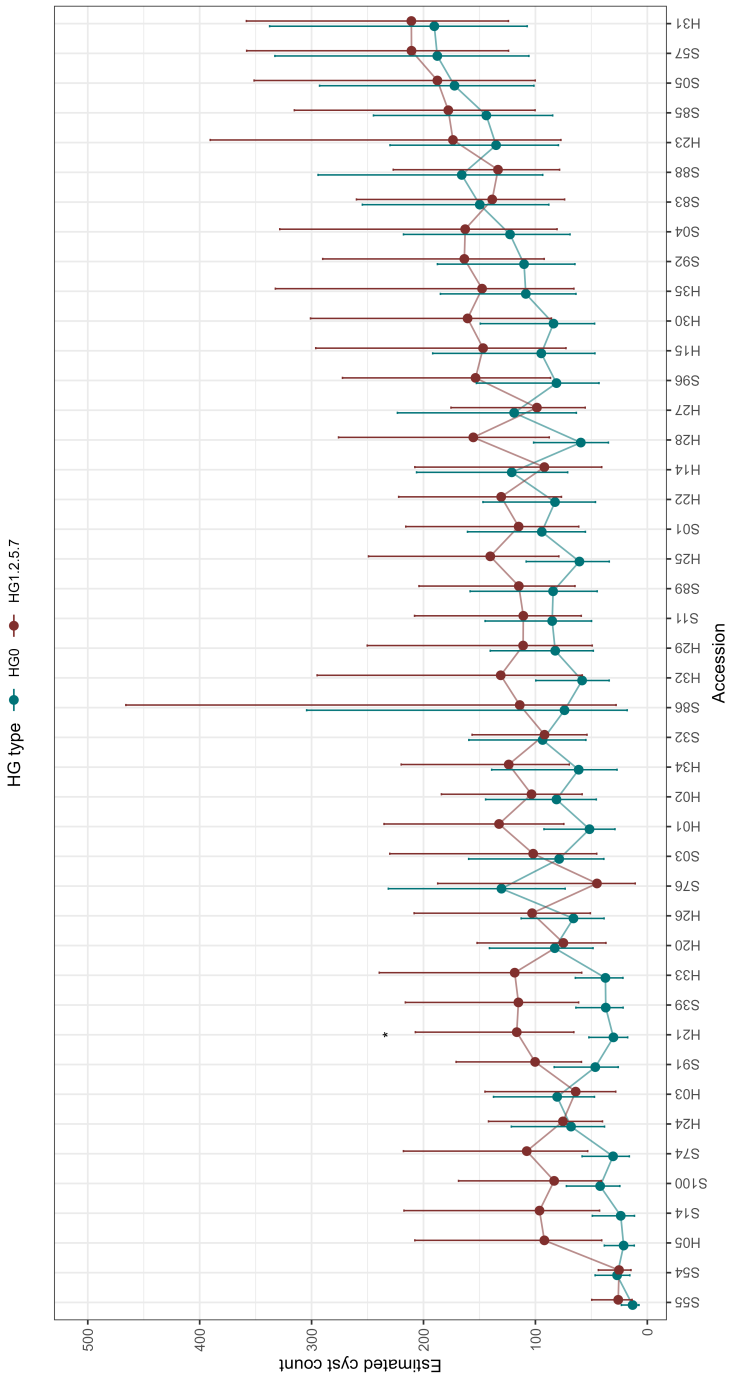

Figure 3.7: Model-estimated cyst counts from the negative binomial generalized linear model showing variation in soybean cyst nematode reproduction when select *G. soja* accessions are infected with SCN populations HG 0 (blue) and HG 1.2.5.7 (red). A star indicates significantly different estimated cyst counts between accessions after Benjamini–Hochberg correction.

3.4 Discussion

Patterns of Resistance in Wild Soybean

Evaluation of two soybean cyst nematode populations revealed substantial variation in resistance phenotype, including broad-spectrum and population-specific responses. A significant accession-pathogen interaction confirmed that SCN reproduction was dependent on specific host-pathogen combinations, indicating non-uniform resistance across SCN populations HG 0 and HG 1.2.5.7. These interactions highlight the complexity of resistance expression in wild soybean, and underscore the importance of evaluating accessions across multiple pathogen populations.

Two accessions, S54 and S55, exhibited strong and consistent resistance to both HG 0 and HG 1.2.5.7. Both maintained Female Index (FI) values less than 10% across both populations. Importantly, they did not show significant differences in cyst counts between pathogen treatments. This pattern suggests effective resistance mechanisms for both the less virulent (HG 0) and more virulent (HG 1.2.5.7) SCN populations. Broad-spectrum resistance of this nature is particularly valuable for soybean breeding. Field populations of SCN are heterogeneous and continually evolving under selection pressures from deployed resistance sources (Gardner et al., 2017).

S54 in particular has emerged as a source of broad-spectrum SCN resistance, both in this study and as a part of Zhang et al.'s 2016 genome-wide association study (GWAS). When resistance classifications from the present study were compared with the prior HG 2.5.7 pre-screen, S54 and S55 emerged as the clearest candidates for broad-spectrum resistance across multiple SCN populations (Table 3). Candidate genes associated with SCN resistance in the GWAS study included genes commonly associated with general plant defense and SCN-specific defense mechanisms, reinforcing the suitability of S54 as a source of SCN resistance. To a lesser degree, S55 also exhibits broad-spectrum SCN resistance. Previously, S55 was found to be moderately resistant to HG 2.5.7 (H. Zhang et al., 2016-a). With FI < 10 for HG 0 and HG 1.2.5.7 in this study, S55 is still an important new source of broad-

spectrum resistance for soybean. The majority of the *G. soja* accessions screened have been found to be susceptible to this pathogen; the identification of broad-spectrum resistance is an important step in the development of new and durable soybean cultivars. (H. Zhang et al., 2016-a).

Table 3.2: Breadth of soybean cyst nematode resistance across selected *Glycine soja* accessions challenged with multiple SCN populations. Accessions were selected from a genome-wide association study of SCN resistance using HG 2.5.7 (Zhang et al., 2016). In this study, HG 0 and HG 1.2.5.7 were used to evaluate resistance in previously identified accessions. Values represent Female Index (FI).

Accession	HG 0	HG 1.2.5.7	HG 2.5.7 (2016)
S54	6.2	8.1	5.2
S55	3.0	8.6	14.1
S100	9.7	26.7	3.3
H05	4.9	29.5	17.5
H21	7.0	37.4	19.1

SCN resistance (FI < 10) was uncommon in both studies, but several accessions only showed relatively minor shifts of resistance. Plant accession H21 was an exception, and only exhibited FI < 10 for HG 0; in this study, cyst count on this accession was significantly higher on HG 1.2.5.7 than on HG 0. In 2016, H21 only maintained moderate resistance (FI = 19.1), though we were unable to determine if there was a significant difference between HG 2.5.7 cyst counts in 2016 and the two populations used in this study.

In contrast, several accessions displayed population-specific resistance patterns. Multiple accessions categorized as resistant or moderately resistant to HG exhibited increased susceptibility to HG 1.2.5.7. This shift in FI ranking for some *G. soja* accessions indicates that certain resistance mechanisms against HG 0 are insufficient against more virulent SCN populations that are capable of reproducing on commonly deployed sources of resistance (Peking and PI 88788). Such population-dependent responses are consistent

with the evolutionary pressure imposed by long-term use of specific resistance genes in commercial soybean production; this adaptation of virulent SCN populations illustrates the vulnerability of relying on a limited set of resistance mechanisms (Crop Science US, 2025; Torabi et al., 2023). It is also notable that though several accessions shifted numerically in FI category between the HG 0 and HG 1.2.5.7 populations, NB-GLM modeling with FDR-corrected contrasts indicated only one accession (H21) exhibited a statistically robust population-specific difference in SCN reproduction.

Moderate resistance (MR) was common among the evaluated accessions. Though more wild soybean accessions displayed moderate resistance to HG 0, nine accessions infected with HG 1.2.5.7 were also categorized as MR. Accessions that displayed moderate resistance may contribute to reduced SCN reproduction over time, particularly when deployed in combination with other resistance sources (Meinhardt et al., 2021). Moderate resistance soybean cultivars have high yield potential, despite higher SCN reproduction than on resistant cultivars, giving them interesting potential in the development of new cultivars with durable SCN resistance (Adee et al., 2008). Moderate resistance, as well as rotation between different resistance sources, generally exerts less selective pressure on pathogenic nematode populations. Germplasm resources with Moderate SCN resistance may be effective for reducing nematode load, if less acting in a less suppressive manner than sources with "full" resistance. Moderately resistant sources of SCN resistance do not force the same rapid, uniform adaptation that stronger forms of resistance like Peking and PI 88788 have in the past (Niblack et al., 2008). Interestingly, both resistant and moderately resistant cultivars seem to produce a carry-over effect on SCN reproduction. In a study by Adee et al., 2008, fields planted with both resistant and moderately resistant cultivars were planted the following year with susceptible cultivars. Yields in the final year were higher in those fields, even with the use of susceptible cultivars (Adee et al., 2008). This illustrates the value of moderate resistance. Rather than being viewed as insufficient for failing to meet the sub-10% Female Index threshold, it should be recognized as a critical component

in the development of diverse SCN resistance mechanisms.

Collectively, these findings demonstrate that *Glycine soja* harbors diverse resistance phenotypes, including both broad-spectrum and population-specific responses. This diversity reinforces the value of soybean wild relative germplasms as a reservoir of resistance variation and highlights the importance of evaluating accessions across multiple SCN populations to accurately characterize resistance durability. The contrasting responses observed between HG 0 and HG 1.2.5.7 suggest different accessions may interfere with distinct stages of SCN infection, such as initial establishment, syncytium development, or female maturation (Torabi et al., 2023).

Pathogen Population Context and Selection Pressures

The contrasting resistance patterns among *Glycine soja* accessions must be interpreted within the broader evolutionary dynamics of *Heterodera glycines* populations. Historically, HG type 0 populations (previously known as race 3) were among the most prevalent in production fields in the United States (Critchfield et al., 2023; Herschman et al., 2008; Tylka & Marett, 2024). HG 0 also remains a population type of concern in other major soybean growing regions, including China and Brazil (You et al., 2024; de Almeida et al., 2020). HG 0 populations are characterized by limited virulence toward commonly deployed resistance sources. However, widespread and prolonged utilization of resistance derived from PI 88788 has imposed strong selection pressures on SCN populations, resulting in the increasing presence of more virulent SCN populations, including HG 1.2.5.7. Since these populations are increasingly capable of reproductive success on both Peking- and PI 88788- sources of resistance, the prolonged durability of these sources is reduced in commercial cultivars.

The differential performance of wild soybean accessions against HG 0 and HG 1.2.5.7 reflects this evolutionary pattern. Accessions that were resistant to HG 0 but moderately resistant or susceptible to HG 1.2.5.7 likely possess mechanisms effective against less virulent populations of SCN, but may be insufficient to suppress reproduction on more

aggressive SCN populations. In contrast, the identification of accessions such as S54 and S55, which maintained low FI values between populations, suggests the presence of resistance mechanisms effective in a broader spectrum of SCN virulence.

Field populations of SCN are never homogeneous. Fields often contain mixtures of HG types, and the relative frequency of virulent populations can shift over time depending on the resistance sources deployed, and sexual reproduction provides a continuous reshuffling of virulence genes. SCN has a short generation time and can survive in fields for up to a decade (Gauthier et al., 2020). Therefore, pathogen populations can respond to selection pressure more rapidly than breeding programs develop new resistant cultivars. As a result, resistance effective against a single HG profile will not remain durable under sustained selection pressure (Mitchum, 2016; McCarville et al., 2017).

The deployment of highly effective resistance sources, while desirable, must be used with caution. The selection of SCN resistant soybean cultivars must be done with care to balance the need for strong resistance in the present without dramatically shifting the virulence of SCN, which may affect future crops. SCN resistance derived from PI 437654 (HG type line 4) is particularly effective in the short term. Although fewer field populations of SCN can reproduce in cultivars with this resistance source, SCN capable of reproducing has been shown to have increased reproductive success in all other resistance indicator lines. Despite its effectiveness, continuous use of this source of resistance is not recommended due to concerns about future virulence of SCN (Gardener et al., 2017). PI 437654 is an illustrative warning of how intense selection pressure on a single resistance source may unintentionally accelerate the emergence of broadly virulent SCN populations.

The results of this study underscore the importance of screening germplasms against multiple SCN populations. Reliance on a single type of SCN may overestimate the breadth or durability of resistance, particularly in regions where virulent populations are increasingly observed. The diversity of resistance responses observed among wild soybean accessions highlights the value of evaluating germplasms under varying virulence pressures to better

anticipate field performance and long-term resistance stability.

Root Architecture Responses to SCN Infection

Variation in root system architecture in wild soybean accessions was substantial and strongly correlated with the accession to wild soybeans and the pathogen population. Among the seven traits evaluated, root as a function of the perimeter (RLP) demonstrated the most consistent and robust statistical signal, exhibiting significant effects of accession and pathogen population, as well as accession x pathogen effects during early SCN infection. These results indicate that root architectural responses to SCN infection are not uniform across genetic backgrounds or pathogen population type, and depend on the specific host-pathogen combination.

Across nearly all accessions, RLP was greater under HG 1.2.5.7 relative to HG 0 after 1 SCN life cycle across diverse genetic backgrounds. In contrast, the perimeter of the root and the area of the root exhibited significant accession-pathogen interactions in smaller subsets of SCN-challenged accessions, indicating that architectural responses were more variable for these secondary traits. The stronger and more uniform response observed for RLP supports its use as the primary root architecture phenotype in this study.

The increase in RLP under HG 1.2.5.7 could reflect compensatory root growth in response to infection or differential allocation of resources triggered by pathogen challenge (Radcliffe et al., 1990; Willig et al., 2023). Because root measurements were obtained at the end of the SCN life cycle, it is not possible to determine whether architectural variation preceded infection or arises as a consequence of it. Nevertheless, consistent pathogen-dependent differences in RLP between accessions indicate that the identity of the SCN population plays a measurable role in shaping host root architecture.

Importantly, RLP and other size-related traits were positively correlated with cyst reproduction. The moderate, positive correlation between RLP and cyst count suggests that larger functional root systems are associated with increased cyst counts across accessions and treatments. However, regression analysis further revealed that this relationship was

pathogen-dependent. Root architecture predicted cyst reproduction under HG 0, but not under HG 1.2.5.7. This suggests that root development may facilitate reproduction in less virulent populations, whereas more aggressive SCN populations are governed more strongly by host resistance mechanisms than by root size alone.

These findings illustrate that smaller root sizes were associated with reduced SCN reproduction only under the HG 0 population. Wild soybean accessions that exhibit broad-spectrum resistance did not consistently show a reduced RLP relative to more susceptible accessions. These results demonstrate that, while root architecture can influence soybean cyst nematode reproduction under certain virulence conditions, it is not a reliable predictor of genetic resistance or lack thereof. Root size can serve as a proxy for soybean health, though comparisons with uninfected roots would be a more robust indicator of the effect of SCN on root development (Noh et al., 2022; Soybean Cyst Nematode | Integrated Pest Management Program, University of Kentucky). Resistance appears to be governed primarily by host-pathogen genetic interactions rather than by large-scale root dynamics alone.

Together, these results indicate that root architecture phenotypes are dynamic host traits influenced by both plant host accession and pathogen population, and that their relationship to soybean cyst nematode reproduction is context dependent. The development of root structure is a continuous process over the course of a growing season. The effects can be small, inconsistent, and depend on both the environment and the timing. Prior studies of early SCN infection reported variable effects of *H. glycines* on soybean root length. Since measurements in this study were taken after approximately one SCN life cycle, the observed differences in RLP likely reflect integrated host responses over the infection period rather than only the effects of early infection (Niblack et al., 1986). Even extremely high infection levels, while affecting nitrogen fixation, leaf area, and leaf color, do not always have a significant impact on root development (Akinrinlola et al., 2024), yet roots may be stunted or distorted by a longer term of infection (Arjoune et al., 2022). The interplay

between root structure variation and pathogen virulence adds a layer of complexity to wild soybean resistance phenotypes. Morphological differences in host traits between pathogen populations highlight the need to consider more than just resistance when evaluating host response to SCN.

Ecological Trade-offs Between Root Growth and Resistance

Plant defenses against pathogens are frequently discussed within the context of growth-defense trade offs. The allocation of resources to resistance mechanisms may reduce growth or reproductive capacity. However, in the soybean-SCN model evidence for consistent growth penalties associated with resistance has been mixed. In the present study, strong resistance phenotypes were not consistently associated with reduced root size relative to more susceptible accessions within the treatments evaluated. Resistant accessions such as S54 and S55 did not exhibit a markedly reduced RLP, perimeter, or root area compared to other accessions under SCN challenge, suggesting that effective resistance in these lines did not impose an obvious cost to the root structure during the experiment.

Similarly, the architectural differences of the roots between HG 0 and HG 1.2.5.7 were largely directional rather than suppressive. The RLP was generally higher with infection with HG 1.2.5.7. This pattern does not support the model in which increased defense against more virulent pathogen populations constrains root growth. Instead, root size responses appear to reflect dynamic host-pathogen interactions rather than a uniform cost of resistance.

It is important to note that this study did not include a non-inoculated control for root measurements. Conclusions about absolute growth penalties associated with resistance cannot be drawn. Root traits were measured following one SCN life cycle, capturing a snapshot of *G. soja* response to infection, rather than its baseline potential for root growth potential. Although no clear trade-off was observed between growth and defense, further work incorporating uninfected controls and extended time points would be beneficial in assessing potential long-term allocation costs in wild soybean.

These early findings are consistent with reports in cultivated soybeans, indicating that the major SCN resistance loci, including Rhg1 and *Rhg4*, do not universally impose severe early growth penalties under SCN infection (Donald et al., 2006). Together, the results suggest that wild soybeans that harbor SCN resistance mechanisms that suppress nematode reproduction without early effects on resource allocation, at least within the timeframe examined.

Breeding for SCN Resistance

Although functional root length (RLP) was positively associated with cyst production in HG 0, this relationship was negligible in the more virulent population of HG 1.2.5.7. These findings suggest that the size of the root system during SCN infection is a dynamic population-specific trait, the magnitude is strongly dependent on host accession, the virulence of the infecting SCN population and other factors (Audette et al., 2020).

Root architecture is not only influenced by the existing host background, but by the specific SCN population encountered. From a breeding perspective, these results do not support the idea that root system size serves as a proxy for SCN resistance, nor do they suggest reduced root growth is inherently associated with lower nematode reproduction. Across accessions, resistance was not consistently accompanied by a diminished root architecture. This absence of a clear trade off between resistance and RLP, root area, or root perimeter indicates the genetics-driven nature of SCN resistance in wild soybean. The root system architecture remains critical for nutrient acquisition, tolerance to abiotic stress, and overall plant vigor. The identification of accessions that maintain strong suppression of SCN reproduction across accessions without apparent disadvantage to root structure underscores the value of broad-spectrum genetic resistance mechanisms that operate independently of root size.

Germplasm Screening and Soybean Breeding Strategy

Reliance on a single SCN population type can overestimate the breadth of resistance and obscure population-specific strengths and weaknesses. Identifying accessions such

as S54 and S55, which suppressed reproduction in both populations without evidence of compromised root architecture, highlights the potential utility of wild soybean as a source of resistance mechanisms that differ from those currently used in *G. max* cultivars.

This study demonstrates that these traits are not proxies for predicting resistance. In particular, RLP demonstrated a statistically significant interaction with HG type in the regression model. This population-specific interaction indicates the interplay between root growth and reproductive success of certain SCN populations, but it does not work as a prediction model for the resistance phenotype. Accessions with larger root systems were not uniformly more susceptible to SCN. Genetic mechanisms, such as those that involve pathogen recognition, feeding site disruption, and cellular defense pathways, operate independently of macro-scale root traits. *Glycine max* resistance loci have previously been found to be linked to genes that regulate root architecture (Dong & Hudson, 2021); *Glycine soja* root traits may exhibit similar patterns and this potential should be investigated more thoroughly.

Together, these findings support a breeding strategy that prioritizes multi-population screening, incorporation of diverse resistance sources, and careful monitoring of pathogen population structure. Given the capacity of SCN populations to adapt rapidly to resistance mechanisms, durable and diverse sources of resistance will remain central to the development and deployment of new SCN resistant cultivars. This will likely require pyramiding of multiple resistance loci, rotation of resistance sources, and continued surveillance of the virulence profiles of SCN populations.

Study Limitations and Experimental Considerations

Several aspects of this study should be taken into account when interpreting the results of this study. First, the root architectural responses were evaluated over a single soybean cyst nematode life cycle (approximately 30 days). While this time frame captures early infection dynamics and initial host-pathogen interactions, it does not reflect the cumulative effects of multiple SCN generations that may occur over the course of multiple

nematode generations in a growing season, or the effects of field conditions in which SCN have already been established. Previous studies have demonstrated that early root responses to *Heterodera glycines* may differ from later season responses, particularly under field conditions where repeated, potentially overlapping, infection cycles may occur. Differences among physiological responses are related not only to the host accession, but also the timing of SCN infection (Wrather & Anand, 1988). Therefore, architectural patterns observed here should be interpreted as early-stage responses, rather than long-term outcomes of SCN infection.

Additionally, root phenotypes were measured only under SCN infected conditions. a non-inoculated control group was not included for architectural comparisons. As such, this study cannot fully interpret the effect of SCN infection on the baseline root morphology differences between *G. soja* accessions. However, the design does allow for robust inference regarding differences between HG 0 and HG 1.2.5.7. Using infection of HG 0, an SCN population with no adaptive advantage over currently deployed sources of SCN resistance, gives a different, and still useful baseline of response to SCN infectivity.

Functional root length (RLP), root area, and root perimeter were derived from the same root system scans, and therefore represent mathematically related but biologically distinct descriptors of root architecture. While these traits are correlated, RLP consistently exhibited the strongest accession and accession-interaction effects, making it the primary root structure metric for interpretation. Root area and root perimeter showed similar directional patterns to RLP. These aligned metrics suggest that the pattern is not the artifact of one specific measurement, but reflect a biologically meaningful relationship between *the Glycine soja* root architecture and the reproduction of the SCN rather than the artifacts of a single measurement.

In this study, plants were grown in sand and inoculated with SCN eggs rather than second-stage juveniles (J2). While sand provides a uniform medium that facilitates cyst and root recovery, and is common in nematology studies (Halbrendt et al., 1992; Kofsky

et al., 2021; H. Zhang et al., 2016-a), it may alter nematode mobility and penetration dynamics relative to field soils (Davis & Tylka, 2021; Koenning et al., 1988; Niblack et al., 1986; Wallace, 1968). Egg inoculation mimics more closely natural infection processes than direct J2 inoculation. Inoculation with J2 bypasses natural hatching signals and can unintentionally alter early infection dynamics relative to egg-based inoculation. (Niblack, 2005). Egg inoculation was also utilized for consistency with methods by Zhang et al., 2016 (H. Zhang et al., 2016-a). However, egg inoculation may introduce additional variability due to potential asynchronous hatch timing between replicates, host accessions, and SCN populations. Differences in root exudates produced by wild soybean accessions with distinct genetic backgrounds may also influence SCN hatching behavior (Tefft & Bone, 1985; C. Wang et al., 2018). Importantly, growth media and egg numbers were consistent across accessions and populations, allowing valid comparative interpretation even if values differ from field environments.

Variability in cyst counts was observed in some accessions. Rather than representing methodological error, this variation is consistent with the quantitative nature of SCN resistance and the differing genetic backgrounds of the wild soybean accessions used in this study. To mitigate inflation of variance, statistical analyses were restricted to accession-pathogen combinations with at least three biological replicates. This filtering step increases confidence in the reported accession-specific comparisons while maintaining a broad representation of the diversity of the germplasm. In the cases of the combinations of S86-HG 0 and S76-HG 1.2.5.7, female indices with insufficient replications were reported for transparency and completeness, not as indications of their full capacity for resistance to SCN or lack thereof. These accessions were previously identified as resistant (R) and moderately resistant to HG 2.5.7, respectively, so their inclusion as potential resistance sources is appropriate if incomplete in this study (Zhang et al., 2016-a).

The results of the generalized negative binomial linear model, which accounts for the overdispersed count data, largely supported the patterns observed in the ANOVA analysis,

indicating that accession effects dominated SCN reproduction, while population-specific differences were limited. ANOVA was sufficient to explain variation within the population and has traditionally been used in soybean-SCN studies. However, NB-GLM provided a more robust description of the effects of accession on differential SCN reproduction. ANOVA suggested several differences in accession x population, yet NB-GLM showed that only H21 had significantly different effects on SCN reproduction between the two HG types. In this way, GLM and the use of the Benjamini-Hochberg FDR correction illustrated the rarity of full resistance and the stability of the response to resistance to wild soybeans in all types of SCN populations.

Finally, greenhouse screening cannot fully replicate the complexity of field environments, where mixed SCN populations, fluctuating environmental conditions, and the potential addition of other abiotic and biotic stressors shape host-pathogen dynamics. However, controlled greenhouse assays are essential to isolate population-specific effects of the pathogen prior to further field validation. Screening in this manner allowed us to narrow down *G. soja* accessions with the potential for broad-spectrum and pathogen-specific resistance to soybean cyst nematodes.

Future Directions

The results of this study highlight several avenues for continued investigation of the interaction between wild soybean resistance and the SCN population. Multi-generational assays would help determine whether the architectural responses observed after a single SCN life cycle persist, amplify, or stabilize over time. The loss of SCN yield is typically associated with cumulative population accumulation, rather than early infection alone. Longer-term microplot or greenhouse studies could reveal whether accession-specific root responses influence subsequent generations of SCN. Integration of genetic or metabolic analysis would strengthen the interpretation of the phenotypic patterns observed in this study. Characterization of the molecular responses of accessions with broad-spectrum resistance compared to pathogen population-specific accessions could determine the mechanisms by

which resistance is achieved. Given that wild soybeans harbor substantial untapped genetic diversity, identification of resistance alleles and molecular responses distinct from those currently in use would be particularly valuable for breeding programs seeking to diversify resistance mechanisms.

The relationship between root system architecture and SCN reproduction warrants further study. Though this study demonstrates population-specific associations between RLP and SCN reproduction, the physiological basis of these differences remains unclear. Controlled experiments examining feeding site establishment and development, or studies examining resource allocation under contrasting SCN populations or other plant stress conditions could help determine whether the architectural variation influences infection success rather than reflecting downstream host responses to SCN development.

These considerations emphasize the importance of integrating population biology, quantitative phenotyping, and genetic analysis to better understand SCN adaptation to resistance mechanisms and improve the long-term durability of SCN resistance.

References

Acharya, K., & Yan, G. (2021). Screening of Early Maturing Soybean Accessions for Resistance Against HG Type 2.5.7 of Soybean Cyst Nematode *Heterodera glycines*. *Plant Health Progress*, 23(2), 166–173. https://doi.org/10.1094/php-07-21-0105-rs

Adee, E. A., Johnson, M. L., & Niblack, T. L. (2008). Effect of soybean cultivars moderately resistant to soybean cyst nematode on SCN populations and yield. *Plant Health Progress*, 9(1). https://doi.org/10.1094/php-2008-0618-03-rs

Anand, A., Subramanian, M., & Kar, D. (2023). Breeding techniques to dispense higher genetic gains. *Frontiers in Plant Science*, 13, 1076094. https://doi.org/10.3389/fpls.2022.1076094

Akinrinlola, R. J., Kelly, H. M., Sinclair, T. R., & Shekoofa, A. (2024). *Heterodera glycines* HG type 1.2.5.7 causes a decrease in soybean (*Glycine max* [L.] Merr.) nitrogen fixation and growth variables. *Journal of Crop Improvement*, 38(4), 299–316 https://doi.org/10.1080/15427528.2024.2336267

Arantes, N. E., Mauro, A. O., & Tihohood, D. (1998). An Alternative Field Method for Screening Soybean Genotypes for Resistance to *Heterodera glycines*. *PubMed*, 30(4S), 542–546. https://pubmed.ncbi.nlm.nih.gov/19274244

Arelli, P. R., Mengistu, A., Nelson, R. L., Cianzio, S. R., & Vuong, T. (2015). New Soybean Accessions Evaluated for Reaction to *Heterodera glycines* Populations. *Crop Science*, 55(3), 1236–1242.

Arjoune, Y., Sugunaraj, N., Peri, S., Nair, S. V., Skurdal, A., Ranganathan, P., & Johnson, B. (2022). Soybean cyst nematode detection and management: a review. *Plant Methods*, 18(1). https://doi.org/10.1186/s13007-022-00933-8

Audette, C., Bélanger, R. R., & Mimee, B. (2020). Coinfection of soybean plants with *Phytophthora sojae* and soybean cyst nematode does not alter the efficacy of resistance genes. *Plant Pathology*, 69(8), 1437–1444. https://doi.org/10.1111/ppa.13227

Bauhus, J., & Messier, C. (1999). Evaluation of fine root length and diameter measure-

ments obtained using RHIZO image analysis. *Agronomy Journal*, 91(1), 142–147. https://doi.org/10.2134/agronj1999.00021962009100010022x

Benjamini, Y., & Yekutieli, D. (2001). The control of the false discovery rate in multiple testing under dependency. *The Annals of Statistics*, 29(4). https://doi.org/10.1214/aos/1013699998

Brozynska, M., Furtado, A., & Henry, R. J. (2016). Genomics of crop wild relatives: expanding the gene pool for crop improvement. *Plant Biotechnology Journal*, 14(4), 1070–1085.

CI-202 Portable Laser Leaf Area Meter. (2020, December 8). CID Bio-Science. https://cid-inc.com/plant-science-tools/leaf-area-measurement/ci-202-portable-laser-leaf-area-meter/

Comas, L., Bouma, T., & Eissenstat, D. (2002). Linking root traits to potential growth rate in six temperate tree species. *Oecologia*, 132(1), 34–43. https://doi.org/10.1007/s00442-002-0922-8

Costa, C., Dwyer, L. M., Zhou, X., Dutilleul, P., Hamel, C., Reid, L. M., & Smith, D. L. (2002). Root morphology of contrasting maize genotypes. *Agronomy Journal*, 94(1), 96–101. https://doi.org/10.2134/agronj2002.9600

Critchfield, R., King, J., Bonkowski, J., Telenko, D., Creswell, T., & Zhang, L. (2023). Characterization of Virulence Phenotypes of *Heterodera glycines* during 2020 in Indiana. *Journal of Nematology*, 55(1). https://doi.org/10.2478/jofnem-2023-0039

Crop Science US. Understanding Soybean cyst nematode Genetic Resistance. (n.d.). Bayer Farmer Experience. https://www.cropscience.bayer.us/articles/bayer/understanding-scn-genetic-resistance

Davis, E L., Tylka, G. L. (2021). Soybean cyst nematode disease. *The Plant Health Instructor*. https://doi.org/10.1094/phi-i-2000-0725-0

De Almeida Moreira, J. A., Tavares, M. C., De Araújo, F. G., & De Menezes, I. P. P. (2020). Genetic diversity of Soybean Cyst Nematode (*Heterodera glycines*) populations in

Southeastern Goiás state, Brasil. *Australian Journal of Crop Science*, 14(7):2020, 1162–1170. https://doi.org/10.21475/ajcs.20.14.07.p2470

Dempewolf, H., Baute, G., Anderson, J., Kilian, B., Smith, C., & Guarino, L. (2017). Past and Future Use of Wild Relatives in Crop Breeding. *Crop Science*, 57(3), 1070–1082.

Donald, P. A., Pierson, P. E., St Martin, S. K., Sellers, P. R., Noel, G. R., Macguidwin, A. E., Faghihi, J., Ferris, V. R., Grau, C. R., Jardine, D. J., Melakeberhan, H., Niblack, T. L., Stienstra, W. C., Tylka, G. L., Wheeler, T. A., & Wysong, D. S. (2006b). Assessing *Heterodera glycines*-Resistant and susceptible cultivar yield response. *PubMed*, 38(1), 76–82. https://pubmed.ncbi.nlm.nih.gov/19259433

Dong, J., & Hudson, M. E. (2021). WI12 Rhg1 interacts with DELLAs and mediates soybean cyst nematode resistance through hormone pathways. *Plant Biotechnology Journal*, 20(2), 283–296. https://doi.org/10.1111/pbi.13709

Fixing the bridge between biologists and statisticians. Correcting for multiplicity in the "emmeans" package. (2026b, January 21). https://www.statforbiology.com/2026/stat_mcp_multivariatet/

Ford-Lloyd, B. V., Schmidt, M., Armstrong, S. J., Barazani, O., Engels, J., Hadas, R., Hammer, K., Kell, S. P., Kang, D., Khoshbakht, K., Li, Y., Long, C., Lu, B., Ma, K., Nguyen, V. T., Qiu, L., Ge, S., Wei, W., Zhang, Z., & Maxted, N. (2011). Crop Wild Relatives—Undervalued, Underutilized and under Threat? *BioScience*, 61(7), 559–565. https://doi.org/10.1525/bio.2011.61.7.10

Gardner, M., Heinz, R., Wang, J., & Mitchum, M. G. (2017). Genetics and adaptation of soybean cyst nematode to broad spectrum soybean resistance. *G3 Genes Genomes Genetics*, 7(3), 835–841. https://doi.org/10.1534/g3.116.035964

Gauthier, N., Kaiser, C., Bradley, C., & University of Kentucky College of Agriculture, Food & Environment Extension Plant Pathology. (2020). Soybean cyst nematode: a potential problem for nurseries. In *Plant Pathology Fact Sheet* (Report PPFS-

OR-W-33). University of Kentucky College of Agriculture, Food and Environment Cooperative Extension Service. https://plantpathology.mgcafe.uky.edu/files/ppfs-or-w-33.pdf

Halbrendt, J. M., Lewis, S. A., & Shipe, E. R. (1992). A Technique for Evaluating *Heterodera glycines* Development in Susceptible and Resistant Soybean. *PubMed*, 24(1), 84–91. https://pubmed.ncbi.nlm.nih.gov/19283206

Herman, T. K., Han, J., Singh, R. J., Domier, L. L., & Hartman, G. L. (2020). Evaluation of wild perennial Glycine species for resistance to soybean cyst nematode and soybean rust. *Plant Breeding*, 139(5), 923–931.

Hershman, D. E., Heinz, R. D., & Kennedy, B. S. (2008). Soybean Cyst Nematode, *Heterodera glycines*, Populations Adapting to Resistant Soybean Cultivars in Kentucky. *Plant Disease*, 92(10), 1475. https://doi.org/10.1094/pdis-92-10-1475b

Hua, C., Li, C., Hu, Y., Mao, Y., You, J., Wang, M., Chen, J., Tian, Z., & Wang, C. (2018). Identification of HG Types of Soybean Cyst Nematode *Heterodera glycines* and Resistance Screening on Soybean Genotypes in Northeast China. *Journal of Nematology*, 50(1), 41–50. https://doi.org/10.21307/jofnem-2018-007

Hwang, E.-Y., Wei, H., Schroeder, S. G., Fickus, E. W., Quigley, C. V., Elia, P., Araya, S., Dong, F., Costa, L., Ferreira, M. E., Cregan, P. B., & Song, Q. (2019). Genetic Diversity and Phylogenetic Relationships of Annual and Perennial 'textitGlycine Species. *G3 Genes|Genomes|Genetics*, 9(7), 2325–2336.

Jacquet, S., Li, S., Mian, R., Kassem, M. A., Rashad, L., Viera, S., Reta, F., Reta, J., & Yuan, J. (2023). Evaluating the Response of *Glycine soja* Accessions to Fungal Pathogen *Macrophomina phaseolina* during Seedling Growth. *Plants*, 12(22), 3807.

Jenkins, W. R. (1964). A rapid centrifugal-flotation technique for separating nematodes from soil. *The Plant Disease Reporter*, 48(9).

Kim, K., Vuong, T. D., Qiu, D., Robbins, R. T., Shannon, J. G., Li, Z., & Nguyen, H. T. (2016). Advancements in breeding, genetics, and genomics for resistance to

three nematode species in soybean. *Theoretical and Applied Genetics*, 129(12), 2295–2311. https://doi.org/10.1007/s00122-016-2816-x

Kim, K-S., Kim, S., Kim, J., Tripathi, P., Lee, J., Chung, Y. S., & Kim, Y. (2021). A large root phenome dataset Wide-Opened the potential for underground breeding in soybean. *Frontiers in Plant Science*, 12, 704239. https://doi.org/10.3389/fpls.2021.704239

Kim, M. Y., Van, K., Kang, Y. J., Kim, K. H., & Lee, S. (2012). Tracing soybean domestication history: From nucleotide to genome. *Breeding Science*, 61(5), 445–452. https://doi.org/10.1270/jsbbs.61.445

Koenning, S. R., Anand, S. C., & Wrather, J. A. (1988). Effect of Within-field Variation in Soil Texture on *Heterodera glycines* and Soybean Yield. *PubMed*, 20(3), 373–380.https://pubmed.ncbi.nlm.nih.gov/19290226

Kofsky, J., Zhang, H., & Song, B.-H. (2021). Novel resistance strategies to soybean cyst nematode (SCN) in wild soybean. *Scientific Reports*, 11(1), 1–13.

La, T., Large, E., Taliercio, E., Song, Q., Gillman, J. D., Xu, D., Nguyen, H. T., Shannon, G., & Scaboo, A. (2019). Characterization of Select Wild Soybean Accessions in the USDA Germplasm Collection for Seed Composition and Agronomic Traits. *Crop Science*, 59(1), 233–251.

Lamichhane, S., & Thapa, S. (2022). Advances from Conventional to Modern Plant Breeding Methodologies. *Plant Breeding and Biotechnology*, 10(1), 1–14. https://doi.org/10.9787/pbb.2022.10.1.1

Leamy, L. J., Lee, C., Song, Q., Mujacic, I., Luo, Y., Chen, C. Y., Li, C., Kjemtrup, S., & Song, B. (2016). Environmental versus geographical effects on genomic variation in wild soybean (*Glycine soja*) across its native range in northeast Asia. *Ecology and Evolution*, 6(17), 6332–6344. https://doi.org/10.1002/ece3.2351

Li, F., Sayama, T., Yokota, Y., Hiraga, S., Hashiguchi, M., Tanaka, H., Akashi, R., & Ishimoto, M. (2024). Assessing genetic diversity and geographical differentiation in a global collection of wild soybean (*Glycine soja* Sieb. et Zucc.) and assigning a

mini-core collection. *DNA Research*, 31(2). https://doi.org/10.1093/dnares/dsae009

Li, L., Tian, R., Pu, Y., Cong, Y., Chen, X., Jia, K., & Li, N. (2024). Comprehensive analysis of the genetic variation dataset among wild soybean (*Glycine soja*) in Shandong Province, China. *BMC Genomic Data*, 25(1), 97. https://doi.org/10.1186/s12863-024-01280-4

Lian, Y., Yuan, M., Wei, H., Li, J., Ding, B., Wang, J., Lu, W., & Koch, G. (2023). Identification of resistant sources from *Glycine max* against soybean cyst nematode. *Frontiers in Plant Science*, 14, 1143676.

McCarville, M.T., Marette, C.C., Mullaney, M.P., Gebhart, G.D., Tylka, G. L. (2017). Increase in Soybean Cyst Nematode Virulence and Reproduction on Resistant Soybean Varieties in Iowa from 2001 to 2015 and the Effects on Soybean Yields. *Plant Health Progress*, 18(3), 146–155. https://doi.org/10.1094/php-rs-16-0062

Mengistu, A., Read, Q. D., Sykes, V., Kelly, H., Kharel, T., Bellaloui, N. (2024). Cover Crop and Crop Rotation Effects on Tissue and Soil Population Dynamics of *Macrophomia phaseolina* and Yield Under No-Till System. *Plant Disease*, 108(2), 302-310. https://doi.org/10.1094/pdis-03-23-0443-re

Meinhardt, C., Howland, A., Ellersieck, M., Scaboo, A., Diers, B., & Mitchum, M. G. (2021). Resistance gene pyramiding and rotation to combat widespread soybean cyst nematode virulence. *Plant Disease*, 105(10), 3238–3243. https://doi.org/10.1094/pdis-12-20-2556-re

Migicovsky, Z., & Myles, S. (2017). Exploiting wild relatives for genomics-assisted breeding of perennial crops. *Frontiers in Plant Science*, 8, 460. https://doi.org/10.3389/fpls.2017.00460

Niblack, T. L. (2005). Soybean Cyst nematode management reconsidered. *Plant Disease*, 89(10), 1020–1026. https://doi.org/10.1094/pd-89-1020

Niblack, T. L., Arelli, P. R., Noel, G. R., Opperman, C. H., Orf, J. H., Schmitt, D. P., Shannon, J. G., & Tylka, G. L. (2002). A Revised Classification Scheme for

Genetically Diverse Populations of *Heterodera glycines*. *Journal of Nematology*, 34(4), 279–288.

Niblack, T. L., Colgrove, A. L., Colgrove, K., & Bond, J. P. (2008). Shift in Virulence of Soybean Cyst Nematode is Associated with Use of Resistance from PI 88788. *Plant Health Progress*, 9(1). https://doi.org/10.1094/php-2008-0118-01-rs

Niblack, T. L., Heinz, R. D., Smith, G. S., & Donald, P. A. (1993). Distribution, Density, and Diversity of *Heterodera glycines* in Missouri. *Journal of Nematology*, 25(4S), 880.

Niblack, T. L., Hussey, R. S., & Boerma, H. R. (1986). Effects of *Heterodera glycines* and *Meloidogyne incognita* on Early Growth of Soybean. *PubMed*, 18(4), 444–450. https://pubmed.ncbi.nlm.nih.gov/19294209

Niblack, T. L., Tylka, G. L., Arelli, P., Bond, J., Diers, B., Donald, P., Faghihi, J., Gallo, K., Heinz, R. D., Lopez-Nicora, H., Von Qualen, R., Welacky, T., & Wilcox, J. (2009). A standard greenhouse method for assessing soybean cyst nematode resistance in soybean: SCE08 (Standardized Cyst Evaluation 2008). *Plant Health Progress*, 10(1). https://doi.org/10.1094/php-2009-0513-01-rv

Noh, E., Fallen, B., Payero, J., & Narayanan, S. (2022). Parsimonious root systems and better root distribution can improve biomass production and yield of soybean. *PLoS ONE*, 17(6), e0270109. https://doi.org/10.1371/journal.pone.0270109

Ortiz, R., Bassi, F. M., Rao, M., & Rubiales, D. (2024). Editorial: Trends and perspectives for the use of crop wild relatives in crop breeding. *Frontiers in Plant Science*, 15, 1424160. https://doi.org/10.3389/fpls.2024.1424160

Pérez-Hernández, O., Giesler, L. J., & Hilbe, J. M. (2019). A Negative Binomial Regression Model of the Observed Population Density of *Heterodera glycines* after Annual Corn Rotation in Nebraska. *Plant Disease*, 103(12), 3093–3100. https://doi.org/10.1094/pdis-03-19-0681-re

Pogorelko, G., Wang, J., Juvale, P. S., Mitchum, M. G., & Baum, T. J. (2020). Screen-

ing soybean cyst nematode effectors for their ability to suppress plant immunity. *Molecular Plant Pathology*, 21(9), 1240–1247. https://doi.org/10.1111/mpp.12972

Posit Software. (2025). RStudio: Integrated Development Environment for R. Posit Software, PBC, Boston, MA. http://www.posit.co/.

Prince, S. J., Song, L., Qiu, D., Santos, J. V. M. D., Chai, C., Joshi, T., Patil, G., Valliyodan, B., Vuong, T. D., Murphy, M., Krampis, K., Tucker, D. M., Biyashev, R., Dorrance, A. E., Maroof, M. S., Xu, D., Shannon, J. G., & Nguyen, H. T. (2015). Genetic variants in root architecture-related genes in a *Glycine soja* accession, a potential resource to improve cultivated soybean. *BMC Genomics*, 16(1), 132. https://doi.org/10.1186/s12864-015-1334-6

Radcliffe, D. E., Hussey, R. S., & McClendon, R. W. (1990). Cyst Nematode vs. Tolerant and Intolerant Soybean Cultivars. *Agronomy Journal*, 82(5), 855–860. https://doi.org/10.2134/agronj1990.00021962008200050001x

Schabenberger, O., Gregoire, T. G., & Kong, F. (2000). Collections of simple effects and their relationship to main effects and interactions in factorials. *The American Statistician*, 54(3), 210–214. https://doi.org/10.1080/00031305.2000.10474547

Sedivy, E. J., Wu, F., & Hanzawa, Y. (2017). Soybean domestication: the origin, genetic architecture and molecular bases. *New Phytologist*, 214(2), 539–553. https://doi.org/10.1111/nph.14418

Shaw, R. G., & Mitchell-Olds, T. (1993). Anova for Unbalanced Data: An Overview. *Ecology*, 74(6), 1638–1645. https://doi.org/10.2307/1939922

Singh, R. J., & Hymowitz, T. (1988). The genomic relationship between *Glycine max* (L.) Merr. and *G. soja* Sieb. and Zucc. as revealed by pachytene chromosome analysis. *Theoretical and Applied Genetics*, 76(5), 705–711. https://doi.org/10.1007/bf00303516

Soybean Cyst Nematode | Integrated Pest Management Program. (n.d.). University of Kentucky. https://ipm.mgcafe.uky.edu/content/soybean-cyst-nematode

Steel, R. G. D. Torrie, J. H. (1980). Principles and Procedures of Statistics: A Biometrical Approach (2nd ed). McGraw-Hill.

Taylor, L. Aggregation, Variance and the Mean. *Nature* 189, 732–735 (1961).https://doi.org/10.1038/189732a0

Tefft, P. M., & Bone, L. W. (1985). Plant-Induced Hatching of Eggs of the Soybean Cyst Nematode *Heterodera glycines*. *PubMed*, 17(3), 275–279. https://pubmed.ncbi.nlm.nih.gov/19294094

Torabi, S., Seifi, S., Geddes-McAlister, J., Tenuta, A., Wally, O., Torkamaneh, D., & Eskandari, M. (2023). Soybean–SCN Battle: Novel Insight into Soybean's Defense Strategies against *Heterodera glycines*. *International Journal of Molecular Sciences*, 24(22), 16232. https://doi.org/10.3390/ijms242216232

Tylka, G. L., & Marett, C. C. (2021). Known Distribution of the Soybean Cyst Nematode, *Heterodera glycines*, in the United States and Canada in 2020. *Plant Health Progress*. https://doi.org/10.1094/PHP-10-20-0094-BR

Tylka, G. L., & Marett, C. C. (2024). Known Distribution of the Soybean Cyst Nematode, *Heterodera glycines*, in the United States and Canada Through 2023. *Plant Health Progress*, 26(1), 51–53. https://doi.org/10.1094/php-08-24-0080-rs

USDA, Agricultural Research Service, National Plant Germplasm System. 2026. Germplasm Resources Information Network (GRIN Taxonomy). National Germplasm Resources Laboratory, Beltsville, Maryland. https://npgsweb.ars-grin.gov/gringlobal/taxon/taxonomydetail?id=17801.

Wallace, H. R. (1968). The dynamics of nematode movement. *Annual Review of Phytopathology*, 6(1), 91–114. https://doi.org/10.1146/annurev.py.06.090168.000515

Wang, C., Masler, E. P., & Rogers, S. T. (2018). Responses of *Heterodera glycines* and *Meloidogyne incognita* Infective Juveniles to Root Tissues, Root Exudates, and Root Extracts from Three Plant Species. *Plant Disease*, 102(9), 1733–1740. https://doi.org/10.1094/pdis-09-17-1445-re

Wang, H.-M., Zhao, H.-H., & Chu, D. (2015). Genetic structure analysis of populations of the soybean cyst nematode, *Heterodera glycines*, from north China. *Nematology*, 17(5), 591–600.

Wen, L., Yuan, C., Herman, T. K., & Hartman, G. L. (2017). Accessions of Perennial Glycine Species With Resistance to Multiple Types of Soybean Cyst Nematode (*Heterodera glycines*). *Plant Disease*. https://doi.org/10.1094/PDIS-10-16-1472-RE

Willig, J., Sonneveld, D., Van Steenbrugge, J. J. M., Deurhof, L., Van Schaik, C. C., Teklu, M. G., Goverse, A., Lozano-Torres, J. L., Smant, G., & Sterken, M. G. (2023). From root to shoot: quantifying nematode tolerance in *Arabidopsis thaliana* by high-throughput phenotyping of plant development. *Journal of Experimental Botany*, 74(18), 5487–5499. https://doi.org/10.1093/jxb/erad266

Winter, S. M. J., Shelp, B. J., Anderson, T. R., Welacky, T. W., & Rajcan, I. (2007). QTL associated with horizontal resistance to soybean cyst nematode in *Glycine soja* PI464925B. *Theoretical and Applied Genetics.*, 114(3), 461–472.

Wrather, J. A., & Anand, S. C. (1988). Relationship Between Time of Infection with *Heterodera glycines* and Soybean Yield. *PubMed*, 20(3), 439–442. https://pubmed.ncbi.nlm.nih.gov/19290235

Xiang, H., Stojilkovic, B., & Gheysen, G. (2025). Decoding Plant–Pathogen interactions: A comprehensive exploration of Effector–Plant transcription factor dynamics. *Molecular Plant Pathology*, 26(1), e70057. https://doi.org/10.1111/mpp.70057

Yu, N., & Diers, B. W. (2017). Fine mapping of the SCN resistance QTL cqSCN-006 and cqSCN-007 from *Glycine soja* PI 468916. *Euphytica*, 213(2), 1–11.

Zhang, H., Li, C., Davis, E. L., Wang, J., Griffin, J. D., Kofsky, J., & Song, B.-H. (2016-a). Genome-Wide Association Study of Resistance to Soybean Cyst Nematode (*Heterodera glycines*) HG Type 2.5.7 in Wild Soybean (*Glycine soja*). *Frontiers in Plant Science*, 7, 215632.

Zhang, H., Mittal, N., Leamy, L. J., Barazani, O., & Song, B. (2016-b). Back into the wild—Apply untapped genetic diversity of wild relatives for crop improvement. *Evolutionary Applications*, 10(1), 5–24. https://doi.org/10.1111/eva.12434

Zhuang, Y., Li, X., Hu, J., Xu, R., & Zhang, D. (2022). Expanding the gene pool for soybean improvement with its wild relatives. *aBIOTECH*, 3(2), 115–125.

CHAPTER 4: WILD SOYBEAN RESPONSES TO COMBINED SCN INFECTION AND WATER DEFICIT STRESS

4.1 Introduction

Agricultural systems are simultaneously exposed to environmental and biological stressors that influence crop growth and productivity. The relationships between host plant genotype, environmental conditions, and pathogen pressure are dynamic and varies across combinations of stressors. Climate change has changed the environmental pressures under which agricultural output must meet the growing demands of a growing population (Change, 2023; Khatri et al., 2023; Pokhrel, 2021). Soybean is an extensively grown commodity with diverse applications; its importance to global food security is underscored by its roles in human nutrition, livestock feed, and industrial production (Dilawari et al., 2022; Fodor et al., 2017). Soybean production systems are vulnerable to both abiotic and biotic stressors, which frequently occur together; early exposure to one stress can increase vulnerability to subsequent challenges (Choudharry & Senthil-Kumar, 2024; Mahecha-Garnica et al., 2022; Martín-Cardoso & San Segundo, 2025).

Among abiotic stressors, lack of water is one of the most significant limitations to soybean productivity worldwide. The water deficit affects soybean growth throughout developmental stages by reducing photosynthesis, altering carbon allocation, and modifying root architecture (Du et al., 2024; Staniak et al., 2023; X. Wang et al., 2022). Tolerance to water shortages is often associated with traits that improve water acquisition or conservation, including increased root depth, altered root to shoot ratios, and improved water-use efficiency (Ku et al., 2013; Valliyodan et al., 2017).

The most economically damaging biotic stressor that affects soybeans is the soybean cyst nematode (SCN, *Heterodera glycines*). SCN infection disrupts root function through

the formation of syncytia. These nematode feeding structures divert host nutrients toward nematode development rather than the host, reducing plant vigor and yield. Between 2015 and 2019, SCN caused more yield loss than any other soybean disease in North America, highlighting its continued importance to soybean production (Bradley et al., 2021; Telenko et al., 2025).

Although SCN infection and water deficit are often studied independently, they are not experienced independently in the field. Combined stress can produce non-additive effects on growth and physiology, complicating the prediction of plant responses and reducing productivity (Zandalinas & Mittler, 2022). The interaction between SCN infection and water deficit is particularly important because both stressors can have serious effects on root function and nutrient acquisition. Water deficit limits water availability and root growth, while SCN infection alters root architecture and nutrient allocation via formation of syncytium. Together, these processes can intensify reductions in water and nutrient uptake, resulting in compounded impacts on plant growth and yield. Early exposure to these stressors is especially consequential; soybean seedlings prioritize root establishment and vegetative development during initial growth stages.

Wild soybean (*Glycine soja*), the progenitor of cultivated soybean (*G. max*), represents an important genetic resource for crop improvement traits, both against abiotic and biotic stressors. Wild soybean populations harbor extensive genetic diversity, and have demonstrated allelic variation associated with stress tolerance and disease resistance that may be useful for breeding programs. Cultivated soybean responses to single water deficit or soybean cyst nematode infection have been well characterized, and there are some studies on SCN infection and water deficit in wild soybean. However, relatively little is known about the combined effects of these stressors in wild soybean (Kofsky et al., 2018; Lin et al., 2024; Nguyen et al., 2024).

Traditional assessment of stress responses in soybean relies on destructive characterization of morphological traits, including biomass, root architecture, and nematode

counts. Destructive measurements provide only a snapshot of plant status at the time of measurement. As a complementary approach, spectral reflectance measurements offer a nondestructive means to assess plant physiological condition at the experimental endpoint. Spectral indices derived from leaf absorbance, reflectance, and transmittance can estimate chlorophyll content, water status, pigment composition, and overall plant health.

In this study, early growth responses of diverse *Glycine soja* accessions were evaluated under SCN infection and combined SCN-water deficit conditions across a single SCN life cycle. By integrating measurements of physiological status in the form of spectral indices as well as phenotypic traits such as SCN reproduction and root and shoot biomass, this study aims to improve understanding of wild soybean physiological responses to single and combined stress conditions and to identify germplasms with potential value for breeding resilient soybean cultivars.

4.2 Materials & Methods

Plant Materials

To assess the effects of soybean cyst nematode infection and combined SCN-water deficit stress on wild soybean plant performance, eighteen wild soybean (*Glycine soja*) accessions and three *Glycine max* cultivars were exposed to SCN and combined SCN-water deficit stress. Seeds were obtained from the United States Department of Agriculture National Plant Germplasm System (USDA Agricultural Research Service, 2025). These accessions were based on previous screenings for soybean cyst nematode resistance at the University of North Carolina at Charlotte, as well as a thorough search of the literature (Table C1).

The seeds were sterilized by immersing them in a 0.5% sodium hypochlorite solution for 30 seconds, then twice in distilled water. Seeds were then scarified to promote uniform germination. They were allowed to germinate for 48 hours on sterile germination paper (Anchor Paper Company, St. Paul, MN, USA). After two days of germination, seedlings with emerged roots were planted in plastic cones (Greenhouse Megastore, Danville IL,

USA) prepared with sterilized sand. Seedlings were watered with 20 mL water twice daily and allowed to grow for 10 days so that the first set of unifoliate leaves had emerged for all plants (Soybean growth stages, n. d).

Spectral Measurements

Leaf reflectance and transmittance spectral indices were measured using the CI-710s Leaf spectrometer (CID Bio-Science, Camas WA, USA). Several indices covering plant health status, chlorophyll and other pigment content, and other indices were measured (Colovic et al., 2022; Joalland et al, 2017; Kup č inskien ė et al., 2023; Mahlein et al., 2012; Oliwa et al., 2023; Parry et al., 2014; Taha et al., 2024). Chlorophyll A and B values, and the derived ratio of Chlorophyll A to B, were estimated using the CI-710s derived spectral absorbance indices. Because measurements are based on in vivo leaf optical properties, resulting values represent relative pigment proxies and are not directly comparable to absolute concentrations or expected chlorophyll A:B ratios reported from extraction based methods (Table C2).

SCN Bioassay & Growth Conditions

Soybean cyst nematodes (SCN, *Heterodera glycines*), were maintained on susceptible *G. max* cultivar Williams 82 for over 50 SCN generations under greenhouse conditions. The population type, HG 1.2.5.7, was maintained separately from other SCN populations to maintain line purity. SCN cysts were extracted from the roots of stock plants and purified by sucrose flotation (Jenkins, 1964). Roots of plants designated for the SCN and combined SCN-water deficit treatments were inoculated with approximately 2000 H. glycine eggs (Brown et al., 2010; Poromarto & Nelson, 2009). Plants grew for three days before initiating water restriction conditions. Throughout the experimental period, greenhouse temperatures ranged from 18 °C to 36 °C; the mean night temperature was 20.40(128) °C; the mean day time temperature was 29.40(246) °C.

SCN-only plants were watered twice daily to maintain moisture levels between 50-75% between watering sessions. Water deficit stress was imposed on combined SCN-

water deficit three days after SCN inoculation by withholding water until growth media water content was depleted and soil moisture meter measurements were found to maintain measurements between 20-25% using the High Frequency Moisture Meter DM300 (X. Wang et al., 2022). Combined SCN-water deficit plants underwent four water-withholding cycles consisting of five days of water deficit, followed by two days of watering for recovery. This regime was maintained for the duration of the experiment, corresponding to one SCN life cycle (30 days). In addition to the soil moisture meter, visual assessments of leaf wilting were conducted using the leaf wilting index of soybean following G. Wang et al (2020). These assessments were used to guide treatment management and confirm plant viability; they were not included in subsequent statistical analysis.

Leaf spectrometer measurements, shoot height measurements, leaf counts, and growth stage determination were taken at the end of the SCN life cycle (30 days after infection) (*Soybean growth stages*, n.d.) before harvesting root and shoot biomass for SCN extraction and biomass measurements. After harvest, the plant shoots were separated from the roots and dried at 60 ° C for 24 hours before taking biomass measurements. SCN cysts were removed from plants stressed with SCN alone and combined SCN-water deficit and counted for analysis of the cyst count. All plant roots were washed to remove growth medium, dried at 60 for 24 hours and biomass was measured. The female index (FI) was calculated using the equation:

$$\text{Female Index (FI)} = \frac{\bar{x}_{\text{test line}}}{\bar{x}_{\text{susceptible check}}} \times 100$$

where the mean cyst count on each wild soybean test line was divided by the mean cyst count on the susceptible check, *G. max* cultivar Williams 82 (Niblack et al., 2009), and multiplied by 100. The root to shoot ratio was calculated from root biomass measurements, and the ratio of chlorophyll a to chlorophyll b was also calculated from leaf spectrometer derived chlorophyll measurements (Dhanapal et al., 2016; Ordóñez et al., 2020).

Statistical Analysis

Differences in soybean cyst nematode cyst count data for SCN-only and combined SCN-water deficit (SCN-WD) stress treatments were analyzed using a two-factor analysis of variance (ANOVA) to evaluate the effects of accession, treatment, and their interaction on SCN reproduction. Models were fit separately for all accessions and wild soybean accessions only. Cyst counts were evaluated using both raw values (x) and transformed via $\log_{10}(x+1)$. Transformation improves variance homogeneity and account for a non-normal data structure, as well as to allow the inclusion of replicates where x = 0. For each dataset and trait scale, ANOVA Type III Sum of Squares was used to determine differences in cyst count between accessions, treatments, and the accession-treatment interaction (McCarville et al., 2017; Mengistu et al., 2024; Niblack et al., 2002; Taylor, 1961). All accessions were represented by a minimum of 3 biological replicates, though most had more. Type III Sum of Squares was utilized to account for this unbalanced design (Acharya & Yan, 2021; Shaw & Mitchell-Olds, 1993).

To evaluate accession-specific responses to combined stress, estimated marginal means were calculated and treatment contrasts (SCN-water deficit vs. SCN-only) were performed. Resulting p-values were adjusted using the Benjamini-Hochberg method to control for false discovery rate across accessions (Benjamini & Yekutieli, 2001).

To assess changes in susceptibility ranking, the female index was calculated for all accessions in SCN-only and SCN-water deficit treatment groups using mean cyst counts across biological replicates according to Niblack et al., 2002. As FI represents a ratio of accession means and not an independent replicate-level response, FI was evaluated descriptively, so that accession-treatment combinations were categorized as follows: resistant (R, FI < 10); moderately resistant (MR, 10-30); moderately susceptible (MS, 30-60), and susceptible (S, FI > 60) (Niblack et al., 2009).

Accession-level female index values were compared between SCN-only and SCN-water deficit treatments by calculating directional changes ($\Delta FI = FI_{\text{SCN-WD}} - FI_{\text{SCN-only}}$) and visualized using slope plots to illustrate treatment associated shifts in susceptibility.

Spearman rank analysis was utilized to assess correlation between FI and cyst counts; and the relationship between treatment-associated changes in ΔFI and Δcyst values.

To identify wild soybean accessions exhibiting higher performance under SCN infection and combined SCN and water deficit stress, accessions were assessed using metrics derived from SCN reproduction and plant growth measurements. Analyses were restricted to wild soybean accessions challenged with SCN alone or combined SCN and water deficit stress.

SCN Reproduction Metrics Two measures of soybean cyst nematode reproduction were used to evaluate resistance: cyst counts summarized as the mean number of cysts per accession within each treatment, and model-estimated means, derived from estimated marginal means (EMMeans). These model adjusted estimates represent the predicted number of cysts produced on each accession under the specified conditions after accounting for variation among replicates Because cyst count data were right skewed, counts were log-transformed prior to modeling using $\log_{10}(x + 1)$.

A linear model including accession, treatment, and their interaction (accession x treatment) was fitted to the log-transformed cyst count data. Estimated marginal means (EMMeans) were then calculated for each accession within each treatment using the emmeans R package. Estimated marginal means represents the expected average number of SCN cysts produced per plant under a given treatment condition after accounting for replication and variation in the linear model. Separate EMMeans were thus obtained for each accession under SCN-only stress and combined SCN-WD stress. Because SCN resistance is expressed as reduced SCN reproduction on the host plant, accessions were ranked within each treatment based on their back-transformed EMMeans cyst counts, with lower predicted cyst numbers indicating stronger resistance. Female index (FI) values were calculated and reported for comparison with standard SCN resistance classifications, but performance rankings were based on cyst reproduction methods (cyst counts or estimated marginal means of cyst counts) because FI represents a linear transformation of cyst counts relative to the

susceptible check.

Stability of SCN reproduction across treatments, the magnitude of change in predicted cyst reproduction between treatments was calculated using the difference between back transformed EMMeans: Δcyst reproduction = $\text{EMMeans}_{\text{SCN-WD}} - \text{EMMeans}_{\text{SCN-only}}$. Accessions were ranked according to the absolute magnitude of change (), with smaller values indicating greater stability of SCN resistance across environmental conditions.

Biomass Metrics

Four biomass-related traits were assessed for their association with SCN cyst count in order to assess wild soybean performance under the two treatment conditions. These included total dry biomass, dry shoot biomass, dry root biomass, and root to shoot ratio (RSR), with all but the last measured in milligrams (mg). Mean values were calculated for each accession within each treatment. Because the goal was to identify a biomass metric most closely associated with nematode resistance, Spearman rank correlations were calculated for each biomass trait and the SCN reproduction metrics (mean cyst counts, back-transformed EMMeans cyst counts, and Female Index). The biomass trait exhibiting the strongest overall correlation with SCN reproduction metrics was selected as the primary indicator of plant performance in subsequent analyses.

Integrated Wild Soybean Performance Classification

To identify accessions exhibiting the best combined performance, as defined as low SCN cyst count and higher relative biomass. These metrics were integrated using a quadrant classification approach. For each treatment separately, accessions were classified relative to the treatment median for: predicted SCN cyst reproduction (back-transformed EMMeans) and total biomass. This produced four performance categories to identify accessions combining strong SCN resistance with high biomass production, representing the most favorable performance under each stress environment (Table 4.1). Treatment-specific medians were used as classification thresholds to divide accessions into high and low groups for both cyst reproduction and biomass. The median provides a robust measure

of central tendency that is less sensitive to skewed distributions and extreme values than the mean, making it suitable for performance classification in biological datasets. This approach is commonly used in quadrant-based analyses to identify relative performance groups when the objective is to compare accessions within an experimental population rather than to define absolute biological thresholds (Zar, 2010). This approach allows the identification of accessions that simultaneously suppress SCN reproduction and maintain plant growth under stress conditions.

Table 4.1: Quadrant ranking framework used to evaluate wild soybean performance under SCN and SCN-water deficit conditions. Accessions were categorized based on relative SCN reproduction metrics and total plant biomass. Low cyst reproduction indicates stronger SCN resistance, whereas higher biomass reflects better plant growth despite stress conditions. The combination of these metrics defines four performance categories used to identify wild soybean accessions exhibiting favorable resistance–growth tradeoffs.

SCN Reproduction	**Biomass Measurement (mg)**	**Classification**
Low reproduction	High biomass	High performing
Low reproduction	Low biomass	Low reproduction & low vigor
High reproduction	High biomass	Tolerant
High reproduction	Low biomass	Low performing

Statistical power for accession, treatment, and accession-treatment effects was estimated using Monte Carlo simulation based on the fitted ANOVA models. For each dataset, 2,000 simulated datasets were generated under the fitted model assumptions; power was calculated as the proportion of simulations yielding $p < 0.05$. This approach provided design specific power estimates reflecting the observed variance and replication structure (Acutis et al., 2012).

Data Preparation and Trait Diagnostics

Prior to downstream analyses, trait data for physiological and phenotypic data were screened for potential anomalies. Traits were evaluated using two complementary data: (1) comparison with literature-based expected ranges for spectral indices and pigment-related

variables (Table C3), and (2) statistical outlier detection using 2 x IQR (interquartile range) method. Because plant phenotype traits frequently exhibit skewed distributions and substantial biological variation among accessions, a broader IQR threshold reduces the likelihood of removing biologically meaningful extreme phenotypes (Wilcox, 2012; Zurr et al., 2010). Observations inconsistent with biologically plausible ranges or attributable to measurement artifacts were replaced with missing values. This resulted in the removal of 368 observations (<1% of all trait measurements). Original missing values resulting from incomplete measurements were retained. Categorical growth stage observations were recorded during data collection, but excluded from the quantitative trait dataset because they represent descriptive development stages rather than continuous measurements. After removal of these variables, the dataset contained 107 missing values across traits. Distribution characteristics of trait variables were evaluated using histograms, Q-Q plots, and summary statistics to identify potential departures from normality prior to correlation-based trait screening.

Trait Screening for Associations with SCN Reproduction

Associations between physiological and phenotypic plant characteristics and soybean cyst nematode reproduction were evaluated using Spearman rank correlation. This non-parametric approach does not assume a linear relationship between variables, and is less sensitive to outliers than Pearson correction. The correlations between the traits of the end-of the experiment plant and three measures of SCN reproduction included cyst count, logarithmic transformed cyst count $\log_{10}(x + 1)$ and female index (FI); these analyses were restricted to accessions of wild soybeans. Because multiple traits were evaluated simultaneously, p-values were adjusted using the Benjamini-Hochberg false discovery method to control for multiple testing. Adjusted p-values were used to identify statistically robust associations for reporting purposes. For subsequent multivariate analyses, a more inclusive screening threshold (raw $p < 0.05$) was used to define the candidate trait predictor pool. This approach allowed retention of biologically relevant traits that may be excluded under strict multiple testing correction, particularly in a dataset with correlated physiological

measurements (e.g. total chlorophyll and greenness index).

Evaluation of Correlations Among Plant Traits

To evaluate relationships among wild soybean physiological and phenotypic traits, and to identify potential redundancy among variables, pairwise correlations and Principal component analysis (PCA) were performed using end-of-experiment trait measurements. Analyses were conducted after extreme values were removed from the dataset. Categorical variables were excluded from quantitative analysis.

Pairwise correlations between traits were evaluated using Spearman rank correlation because many plant physiological traits exhibited non-normal distributions and potential skewness; this nonparametric approach does not require normally distributed variables, and provides robustness to outliers and monotonic transformations of the data. To evaluate the influence of plant size variables on trait correlations, analyses were performed both with biomass traits included and excluded. Pairwise correlation matrices were calculated, and trait pairs exhibiting strong correlations ($|\rho| \geq 0.80$) were identified as potentially redundant variables.

Principal component analysis was performed to further evaluate the relationships among traits and to identify major trends in phenotypic and physiological variation among plants. Prior to PCA, trait variables were standardized using z-score transformation to place all variables on a common scale. PCA was performed on two datasets (1) all measured traits, including biomass variables, and (2) the subset of traits significantly associated with SCN reproduction. Plant biplots were generated to display the distribution of individual plants in principal component space.

Results of the trait-trait correlation and PCA were used to identify groups of correlated traits representing similar physiological processes (e.g. total chlorophyll content, chlorophyll A content, or all biomass traits). From each group of correlated traits, representative variables were selected to reduce redundancy prior to regression analysis. Traits were selected to capture distinct physiological processes, including canopy vigor, plant size,

pigment-based stress responses, water status, and biomass allocation. The reduced trait set was subsequently utilized for regression analysis using a structured, biologically informed selection framework to elucidate the associations between plant traits and soybean cyst nematode reproduction.

Multivariate Modeling

To evaluate the combined effects of physiological and phenotypic traits on SCN reproduction, a multivariate regression framework was implemented using the end of experiment trait measurements. These analyses were restricted to wild soybean accessions exposed to SCN infection to ensure variation in cyst counts reflected true differences in infection intensity. Candidate predictor traits included biomass and spectral index traits. Traits correlated with SCN reproduction were initially identified using Spearman rank correlations. A threshold of $p < 0.05$ was used to define the pool of potential candidate traits. This inclusive threshold was used to retain biologically relevant traits that may not meet stricter multiple-testing criteria, particularly in datasets with correlated physiological measurements. Benjamini-Hochberg (BH)-adjusted p-values were retained for reporting and used to assess statistical robustness, but were not used as a filtering criteria at this stage.

To reduce redundancy among predictors, pairwise-trait correlations were evaluated with Spearman's rank correlation. Traits exhibiting strong correlations 0.80 were grouped into clusters and a single representative trait from each trait was chosen. Within each cluster, representative traits were prioritized based on a combination of screening criteria, strength of association with SCN reproduction (), and magnitude of loading in principal component analysis (PCA).

PCA was used to identify major axes of physiological variation among traits and to guide final predictor selection. Traits were assigned to principal components (PCs) based on their highest loading. To ensure biological interpretability and inclusion of distinct physiological processes, a reduced model (i.e, the model used a subset of all traits measured) was constructed selecting predictors across major PCA-defined axes. These included: a

predictor representing canopy status, one representing growth or biomass, and up to two representing stress- or pigment-related processes when available. An additional predictor from a distinct correlation cluster was included when supported by screening results and PCA structure. This approach used screening to build a biologically informed model that captured multiple physiological dimensions of wild soybean response to SCN infection while minimizing redundancy.

Two models were constructed. A rule-based full model included all screened, non-redundant cluster representatives. A reduced model included the explicitly selected predictors representing distinct physiological axes. Model performance was evaluated primarily using the reduced model due to its interpretability and parsimony.

Regression analyses were performed using ordinary least squares (OLS), while model performance was evaluated using Akaike Information Criterion (AIC), adjusted coefficient of determination (adjusted R2), and root mean square error (RMSE). Multicollinearity among predictors was assessed using variance inflation factors (VIF). Model assumptions were checked with standard diagnostic plots. Influence diagnostics, including Cook's distance and leverage values, were examined to identify potentially influential observations.

To evaluate the robustness of biomass predictors, a sensitivity analysis was performed by substituting highly correlated alternative biomass or size-related variables (e.g., shoot height, total biomass, root biomass, shoot biomass, and root to shoot ratio) into the reduced model while holding other predictors constant. Model performance metrics were compared across these alternatives to identify the most appropriate representation of plant growth or biomass allocation in the final model. All analyses were performed using R 4.5.2.

4.3 Results

Wild Soybean Responses To Combined SCN-Water Deficit Stress

Significant variation of the log-transformed cyst count data was revealed for wild soybean accessions ($F=4.92$, $p < 0.001$, df: 18). In contrast the treatment main effect

(SCN-only vs SCN-WD) was not significant (F=0.001, p = 0.97). The accession-treatment interaction was also not significant (F = 0.85, p =0.64). A full comparison of type III ANOVA results across all data transformations and accession subsets is presented in Table C4, including models to fit to raw and log-transformed data for both the complete dataset and the wild accession subset.

Statistical power for accession, treatment and accession-treatment effects was estimated using Monte-Carlo simulation based on the fitted ANOVA model for the log-transformed cyst count data of wild soybean accessions. For each model, 2000 simulated datasets were generated and power was calculated as the proportion of simulations producing $p < 0.05$. Power to detect accessions was 1.00, while power for the accession-treatment interaction was 0.64. Power to detect the treatment main effect was 0.054, indicating limited ability to detect treatment effects. Summaries of the power analysis for all datasets are presented in Table C5.

To evaluate accession-specific responses to combined SCN infection and water deficit stress, estimated marginal means (EMMeans) contrasts of the log-transformed model were analyzed; no significant differences were found between accessions infected only with wild soybeans and the same accessions under combined SCN and water deficit stress following correction for false discovery rate. A full comparison of all models and data transformations is included in Table C6.

Despite the absence of significant contrasts, directional variation among wild soybean accessions was evident. A forest plot of model-based treatment contrasts (SCN-WD - SCN-only) showed heterogeneous directional responses among wild soybean accessions. Several accessions trend towards increased cyst counts under SCN-WD stress; others trend toward decreases. Confidence intervals generally overlapped zero, consistent with the non-significant accession-treatment interaction and the absence of significant within-accession contrasts after multiple testing correction (Figure 4.1).

Accessions with reduced cyst counts under SCN-water deficit treatment include S100

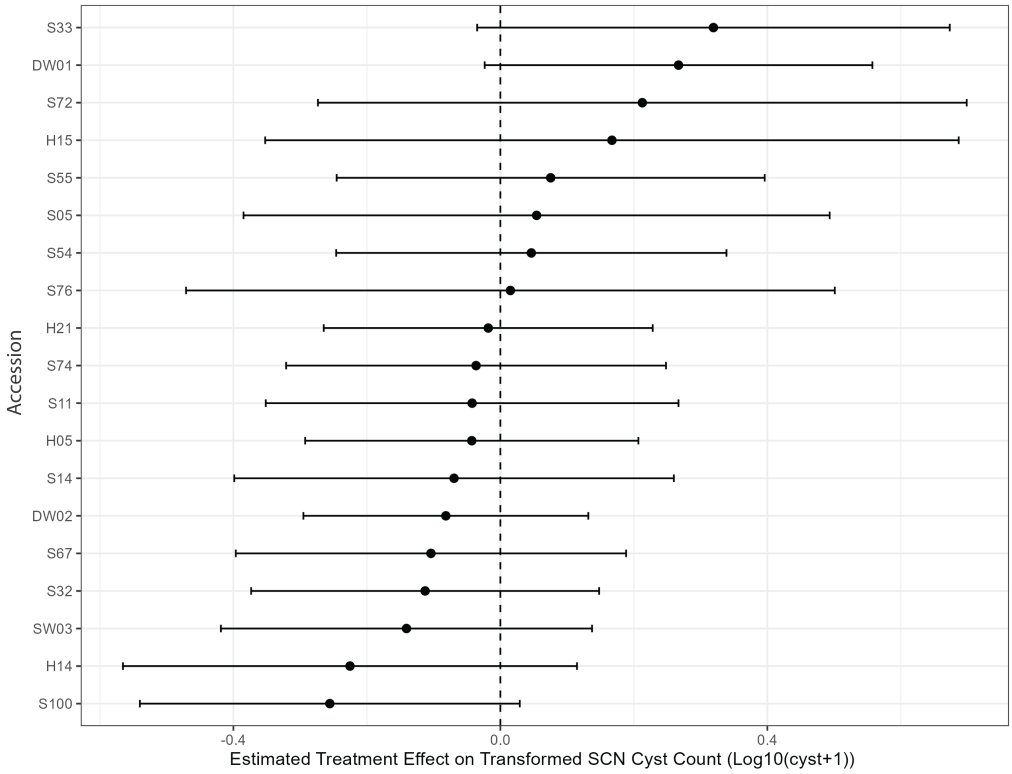

Figure 4.1: Forest plot illustrating accession-specific treatment contrasts between SCN-water deficit and SCN-only treatments for log-transformed cyst counts of wild soybean accessions. Points represent estimated marginal mean differences within wild soybean accession accessions. Horizontal bars indicate 95% confidence intervals. Positive values indicate increased cyst counts under SCN- water deficit stress, whereas negative values indicate reduced cyst counts.

and H14. In contrast, other accessions, including DW01, showed increased cyst production under combined stress. Many accessions displayed minimal differences between treatments, and residual variability limited statistical detection of accession-specific contrasts within the accessions tested.

To visualize accession responses on the original model scale, estimated marginal means of the transformed cyst count were plotted for each accession under SCN-only and combined SCN-WD. Across wild accessions, model-estimated cyst counts differed in baseline magnitude between accessions. In contrast, the mean shift between SCN-only and SCN-WD stress was generally small for most accessions; reaction norm lines were largely parallel (Figure 2).

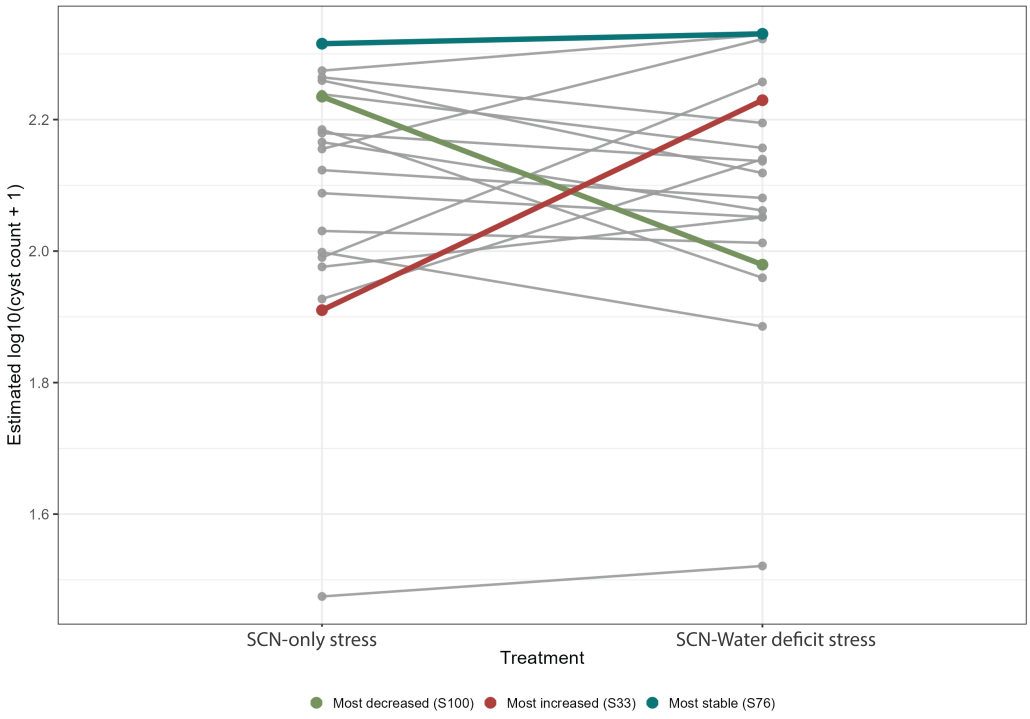

Figure 4.2: Reaction norms of model-estimated transformed cyst counts ($\log_{10}(x + 1)$) for SCN-only and SCN-water deficit treatments for wild soybean accessions. Grey lines represent individual accessions; highlighted accessions illustrate the most negative (S100), smallest magnitude (S76), and most positive treatment contrasts (S33) in SCN reproduction (SCN-water deficit vs. SCN only stress). Most accessions exhibited modest treatment-associated shifts, with largely parallel responses between treatments.

Female index (FI) represents relative susceptibility normalized to a susceptible

check; thus patterns in FI were examined to determine if SCN-WD treatment altered resistance expression independent of absolute cyst production (Niblack et al., 2002). Across wild soybean accessions tested in this study, FI generally increased under combined SCN-WD stress relative to SCN only conditions. Directional increases in FI were evident for several accessions; of note, H15, DW01, and S33 illustrated greater relative susceptibility under combined stress treatment. Spearman correlation analysis revealed strong rank agreement between FI and cyst count across accessions under both SCN-only and SCN-WD treatments ($p < 0.001$, $\rho = 1.00$ and $p < 0.001$ and $\rho = 1.00$, respectively).

Accession-level changes in FI across treatments were strongly associated with changes in cyst counts, indicating that FI captured additional variation related to normalization against the susceptible check (ΔFI vs. Δcyst count: $\rho = 0.79$, $p < 0.001$). Spearman correlations between FI and cyst count were equal to 1.0 under both stress environments.

The resistance stability was evaluated, revealing that the majority of accessions (14 of 21) changed the FI category under combined stress, most frequently shifting towards greater susceptibility.

Integrated Performance Metrics

Wild soybean performance under soybean cyst nematode (SCN) infection and combined SCN-water deficit stress was evaluated using cyst reproduction metrics and plant biomass metrics. Wild soybean accessions exhibited substantial variation in SCN reproduction across both treatment environments. Mean cyst counts varied widely among accessions under both SCN-only and combined SCN-WD treatments, indicating considerable diversity in resistance levels within the wild soybean panel (Table 4.2).

Model-estimated cyst reproduction derived from the log-transformed linear model further clarified differences in SCN reproduction by accession. EMMeans revealed pronounced differences in predicted cyst reproduction among accessions under the two stress treatments, as described in Tables C7 and C8, respectively.

Female index values calculated from accession-level cyst means provided an addi-

Table 4.2: Wild soybean accessions ranked by mean SCN cyst counts under SCN-only and combined SCN-water deficit (SCN-WD) treatments. Lower cyst counts indicate stronger resistance to *Heterodera glycines*. Rankings are ordered from lowest to highest cyst reproduction (rank 1 = strongest resistance).

(a) SCN-only

Rank	Accession	Mean cyst count
1	S54	40.5
2	S72	95.0
3	S55	105.4
4	S32	118.8
5	H21	124.8
6	S74	134.4
7	S33	136.2
8	DW01	139.1
9	S11	139.3
10	H15	142.3
11	S67	159.0
12	H05	163.3
13	H14	164.4
14	S100	183.4
15	SW03	184.5
16	DW02	184.6
17	S14	188.6
18	S05	190.6
19	S76	206.7

(b) SCN-WD

Rank	Accession	Mean cyst count
1	S54	44.3
2	S32	106.4
3	H21	108.6
4	S74	124.9
5	S11	131.1
6	S100	137.2
7	S55	138.7
8	S67	142.1
9	H05	145.0
10	S72	148.5
11	DW02	155.9
12	SW03	171.1
13	H14	174.1
14	S33	174.3
15	S14	183.1
16	DW01	183.4
17	H15	210.0
18	S05	212.3
19	S76	216.0

tional measure of relative SCN resistance (Table C9). A slope plot was utilized to visualize changes of FI between SCN-only and SCN-WD treatments; many accessions showed an increase in FI from SCN-only stress and SCN-water deficit stress treatments. The accession that showed the least FI change was S100, while H15 exhibited the most change in FI. No negative FI change (lower resistance categorization under combined stress relative to single SCN stress) was observed (Figure C1).

Biomass traits measured at the end of the experiment exhibited variation among wild soybean accessions under both SCN-only and combined SCN-WD stress conditions. Under SCN-only stress, mean total biomass across accessions was 46.60 mg (SD = 18.23), while mean root biomass and mean shoot biomass were 22.54 ± 8.24 mg and 24.07 ± 10.28 mg, respectively. Under combined SCN-WD stress, biomass values were generally lower; total biomass was reduced to 38.61 ± 8.40 mg. Root biomass decreased to 19.27 ± 4.51 mg, and shoot biomass mean was reduced to 19.34 ± 4.74 mg.

Root to shoot ratios were similar across treatments, ranging from 1.0-1.1 across accessions (Table 2). Descriptive statistics and diagnostic distribution in the form of Q-Q plot visualization confirmed that biomass traits were approximately normally distributed across accessions within treatments (Table C10, Figure C2, and Figure C3).

Table 4.3: Descriptive statistics of biomass traits for wild soybean accessions under SCN-only and combined SCN–water deficit stress treatments. Values represent accession means ± standard deviation (SD) for root biomass, shoot biomass, total biomass (mg), and root:shoot ratio measured at the conclusion of the experiment.

Treatment	Biomass metric	Mean ± SD	Median
SCN-only	Root	22.54 ± 8.24	22.43
	Shoot	24.07 ± 10.28	20.31
	Total biomass (root + shoot)	46.61 ± 18.23	40.80
	Root:shoot ratio	1.01 ± 0.19	0.96
SCN–water deficit	Root	19.27 ± 4.51	20.46
	Shoot	19.34 ± 4.74	18.47
	Total biomass (root + shoot)	38.61 ± 8.40	38.38
	Root:shoot ratio	1.07 ± 0.22	1.03

Biomass traits measured at the end of the experiment were evaluated as metrics of plant vigor. Four biomass-related metrics were considered: total biomass (dry root & shoot mass), shoot dry mass, root dry mass, and root to shoot ratio. Biomass metrics were evaluated to identify the variable most consistently associated with EMMeans cyst count. The metric with the highest mean absolute correlation coefficient $|\rho|$ across nematode reproduction measures was selected as the primary indicator of plant performance under nematode stress. These analyses showed that total biomass had the strongest overall association with SCN reproduction (average $|\rho| \approx 0.30 - 0.43$). The direction of the relationship between plant total biomass cyst count differed between treatments, with a positive association under SCN-only conditions, and a negative association under combined SCN-water deficit stress. Metric selection was based on the magnitude of the correlation coefficients rather than the p-values, as the objective was to identify the biomass variable most strongly associated with nematode count metrics, rather than to test a specific null hypothesis (Muff et al., 2022; Nakagawa et al., 2007; Schober et al., 2018; Sullivan & Feinn, 2012).Total biomass was selected as the primary growth metric for evaluating wild soybean performance across accessions and treatments (Table C11).

Wild Soybean Performance with SCN and Combined SCN-Water Deficit Stress

Integration of predicted SCN reproduction and total biomass revealed clear differences in overall performance among accessions in both treatments. Accessions were assessed using a median-based quadrant classification approach. For each treatment, accessions were classified relative to the treatment-specific median values of predicted cyst reproduction and total biomass. This approach partitioned accessions into four performance groups representing combinations of resistance (lower relative SCN reproduction) and plant growth (higher relative biomass), allowing identification of accessions that simultaneously suppress SCN reproduction and maintain plant vigor, thus representing the most favorable performance under stress treatment.

Performance of wild soybean accessions under a single stressor (SCN infection) was

evaluated to establish a baseline of resistance and plant growth responses in the absence of water restriction. Four accessions - S54, S32, S11, and H15 - were classified as high performing in this experimental setting for the SCN-only treatment group. These combined low SCN reproduction with above-median biomass production. The remaining accessions also maintained relatively low cyst reproduction while producing substantial biomass, indicating the ability to suppress SCN reproduction and sustain plant growth during early SCN infection (Figure 4.3A).

A second set of accessions was classified as a potential trade-off class These accessions expressed relatively stronger SCN resistance, but reduced plant vigor relative to other accessions. These include S33, S72, S55, DW01, H21, and S74. These accessions exhibited cyst reproduction below the treatment median, but produced comparatively lower biomass.

Several accessions were classified as tolerant, as they produced high SCN reproduction, but also high biomass. These accessions include S67, S100, SW03, S14, S05, and S76. They maintained high biomass production while supporting higher levels of nematode reproduction.

Finally, three accessions were classified as low performing. These accessions exhibited both high SCN reproduction and below-median biomass and were H05, H14, and DW02. These results demonstrate considerable diversity among wild soybean accessions in both SCN resistance and plant growth responses under the single stressor of SCN infection (Figure 4.3A).

Under combined SCN-water deficit stress, eight accessions were classified as high performing, exhibiting both below-median predicted SCN reproduction and above-median total biomass. These accessions included: S54, S32, H14, S100, H21, S67, S11, and SW03 (Figure 4.3B). A few accessions displayed elevated SCN reproduction and reduced biomass, indicating comparatively poor performance under dual-stress conditions; these were: H05, S72, DW02, S33, DW01, H15, and S76. A small number of accessions exhibited high

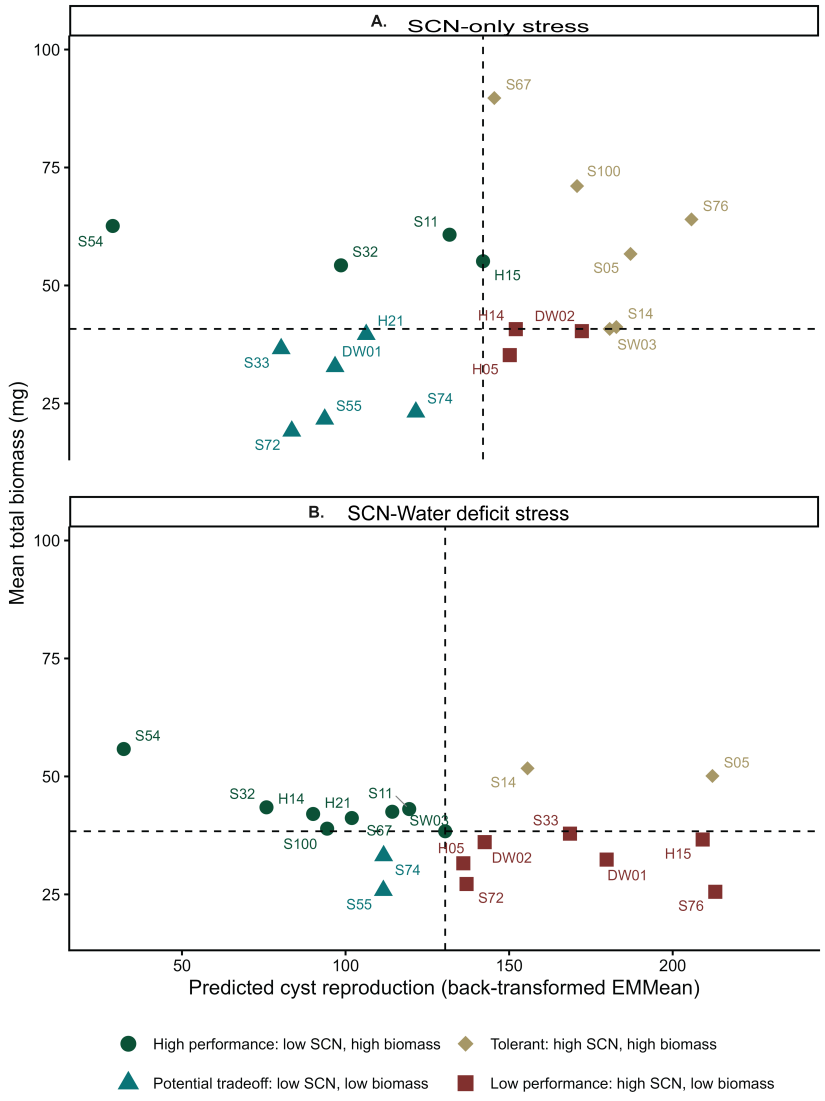

Figure 4.3: Performance classification of wild soybean accessions. Quadrant plot integrates modeled SCN cyst count and total biomass to classify accession responses. The x-axis shows the modeled SCN cyst count of back-transformed estimated marginal means from the $\log_{10}$(cyst + 1) model, while the y-axis shows median total biomass (mg). Dashed vertical and horizontal lines represent the median cyst count and median biomass within each treatment, respectively. Medians partition accessions into four performance categories: High performance (low SCN cyst count and high biomass); Potential trade off (low SCN cyst count, low biomass); Tolerant (higher cyst count, higher biomass); and Low performance (high SCN cyst count and low biomass). Panel A shows results for SCN-only stress; panel B shows combined SCN-water deficit results.

biomass despite relatively high SCN reproduction, suggesting potential tolerance rather than resistance; these included S14 and S05 (Figure 4.3B).

Trait Screening for Associations with SCN Reproduction

Visual inspection of histograms and Q-Q plots indicated that many physiological and phenotypic traits exhibited right-skewed distributions, while vegetation indices were generally bounded within expected ranges (Table C12). Overall, these checks indicated that the data set was largely free of measurement artifacts and suitable for trait-resistance analyzes.

Spearman correlation analysis identified several end-of-experiment traits that were significantly associated with SCN reproduction after Benjamini-Hochberg correction. The magnitude of these relationships was generally small ($|\rho| \approx 0.14$–0.24, $p < 0.05$). Several vegetation indices were found to be associated with plant physiological status (Figure C3). Among those negatively correlated with transformed SCN reproduction, PRI, NDVI, Greenness, and CNDVI had the highest magnitude, ranging from $|\rho| \approx -0.16$–-0.22. Traits that were positively correlated with the logarithmic transformation cyst counts included PSRI, root to shoot ratio, shoot height, and ARI1; for these, ρ ranged from 0.14 to 0.24 ($p < 0.01$ for all of these). Table C13 summarizes all all Spearman plant trait and cyst count results correlation results.

Evaluation of Correlations Among Trait Plants

Pairwise Spearman correlations were calculated among 21 end-of-experiment traits of wild soybean under SCN infection to evaluate the relationships among traits and identify potential redundancy among variables. Strong correlations were defined as $|\rho| \geq 0.80$, and 13 trait pairs met this criteria. Several clusters of strongly correlated traits were observed with statistical significance and are illustrated in Figure 4.4 (Table C14).

Chlorophyll-related measurements exhibited the strongest correlations in the dataset. Chlorophyll A and total chlorophyll were strongly correlated (ρ =0.980), as were Chlroophyll B and total chlorophyll (ρ =0.987). Chlorophyll A and chlorophyll B were also strongly

correlated to one another (ρ = 0.940). Leaf greenness and canopy reflectance indices also showed strong positive correlations: SPAD and CCI values were highly correlated (ρ = 0.948), while NDVI was strongly correlated with both the greenness value and CNDVI (ρ =0.885 and 0.865 respectively). Biomass related traits also exhibited strong correlations; root mass and shoot mass were both strongly correlated with total biomass (ρ = 0.941 and ρ = 0.941 respectively). High correlations were observed between chlorophyll measurements and certain spectral indices, including correlations between CCI and chlorophyll A (ρ = 0.842) and between SPAD and chlorophyll A (ρ = 0.821).

To further examine multivariate relationships among traits, principal component analysis (PCA) was conducted. PCA was performed on two datasets: (1) all measured traits, including biomass variables, and (2) the subset of traits significantly associated with SCN reproduction following Benjamini-Hochberg (BH) correction for multiple testing.

In the PCA that includes all traits, including biomass variables, the first four Principal components (PCs) explained 69.9% of the total variance. PC1 accounted for 43.3% of variance, followed by PC2 (11.2%), PC3 (9.1%) and PC4 (6.1%) (Figure 4.5, Figure C4). Traits with the strongest loadings on PC1 included chlorophyll measurements (chlorophyll A, chlorophyll B, and total chlorophyll), as well as spectral indices associated with leaf greenness , including NDVI, SPAD, and CNDVI. PC2 was characterized by loadings from biomass-related traits, including shoot mass, root mass, total biomass, and shoot height (Figure C5). PC3 was associated with several pigment- and stress-related indices: the ratio of Chlorophyll A to Chlorophyll B (Chlorophyll A:B), water band index (WBI), plant senescence reflectance index (PSRI) and carotenoid reflectance index (CRI) (Figure C5).

The PCA performed using the subset of traits significantly associated with SCN reproduction after Benjamini-Hochberg correction, the first four components explained 78.4% of the total variance (Figure C6). PC1 accounted for 52.9% of variance, followed by PC2 (10.5%), PC3 (8.0%) and PC4 (6.9%) . A similar pattern of clustering was observed in this subset: chlorophyll-related measurements and leaf greenness indices showed the

strongest loadings on PC1. PC2 included strong loadings from several physiological and pigment related indices, including WBI, ARI, PSRI(Figure C6). PC3 also included contributions from several pigment- and stress related indices. Together, the correlation analysis of traits and PCA revealed clear patterns of association among end-of-experiment traits, including clusters of strongly related chlorophyll measurements, leaf greenness indices, and biomass-related traits.

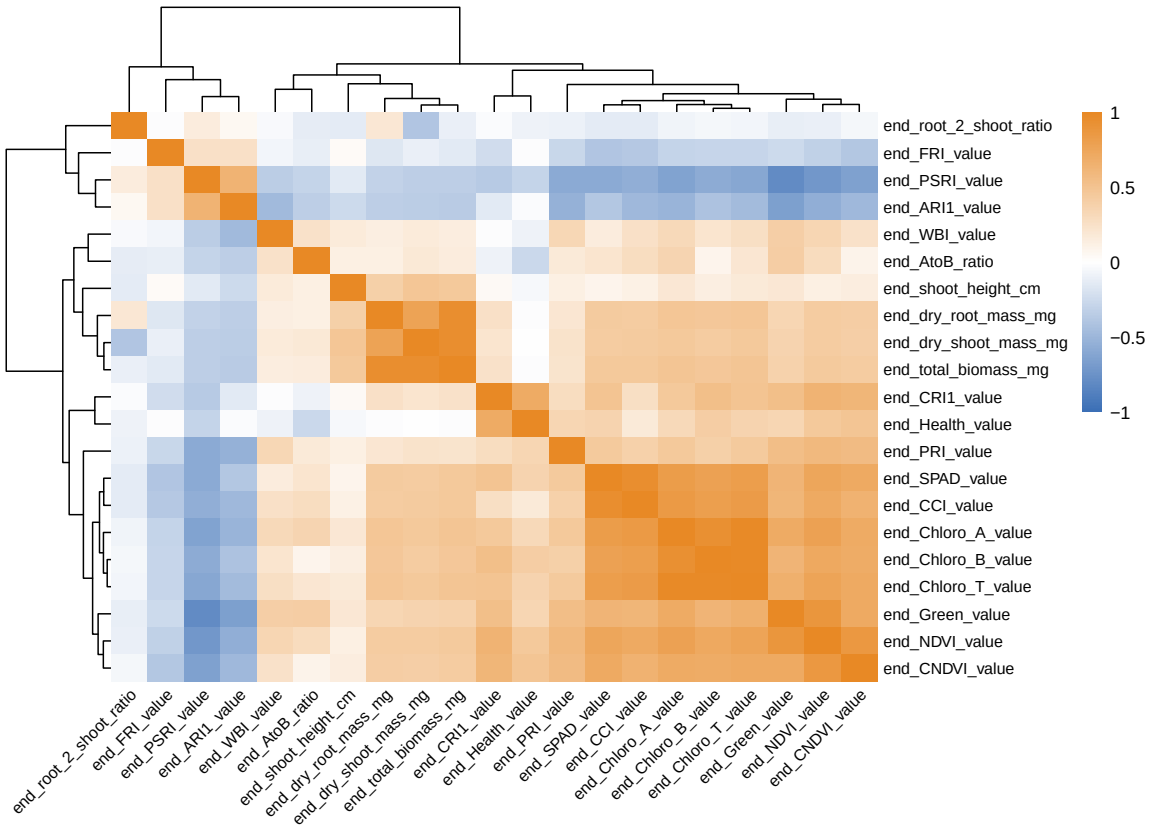

Figure 4.4: Heatmap of Spearman correlation analysis among 21 end-of-experiment traits measured in wild soybean infected with SCN. Color intensity indicates correlation strength (ρ). Clusters of strongly correlated traits include chlorophyll measurements, leaf greenness indices, and biomass-related traits..

Multivariate Modeling of SCN Reproduction

The combined influence of plant physiological and phenotypic traits on SCN reproduction was assessed utilizing multiple regression models using a set of predictors that represent distinct physiological processes. The final modeling dataset included 295 obser-

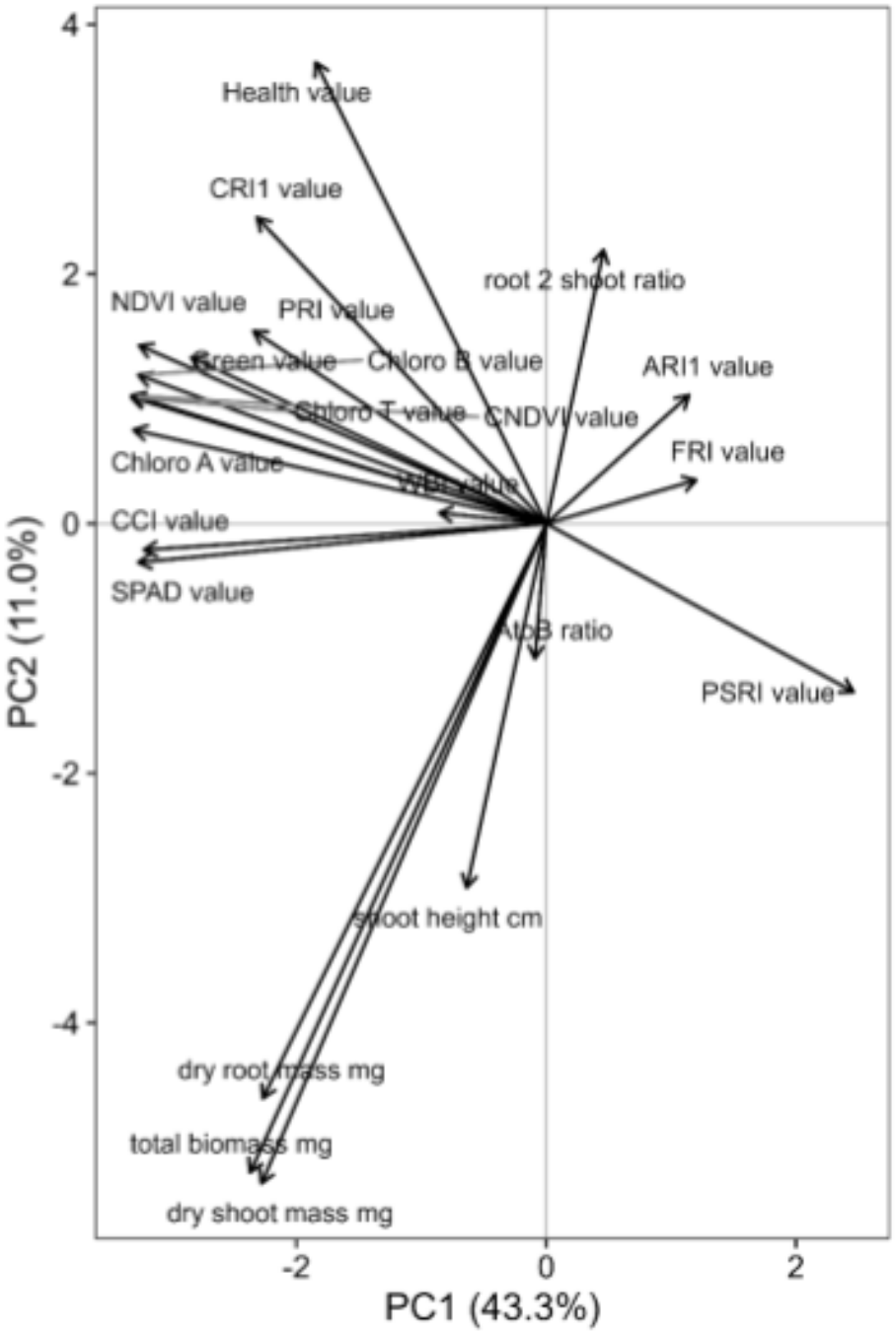

Figure 4.5: Principal component analysis (PCA) of traits measured at the end of the SCN life cycle. PC1 explained 43.3% of the total variance, and was primarily associated with chlorophyll and leaf greenness indices. PC2 explained 11.0% of variance and was associated with biomass traits, such as shoot mass, root mass, and total biomass.

vations. The reduced model consisted of four predictor traits: plant senescence reflectance index (PSRI), photochemical reflectance index (PRI), normalized difference vegetation index, (NDVI), and root-to-shoot ratio.

Model comparison indicated the reduced model provided the best balance between model fit and model complexity. The reduced ordinary least squares (OLS) model illustrated the lowest Akaike Information Criterion (AIC = 204.22), an adjusted R^2 of 0.115, and RMSE of 0.335. The reduced model explained approximately 11.5% of the variation in log-transformed cyst counts ($R^2 = 0.115$).

Three of the four predictor traits from the reduced model were found to be significantly associated with log-transformed cyst counts. The photochemical reflectance index (PRI) and normalized difference vegetation index (NDVI) were negatively correlated with cyst counts ($\beta = -3.27,\ p < 0.001$ and $\beta = -0.46,\ p < 0.05$, respectively). Root-to-shoot ratio (RSR) was positively correlated with cyst counts ($\beta = 0.18, p < 0.001$) and plant senescence reflectance index (PSRI) was not significantly associated with cyst counts ($\beta = -0.51, p = 0.198$).

4.4 Discussion

Wild Soybean Response to SCN and Combined SCN-Water Deficit Stress

The responses of wild soybeans to SCN and combined SCN-water deficit stress were characterized by substantial differences between soybean accessions. Accessions tested in this study exhibited significant variation in cyst counts. While some accessions noted a shift in FI, SCN resistance was not significantly different between treatment groups. However, this result should be interpreted with caution; power to detect treatment differences was extremely low, indicating analysis had limited sensitivity to detect treatment-driven effects. There were no significant interactions between accession and treatment, suggesting that accession-specific responses were modest relative to residual variability.

For example, S100 exhibited a reduction in model-estimated cyst counts, but an increase in the female index (FI) ranking between treatments (FI = 45.3, rank = MR) and

SCN-water deficit stress (FI = 63.4, rank = S). This likely represents differences between model-adjusted estimates and raw-mean-based ratios when treatment effects are small (Figure 2). Category shifts reflected relative changes around treatment medians rather than large absolute differences (Figure 4.3). Small changes in trait values or shifts among other accessions could alter performance classification without statistically significant differences.

Nineteen *G. soja* accessions were investigated. Of these, sixteen had previously noted SCN resistance, and two had been reported to have drought tolerance traits. The third, S67, has been reported to be susceptible to SCN, and was included as a *G. soja* check for SCN susceptibility (H. Zhang et al., 2017). One of the accessions previously noted to exhibit a drought tolerance trait (slow wilting) was found to have moderate SCN resistance (FI 10-30) in an unpublished study using the same SCN HG type used in this work, HG 1.2.5.7. Here it exhibited high nematode reproduction across both treatment groups. It did not show resistance or improved performance under either condition, providing a useful baseline for comparison of the other *G. soja* accessions. Cultivated checks (e.g., Williams 82, PI 88788) were excluded to avoid confounding effects of divergent genetic backgrounds.

When exposed to combined SCN-water deficit conditions, nearly all wild soybean accessions exhibited higher cyst counts in the combined stress environment. Interestingly, none of these differences in cysts counts were found to be statistically significant after Benjamini-Hochberg correction for multiple testing. While only one SCN life cycle was represented in this study, this provides promising preliminary data on the durability of SCN resistance in the face of a harmful abiotic stress when combined with SCN infection.

A few accessions stood out in their responses to SCN infection and combined SCN-water deficit. Accession S54 was found to be resistant under SCN stress (FI = 9.6), and remained moderately resistant (FI =16.1) under the combination stress environment. S54 was able to maintain a degree of SCN resistance to a virulent HG type while also maintaining higher biomass than the median for that trait (Figure 4.3). Since SCN has been shown to reduce both root and shoot biomass, the maintenance of resistance and relative

biomass performance illustrates its durability and potential usefulness in improving soybean germplasm. Another accession with established SCN resistance, S55, was able to maintain its performance classification from SCN stress while under combined SCN-water deficit conditions. It was previously found to be resistant to both resistant HG 0 and HG 1.2.5.7 (see Chapter 3); during this trial S55 exhibited a shift in FI from moderately resistant to moderately susceptible (FI = 24.9 and FI = 50.4, respectively). Additional studies are needed to determine the limits of SCN resistance stability in wild soybean.

S100 showed a different pattern of SCN reproduction, displaying the most reduction in estimated cyst counts between the two treatments (Figure 2) and an increase in FI (SCN-only: FI = 43.5, SCN-water deficit: FI = 49.9). The estimated marginal means are not reflective of FI, but are a relative measure of cyst count to adjust for replication differences and variance. When the average number of cysts increases for the combined stress of susceptible check (Williams 82), EMMeans and FI can move in opposite directions. This is an example of the weak treatment effect; different metrics give seemingly opposite signals.

As illustrated in Figure 4.3, S100 was considered tolerant under SCN-only stress, while it shifted to a High Performance rating under combined stress. Performance category shifts like this can occur when, as in this study, performance categories were defined relative to treatment-specific medians. Accessions that maintain their performance ranking may be more durable under SCN and combined SCN stress, but that is within the framework of the experiment, and cannot be globally applied. However, it does provide a way to assess accessions within the experimental setting in which they are found.

Wild Soybean Performance Under SCN and Combined Stress

In general, the changes in SCN reproduction and biomass accumulation between the SCN-only and combined stress treatments were modest and largely non-significant; relative differences between accessions resulted in notable stability in resistance rankings and performance classification between the two treatments (Table 1). With regards to performance classification, three accessions stayed in the same High performance category

across treatment groups.

Standout accession S54 remained in the High Performance classification across single and combined stress conditions. Although S54 experienced an increase in SCN reproduction, the shift was not statistically significant. As previously described in Chapter 2 and Chapter 3, S54 has consistently distinguished itself as a source of SCN resistance to multiple HG types (HG 0, HG 1.2.5.7, and HG 2.5.7 per Zhang et al., 2016). This study showed that S54 has potential for durability under combined SCN and abiotic stress, including water deficit. Accessions S32, and S11 also remained in the high performance classification group between treatments.

Within the Potential trade off classification, S55 and S74 remained in the same classification group between SCN-only treatment and SCN-WD treatment. The Tolerance classification quadrant retained S05 and S14, while the Low performance quadrant retained DW02 and H05 (Figure 4.3).

In independent screenings of HG standard cultivars, accession DW01 had previously been classified as moderately susceptible and moderately resistant to HG 1.2.5.7. It has independently been tested for slow wilting (Seversike et al., 2012). In this study, DW01 had relatively lower SCN and biomass, but shifted to the poor performance quadrant under the combination of SCN and water deficit reflecting an increase in relative cyst production and/or reduced biomass compared to other accessions. This shift highlights the sensitivity of some accessions to combined stress, where relatively modest changes in SCN reproduction or biomass result in decreased performance relative to other accessions in the same conditions.

Some accessions remained in the same classification quadrant while exhibiting shifts in relative cyst count and biomass between treatments. All other accessions shifted from their SCN stress classification quadrant. These results revealed important considerations related to accession type, their genetic background, and environment. Classification of estimated means for SCN reproduction and total biomass was determined based on the treatment specific median for both of those metrics. As some accessions within the High

performance classification or the Trade off classification represented SCN reproduction relative to the median, not a defined metric of "good vs bad" SCN reproduction.

Accession-specific responses to SCN and combined SCN-WD stress such as these likely reflect differences in evolutionary backgrounds and the timing of the applied stressors. Here SCN infection was applied prior to water restriction cycles. Elsewhere, water deficit has been applied before other stress conditions. There is evidence that water deficiency may act as a defensive primer for plants that later improves tolerance or resistance to pathogens by activating the plant immune response early as a form of "stress memory". This may be especially beneficial if the abiotic stress (water restriction) is mild in nature. However, experimental designs that impart mild water deficit before SCN infection should be interpreted cautiously in the context of SCN infection and resistance. In SCN-infested soils, soybean roots may encounter the nematode early in development. Early infection by a biotic agent may influence subsequent responses to additional abiotic or biotic stressors in less beneficial ways (Hilker et al., 2015; Sintaha et al., 2022; Tang et al., 2023).

Integration of SCN reproduction and biomass further elucidated the variation in accession performance that is consistent with potential trade-offs or alternative response strategies. While some accessions, such as S54, combined lower cyst reproduction with higher biomass, others exhibited low SCN but reduced biomass, indicating their relative resistance may not coincide with strong growth performance. In contrast, some accessions maintained relatively high biomass despite supporting higher SCN reproduction, suggesting tolerance rather than resistance. These patterns indicate that wild soybean accessions differ in how they allocate resources between growth and defense, and that resistance and biomass production are not universally aligned traits.

Plant Performance Evaluation Metrics

To evaluate accession responses beyond relative changes in SCN reproduction, plant performance was assessed by integrating cyst reproduction metrics (EMMeans) with a plant vigor trait. EMMeans provides estimates of accession performance that account for

variation in replication and model structure, offering a more stable and comparable measure of cyst production across accessions and treatments. Cyst count data were right skewed and heteroskedastic, thus the use of this model improved variance stabilization while retaining interpretability of SCN reproduction.

In contrast, the Female Index represents a linear normalization of the accession means relative to a susceptible check and does not incorporate a model-based variance adjustment. Thus, EMMeans were used as the primary metric of SCN reproduction, while FI was retained as a complementary measure for comparison with established resistance classifications.

Total biomass was selected as the primary indicator of plant performance as it showed the strongest and most consistent association with SCN reproduction among the biomass-related traits measured. Spearman rank correlation analysis indicated that total biomass had the highest average magnitude of association in cyst count, model-estimated cyst counts, and female index compared to root and shoot biomass or root to-stem ratio (RSR). Total biomass was selected based on the strength and consistency of these associations rather than statistical significance alone, as the objective was to identify a biological meaningful indicator of plant performance under stress. As such, total biomass is a comprehensive measure of plant vigor and the ability to maintain growth under SCN infection and combined stress conditions, making it a suitable choice for evaluating overall accession performance in conjunction with SCN reproduction.

Treatment-specific medians were used to define performance categories because they provide a robust distribution-independent threshold that is less sensitive to skew and extreme values than the mean. This allowed accessions to be classified based on relative performance within each stress environment rather than absolute trait values.

Host genotype, pathogen virulence, and stress timing likely influence responses to combined stress. In this study, SCN eggs were applied to roots before water restriction was applied to more closely mimic field conditions. Roots encounter SCN cysts and

eggs immediately after emergence, and their exudates can either promote or inhibit egg hatching and SCN juvenile infection. Root pathogens such as SCN may damage roots and interfere with water uptake, exacerbating the effect of water deficit. In some cases, beneficial microbes may prime soybeans for water deficit, exhibiting more lateral root growth that enhances drought tolerance. In general, hot and dry weather conditions have been found to enhance SCN reproduction, are negatively associated with precipitation, and are positively correlated with temperature. Virulent populations were also shown to increase, and were able to overcome common resistance genes such as PI 88788. There is evidence that increasingly hot and dry conditions may accelerate the SCN life cycle, both by lengthening warmer months in which SCN hatch, and by accelerating SCN development from the current 28 day life cycle to 15-18 days (McCarville et al., 2017). Understanding the effects of combined SCN-water deficit stress is an important consideration when evaluating soybean responses to these stressors.

Phenotypic and Physiological Associations with SCN Reproduction

A subset of the 15 traits of the spectral index and five traits of biomass and growth measured in this study collectively explained the variation in the reproduction of SCN. The model utilized a reduced subset of these traits explained approximately 11.5% of variation in log-transformed cyst counts. These four traits are the normalized vegetation index (NDVI), the photochemical reflectance index (PRI), the plant senescence reflectance index (PSRI), and the root-to-shoot ratio.

NDVI, or normalized vegetation index, was also negatively correlated with SCN reproduction.. NDVI is an assessment of plant health and greenness. It has been used to detect changes in chlorophyll content. As pathogen damage and pathogen load increases, chlorophyll photosystems are damaged and degraded. However, soybeans can be both highly infected (stressed) and green before the onset of chlorosis. Cultivated soybean can withstand increasing densities of the SCN population and long duration of infection (60-70 days) before chlorophyll degradation leads to chlorosis. Chlorosis, as a symptom of

SCN infection, lags a little behind female development after infection is established. The syncytium is a nutrient sink, making NDVI assessment of chlorohpyll and chlorosis at 30 days an indicator of SCN reproduction (Bent, 2022).

PRI was negatively correlated with cyst counts. PRI, the photochemical reflectance index, is related to xanthophyll pigment composition. These carotenoid pigments act as crucial stress-response machinery. *Arabidopsis thaliana* infected with *Heterodera schachtii* (beet cyst nematode) have exhibited decreased carotenoid content compared to controls. Xanthophylls function as photoprotective agents; but their effectiveness is reduced in the case of some root-based pathogens, as the photosynthetic apparatus is damaged by the SCN feeding process, which causes chlorosis. In contrast to NDVI, which measures how much light is absorbed (structure of the photosynthetic apparatus), PRI provides a metric for how efficiently intercepted light is used for photosynthesis (function of the photosynthetic apparatus). PRI is highly sensitive to rapid changes in photosynthesis related to water stress or other light conditions. In the case of SCN and SCN-WD conditions in this study, the decrease of PRI-related xanthophylls is likely an accumulation of photosystem breakdown after one SCN life cycle; it has previously exhibited high correlation with soybean disease after 98-105 days after infection. NDVI changes more slowly over time, reflecting slower structural changes over time, making these two indices complementary measurements of the effects of SCN infection.

The root to shoot ratio (RSR) was positively correlated with cyst counts. Higher allocation of root biomass may be an example of an ecological tradeoff between enhancing adaptation to the water deficit while simultaneously increasing host biomass for SCN infection and development. Biomass allocation patterns in this study associated with to SCN susceptibility under stress. RSR reflects how plants allocate carbon above- and below-ground in response to environmental conditions. In favorable conditions, shoot growth is prioritized to support energy acquisition and reproductive success. In unfavorable conditions, particularly water deficit, allocation shifts to below ground growth to prioritize

water and nutrient uptake (Kurepa & Small, 2022).

The relationship between RSR and SCN reproduction in this study suggests that root allocation is not indicative of tolerance. Accessions with high RSR may reflect altered carbon allocation in response to stress without limiting nematode reproduction. Accessions with higher RSR may produce more root mass(e.g., lateral roots) as a way to tolerate larger SCN cyst loads that cannot be eliminated via host resistance. In field conditions, this may facilitate sustained SCN infection until environmental constraints (e.g., lower temperatures) or crops are harvested and further development is limited for that season. However, since SCN can survive in soil during colder seasons and over a period of years, subsequent plantings may be at risk for high levels of infection and lower yields. In *G. max* cultivars, high SCN population density is typically associated with susceptible accessions, and resistance loci such as *rhg 1* reduce SCN reproduction. In *G. soja*, variation in resistance and tolerance strategies can result in accession that maintains growth despite infection while still supporting relatively high nematode populations, consistent with the positive association observed between RSR and cyst counts (Du et al., 2020; Medina López et al., 2025)..

Water deficit conditions, which reallocate growth from above-ground biomass to root development, may compromise moderate SCN resistance mechanisms found in accessions like DW01. This accession has exhibited variation in SCN resistance from moderate resistance to the moderate susceptibility and full susceptibility observed in this study (FI = 32.9 and FI = 66.7 for SCN only and SCN-water deficit stress, respectively). Notably, DW01 and DW02, have been reported to harbor traits that allow them to tolerate water deficit, slow wilting and variable wilting, respectively (Seversike et al., 2012).

Wilting represents a short-term physiological response that reduces transpiration and conserves water, but also reduces photosynthesis and does not directly alleviate below ground resource limitations. Wilting may be a temporary mitigation strategy rather than a sustainable mechanism under prolonged water deficit. Though slow-wilting accessions

can maintain higher yields and recover more effectively following water restoration, the combination of SCN infection and water deficit in this study may have exceeded the adaptive capacity of DW01 and DW02 over the course of the SCN life cycle. This suggests that while wilting-related traits can confer drought tolerance, especially in the short term, they do not protect against SCN infection stress in a meaningful way and may coincide with reduced overall plant performance under combined SCN-water deficit conditions (Du et al., 2020). DW01's previous performance for partial or moderate SCN resistance indicates some potential for future studies to investigate the relationship between biotic stress resistance and abiotic stress tolerance, but does not necessarily make it an immediate candidate for soybean improvement.

The plant senescence reflectance index (PSRI) was the final trait that explained the variation in the reproduction of the SCN in this study. Used to assess canopy stress, senescence, and fruit ripening, PSRI was the only one of these traits not significantly associated with cyst counts. Higher PSRI values in general indicate higher stress and chlorophyll degradation, key aspects of both plant maturity and age- and stress-related senescence. It is sensitive to the accumulation of carotenoids relative to chlorophyll breakdown, and is often used as a monitor for crop health In soybean, it is often used to track seed protein content at the end of the growing season (Arjoune et al., 2022).

Predictive traits were chosen to represent distinct physiological processes, not solely based on correlative statistical significance. The structured selection of traits was based on a combination of correlation screening, redundancy filtering, and PCA axis representation. In the case of PSRI, inclusion in this analysis represents a unique physiological state where stress pigments, carotenoids, and senescence are captured together. PSRI is a widely used stress and senescence indicator relevant to plant-pathological interactions. Predictor selection prioritized biological representation of independent trait dimensions rather than individual p-value significance. The reduced, four-trait model, supports its inclusion, while maintaining representation of multiple physiological processes related to plant vigor, stress

response, and biomass allocation.

The selected predictors represent distinct physiological processes, but are not entirely independent, reflecting the interconnectedness of plant physiological systems. Both PSRI and PRI are influenced by carotenoid dynamics, while PSRI incorporates variation in chlorophyll content. Similarly, NDVI reflects canopy greenness and chlorophyll status, which are linked to photosynthetic efficiency captured by PRI. Though multicollinearity was low based on variance inflation factors (VIF < 3), these relationships indicate some shared biological variance. Together, these traits represent a coordinated physiological system in which photosynthetic function, canopy structure, pigment dynamics, and biomass allocation respond in an integrated manner to SCN infection and environmental stress. Rather than behaving independently, these processes are biologically linked, contributing to shared and complementary information to the model.

Combined Stress Biology: SCN and Water Deficit Interaction

Interactions between soybean cyst nematode (SCN) and water deficit stress is a distinct physiological condition shaped by interacting biological processes. The combination of SCN and water deficit did not result in significant increases in cyst reproduction relative to SCN-only conditions, indicating that water deficit treatment did not substantially amplify nematode reproduction under experimental conditions. Instead, differences between accessions in SCN reproduction remained the dominant factor, with comparatively small treatment effects.

Water deficiency stress can impose opposing effects on plant-nematode interactions, including reduced root development and resource availability that may limit nematode development, alongside potential suppression of host defenses that could increase susceptibility. These influences may counteract each other, resulting in minimal changes in cyst production. The sequence of stress application is likely an important factor. In this study, SCN infection preceded water restriction treatment, which may have influenced host physiological responses and the progression of nematode development. Early-stage infection may

establish feeding sites prior to the onset of water limitation, reducing the extent to which water deficit alters subsequent nematode reproduction. The stress first applied may set the tone for plant physiological responses. In some cases, water restriction applied before more severe water deficit or other stress factors may prime the host immune system with a low level of stress, making it more robust to subsequent stress applications. However, application of the pathogen before the abiotic stress, though perhaps closer to most field conditions, may prime the host for reduced resistance rather than to defense.

Host genetic background likely plays a strong role as well, as the direction of SCN cyst counts and model-estimated cyst counts was not consistent between accessions. The modest and non-significant treatment effects observed here are also consistent with the possibility that plant physiological responses to combined stress are buffered or regulated in a manner that maintains overall system stability. Rather than producing large shifts in SCN reproduction, combined stress may alter relative accession performance, as reflected in shifts in resistance rankings and performance classifications. This context dependence is illustrated further by the reversal in the relationship between plant biomass and nematode cyst numbers. Under single SCN conditions, total biomass was positively associated with cyst counts; in contrast, under combined SCN-WD stress the relationship was negative. Shifts like these indicate that plant growth and SCN reproduction is not fixed, but depends on the environmental context. This may reflect differences in resource allocation, stress physiology, and host pathogen interactions under combined stress conditions. These results highlight the importance of considering any combined stress as a unique biological context, where interactions among host physiology, environmental conditions, and pathogen dynamics shape outcomes in ways that are not predictable from either single stress alone.

Understanding these interactions is particularly important in agricultural systems, where crops are frequently exposed to multiple stressors simultaneously. The results of this study suggest that, at least under the conditions tested, the resistance to SCN in wild soybean did not show a statistically detectable reduction in resistance when exposed to

a relatively severe early onset water deficit, although the ability to detect treatments was low. This limits the ability to draw strong conclusions about treatment-driven differences. While subtle context dependent shifts in performance may still occur among accessions, this reinforces the need to evaluate plant responses under combined stress conditions directly, rather than attempting to infer outcomes from single-stress studies.

Broader Implications for Soybean Improvement and Stress Biology

The results of this study have several implications for soybean improvement under conditions of combined biotic and abiotic stress. The relative stability of SCN resistance across single SCN and combined SCN-water deficit conditions suggests no statistically significant reduction in resistance as measured by SCN reproduction when under combined SCN-WD stress during early growth. However, limited power to detect treatment effects restricts the ability to draw strong conclusions about whether resistance mechanisms are compromised. This supports the potential utility of wild soybean germplasm as a source of durable SCN resistance under variable environmental conditions, though stronger powered studies will provide more reliable insight.

Integration of SCN reproduction metrics with plant biomass highlights the importance of evaluating accession performance using multiple complementary traits. While resistance, defined as nematode reproduction relative to a susceptible check, remains the primary breeding objective, the results demonstrate that resistance alone does not fully capture plant performance under stress. Accessions differed in their ability to maintain biomass while limiting SCN reproduction, indicating the potential for alternative strategies such as tolerance or growth-defense trade-offs. Ravelombola et al., 2020 has already incorporated a biomass-centered framework in their work to identify SCN resistance in cultivated soybean by incorporating a biomass metric, the Tolerance Index (TI) which evaluates the biomass a line infested with SCN with the biomass of the line without SCN. Their genome-wide association study identified genes associated with the ability to host SCN rather than to attempt to eliminate SCN infection without a large reduction in biomass.

Identification of physiological traits associated with SCN reproduction, including indices related to photosynthetic efficiency, canopy condition, and biomass allocation, suggests that plant physiological state contributes to variation in nematode performance. Although the proportion of variance explained was modest (11.5%), these traits offer insight into the underlying biological processes associated with host-parasite interactions. This supports the potential for high-throughput phenotyping approaches such as spectral reflectance indices, into breeding and selection strategies aimed at improving soybean resilience.

More broadly, this study underscores the importance of evaluating plant responses under combined stress conditions. The absence of strong additive effects of water deficit on SCN reproduction, coupled with shifts in relative accession performance highlights how combined stress represents a distinct biological context rather than a simple summation of individual stress effects. As climate variability increases the frequency and intensity of concurrent stressors and expands the range of crops and their pathogens, understanding these interactions will be critical for the development of resilient crop varieties.

Together these finds support a multi-dimensional approach to soybean improvement that integrates genetic resistance, physiological performance, and environmental context. Wild soybean is a valuable resource for identifying resilience traits, and continued evaluation across diverse stress combinations and pathogen populations will be essential for translating these insights into applied breeding programs.

Methodological Considerations

Several factors should be considered when interpreting this study. Water deficit stress was imposed under controlled conditions without direct physiological measurement of plant water status such as stomatal conductance or relative water content. Stomatal conductance measurements were not taken due to instrument limitations during the study period, and soil water content was not directly quantified because plants were grown in a sand-based medium, where standard soil moisture measurements are less applicable. As a result, the degree of water deficit experienced by plants was inferred by treatment

conditions rather than quantified directly. This allowed for consistent application across treatments, although it limited the ability to precisely characterize the intensity of the water deficit and the water status of the plants. Future studies incorporating direct physiological and environmental measurements would allow for a more precise characterization of the intensity of the water deficit and its interaction with SCN infection.

The plant-level regression identified endpoint traits associated with log-transformed cyst counts. However, multiple observations were observed within accessions, and so the assumption of independent residuals under an ordinary least squares (OLS) model may have not been met. Coefficient significance and model explanatory power should be interpreted cautiously. A mixed-effects model with accession included as a random effect would likely provide a more rigorous test of whether these associations persist after accounting for accession level clustering. Associations identified in the OLS framework should be interpreted as plant-level relationships that partially reflect shared accession effects. Incorporating accession (and therefore, shared genetic background) as a random effect would allow for evaluation of whether trait-cyst count relationships persist after accounting for accession-level variation (Zuur et al., 2009).

The reduced model explained a relatively small proportion of the total variation in SCN reproduction ($R^2 = 0.115$), indicating a substantial proportion of variability remained unexplained by the measured traits. This likely reflects the complexity of SCN-host interactions, which are influenced by additional genetic, physiological, and environmental factors not captured in the current study. As such, the identified trait associations should be interpreted as contributing factors, rather than as comprehensive predictors of SCN reproduction.

Future Directions

Building on the findings of this study, several avenues for future research can advance understanding of wild soybean responses to combined stressors. First, evaluation of wild soybeans across multiple SCN populations would provide insight into the breadth and

durability of resistance observed here. Because SCN resistance is often population specific, testing accessions against diverse populations of SCN will be important for accessing their utility in breeding programs. The accessions assessed here were previously found to have SCN resistance, but the resistance response is variable dependent on the HG type of *H. glycines* under study.

Integrating physiological phenotyping with genomic approaches represents a promising direction for improving predictive understanding of SCN resistance in wild soybean. Linking traits such as photosynthetic efficiency, canopy condition, and biomass allocation with quantitative trait loci and genome-wide association analysis could identify genetic mechanisms underlying the observed phenotypic patterns. In this context, the combined use of resistance and performance metric offers particular promise. Approaches such as tolerance indices (Ravelombola et al., 2020), when used in conjunction with female index (FI), may provide a powerful framework for identifying loci associated with SCN resistance and plant performance. Incorporating these two complementary metrics enables a more comprehensive assessment of the potential of wild soybean resistance and resistance durability; this mixed approach can capture multiple dimensions of plant responses that are relevant for soybean improvement.

Future studies should continue to broaden our understanding of plant phenotypic responses under a broader range of environmental conditions. The severity of one stressor can influence plant responses, thus experiments that manipulate the timing of SCN infection and water deficit would provide further insight into combined stress biology. Genes for SCN resistance and water deficit tolerance provide the basis of potential plant response. Precise phenotyping elucidates the actual response to environmental conditions. Genetic markers are robust tools for identifying traits of interest, but they do not capture environmental effects on gene expression. In this study phenotyping integrated SCN resistance, biomass, and physiology, validating the real-world effectiveness of potential resistance loci in wild soybean. This complementary approach offers a comprehensive framework for improving

soybean resilience

Integration of phenotypic and genotypic approaches is essential in order to translate these findings into soybean improvement outcomes. Marker-assisted selection (MAS) and genomic approaches can be used to identify and track resistance loci, while phenotypic screening ensures selected accessions maintain desirable agronomic traits, such as biotic and abiotic stress resilience. Breeding strategies may include the incorporation of favorable alleles from wild soybean into elite germplasm through traditional crosses, followed by selection using molecular markers and performance-based metrics. The development of multi-parent advanced generation intercross (MAGIC) lines provides an opportunity to recombine diverse genetic backgrounds and capture complex trait interactions, including those associated with combined stress responses. The combined use of distinct, yet linked resistance metrics can guide selection towards wild soybean accessions that both suppress SCN reproduction and maintain growth under harsh conditions. Targeted gene editing will further accelerate the identification and deployment of favorable trait combinations. Such integrated approaches are critical for the next generation of soybean cultivars to be capable of maintaining productivity under combined abiotic and biotic stress conditions.

Collectively, these findings highlight the value of multidimensional approaches to soybean improvement, where resistance, physiology, and performance are considered together to develop soybean cultivars capable of maintaining productivity under complex stress environments.

References

Acharya, K., & Yan, G. (2021). Screening of Early Maturing Soybean Accessions for Resistance Against HG Type 2.5.7 of Soybean Cyst Nematode *Heterodera glycines*. *Plant Health Progress*, 23(2), 166–173. https://doi.org/10.1094/php-07-21-0105-rs

Acutis, M., Scaglia, B., Confalonieri, R. (2012). Perfunctory analysis of variance in agronomy, and its consequences in experimental results interpretation. *European Journal of Agronomy*, 43, 129–135. https://doi.org/10.1016/j.eja.2012.06.006

Benjamini, Y., & Yekutieli, D. (2001). The control of the false discovery rate in multiple testing under dependency. *The Annals of Statistics*, 29(4). https://doi.org/10.1214/aos/1013699998

Bradley, C. A., Allen, T. W., Sisson, A. J., Bergstrom, G. C., Bissonnette, K. M., Bond, J., Byamukama, E., Chilvers, M. I., Collins, A. A., Damicone, J. P., Dorrance, A. E., Dufault, N. S., Esker, P. D., Faske, T. R., Fiorellino, N. M., Giesler, L. J., Hartman, G. L., Hollier, C. A., Isakeit, T., . . . Wise, K. A. (2021). Soybean Yield Loss Estimates Due to Diseases in the United States and Ontario, Canada, from 2015 to 2019. *Plant Health Progress*, 22(4), 483–495. https://doi.org/10.1094/php-01-21-0013-rs

Brown, S., Yeckel, G., Heinz, R., Clark, K., Sleper, D., & Mitchum, M. G. (2010). A High-Throughput Automated Technique for Counting Females of *Heterodera glycines* using a Fluorescence-Based Imaging System. *PubMed*, 42(3), 201–206. https://pubmed.ncbi.nlm.nih.gov/22736857

Burton, J., Carter, T., Fountain, M., & Bowman, D. (2006). Registration of 'NC-Raleigh' Soybean. *Crop Science*, 46(6), 2710–2711. https://doi.org/10.2135/cropsci2005.11.0410

Change, I. P. O. C. (2023). Climate Change 2022 – Impacts, adaptation and vulnerability. In *Cambridge University Press eBooks*. https://doi.org/10.1017/9781009325844

Colovic, M., Yu, K., Todorovic, M., Cantore, V., Hamze, M., Albrizio, R., & Stellacci, A. M. (2022). Hyperspectral vegetation indices to assess water and nitrogen status of sweet

maize crop. *Agronomy*, 12(9), 2181. https://doi.org/10.3390/agronomy12092181

Cerovic, Z. G., Samson, G., Morales, F., Tremblay, N., & Moya, I. (1999). Ultraviolet-induced fluorescence for plant monitoring: present state and prospects. *Agronomie*, 19(7), 543–578. https://doi.org/10.1051/agro:19990701

Dhanapal, A. P., Ray, J. D., Singh, S. K., Hoyos-Villegas, V., Smith, J. R., Purcell, L. C., & Fritschi, F. B. (2016). Genome-wide association mapping of soybean chlorophyll traits based on canopy spectral reflectance and leaf extracts. *BMC Plant Biology*, 16(1), 174. https://doi.org/10.1186/s12870-016-0861-x

Dilawari, R., Kaur, N., Priyadarshi, N., Prakash, I., Patra, A., Mehta, S., Singh, B., Jain, P., & Islam, M. A. (2022). Soybean: A Key Player for Global Food Security. In *Soybean Improvement* (pp. 1–46). https://doi.org/10.1007/978-3-031-12232-3_1

Du, X., Zhang, X., Chen, X., Jin, W., Huang, Z., & Kong, L. (2024). Drought stress reduces the photosynthetic source of subtending leaves and the transit sink function of podshells, leading to reduced seed weight in soybean plants. *Frontiers in Plant Science*, 15, 1337544. https://doi.org/10.3389/fpls.2024.1337544

Ergin, N., Kulan, E. G., Harmancı, P., & Kaya, M. D. (2025). Morpho-physiological and water use performance of soybean cultivars under drought stress at early growth stages. *International Journal of Agriculture Environment and Food Sciences*, 9(1), 13–21. https://doi.org/10.31015/2025.1.2

Fodor, N., Challinor, A., Droutsas, I., Ramirez-Villegas, J., Zabel, F., Koehler, A., & Foyer, C. H. (2017). Integrating Plant Science and Crop Modeling: Assessment of the impact of climate change on soybean and maize production. *Plant and Cell Physiology*, 58(11), 1833–1847. https://doi.org/10.1093/pcp/pcx141

Gamon, J. A., Peñuelas, J., & Field, C. B. (1992). A narrow-waveband spectral index that tracks diurnal changes in photosynthetic efficiency. *Remote Sensing of Environment*, 41(1), 35–44.

Gitelson, A., & Merzlyak, M. N. (1994). Quantitative estimation of chlorophyll-a using

reflectance spectra: Experiments with autumn chestnut and maple leaves. *Journal of Photochemistry and Photobiology B Biology*, 22(3), 247–252. https://doi.org/10.1016/1011-1344(93)06963-4

Gitelson, A. A., Merzlyak, M. N., & Chivkunova, O. B. (2001). Optical properties and nondestructive estimation of anthocyanin content in plant leaves. *Photochemistry and Photobiology*, 74(1), 38–45.

Guo, B., Chen, L., Dong, L., Yang, C., Zhang, J., Geng, X., Zhou, L., & Song, L. (2023). Characterization of the soybean KRP gene family reveals a key role for GmKRP2a in root development. *Frontiers in Plant Science*, 14, 1096467. https://doi.org/10.3389/fpls.2023.1096467

Hilker, M., Schwachtje, J., Baier, M., Balazadeh, S., Bäurle, I., Geiselhardt, S., Hincha, D. K., Kunze, R., Mueller-Roeber, B., Rillig, M. C., Rolff, J., Romeis, T., Schmülling, T., Steppuhn, A., Van Dongen, J., Whitcomb, S. J., Wurst, S., Zuther, E., & Kopka, J. (2015). Priming and memory of stress responses in organisms lacking a nervous system. *Biological Reviews of the Cambridge Philosophical Society*, 91(4), 1118–1133. https://doi.org/10.1111/brv.12215

Jenkins, W. R. (1964). A rapid centrifugal-flotation technique for separating nematodes from soil. *Plant Disease Reporter*, 48(692).

Joalland, S., Screpanti, C., Liebisch, F., Varella, H. V., Gaume, A., & Walter, A. (2017). Comparison of visible imaging, thermography and spectrometry methods to evaluate the effect of *Heterodera schachtii* inoculation on sugar beets. *Plant Methods*, 13(1), 73. https://doi.org/10.1186/s13007-017-0223-1

Khatri, P., Kumar, P., Shakya, K. S., Kirlas, M. C., & Tiwari, K. K. (2023). Understanding the intertwined nature of rising multiple risks in modern agriculture and food system. *Environment Development and Sustainability*, 26(9), 24107–24150. https://doi.org/10.1007/s10668-023-03638-7

Kofsky, J., Zhang, H., & Song, B. (2018). The Untapped Genetic Reservoir: The Past,

Current, and Future Applications of the Wild Soybean (*Glycine soja*). *Frontiers in Plant Science*, 9, 949. https://doi.org/10.3389/fpls.2018.00949

Ku, Y., Au-Yeung, W., Yung, Y., Li, M., Wen, C., Liu, X., & Lam, H. (2013). Drought stress and tolerance in Soybean. In *InTech eBooks*. https://doi.org/10.5772/52945

Kupčinskienė, A., Brazaitytė, A., Rasiukevičiūtė, N., Valiuškaitė, A., Morkeliūnė, A., & Vaštakaitė-Kairienė, V. (2023). Vegetation Indices for Early Grey Mould Detection in Lettuce Grown under Different Lighting Conditions. *Plants*, 12(23), 4042. https://doi.org/10.3390/plants12234042

Lichtenthaler, H. K., & Wellburn, A. R. (1983). Determinations of total carotenoids and chlorophylls a and b of leaf extracts in different solvents. *Biochemical Society Transactions*, 11(5), 591–592.

Lin, S., Zhang, W., Wang, G., Hu, Y., Zhong, X., & Tang, G. (2024). Physiological Regulation of Photosynthetic-Related Indices, Antioxidant Defense, and Proline Anabolism on Drought Tolerance of Wild Soybean (*Glycine soja* L.). *Plants*, 13(6), 880. https://doi.org/10.3390/plants13060880

Lumactud, R. A., Dollete, D., Liyanage, D. K., Szczyglowski, K., Hill, B., & Thilakarathna, M. S. (2022). The effect of drought stress on nodulation, plant growth, and nitrogen fixation in soybean during early plant growth. *Journal of Agronomy and Crop Science*, 209(3), 345–354. https://doi.org/10.1111/jac.12627

Mahecha-Garnica, S., Ye, W., Schumacher, L. A., & Gorny, A. M. (2022). Soybean Cyst Nematode of Soybean: a Diagnostic guide. *Plant Health Progress*, 23(4), 507–513. https://doi.org/10.1094/php-11-21-0138-dg

Mahlein, A., Rumpf, T., Welke, P., Dehne, H., Plümer, L., Steiner, U., & Oerke, E. (2012). Development of spectral indices for detecting and identifying plant diseases. *Remote Sensing of Environment*, 128, 21–30. https://doi.org/10.1016/j.rse.2012.09.019

Markwell, J., Osterman, J. C., & Mitchell, J. L. (1995). Calibration of the Minolta SPAD-502 leaf chlorophyll meter. *Photosynthesis Research*, 46(3), 467–472.

Martín-Cardoso, H., San Segundo, B. (2025). Impact of Nutrient Stress on Plant Disease Resistance. *International Journal of Molecular Sciences*. 26(4), 1780. https://doi.org/10.3390/ijms26041780

Maxwell, K., & Johnson, G. N. (2000). Chlorophyll fluorescence—a practical guide. *Journal of Experimental Botany*, 51(345), 659–668. https://doi.org/10.1093/jexbot/51.345.659

McCarville, M. T., Marette, C.C., Mullaney, M.P., Gebhart, G. D., Tylka, G. L. (2017). Increase in Soybean Cyst Nematode Virulence and Reproduction on Resistant Soybean Varieties in Iowa from 2001 to 2015 and the Effects on Soybean Yields. *Plant Health Progress*, 18(3), 146–155. https://doi.org/10.1094/php-rs-16-0062

Mengistu, A., Read, Q. D., Skyes, V., Kelly, H., Kharel, T., & Bellaloui, N. (2024). Cover Crop and Crop Rotation Effects on Tissue and Soil Population Dynamics of Macrophomia phaseolina and Yield Under No-Till System. *Plant Disease*, 108(2), 302-310. https://doi.org/10.1094/pdis-03-23-0443-re

Merzlyak, M. N., Gitelson, A. A., Chivkunova, O. B., & Rakitin, V. Y. (1999). Non-destructive optical detection of pigment changes during leaf senescence and fruit ripening. *Physiologia Plantarum*, 106(1), 135–141.

Nguyen, T. C., Tran, H. A., Lee, J., Seo, H. S., Jo, H., & Song, J. T. (2024). Genetic Control of Tolerance to Drought Stress in Wild Soybean (*Glycine soja*) at the Vegetative and the Germination Stages. *Plants*, 13(14), 1894. https://doi.org/10.3390/plants13141894

Niblack, T. L., Arelli, P. R., Noel, G. R., Opperman, C. H., Orf, J. H., Schmitt, D. P., Shannon, J. G., & Tylka, G. L. (2002). A Revised Classification Scheme for Genetically Diverse Populations of *Heterodera glycines*. *Journal of Nematology*, 34(4), 279–288.

Niblack, T. L., Tylka, G. L., Arelli, P., Bond, J., Diers, B., Donald, P., Faghihi, J., Gallo, K., Heinz, R. D., Lopez-Nicora, H., Von Qualen, R., Welacky, T., & Wilcox, J. (2009). A standard greenhouse method for assessing soybean cyst nematode resistance in

soybean: SCE08 (Standardized Cyst Evaluation 2008). *Plant Health Progress*, 10(1). https://doi.org/10.1094/php-2009-0513-01-rv

Oliwa, J., Skoczowski, A., Rut, G., & Kornaś, A. (2023). Water-Deficit Stress in the Epiphytic Elkhorn Fern: Insight into Photosynthetic Response. *International Journal of Molecular Sciences*, 24(15), 12064. https://doi.org/10.3390/ijms241512064

Ordóñez, R. A., Archontoulis, S. V., Martinez-Feria, R., Hatfield, J. L., Wright, E. E., & Castellano, M. J. (2020). Root to shoot and carbon to nitrogen ratios of maize and soybean crops in the US Midwest. *European Journal of Agronomy*, 120, 126130. https://doi.org/10.1016/j.eja.2020.126130

Parry, C., Blonquist, J. M., & Bugbee, B. (2014). In situ measurement of leaf chlorophyll concentration: analysis of the optical/absolute relationship. *Plant Cell & Environment*, 37(11), 2508–2520. https://doi.org/10.1111/pce.12324

Pathan, M. S., Lee, J., Shannon, J. G., & Nguyen, H. T. (2007). Recent Advances in Breeding For Drought and Salt Stress Tolerance in Soybean. In *Recent Advances in Breeding for Drought and Salt Stress Tolerance in Soybean* (pp. 739–773). https://doi.org/10.1007/978-1-4020-5578-$2_3$0

Peñuelas, J., Piñol, J., Ogaya, R., & Filella, I. (1997). Estimation of plant water concentration by the reflectance Water Index WI (R900/R970). *International Journal of Remote Sensing*, 18(13), 2869–2875.

Pettorelli, N., Vik, J. O., Mysterud, A., Gaillard, J., Tucker, C. J., & Stenseth, N. C. (2005). Using the satellite-derived NDVI to assess ecological responses to environmental change. *Trends in Ecology & Evolution*, 20(9), 503–510. https://doi.org/10.1016/j.tree.2005.05.011

Pokhrel, A. (2021). Role of Individual Components of Disease Triangle in Disease Development: A Review. *Journal of Plant Pathology & Microbiology*, 12(9), 573.https://doi.org/10.35248/2157-7471.21.12.573

Poromarto, S. H., & Nelson, B. D. (2009). Reproduction of soybean cyst nematode on dry

bean cultivars adapted to North Dakota and Northern Minnesota. *Plant Disease*, 93(5), 507–511. https://doi.org/10.1094/pdis-93-5-0507

Prince, S. J., Valliyodan, B., Ye, H., Yang, M., Tai, S., Hu, W., Murphy, M., Durnell, L. A., Song, L., Joshi, T., Liu, Y., Van De Velde, J., Vandepoele, K., Shannon, J. G., & Nguyen, H. T. (2018). Understanding genetic control of root system architecture in soybean: Insights into the genetic basis of lateral root number. *Plant Cell & Environment*, 42(1), 212–229. https://doi.org/10.1111/pce.13333

Richardson, A. D., Duigan, S. P., & Berlyn, G. P. (2002). An evaluation of noninvasive methods to estimate foliar chlorophyll content. *New Phytologist*, 153(1), 185–194. Seversike, T. M., Sermons, S. M., Sinclair, T. R., Carter, T. E., & Rufty, T. W. (2012). Temperature interactions with transpiration response to vapor pressure deficit among cultivated and wild soybean genotypes. *Physiologia Plantarum*, 148(1), 62–73. https://doi.org/10.1111/j.1399-3054.2012.01693.x

Shaw, R. G., & Mitchell-Olds, T. (1993). Anova for Unbalanced Data: An Overview. *Ecology*, 74(6), 1638–1645. https://doi.org/10.2307/1939922

Sintaha, M., Man, C., Yung, W., Duan, S., Li, M., & Lam, H. (2022). Drought stress priming improved the drought tolerance of soybean. *Plants*, 11(21), 2954. https://doi.org/10.3390/plants11212954

Sonobe, R., Yamashita, H., Mihara, H., Morita, A., & Ikka, T. (2020). Estimation of Leaf Chlorophyll a, b and Carotenoid Contents and Their Ratios Using Hyperspectral Reflectance. *Remote Sensing*, 12(19), 3265. https://doi.org/10.3390/rs12193265

Soybean growth stages. (n.d.). *Integrated Crop Management*. https://crops.extension.iastate.edu/encyclopedia/soybean-growth-stages

Staniak, M., Szpunar-Krok, E., & Kocira, A. (2023). Responses of soybean to selected Abiotic Stresses—PhotoPeriod, Temperature and water. *Agriculture*, 13(1), 146. https://doi.org/10.3390/agriculture13010146

Tang, X., Xue, Y., Cao, D., Luan, X., Zhao, K., Liu, Q., Ren, Y., Zhu, Z., Li, Y., &

Liu, X. (2023). Identification of Candidate Genes for Drought Resistance during Soybean Seed Development. *Agriculture*, 13(5), 949. https://doi.org/10.3390/agriculture13050949

Taylor, L. Aggregation, Variance and the Mean. *NatureNature*, 189, 732–735. https://doi.org/10.1038/189732a0

Taha, M. F., Mao, H., Wang, Y., ElManawy, A. I., Elmasry, G., Wu, L., Memon, M. S., Niu, Z., Huang, T., & Qiu, Z. (2024). High-Throughput analysis of leaf chlorophyll content in aquaponically grown lettuce using hyperspectral reflectance and RGB images. *Plants*, 13(3), 392. https://doi.org/10.3390/plants13030392

Telenko, D. E. P., Allen, T., Sisson, A. J., Bissonnette, K., Bonkowski, J., Bradley, C. A., Byamukama, E., Camiletti, B., Chilvers, M. I., Collins, A., Damicone, J., Dufault, N., Duffeck, M., Esker, P., Faske, T. R., Harbach, C., Isakeit, T., Jackson, T. A., Kleczewski, N., . . . Zeng, Y. (2025). Estimated soybean yield and economic losses caused by diseases in the United States and Ontario, Canada from 2020 to 2024. *Plant Health Progress*. https://doi.org/10.1094/php-09-25-0227-rs

USDA, Agricultural Research Service, National Plant Germplasm System. (2026). Germplasm Resources Information Network (GRIN Taxonomy). National Germplasm Resources Laboratory, Beltsville, Maryland. https://npgsweb.ars-grin.gov/gringlobal/taxon/taxonomydetail?id=17801

Valliyodan, B., Ye, H., Song, L., Murphy, M., Shannon, J. G., & Nguyen, H. T. (2016). Genetic diversity and genomic strategies for improving drought and waterlogging tolerance in soybeans. *Journal of Experimental Botany*, 68(8), erw433. https://doi.org/10.1093/jxb/erw433

Wang, G., Zhou, Q., He, M., Zhong, X., & Tang, G. (2020). Wilting index and root morphological characteristics used as drought-tolerance variety selection at the seedling stage in soybean (*Glycine max* L.). *Plant Growth Regulation*, 92(1), 29–42. https://doi.org/10.1007/s10725-020-00617-0

Wang, X., Wu, Z., Zhou, Q., Wang, X., Song, S., & Dong, S. (2022). Physiological response of soybean plants to water deficit. *Frontiers in Plant Science*, 12, 809692. https://doi.org/10.3389/fpls.2021.809692

Zandalinas, S. I., & Mittler, R. (2022). Plant responses to multifactorial stress combination. *New Phytologist*, 234(4), 1161–1167. https://doi.org/10.1111/nph.18087

Zar, J.H. (2010) Biostatistical Analysis. 5th Edition, *Prentice-Hall/Pearson*, Upper Saddle River, xiii, 944 p.

Zhang, H., Kjemtrup-Lovelace, S., Li, C., Luo, Y., Chen, L. P., & Song, B. (2017). Comparative RNA-Seq Analysis Uncovers a Complex Regulatory Network for Soybean Cyst Nematode Resistance in Wild Soybean (*Glycine soja*). *Scientific Reports*, 7(1), 9699. https://doi.org/10.1038/s41598-017-09945-0

Zhang, H., Li, C., Davis, E. L., Wang, J., Griffin, J. D., Kofsky, J., & Song, B. (2016). Genome-Wide Association Study of Resistance to Soybean Cyst Nematode (*Heterodera glycines*) HG Type 2.5.7 in Wild Soybean (*Glycine soja*). *Frontiers in Plant Science*, 7, 1214. https://doi.org/10.3389/fpls.2016.01214

Zuur, A. F., Ieno, E. N., Walker, N., Saveliev, A. A., & Smith, G. M. (2009). Mixed effects models and extensions in ecology with R. In *Statistics for biology and health*. https://doi.org/10.1007/978-0-387-87458-6

CHAPTER 5: SYNTHESIS & CONCLUSIONS

Framing SCN Resistance: Insights from Wild Relatives

Current frameworks for evaluating soybean cyst nematode resistance fails to fully capture the complexity of host responses across genetic, physiological, and environmental dimensions. Decades of resistance deployment have imposed strong directional selection on SCN populations, leading to increased virulence in ways that differ from more balanced host-pathogen coevolution in natural systems. As such, resistance must be understood as a multidimensional, context-dependent trait that extends beyond pathogen suppression to include plant performance and environmental response. Plant performance directly influences yield, the central outcome of soybean production, and varies across environmental conditions, including pathogen type and weather. This dissertation investigates the genetic, phenotypic, and environmental context in which wild soybean (*Glycine soja*) harnesses innate sources of resistance to protect itself from SCN. This work provides insight into, though not fully encompassing, the complexity of plant host and pathogen interactions within the wild soybean model.

To capture this complexity, multiple dimensions of resistance were investigated. Genetic mapping of wild soybean uncovered novel loci and epistatic interactions associated with SCN resistance. Phenotypic screening of wild soybean accessions evaluated the effect of distinct SCN population types on resistance. Combined stress experiments tested the resilience of SCN resistance by assessing wild soybean accessions while under single and combined SCN-drought conditions. Interpretation of treatment effects in this chapter should be made with caution, as the study had limited ability to detect differences between treatments. These findings illustrate the multidimensional nature of SCN resistance in wild soybean and point to key considerations when assessing wild soybean germplasm for

soybean improvement.

SCN Resistance Is A Multidimensional Trait System

Soybean cyst nematode resistance (*Heterodera glycines*) is a complex trait integrating host plant genetic, physiological and developmental factors, in addition to environmental and pathogen cues. The wild progenitor of soybean, *Glycine soja*, provides a diverse reservoir of SCN resistance. These studies have demonstrated the complexity of wild soybean response to SCN by identifying SCN resistance loci and epistatic interactions, screening for resistance between differential SCN populations, and testing the resilience of wild soybean resistance across contrasting environmental conditions. Collectively, these findings indicate that SCN resistance includes both pathogen suppression and plant performance so that some accessions maintain favorable physiological and phenotypic traits despite SCN infection. In this way, the understanding of SCN resistance becomes not a binary of resistance/susceptibility, or only a hierarchical ranking of resistance levels, but an integrated collection of traits that when deployed provide robust defenses against this damaging pathogen.

Resistance can also reflect tradeoffs between resource allocation. A root-based parasite, SCN infection affects plant growth and development, and the process of resistance may require ecological tradeoffs, reducing biomass production in favor of reducing pathogen load. Tolerance, on the other hand, may include the reallocation of biomass that results in pathogen maintenance, not suppression. There was some evidence for biological tradeoffs, but the relationship between biomass and resistance was weak. The direction of association differed between SCN-only and combined SCN-drought conditions (Chapter 4). Some accessions, such as S54, retained higher median biomass and lower resistance levels across stress conditions, while others had lower levels of resistance (though not full resistance) and lower than median biomass. This supports differential allocation strategies between accessions, suggesting yield and resistance are not inherently incompatible, promising results for producers who aim to increase yields while utilizing the most efficient form of

SCN suppression - host resistance.

Elucidation of the complex nature of SCN resistance in wild soybean is crucial in the face of increasingly harmful impacts of climate change. The functional host resistance in normal conditions is variably stable across harsher environmental contexts, including drought. Differences in environmental conditions, such as increased pressure on host resistance due to drought, are not clearly resolved. Statistical differences between single and combined stress conditions were not detectable. However, power to detect treatment effects was low, limiting the ability to draw strong conclusions. The inclusion of one additional stress factor has been shown to shift the performance of several wild soybean accessions. Host responses to multiple stressors are not simply the sum of responses to each stress applied individually. Plants have a marvelous capacity for plasticity in responses to environmental conditions, and this was seen through the lens of wild soybean response to differing SCN populations (Chapter 3) and changed environmental conditions (Chapter 4). Some accessions shifted root architecture and biomass traits in response to these changes, while others were able to maintain resistance and root traits.

Taken together, these findings indicate that SCN resistance cannot be attributed to a single underlying mechanism; instead resistance reflects the interaction of multiple genetic and physiological processes. In Chapter 2, novel loci associated with SCN resistance were identified, providing promising new avenues for the genetic improvement of soybean. Most interesting was the discovery of epistatic interactions between these loci and other parts of the *G. soja* genome and each other. These highlight the complex genetic architecture of pathogen resistance, where loci do not act independently, but in concert with one another and with other regions to express genes necessary for SCN suppression.

Screening of wild soybean (Chapter 3) expanded knowledge of the complex nature of SCN resistance by detailing the effects SCN population structure has on resistance and root traits. While some accessions of wild soybean were able to maintain their resistance, others shifted when exposed to more virulent SCN populations. While a few accessions

were able to maintain resistance, others shifted in response to exposure to nematodes with stronger pathogenicity and a wider virulence profile. However, many shifts in Female Index (FI) were not statistically significant, potentially indicating a stability towards the pathogen groups under study, providing crucial information for our understanding of wild soybean response when faced with the types of SCN populations found in soybean growing regions.

Chapter 4 provided another dimension, that of resistance and resilience in the face of harsh conditions. No accession showed a significant shift in SCN reproduction between the two treatment groups, though power to detect treatment effects was low. Though no detectably meaningful differences were found, in general cyst counts increased when wild soybean accessions faced drought, and physiological processes shifted in response to the differing environments.

These studies illustrate the multidimensional nature of wild soybean resistance. These crop wild relatives originate from a variety of environments which shaped their evolutionary history, and their responses to various conditions reflects the diversity of genetic, physiological, and phenotypic responses of which they are capable. No single genetic loci, function, or response explains why one accession performs better than another, especially in different stress conditions.

Accessions S54 and S55 provide an example of this complexity. These lines originate from neighboring provinces of South Korea, approximately 120 kilometers apart, representing geographically proximate environments with broadly similar climates. Across SCN HG types evaluated in this and previous studies, both exhibited comparable responses to infection. However, their responses diverged under combined SCN-drought stress. While both remained within their respective performance classifications, the female index of S55 increased substantially under drought conditions. This divergence, despite similar baseline resistance, highlights the context-dependent nature of SCN resistance and suggests the conclusion that resistance outcomes are shaped by interacting genetic and environmental factors rather than a single underlying mechanism. While underlying genetic differences

between these accessions likely contribute to their differential responses under combined SCN-drought, the divergence observed indicates that resistance cannot be fully understood without considering environmental context and genotype-by-environment interactions.

To understand the multifaceted nature of SCN resistance, a multi-metric approach is necessary to disentangle the complex intertwining of genetic control, environmental context, and phenotypic response. Differing metrics help elucidate distinct aspects of wild soybean resistance. Female index represents a normalized, rescaled form of cyst count relative to a susceptible check; it is not an independent metric, but standardized expression of SCN reproduction. Spectral indices such as NDVI and PSRI reflect canopy greenness and stress response, respectively, while biomass metrics such as root to shoot ratios provide insight on carbon allocation and, to a degree, biomass. No single metric fully describes whether an accession is resistant to SCN, however. They are tools that provide a snapshot of a single aspect of host response to SCN. As useful as they have been in identifying traits of interest, they represent one part of the organism, and the whole plant, or at least many aspects of it, must be considered to successfully develop resilient crop cultivars.

The aim of agricultural breeding is to increase productivity, and cultivars have been carefully developed to achieve that goal. Soybean breeders have increased important agronomic traits, reduced the need for inputs, and controlled infectivity of pathogens. However, a beneficial trait does not automatically cause an increase in productivity. Similarly, biological performance can mask susceptibility. A cultivar susceptible to HG 1.2.5.7 such as PI 88788 is able to maintain a heavy cyst load, and even reproduce, yet the problem of SCN avirulence to the *Rhg1* is not avoided, but rather promoted and advanced to the next growing season. By investigating multiple traits related to resistance, the understanding of its mechanics and outcomes will be better understood. The use of FI alone as a resistance metric would eliminate many accessions, as described in Chapter 4.

Multiple metrics must be considered together because they represent different facets of the physiological state of the individual organism. Analyses combining metrics allow for

a better understanding of host resource allocation strategy under pathogen infection. Some mechanisms limit pathogen infection altogether, while others limit the damage caused by the pathogen or other agent. Where a single metric captures only one mechanism, while crop breeding strategies depend upon multiple phenotypic considerations, such as biomass and measurements of response to environmental cues like pathogen infection. Resistance is a system-level phenotype, thus the metrics by which we assess resistance must consider as many processes as practicable to make balanced, robust decisions about which *G. soja* accessions to incorporate into soybean germplasm.

Because these metrics capture distinct aspects of host plant response, their integration reveals that resistance is regulated by multiple interacting processes rather than a single controlling mechanism. This more sophisticated process of trait choice development allows breeders to better balance resistance and performance and reduce the potential for the introgression of undesirable traits into new cultivars, which may require further breeding efforts (i.e. negative selection or culling) to reduce incidence of those traits.

Further, multi-trait assessment of wild soybean phenotypes will help to improve stability of resistance in the face of differential pathogenic and environmental conditions. Diversity of resistance strategies is better suited to improved field performance, leading to better outcomes. Stability of performance, or resilience, may promote the persistence of resistance mechanisms in the presence of continuously adapting pathogen populations. Using a wider array of traits will allow soybean breeders to fully leverage the diversity of wild soybean germplasm, instead of relying on a single, relatively rare metric.

With the incorporation of diverse traits contributing to resilience the potential of wild soybean germplasm as a source of useful genetic and physiological tools for crop improvement expands beyond its current usage. Wild soybean traits have already been utilized for crop improvement traits, improving both cultivar durability and yield traits. Both broad-spectrum and pathogen-specific mechanisms can be incorporated into existing cultivars, as well as assisting in the development of new, improved elite lines. Evaluating these

traits across genotype-by-environment conditions will support more informed selection of cultivars for specific production environments.

Those field conditions do and will experience a combination of pathogen infection and weather variability, producing unique stress conditions for crops plants. Instead of a single stressor with relatively predictable effects on crops and yields, the combined effects of different stressors during field conditions result in complex, non-additive plant responses, highlighting the importance of leveraging diverse wild soybean traits to develop cultivars capable of maintaining performance across variable field environments.

Methodological Considerations

The integration of genetic, phenotypic, and environmental analyses in this work also highlights the importance of biological consistency when evaluating SCN resistance. Differences in experimental design, including inoculum levels, plant growth conditions, and trait measurement approaches complicate comparisons across studies and limit the ability to synthesize findings at a broader scale. Variation in methodology is often necessary or unavoidable to address specific research questions, greater standardization in key components of SCN phenotyping would improve reproducibility and comparability across experiments.

One important consideration is the quantification of SCN infection. Female index and cyst counts are widely used metrics, yet interpretation can vary depending on experimental conditions and thresholds applied. As demonstrated in this work, reliance on a single metric can obscure meaningful biological differences among wild soybean accessions. Incorporating complementary measurements of plant performance alongside pathogen reproduction provides a more complete assessment of resistance and resilience. Standardizing how these metrics are collected and reported would facilitate clearer comparisons among QTL, screening, and stress response studies.

Variation in inoculum density across studies presents a challenge for interpreting resistance levels. SCN egg counts can vary widely, influencing both infection pressure and plant response. Although field conditions are inherently heterogeneous, establishing

more consistent laboratory benchmarks would allow for more reliable comparisons between studies and environments. Such standardization would be particularly valuable in integrating findings from genetic mapping, phenotyping, and breeding programs.

This alignment of methodologies across SCN research will support the identification of robust resistance traits and improve the translation of experimental findings into breeding applications. As resistance is increasingly understood as a multidimensional and context-dependent phenotype, experimental approaches must evolve to capture this complexity in a consistent and reproducible manner.

Synthesis and Future Directions

This dissertation demonstrates that wild soybean resistance to SCN is not a singular trait, but a phenotype representing the complex interplay of genetic, physiological, and environmental factors. Across genetic mapping, phenotypic screening, and combined stress experiments, wild soybean resistance was shown to encompass both the suppression of pathogen reproduction and the maintenance of plant performance. These findings challenge traditional classifications of resistance and highlight the importance of evaluating host response though integrated, multi-metric frameworks.

Wild soybean (*Glycine soja*) emerges from this work as a valued and underutilized source of diverse resistance strategies. Rather than providing a single solution to SCN management, wild soybean germplasm offers a range of mechanisms–including resistance, tolerance, and resilience–that can be leveraged to improve both durability and productivity in cultivated soybean. Importantly, the expression of these traits is influenced by environmental context, with combined stress conditions revealing responses that are not predictable from single-stress evaluations alone.

Together, these results underscore the need for crop breeding strategies that integrate multiple traits and consider genotype-by-environment interactions. By including diverse resistance-associated traits and evaluating performance under realistic field conditions, it is possible to develop soybean cultivars that maintain stable productivity under realistic

field conditions while limiting pathogen proliferation. As agricultural systems face increasing environmental variability and pathogen pressure, such integrative approaches will be essential to maintain crop performance and long-term resistance durability of soybean.

APPENDIX A: SUPPLEMENTARY MATERIALS FOR CHAPTER 2 – QTL MAPPING *GLYCINE SOJA* FOR SCN RESISTANCE

Table A.1: Summary statistics of the parental lines and 185 F_4 progeny developed from a cross between NC-Raleigh and S54 in response to infection by soybean cyst nematode HG Type 1.2.5.7.

Mean	Min	Max	Std. Dev.	Shapiro–Wilk (w)	Skewness (γ)	Kurtosis
44.16	0	130.87	24.52	0.9718	0.2754	-0.1889

Table A.2: HG test results for 7 *Glycine max* indicator lines (Niblack et al. 2009). Resistance is ranked R (FI < 10); moderate resistance is ranked MR (10 < FI < 30); moderate susceptibility is categorized as MS (30 < FI < 60); and fully susceptible genotypes are ranked S (> 60).

Indicator line	PI#	Female index (FI)	Resistance rating
1	Peking (PI 548402)	40.4	MS
2	PI 88788	53.4	MS
3	PI 90763	8.8	R
4	PI 437654	0.0	R
5	PI 209332	72.0	S
6	PI 89772	3.3	R
7	PI 548316	59.4	MS

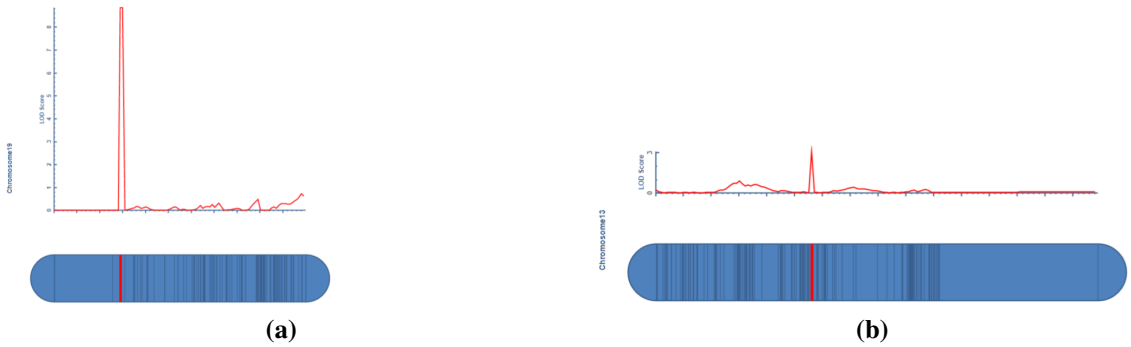

(a) (b)

Figure A.1: Supplemental Figure 1: Linkage maps made with IciMapping (Meng et al., 2015) with LOD scores of QTL associated with SCN 1.2.5.7; linkage map A represents QTL-19 (LOD = 8.84), while linkage map B represents QTL-13 (LOD = 3.06). Only loci with significant QTL (LOD ≥ 3) are shown.

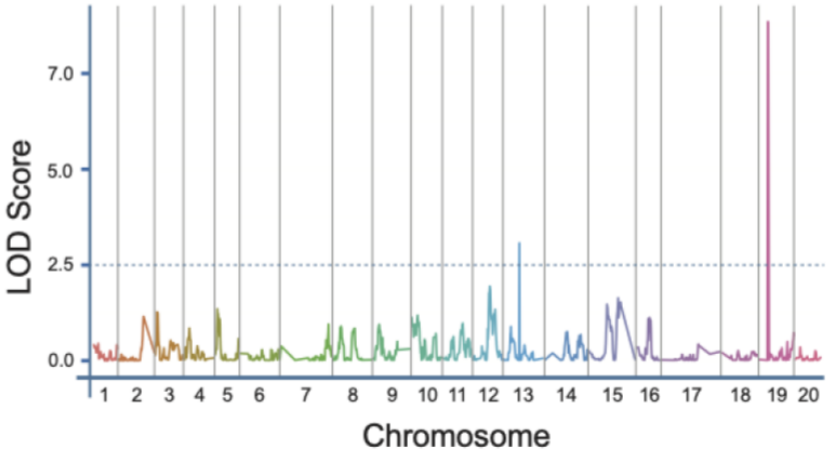

Figure A.2: Genome-wide scan of significant QTL in wild soybean mapping population.

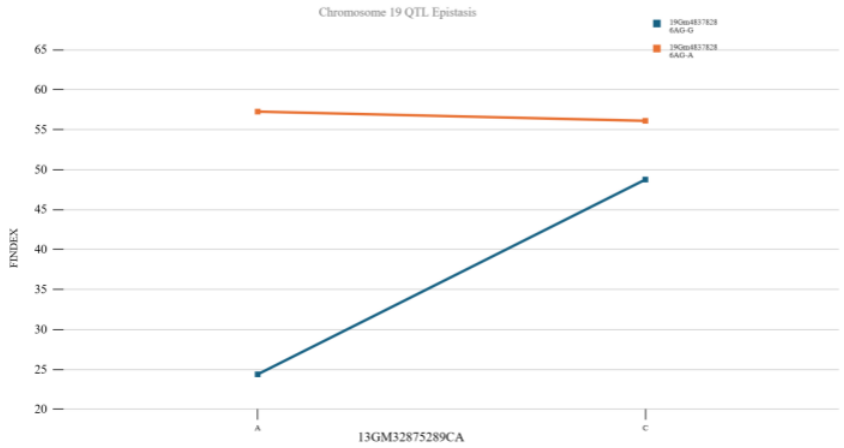

(a)

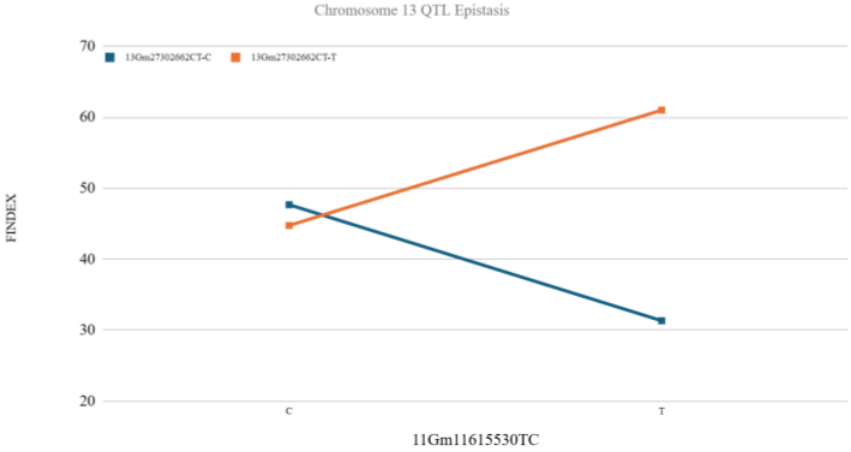

(b)

Figure A.3: Interaction plots of QTL-19 interacting with epistatic SNP 13 (Epi-13) (a) and QTL-13 interacting with epistatic SNP 11 (Epi-11) (b).

Table A.3: Results of 1,000-permutation testing used to determine the genome-wide LOD significance threshold for QTL detection in the recombinant inbred line (RIL) population derived from the cross between S54 and NC-Raleigh. Additive effect is indicated by "Add".

QTL loci	Left marker	Right marker	LOD	PVE (%)	Add
QTL-19	19Gm48378286	Gm48433644	8.8386	18.9939	-10.1254
QTL-13	13Gm27373181	13Gm27302662	3.061	6.341	-6.174

Table A.4: Distribution of SNP markers across 20 chromosomes for QTL mapping of SCN resistance.

Chr[a]	#Markers	Total distance (cM)	Average interval (cM)
1	149	89.5	0.60
2	172	89.8	0.52
3	136	87.5	0.64
4	130	85.9	0.66
5	120	79.5	0.66
6	163	80.9	0.49
7	173	88.4	0.51
8	227	89.7	0.40
9	127	87.6	0.68
10	169	88.1	0.52
11	147	89.6	0.61
12	134	88.9	0.66
13	193	88.5	0.46
14	135	89.0	0.66
15	165	89.4	0.54
16	115	85.3	0.74
17	133	88.5	0.67
18	205	89.8	0.44
19	157	76.1	0.48
20	136	83.1	0.61
Total	3086	1735.1	0.58

[a] Chr = chromosome.

Table A.5: Results of Kruskal–Wallis tests comparing female index (FI) distributions among genotype classes at peak markers within the QTL-19 and QTL-13 intervals. P-values are reported for comparisons among genotype classes; “ns” indicates non-significant results.

Marker	Marker side	Comparison	Adjusted p-value
13Gm27302662_CT	left	CC vs TT	4.11E-04
13Gm27302662_CT	left	CC vs CT	0.715764
13Gm27302662_CT	left	TT vs CT	0.035706
13Gm27373181_AG	right	AA vs GG	1.77E-04
13Gm27373181_AG	right	AA vs AG	0.020845
13Gm27373181_AG	right	GG vs AG	0.798438
19Gm48378286_AG	left	AA vs GG	2.10E-08
19Gm48378286_AG	left	AA vs AG	0.058485
19Gm48378286_AG	left	GG vs AG	0.058485
19Gm48433644_AG	right	AA vs GG	6.99E-09
19Gm48433644_AG	right	AA vs AG	0.054658
19Gm48433644_AG	right	GG vs AG	0.069911

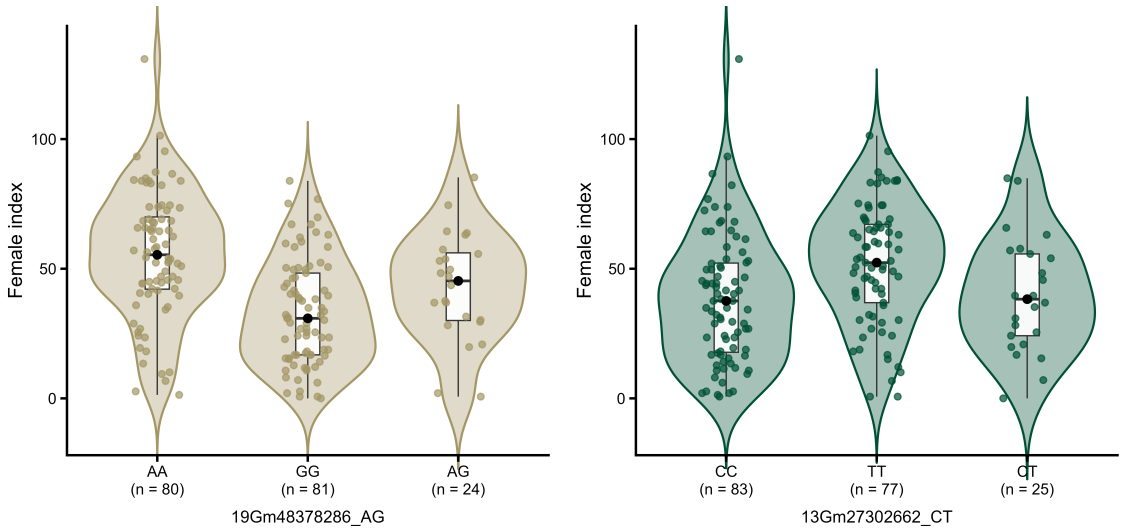

Figure A.4: Allele effects at peak left markers associated with SCN resistance. Female index distributions of recombinant inbred lines grouped by genotype at peak markers at QTL-19 (left) and QTL-13 (right). Violin plots showing phenotype distributions with overlaid boxplots indicating medians and interquartile ranges. Points represent individual RILs; sample size for genotype classes are shown on the x-axis. Statistical differences among genotype classes were assessed using Kruskal-Wallis tests followed by Dunn's post hoc test with Benjamini-Hochberg correction.

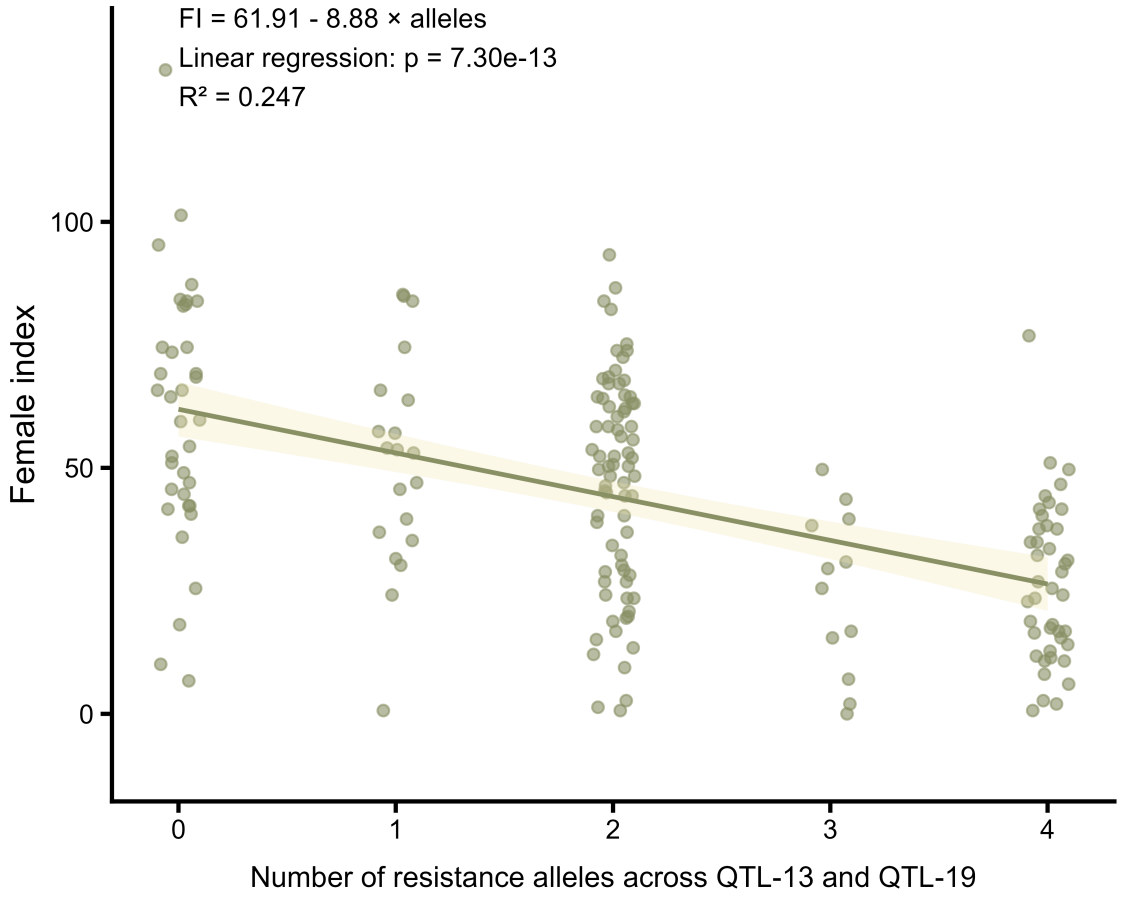

Figure A.5: Female index (FI) of recombinant inbred lines plotted against total number of resistance alleles present across QTL-19 and QTL-13. The G allele at each peak marker was associated with reduced SCN reproduction and was counted as the resistance allele . Points represent individual RILs; the fitted line represents the linear regression relationship between allele count and FI. The highlighted region indicates the 95% confidence interval of the regression line. FI declined significantly with increasing numbers of resistance alleles ($p < 0.001$, $R^2 = 0.247$), consistent with the additive effects of QTL-19 and QTL-13.

Table A.6: Results for Spearman rank correlation testing and Jonckheere–Terpstra trend test for the stacking of SCN-resistance associated alleles.

Test	Comparison	Term	Estimate	Statistic	p-value
Spearman rank correlation	N/A	ρ	-0.50134	1558722.9	4.21×10^{-13}
Jonckheere–Terpstra	Ordered trend	JT	N/A	3434.5	2.32×10^{-12}

Table A.7: Candidate genes located within the major QTL and epistatic intervals identified in this study, based on annotations from the *Glycine max* Williams 82 reference genome assembly (Glyma.Wm82.gnm6) available through SoyBase.

Locus	Gene ID	Genomic Position	Annotation
QTL-19	Glyma.19G194300	Gm19:48249528–48251223	Flowering locus protein T
QTL-19	Glyma.19G194366	Gm19:48262136–48266894	Alpha/beta-hydrolase superfamily protein (methylesterase)
QTL-19	Glyma.19G194500	Gm19:48267753–48273017	bZIP transcription factor family protein
QTL-19	Glyma.19G194600	Gm19:48273809–48275841	F-box/LRR plant protein
QTL-19	Glyma.19G194700	Gm19:48276907–48281484	Iron-sulfur cluster assembly protein IscA
QTL-19	Glyma.19G194800	Gm19:48282040–48290392	Cell division FtsZ-like protein
QTL-19	Glyma.19G194900	Gm19:48293498–48300554	Uncharacterized protein LOC100793911 isoform X5
QTL-19	Glyma.19G194915	Gm19:48301221–48303727	Ubiquinol-cytochrome c reductase complex protein
QTL-19	Glyma.19G194922	Gm19:48305667–48310287	Ribosomal protein L1p/L10e family
QTL-19	Glyma.19G194929	Gm19:48311707–48312409	Glucosamine 6-phosphate N-acetyltransferase
QTL-19	Glyma.19G194936	Gm19:48315731–48320941	SOUL heme-binding family protein
QTL-19	Glyma.19G194943	Gm19:48322974–48323713	Uncharacterized protein At1g66480-like
QTL-19	Glyma.19G194950	Gm19:48335499–48338055	Uncharacterized protein At5g39865-like
QTL-19	Glyma.19G194957	Gm19:48345030–48346669	Micronuclear linker histone polyprotein-like
QTL-19	Glyma.19G194964	Gm19:48354779–48363614	F-box family protein
QTL-19	Glyma.19G194971	Gm19:48364484–48373283	RNA-binding protein 24-A-like isoform X3
QTL-19	Glyma.19G194974	Gm19:48375057–48375584	Nucleic acid-binding, OB-fold-like protein
QTL-19	Glyma.19G194978	Gm19:48377992–48379164	Unknown protein
QTL-19	Glyma.19G194985	Gm19:48380528–48387316	Signal recognition particle SRP54
QTL-19	Glyma.19G194992	Gm19:48387994–48392825	Rho GTPase-activating protein 1-like
QTL-19	Glyma.19G195000	Gm19:48394725–48395695	Unknown protein
QTL-19	Glyma.19G195100	Gm19:48401087–48402520	Small nuclear ribonucleoprotein family protein
QTL-19	Glyma.19G195200	Gm19:48404236–48405470	SAUR-like auxin-responsive protein
QTL-19	Glyma.19G195300	Gm19:48408085–48414725	ATP-binding microtubule motor family protein
QTL-19	Glyma.19G195400	Gm19:48417837–48422828	Cell wall invertase I
QTL-19	Glyma.19G195500	Gm19:48424685–48425799	Ubiquitin 4
QTL-19	Glyma.19G195600	Gm19:48428425–48432333	Alpha/beta hydrolase domain protein
QTL-19	Glyma.19G195700	Gm19:48433206–48435427	Uncharacterized protein LOC102669414
QTL-19	Glyma.19G195800	Gm19:48449350–48451571	NAC domain protein
QTL-19	Glyma.19G195900	Gm19:48459450–48462523	VPS55 family protein
QTL-19	Glyma.19G196000	Gm19:48471390–48489114	SPINDLY-like N-acetylglucosaminyltransferase
QTL-19	Glyma.19G196100	Gm19:48489790–48492189	Cyclophilin-like isomerase
QTL-19	Glyma.19G196202	Gm19:48492088–48496006	Mitochondrial fission protein ELM1-like
QTL-19	Glyma.19G196300	Gm19:48497058–48501078	mRNA-decapping enzyme-like protein
QTL-19	Glyma.19G196400	Gm19:48507994–48509293	F-box family protein

Continued on next page

Table A.7: Table A7 (continued).

Locus	Gene ID	Genomic Position	Annotation
QTL-19	Glyma.19G196500	Gm19:48517788–48520406	Embryo defective 2735
QTL-13	Glyma.13G153800	Gm13:27177228–27177813	Uncharacterized protein LOC10079395
QTL-13	Glyma.13G153900	Gm13:27203887–27205266	Ubiquitin-like superfamily protein
QTL-13	Glyma.13G154000	Gm13:27211702–27222015	Glutathione S-transferase
QTL-13	Glyma.13G154100	Gm13:27224490–27228806	Lipid-transfer/seed storage protein
QTL-13	Glyma.13G154200	Gm13:27250451–27257953	Ubiquitin carboxyl-terminal hydrolase
QTL-13	Glyma.13G154300	Gm13:27270349–27272708	Uncharacterized protein LOC100795534
QTL-13	Glyma.13G154400	Gm13:27280959–27285540	F-box family protein
QTL-13	Glyma.13G154433	Gm13:27285780–27294764	ABC transporter B family member 29
QTL-13	Glyma.13G154500	Gm13:27295130–27296268	Uncharacterized protein LOC102670030
QTL-13	Glyma.13G154600	Gm13:27299453–27303427	Phosphopantetheinyl transferase
QTL-13	Glyma.13G154700	Gm13:27310117–27314533	PPR superfamily protein
QTL-13	Glyma.13G154800	Gm13:27318160–27323263	Heme ABC exporter CcmA
QTL-13	Glyma.13G155100	Gm13:27328420–27333886	Glycerophosphoryl diester phosphodiesterase
QTL-13	Glyma.13G155200	Gm13:27335483–27337373	Temperature-induced lipocalin
QTL-13	Glyma.13G155300	Gm13:27339158–27340826	Ribosomal protein L10
QTL-13	Glyma.13G155400	Gm13:27341986–27345863	Response regulator ARR12-like
QTL-13	Glyma.13G155600	Gm13:27357495–27363947	Alpha/beta hydrolase
QTL-13	Glyma.13G155700	Gm13:27368045–27372751	Calcineurin-like phosphoesterase
QTL-13	Glyma.13G155800	Gm13:27383667–27385976	Glycosyl hydrolase with chitinase domain
QTL-13	Glyma.13G155900	Gm13:27386877–27391103	Cullin neddylation protein
QTL-13	Glyma.13G156000	Gm13:27396425–27401989	Plasma membrane H+-ATPase
QTL-13	Glyma.13G156200	Gm13:27407081–27411027	WD repeat protein
QTL-13	Glyma.13G156300	Gm13:27415157–27417982	WD repeat protein
QTL-13	Glyma.13G156350	Gm13:27419912–27422644	DNA replication licensing factor MCM5
QTL-13	Glyma.13G156400	Gm13:27422645–27425883	DNA replication licensing factor MCM5
Epi-13	Glyma.13G210800	Gm13:32728989–32735033	Glutamine synthetase 2
Epi-13	Glyma.13G210900	Gm13:32735685–32744704	Uncharacterized protein LOC100500244 isoform X4
Epi-13	Glyma.13G211000	Gm13:32749359–32751552	F-box interaction domain protein
Epi-13	Glyma.13G211100	Gm13:32758293–32759126	RING-H2 zinc finger protein
Epi-13	Glyma.13G211200	Gm13:32762583–32766392	FAR1-related sequence 7-like protein
Epi-13	Glyma.13G211300	Gm13:32770699–32772182	Bax inhibitor-1 family protein
Epi-13	Glyma.13G211400	Gm13:32774492–32776650	BSD domain-containing protein
Epi-13	Glyma.13G211500	Gm13:32778123–32787710	Mo25 family protein
Epi-13	Glyma.13G211600	Gm13:32792371–32799964	F-box/LRR protein
Epi-13	Glyma.13G211700	Gm13:32812757–32814150	Adenosylmethionine decarboxylase
Epi-13	Glyma.13G211800	Gm13:32822799–32827324	Protein phosphatase 2C

Continued on next page

Table A.7: Table A7 (continued).

Locus	Gene ID	Genomic Position	Annotation
Epi-13	Glyma.13G211900	Gm13:32829491–32846136	SAC3/GANP/eIF-3 p25 family protein
Epi-13	Glyma.13G212000	Gm13:32847734–32849156	Methionine sulfoxide reductase B2
Epi-13	Glyma.13G212100	Gm13:32853428–32854816	Cox19-like CHCH protein
Epi-13	Glyma.13G212200	Gm13:32856716–32862345	E3 ubiquitin-protein ligase RF298-like
Epi-13	Glyma.13G212300	Gm13:32865905–32868333	Endonuclease/exonuclease/phosphatase protein
Epi-13	Glyma.13G212400	Gm13:32869730–32870793	DUF679 membrane protein
Epi-13	Glyma.13G212500	Gm13:32877870–32880141	Uncharacterized protein LOC100820034
Epi-13	Glyma.13G212600	Gm13:32889276–32894977	Protein kinase superfamily protein
Epi-13	Glyma.13G212700	Gm13:32896237–32900611	Oxidoreductase protein
Epi-13	Glyma.13G212800	Gm13:32905745–32908810	Histidine phosphotransfer protein 6
Epi-13	Glyma.13G212900	Gm13:32909346–32917452	Nucleoside hydrolase family protein
Epi-13	Glyma.13G213000	Gm13:32922496–32932618	Nucleoside hydrolase family protein
Epi-13	Glyma.13G213100	Gm13:32936361–32942580	WD-40 repeat protein
Epi-13	Glyma.13G213200	Gm13:32944409–32950811	Integral membrane protein
Epi-13	Glyma.13G213300	Gm13:32951417–32956489	Integral membrane protein
Epi-13	Glyma.13G213400	Gm13:32962156–32969518	SPL7 transcription factor
Epi-13	Glyma.13G213500	Gm13:32983205–32988071	1-deoxy-D-xylulose 5-phosphate synthase
Epi-13	Glyma.13G213600	Gm13:32999898–33006091	Zinc finger superfamily protein
Epi-11	Glyma.11G152542	Gm11:11495510–11501397	RING/U-box zinc finger protein
Epi-11	Glyma.11G152751	Gm11:11507276–11511795	Alpha/beta-hydrolase protein
Epi-11	Glyma.11G152960	Gm11:11512633–11535868	Translation elongation factor EF-1
Epi-11	Glyma.11G153169	Gm11:11534958–11540084	Ribosomal protein L28
Epi-11	Glyma.11G153378	Gm11:11540445–11544149	Morphology protein precursor
Epi-11	Glyma.11G153587	Gm11:11545092–11548974	Allergen Gly m Bd 28 kDa protein
Epi-11	Glyma.11G153796	Gm11:11552230–11553015	Hypothetical protein
Epi-11	Glyma.11G154005	Gm11:11558158–11568648	SUMO ligase SIZ1-like protein
Epi-11	Glyma.11G154214	Gm11:11570192–11574472	Transmembrane protein
Epi-11	Glyma.11G154423	Gm11:11578635–11585711	Isovaleryl-CoA dehydrogenase
Epi-11	Glyma.11G154632	Gm11:11585739–11592808	Auxin response factor 4
Epi-11	Glyma.11G154841	Gm11:11607222–11609520	Uncharacterized protein LOC102663390
Epi-11	Glyma.11G155259	Gm11:11642039–11643106	Sec61-beta subunit protein
Epi-11	Glyma.11G155468	Gm11:11645172–11647904	Programmed cell death protein
Epi-11	Glyma.11G156304	Gm11:11684148–11685282	Fasciclin-like arabinogalactan protein 11
Epi-11	Glyma.11G156513	Gm11:11689454–11690631	Fasciclin-like arabinogalactan protein 12
Epi-11	Glyma.11G156722	Gm11:11691299–11698947	Beta-galactosidase 8
Epi-11	Glyma.11G156931	Gm11:11709305–11713449	INO80 complex subunit C
Epi-11	Glyma.11G157140	Gm11:11718120–11731172	Uncharacterized protein LOC100797428

Continued on next page

Table A.7: Table A7 (continued).

Locus	Gene ID	Genomic Position	Annotation
Epi-11	Glyma.11G157349	Gm11:11735638–11737136	bZIP transcription factor bZIP122
Epi-02	Glyma.02G133700	Gm02:14371190–14373199	Cyclin-dependent kinase inhibitor
Epi-02	Glyma.02G133800	Gm02:14383319–14386007	Carboxylesterase-like protein
Epi-02	Glyma.02G133900	Gm02:14387498–14388944	Carboxylesterase-like protein
Epi-02	Glyma.02G134000	Gm02:14392144–14394816	Carboxylesterase-like protein
Epi-02	Glyma.02G134100	Gm02:14396336–14400861	Carboxylesterase-like protein
Epi-02	Glyma.02G134200	Gm02:14401968–14403164	Carboxylesterase-like protein
Epi-02	Glyma.02G134300	Gm02:14416590–14421640	P-loop NTP hydrolase protein
Epi-02	Glyma.02G134400	Gm02:14429462–14434201	RNA-binding protein
Epi-02	Glyma.02G134500	Gm02:14442561–14444201	Uncharacterized protein LOC100803045
Epi-02	Glyma.02G134600	Gm02:14454255–14459665	Calcium/calmodulin-dependent protein kinase
Epi-02	Glyma.02G134700	Gm02:14472518–14473880	Plastocyanin-like protein

APPENDIX B: SUPPLEMENTARY MATERIALS FOR CHAPTER 3 – SCREENING *GLYCINE SOJA* FOR SCN RESISTANCE

Table B.1: Accessions used in this experiment, their accession ID, and their Female Index as calculated in Zhang et al. (2016a).

Accession	Accession ID	Female Index (Zhang et al. 2016a)	FI Rating (HG 2.5.7)	Purpose
Test Lines				
PI 578345	S100	3.3	R	Test line
PI 424093	S54	5.2	R	Test line
PI 464937 A	H01	5.7	R	Test line
PI 508067	S86	5.8	R	Test line
PI 507615	H20	8.3	R	Test line
PI 464936 B	H02	9.0	R	Test line
PI 487428	S74	9.0	R	Test line
PI 507667	S83	9.9	R	Test line
PI 464927 B	H03	11.5	MR	Test line
PI 424002	H26	11.8	MR	Test line
PI 424096	S55	14.1	MR	Test line
PI 366120	S04	16.3	MR	Test line
PI 562550	S96	16.3	MR	Test line
PI 507739 B	H05	17.5	MR	Test line
PI 366122	S05	18.1	MR	Test line
PI 468918	H21	19.1	MR	Test line
PI 549037	S92	19.1	MR	Test line
PI 522179	S88	19.4	MR	Test line
PI 522200 A	H33	20.0	MR	Test line
PI 378699 A	H24	20.6	MR	Test line
PI 378698	S11	21.5	MR	Test line
101404_B	S01	21.7	MR	Test line
PI 447003 A	H27	21.7	MR	Test line
PI 578338 A	H22	24.1	MR	Test line
PI 507839	H30	24.3	MR	Test line
PI 532453 A	S91	24.5	MR	Test line
PI 378684 A	H23	25.7	MR	Test line
PI 424117	S57	25.7	MR	Test line
PI 522193	H31	26.0	MR	Test line
PI 407037	S14	26.4	MR	Test line
PI 507738	H28	26.6	MR	Test line

Continued on next page

Table B.1: Table B.1 (continued).

Accession	Accession ID	Female Index (Zhang et al. 2016a)	FI Rating (HG 2.5.7)	Purpose
PI 407308	H25	26.9	MR	Test line
PI 522180	S89	27.1	MR	Test line
PI 522223	H34	27.1	MR	Test line
PI 507805	S85	27.6	MR	Test line
522198_A	H14	27.6	MR	Test line
PI 339871 A	S03	28.0	MR	Test line
PI 487431	S76	28.5	MR	Test line
PI 562534	H15	28.7	MR	Test line
PI 522196 A	H32	28.8	MR	Test line
PI 407254	S39	29.4	MR	Test line
PI 407217	S32	29.7	MR	Test line
PI 522229	H35	29.9	MR	Test line
PI 507776	H29	30.0	MS	Test line
Check Lines				
NC Dunphy	NCD	n/a	n/a	Susceptible cultivar
NC Raleigh	NCR	n/a	n/a	Susceptible cultivar
Williams 82	W82	n/a	n/a	Susceptible check
Lee 74	L74	n/a	n/a	Susceptible check

Table B.2: Results for HG testing using both Williams 82 and Lee 74 as susceptible checks. Two populations of soybean cyst nematode (SCN) were tested: HG 1.2.5.7 (top) and HG 0 (bottom).

Test Line #	Test Line Accession	FI (W82 × HG 1.2.5.7)	Rating	FI (L74 × HG 1.2.5.7)	Rating
HG 1.2.5.7					
1	PI 548404 (Peking)	30.4	MS	30.3	MS
2	PI 88788	50.2	MS	50.0	MS
3	PI 90763	1.9	R	1.8	R
4	PI 437654	0.0	R	0.0	R
5	PI 209332	50.5	MS	50.3	MS
6	PI 89772	3.2	R	3.1	R
7	PI 548316	30.7	MS	30.6	MS
HG 0					
Test Line #	**Test Line Accession**	**FI (W82 × HG 0)**	**Rating**	**FI (L74 × HG 0)**	**Rating**

Continued on next page

Table B.2: Table B.2 (continued).

Test Line #	Test Line Accession	FI (W82 × HG 1.2.5.7)	Rating	FI (L74 × HG 1.2.5.7)	Rating
1	PI 548404 (Peking)	5.1	R	3.4	R
2	PI 88788	0.0	R	0.0	R
3	PI 90763	0.0	R	0.0	R
4	PI 437654	0.0	R	0.0	R
5	PI 209332	9.5	R	7.4	R
6	PI 89772	0.1	R	0.1	R
7	PI 548316	0.1	R	0.1	R

Table B.3: Results of two-way ANOVA using sum of squares (Sum Sq) for all plant accessions, as well as a subset filtered for accessions with $n \geq 3$ replicates. Degrees of freedom (df) varied depending on dataset.

Source of Variation	Sum Sq	df	F-value	P-value
Subset: $n \geq 3$ replicates				
Intercept	1717.049	1	9066.654	8.526
Accession (A)	138.617	51	14.352	9.648
HG Type (P)	16.724	1	88.307	2.148
A × P Interaction	31.315	51	3.242	1.387
Residuals	92.607	489	NA	NA
All genotypes				
Intercept	1601.785	1	8305.019	1.944
Accession (A)	140.723	54	13.512	4.565
HG Type (P)	17.310	1	89.750	1.062
A × P Interaction	33.697	54	3.234	4.760
Residuals	96.820	502	NA	NA

Table B.4: Spearman's rank correlation (ρ) analysis results for all accessions, as well as a subset filtered for accessions with $n \geq 3$ replicates.

Dataset	ρ	P-value
All accessions	0.6859	2.89
Subset ($n \geq 3$)	0.7500	1.79

Table B.5: Results of ANOVA analyses for root–SCN cyst data. Analyses are shown for all accessions (All) and for a subset with $n \geq 3$ replicates (n3).

Trait (unit)	Dataset	Effect	Sum Sq	df	F value	P-value
Subset: $n \geq 3$ replicates						
Area (cm^2)	n3	Accession (A)	1.600	41	3.520	5.64
		HG type (P)	0.000	1	0.026	8.7107
		A × P	1.613	41	3.548	4.15
		Residuals	4.290	387	NA	NA
Length (cm)	n3	Accession (A)	1.919	41	4.244	1.92
		HG type (P)	0.036	1	3.302	6.995
		A × P	1.452	41	3.212	1.65
		Residuals	4.268	387	NA	NA
Width (cm)	n3	Accession (A)	0.414	41	0.344	9.9996
		HG type (P)	0.063	1	2.130	1.4524
		A × P	2.905	41	2.410	7.96
		Residuals	11.376	387	NA	NA
Perimeter (cm)	n3	Accession (A)	3.774	41	3.843	1.61
		HG type (P)	0.023	1	0.939	3.3309
		A × P	3.803	41	3.872	1.17
		Residuals	9.271	387	NA	NA
Aspect ratio	n3	Accession (A)	1.882	41	0.740	8.8140
		HG type (P)	0.204	1	3.293	7.037
		A × P	4.761	41	1.871	1.39
		Residuals	24.023	387	NA	NA
Root Length (RLP) (cm)	n3	Accession (A)	1.614	41	2.353	1.41
		HG type (P)	0.366	1	21.910	3.96
		A × P	2.822	41	4.116	7.89
		Residuals	6.473	387	NA	NA
Length (manual) (cm)	n3	Accession (A)	4.954	41	2.340	1.62
		HG type (P)	0.002	1	0.048	8.2700
		A × P	2.734	41	1.291	1.1535
		Residuals	19.986	387	NA	NA
All accessions						
Area (cm^2)	All	Accession (A)	1.601	43	3.355	1.57
		HG type (P)	0.000	1	0.026	8.7113
		A × P	1.622	43	3.399	9.47
		Residuals	4.350	392	NA	NA
Length (cm)	All	Accession (A)	1.946	43	4.115	2.64

Continued on next page

Table B.5: Table B.5 (continued).

Trait (unit)	Dataset	Effect	Sum Sq	df	F value	P-value
		HG type (P)	0.036	1	3.311	6.950
		A × P	1.461	43	3.090	3.15
		Residuals	4.311	392	NA	NA
Width (cm)	All	Accession (A)	0.431	43	0.344	9.9997
		HG type (P)	0.063	1	2.151	1.4332
		A × P	2.914	43	2.327	1.26
		Residuals	11.413	392	NA	NA
Perimeter (cm)	All	Accession (A)	3.789	43	3.691	3.39
		HG type (P)	0.023	1	0.943	3.3220
		A × P	3.822	43	3.724	2.33
		Residuals	9.357	392	NA	NA
Aspect ratio	All	Accession (A)	2.052	43	0.774	8.4756
		HG type (P)	0.204	1	3.316	6.939
		A × P	4.766	43	1.798	2.19
		Residuals	24.164	392	NA	NA
Root length (RLP) (cm)	All	Accession (A)	1.637	43	2.292	1.82
		HG type (P)	0.366	1	22.064	3.66
		A × P	2.849	43	3.988	1.13
		Residuals	6.511	392	NA	NA
Length (manual) (cm)	All	Accession (A)	5.081	43	2.259	2.56
		HG type (P)	0.002	1	0.047	8.2809
		A × P	2.738	43	1.217	1.7182
		Residuals	20.505	392	NA	NA

Table B.6: Spearman correlation (ρ) analysis results for root–cyst data. Analyses were performed on all data (All) and on a subset with $n \geq 3$ replicates (n3). All traits are reported in centimeters (cm) unless otherwise noted.

Trait (unit)	Dataset	ρ	P-value
All data			
Area (cm^2)	All	0.3625	2.35
Length (cm)	All	0.3252	2.76
Width (cm)	All	0.0934	4.09
Perimeter (cm)	All	0.3426	1.15
Aspect ratio	All	0.0924	4.30
Functional root length (RLP) (cm)	All	0.4026	3.94

Continued on next page

Table B.6: Table B.6 (continued).

Trait (unit)	Dataset	ρ	P-value
Length (manual) (cm)	All	0.3275	1.84
Subset: $n \geq 3$ replicates			
Area (cm^2)	n3	0.3582	1.06
Length (cm)	n3	0.3202	1.08
Width (cm)	n3	0.0839	6.90
Perimeter (cm)	n3	0.3389	4.00
Aspect ratio	n3	0.0979	3.36
Functional root length (RLP) (cm)	n3	0.4072	3.09
Length (manual) (cm)	n3	0.3214	8.92

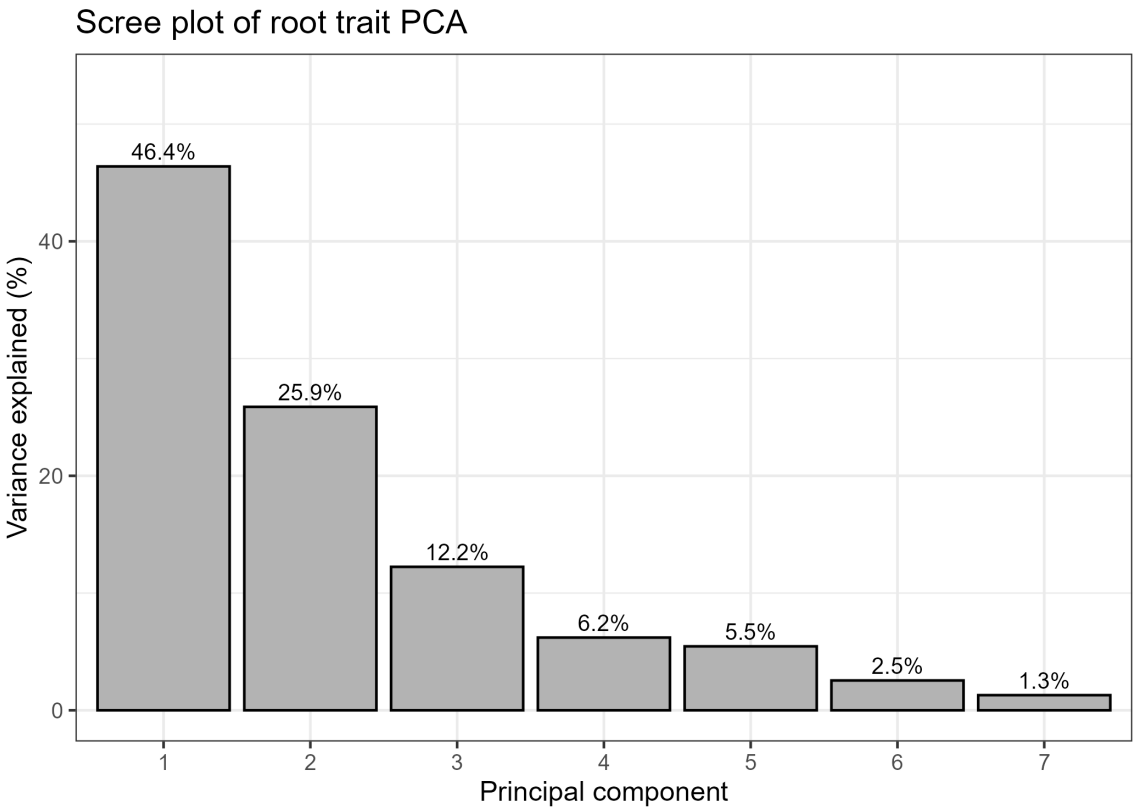

Figure B.1: Scree plot showing the proportion of variance explained by each principal component (PC) in the root traits of *Glycine soja* accessions infected with SCN HG types 0 and 1.2.5.7. The first two PCs explain the majority of variation in root morphology (PC1 = 46.4%, PC2 = 25.9%), together accounting for 72.3% of total variance.

Table B.7: Contrasts of cyst counts for wild soybean accessions infected with soybean cyst nematode HG types HG 0 and HG 1.2.5.7. Benjamini–Hochberg adjusted P-values (Adj. P-value) control the false discovery rate.

Accession ID	Ratio	SE	z	P-value	Adj. P-value
H01	0.3899	0.1625	−2.2606	0.0238	0.1308
H02	0.7842	0.3259	−0.5848	0.5587	0.8204
H03	1.2589	0.6276	0.4619	0.6442	0.8204
H05	0.2301	0.1185	−2.8537	0.0043	0.0872
H14	1.3168	0.6535	0.5544	0.5793	0.8204
H15	0.6457	0.3279	−0.8614	0.3890	0.8151
H20	1.1029	0.4985	0.2166	0.8285	0.8882
H21	0.2596	0.1049	−3.3390	0.0008	0.0370
H22	0.6318	0.2528	−1.1474	0.2512	0.6141
H23	0.7782	0.3848	−0.5072	0.6120	0.8204
H24	0.9041	0.3952	−0.2307	0.8175	0.8882
H25	0.4323	0.1798	−2.0162	0.0438	0.2140
H26	0.6408	0.2893	−0.9857	0.3243	0.7134
H27	1.2061	0.5248	0.4306	0.6668	0.8204
H28	0.3822	0.1531	−2.4011	0.0163	0.1027
H29	0.7413	0.3679	−0.6032	0.5464	0.8204
H30	0.5220	0.2271	−1.4945	0.1351	0.4211
H31	0.9027	0.3594	−0.2572	0.7970	0.8882
H32	0.4449	0.2209	−1.6310	0.1029	0.4115
H33	0.3159	0.1431	−2.5442	0.0110	0.0872
H34	0.4953	0.2527	−1.3769	0.1685	0.4534
H35	0.7352	0.3640	−0.6212	0.5345	0.8204
S01	0.8199	0.3451	−0.4718	0.6370	0.8204
S03	0.7721	0.4245	−0.4705	0.6380	0.8204
S04	0.7537	0.3489	−0.6109	0.5413	0.8204
S05	0.9184	0.3851	−0.2031	0.8391	0.8882
S11	0.7671	0.3231	−0.6294	0.5291	0.8204
S14	0.2465	0.1372	−2.5154	0.0119	0.0872
S32	1.0187	0.3919	0.0481	0.9617	0.9617
S39	0.3224	0.1366	−2.6717	0.0075	0.0872
S54	1.0678	0.4216	0.1662	0.8680	0.8882
S55	0.5055	0.2218	−1.5550	0.1199	0.4211
S57	0.8906	0.3546	−0.2909	0.7711	0.8882
S74	0.2840	0.1383	−2.5852	0.0097	0.0872
S76	2.8963	2.2718	1.3557	0.1752	0.4534

Continued on next page

Table B.7: Table B.7 (continued).

Accession ID	Ratio	SE	z	P-value	Adj. P-value
S83	1.0802	0.4536	0.1837	0.8542	0.8882
S85	0.8089	0.3225	−0.5318	0.5948	0.8204
S86	0.6491	0.6609	−0.4244	0.6713	0.8204
S88	1.2429	0.4957	0.5451	0.5857	0.8204
S89	0.7332	0.3195	−0.7122	0.4763	0.8204
S91	0.4637	0.1866	−1.9095	0.0562	0.2473
S92	0.6737	0.2689	−0.9897	0.3223	0.7134
S96	0.5290	0.2303	−1.4627	0.1436	0.4211
S100	0.5062	0.2296	−1.5012	0.1333	0.4211

Table B.8: Resistance breadth of selected wild soybean accessions across soybean cyst nematode (SCN) populations HG 0 and HG 1.2.5.7. Female Index (FI) categories are defined as: FI < 10 = resistant (R); FI 10–30 = moderately resistant (MR); FI 30–60 = moderately susceptible (MS); FI > 60 = susceptible (S). Accessions that maintain resistant or moderately resistant classifications across both SCN populations are shown in bold, indicating stable resistance across environments.

Accession ID	FI (HG 0)	Rank	FI (HG 1.2.5.7)	Rank
H01	11.9	MR	42.4	MS
H02	18.7	MR	33.1	MS
H03	**18.6**	**MR**	**20.5**	**MR**
H05	**4.9**	**R**	**29.5**	**MR**
H14	**28.0**	**MR**	**29.5**	**MR**
H15	21.9	MR	47.0	MS
H20	**19.1**	**MR**	**24.0**	**MR**
H21	7.0	R	37.4	MS
H22	23.4	MR	41.8	MS
H23	36.3	MS	55.6	MS
H24	**15.7**	**MR**	**24.1**	**MR**
H25	12.0	MR	44.9	MS
H26	**15.2**	**MR**	**26.4**	**MR**
H27	32.0	MS	31.6	MS
H28	13.7	MR	49.8	MS
H29	19.0	MR	33.8	MS
H30	19.3	MR	56.8	MS
H31	43.9	MS	67.5	S

Continued on next page

Table B.8: Table B.8 (continued).

Accession ID	FI (HG 0)	Rank	FI (HG 1.2.5.7)	Rank
H32	**21.6**	**MR**	**29.4**	**MR**
H33	8.6	R	37.9	MS
H34	7.8	R	39.6	MS
H35	25.1	MR	44.2	MS
NCD	145.9	S	85.5	S
NCR	151.9	S	92.3	S
S01	21.8	MR	36.8	MS
S03	14.8	MR	32.7	MS
S04	28.3	MR	52.1	MS
S05	39.8	MS	60.1	S
S100	**9.7**	**R**	**26.7**	**MR**
S11	19.6	MR	30.0	MS
S14	4.2	R	30.8	MS
S32	**21.6**	**MR**	**29.4**	**MR**
S39	8.6	R	36.9	MS
S54	**6.2**	**R**	**8.1**	**R**
S55	**3.0**	**R**	**8.6**	**R**
S57	43.3	MS	67.5	S
S74	8.2	R	34.5	MS
S76	30.1	MS	14.4	MR
S83	34.6	MS	42.0	MS
S85	33.2	MS	56.9	MS
S86	17.1	MR	37.1	MS
S88	38.3	MS	42.7	MS
S89	19.4	MR	36.8	MS
S91	12.5	MR	32.1	MS
S92	25.4	MR	52.3	MS
S96	15.7	MR	49.1	MS

APPENDIX C: SUPPLEMENTARY MATERIALS – *GLYCINE SOJA* PERFORMANCE UNDER COMBINED STRESS

Table C.1: *Glycine soja* and *Glycine max* accessions included in this study and their reported stress-related traits. Accessions were selected based on published literature on SCN resistance and drought tolerance traits, supplemented with unpublished laboratory screening where available.

Accession ID	Accession	Species	Reported Trait(s)	Citation
DW01	549033	*G. soja*	Slow wilting, drought tolerance; SCN resistance	Seversike et al. (2012); unpublished data
DW02	468917	*G. soja*	Variable wilting, drought tolerance	Seversike et al. (2012)
H05	507739 B	*G. soja*	SCN resistance	Zhang et al. (2016)
H14	522198 A	*G. soja*	SCN resistance	Unpublished data
H15	562534	*G. soja*	Advantageous root growth mutation	Guo et al. (2023)
H21	468918	*G. soja*	Lateral root traits; SCN resistance	Prince et al. (2018); Zhang et al. (2016)
S05	366122	*G. soja*	SCN resistance	Zhang et al. (2016)
S11	378698	*G. soja*	SCN resistance	Zhang et al. (2016)
S14	407037	*G. soja*	SCN resistance	Zhang et al. (2016)
S32	407217	*G. soja*	SCN resistance	Zhang et al. (2016)
S33	407221	*G. soja*	SCN resistance	Anand et al. (1984)
S54	424093	*G. soja*	SCN resistance	Zhang et al. (2016)
S55	424096	*G. soja*	SCN resistance	Zhang et al. (2016)
S67	468396 B	*G. soja*	*G. soja* susceptible benchmark	Zhang et al. (2017)
S72	483468 A	*G. soja*	Osmotic stress tolerance	Pathan et al. (2007)
S74	487428	*G. soja*	SCN resistance	Zhang et al. (2016)
S76	487431	*G. soja*	SCN resistance	Zhang et al. (2016)
S100	578345	*G. soja*	SCN resistance	Zhang et al. (2016); unpublished data
SW03	483463	*G. soja*	Osmotic stress tolerance	Valliyodan et al. (2017)
NCR	NC-Raleigh	*G. max*	*G. max* susceptible benchmark	Burton et al. (2006)
HG2	PI 88788	*G. max*	SCN resistance	Niblack et al. (2002)
W82	Williams 82	*G. max*	Susceptible check	Niblack et al. (2002)

Table C.2: Spectral indices and leaf pigment parameters derived from CI-710s leaf spectrometer measurements. R_λ, A_λ, and T_λ reflect leaf absorbance, reflectance, and transmittance at wavelength λ (nm), respectively. Parameters indicated with an asterisk (*) represent estimated pigment concentrations (μg/cm^3).

Parameter	Index	Biological Meaning	Formula	Citation
Anthocyanin Reflectance Index 1	ARI1	Stress-induced pigment production	$(1/R_{550}) - (1/R_{700})$	Kupčinskienė et al. (2023)
Carotenoid Reflectance Index 1	CRI1	Photoprotective pigment accumulation under stress	$(1/R_{510}) - (1/R_{550})$	Kupčinskienė et al. (2023)
Chlorophyll A*	CPHL A	Measure chlorophyll-a content of leaves	$(12.7A_{663}) - (2.59A_{645})$	Parry et al. (2014)
Chlorophyll B*	CPHL B	Measure chlorophyll-b content of leaves	$(22.9A_{645}) - (4.7A_{663})$	Parry et al. (2014)
Chlorophyll Total*	CPHL T	Measure total chlorophyll content	$(8.2A_{663}) + (20.2A_{645})$	Parry et al. (2014)
Chlorophyll Content Index	CCI	Photosynthetic capacity and nitrogen status	T_{931}/T_{653}	Parry et al. (2014)
Chlorophyll Normalized Difference Vegetation Index	CNDVI	Estimation of photosynthetic quality and metabolic health	$(R_{750} - R_{705})/(R_{750} + R_{705})$	Taha et al. (2024)
Flavanol Reflectance Index	FRI	Secondary metabolites linked to stress defense	$(1/R_{410} - 1/R_{460})\, R_{800}$	Kupčinskienė et al. (2023)
Greenness	G	Relative chlorophyll content	R_{554}/R_{677}	Kupčinskienė et al. (2023)
Health Index	HI	Indicator of pathogen-induced stress	$(R_{534} - R_{698})\,/(R_{534} + R_{698}) - (R_{704}/2)$	Joalland et al. (2017); Mahlein et al. (2012)
Normalized Difference Vegetation Index	NDVI	Greenness and general plant health	$(R_{800} - R_{680})/(R_{800} + R_{680})$	Joalland et al. (2017); Kupčinskienė et al. (2023)
Photochemical Reflectance Index	PRI	Photosynthetic efficiency and plant stress	$(R_{531} - R_{570})/(R_{531} + R_{570})$	Joalland et al. (2017); Kupčinskienė et al. (2023)
Plant Senescence Reflectance Index	PSRI	Stress-induced aging	$(R_{680} - R_{500})/R_{750}$	Kupčinskienė et al. (2023)
Soil-Plant Analysis Development	SPAD	Relative chlorophyll content and leaf nitrogen	$-42.9 + 42.1(T_{931}/T_{653})^{0.215}$	Parry et al. (2014)
Water Band Index	WBI	Relative leaf water content	R_{900}/R_{970}	Colovic et al. (2022); Oliwa et al. (2023)

Table C.3: Vegetation indices and their typical ranges as supported in the literature. Ranges reflect values reported under typical leaf-level measurements as cited by the included authors.

Index	Parameter	Range	Citation
NDVI	Normalized Difference Vegetation Index	-1 to 1 (leaf scale typically $\sim$ 0.2–0.9)	Pettorelli et al. (2005)
CNDVI	Chlorophyll NDVI	-1 to 1 (leaf scale $\sim$ 0.1–0.6)	Gitelson & Merzlyak (1994)
PRI	Photochemical Reflectance Index	approximately -0.1 to 0.1	Gamon et al. (1992)
WBI	Water Band Index	$\sim$ 0.8–1.2 (healthy leaves $\sim$ 0.9–1.05)	Peñuelas et al. (1997)
PSRI	Plant Senescence Reflectance Index	approximately -0.2 to 0.4	Merzlyak et al. (1999)
G	Greenness Index	$\sim$ 0.5–2.0	Gitelson et al. (2002)
CRI1	Carotenoid Reflectance Index 1	approximately -1 to 2 (reported -5 to 5)	Gitelson et al. (2001)
ARI1	Anthocyanin Reflectance Index 1	$\sim$ 0–5	Gitelson et al. (2001)
FRI	Flavanols Reflectance Index	$\sim$ 0–3	Cerovic et al. (2002)
CCI	Chlorophyll Content Index	$\sim$ 0–3	Richardson et al. (2002)
SPAD	SPAD chlorophyll index	$\sim$ 0–60 SPAD units	Markwell et al. (1995)
Chl a	Chlorophyll a	$\sim$ 5–30 μg cm^{-2}	Lichtenthaler & Wellburn (1983)
Chl b	Chlorophyll b	$\sim$ 2–15 μg cm^{-2}	Lichtenthaler & Wellburn (1983)
Total Chl	Total chlorophyll	$\sim$ 10–45 μg cm^{-2}	Lichtenthaler & Wellburn (1983)
Chl a:b	Chlorophyll a:b ratio	typically $\sim$ 2–4	Lichtenthaler & Wellburn (1983)
HI	Health Index	-1 to 1	Mahlein et al. (2012)

Table C.4: Type III ANOVA results for models including all accessions and for *Glycine soja* accessions only. Analyses were conducted on raw cyst count data and on log-transformed data using $\log_{10}(\text{cyst}+1)$. Reported values include degrees of freedom (df), sums of squares (Sum Sq), F-statistics, and P-values.

Model	Effect	df	Sum Sq	F value	P-value
All accessions (raw data)					

Continued on next page

Table C.4: Table C.4 (continued).

Model	Effect	df	Sum Sq	F value	P-value
	Accession (A)	21	1.86	12.59	2.93
	Treatment (T)	1	5.77	0.82	3.66
	A × T	21	1.90	1.28	1.84
All accessions ($\log_{10}$ transformed)					
	Accession (A)	21	1.48	7.05	5.44
	Treatment (T)	1	1.96	0.20	6.58
	A × T	21	1.87	0.89	6.04
***Glycine soja* only (raw data)**					
	Accession (A)	18	4.19	5.90	3.74
	Treatment (T)	1	2.06	0.52	4.70
	A × T	18	5.69	0.80	6.98
***Glycine soja* only ($\log_{10}$ transformed)**					
	Accession (A)	18	9.34	4.92	1.00
	Treatment (T)	1	1.42	0.001	9.71
	A × T	18	1.62	0.85	6.38

Table C.5: Monte Carlo power analysis for Type III ANOVA models fitted to cyst count data. Analyses were conducted for all accessions (including *Glycine max* and *Glycine soja*) and for *G. soja* accessions only, using both raw cyst count data and log-transformed data ($\log_{10}(\text{cyst\_count} + 1)$). Reported values represent empirical power estimates for detecting accession (A), treatment (T), and accession × treatment (A × T) effects based on 2,000 simulations at $\alpha = 0.05$.

Dataset	Effect tested	Power	Simulations	α
All accessions (raw cyst count data)				
	Accession (A)	1.0000	2000	0.05
	Treatment (T)	0.1555	2000	0.05
	A × T	0.8875	2000	0.05
All accessions ($\log_{10}$ transformed)				
	Accession (A)	1.0000	2000	0.05
	Treatment (T)	0.0735	2000	0.05
	A × T	0.7045	2000	0.05
***Glycine soja* only (raw cyst count data)**				
	Accession (A)	1.0000	2000	0.05
	Treatment (T)	0.1120	2000	0.05

Continued on next page

Table C.5: Table C.5 (continued).

Dataset	Effect tested	Power	Simulations	α
	A × T	0.6145	2000	0.05
***Glycine soja* only ($\log_{10}$ transformed)**				
	Accession (A)	1.0000	2000	0.05
	Treatment (T)	0.0540	2000	0.05
	A × T	0.6430	2000	0.05

Table C.6: Results of simple effects analyses for contrasts in SCN cyst counts between combined SCN and water deficit stress and SCN-only treatments. Analyses were conducted for all accessions and for *Glycine soja* accessions only, using both raw cyst count data and log-transformed data ($\log_{10}(x+1)$). Reported values include estimated contrasts (Estimate), standard errors (SE), test statistics (z), and Benjamini–Hochberg adjusted P-values (Adj. P-value).

Dataset	Accession	Estimate	SE	z	Adj. P-value
All accessions (raw data)					
	DW01	44.291	38.336	1.1550	0.2490
	DW02	−28.725	28.171	−1.0197	0.3090
	H05	−18.308	32.944	−0.5560	0.5790
	H14	−3.607	43.469	−0.0830	0.9340
	H15	67.667	68.578	0.9870	0.3240
	H21	−16.217	32.529	−0.4990	0.6180
	NCR	−122.714	42.327	−2.9000	0.00399
	PI 88788	−14.400	53.120	−0.2710	0.7860
	S05	21.762	57.959	0.3750	0.7080
	S100	−46.200	37.566	−1.2230	0.2200
	S11	−8.208	40.812	−0.2010	0.8410
	S14	−5.482	43.469	−0.1260	0.9000
	S32	−12.434	34.409	−0.3610	0.7180
	S33	38.119	46.728	0.8160	0.4150
	S54	3.833	38.591	0.0990	0.9210
	S55	33.238	42.327	0.7850	0.4330
	S67	−16.889	38.591	−0.4380	0.6620
	S72	53.500	64.149	0.8340	0.4050
	S74	−9.500	37.562	−0.2530	0.8000
	S76	9.333	64.149	0.1450	0.8840
	SW03	−13.354	36.698	−0.3640	0.7160

Continued on next page

Table C.6: Table C.6 (continued).

Dataset	Accession	Estimate	SE	z	Adj. P-value
	W82	−146.875	39.840	−3.6870	0.6470
All accessions ($\log_{10}$ transformed)					
	DW01	0.267	0.145	0.0660	0.5280
	DW02	−0.082	0.106	0.4420	0.9310
	H05	−0.043	0.124	0.7300	0.9310
	H14	−0.257	0.164	0.1180	0.6510
	H15	0.167	0.258	0.5180	0.9310
	H21	−0.018	0.123	0.8820	0.9500
	NCR	−0.199	0.160	0.2120	0.9290
	PI 88788	0.022	0.200	0.9120	0.9500
	S05	0.054	0.218	0.8040	0.9310
	S100	−0.256	0.142	0.0720	0.5280
	S11	−0.042	0.154	0.7830	0.9310
	S14	−0.069	0.164	0.6720	0.9310
	S32	−0.113	0.130	0.3850	0.9310
	S33	0.319	0.176	0.0710	0.5280
	S54	0.046	0.145	0.7500	0.9310
	S55	0.075	0.160	0.6370	0.9310
	S67	−0.104	0.145	0.4750	0.9310
	S72	0.213	0.242	0.3800	0.9310
	S74	−0.036	0.142	0.7970	0.9310
	S76	0.015	0.242	0.9500	0.9500
	SW03	−0.141	0.138	0.3100	0.9310
	W82	−0.172	0.150	0.2530	0.9290
***Glycine soja* only (raw data)**					
	DW01	44.292	28.662	0.1230	0.7990
	DW02	−28.725	21.062	0.1740	0.7990
	H05	−18.308	24.630	0.4580	0.8940
	H14	9.714	33.565	0.7720	0.8940
	H15	67.667	51.271	0.1880	0.7990
	H21	−16.217	24.320	0.5050	0.8940
	S05	21.762	43.332	0.6160	0.8940
	S100	−46.200	28.083	0.1010	0.7990
	S11	−8.208	30.513	0.7880	0.8940
	S14	−5.482	32.499	0.8660	0.8940
	S32	−12.434	25.725	0.6290	0.8940

Continued on next page

Table C.6: Table C.6 (continued).

Dataset	Accession	Estimate	SE	z	Adj. P-value
	S33	38.119	34.936	0.2760	0.7990
	S54	3.833	28.852	0.8940	0.8940
	S55	33.238	31.645	0.2940	0.7990
	S67	−16.889	28.852	0.5590	0.8940
	S72	53.500	47.960	0.2660	0.7990
	S74	−9.500	28.083	0.7350	0.8940
	S76	9.333	47.960	0.8460	0.8940
	SW03	−13.355	27.437	0.6270	0.8940
***Glycine soja* only ($\log_{10}$ transformed)**					
	DW01	0.267	0.148	0.0730	0.5030
	DW02	−0.082	0.109	0.4540	0.9040
	H05	−0.043	0.127	0.7370	0.9040
	H14	−0.225	0.174	0.1950	0.9040
	H15	0.167	0.265	0.5290	0.9040
	H21	−0.018	0.126	0.8850	0.9340
	S05	0.054	0.224	0.8090	0.9040
	S100	−0.256	0.145	0.0790	0.5030
	S11	−0.042	0.158	0.7890	0.9040
	S14	−0.069	0.168	0.6800	0.9040
	S32	−0.113	0.133	0.3970	0.9040
	S33	0.319	0.181	0.0780	0.5030
	S54	0.046	0.149	0.7560	0.9040
	S55	0.075	0.164	0.6450	0.9040
	S67	−0.104	0.149	0.4860	0.9040
	S72	0.213	0.248	0.3920	0.9040
	S74	−0.036	0.145	0.8020	0.9040
	S76	0.015	0.248	0.9520	0.9520

Table C.7: Estimated marginal means (EMMeans) of SCN reproduction under the SCN-only treatment. Model-adjusted means were estimated on the log-transformed scale and back-transformed (BT) to the original scale for interpretation. Reported values include EMMeans on the log scale, back-transformed EMMeans, corresponding back-transformed lower and upper confidence intervals (CI), and genotype rankings from lowest to highest predicted SCN reproduction.

Genotype	EMMean	BT EMMean	Lower CI (BT)	Upper CI (BT)	Rank
S54	1.470	28.84	17.74	46.51	1
S33	1.910	80.32	43.60	147.25	2
S72	1.930	83.56	35.17	196.70	3
S55	1.977	93.68	53.28	164.01	4
DW01	1.990	96.78	62.95	148.53	5
S32	2.000	98.60	62.92	154.21	6
H21	2.030	106.31	72.40	155.90	7
S74	2.090	121.45	75.92	194.05	8
S11	2.120	131.80	80.32	215.84	9
H15	2.160	142.02	60.17	333.40	10
S67	2.167	145.47	90.99	232.23	11
H05	2.180	150.19	99.54	226.37	12
H14	2.180	152.04	86.76	265.85	13
S100	2.230	170.76	106.87	272.50	14
DW02	2.240	172.23	123.65	239.70	15
SW03	2.260	180.74	115.63	282.19	16
S14	2.260	182.77	108.24	308.14	17
S05	2.270	187.11	106.88	327.01	18
S76	2.320	205.74	87.42	482.37	19

Table C.8: Estimated marginal means (EMMeans) of SCN reproduction under the combined SCN and water deficit treatment. Model-adjusted means were estimated on the log-transformed scale and back-transformed (BT) to the original scale for interpretation. Reported values include EMMeans on the log scale, back-transformed EMMeans, corresponding back-transformed lower and upper confidence intervals (CI), and genotype rankings from lowest to highest predicted SCN reproduction.

Genotype	EMMean	BT EMMean	Lower CI (BT)	Upper CI (BT)	Rank
S54	1.520	32.20	19.33	53.22	1
S32	1.890	75.83	50.09	114.54	2
H14	1.960	90.09	51.24	157.83	3

Continued on next page

Table C.8: Table C.8 (continued).

Genotype	EMMean	BT EMMean	Lower CI (BT)	Upper CI (BT)	Rank
S100	1.980	94.37	58.89	150.86	4
H21	2.010	101.91	66.30	156.37	5
S55	2.050	111.56	67.93	182.80	6
S74	2.050	111.64	69.74	178.36	7
S67	2.060	114.28	69.60	187.24	8
S11	2.080	119.46	70.61	201.63	9
SW03	2.120	130.45	81.55	208.32	10
H05	2.140	136.00	90.10	205.02	11
S72	2.140	136.99	65.13	286.93	12
DW02	2.160	142.52	98.36	206.32	13
S14	2.190	155.62	88.82	272.11	14
S33	2.230	168.60	96.26	294.73	15
DW01	2.260	179.81	106.48	303.16	16
H15	2.320	209.16	88.89	490.38	17
S05	2.330	212.14	90.16	497.35	18
S76	2.330	213.02	101.57	445.57	19

Table C.9: Ranked Female Index (FI) values for *Glycine soja* accessions under SCN-only and combined SCN and water deficit treatments. FI was calculated as the mean cyst count on each accession relative to a susceptible check and used to compare SCN resistance across accessions and treatments. Accessions are ranked from lowest (most resistant) to highest (most susceptible) FI within each treatment.

Accession	SCN-only			SCN + water deficit		
	FI	Class	Rank	FI	Class	Rank
S54	9.6	R	1	16.1	MR	1
S72	22.5	MR	2	38.7	MS	2
S55	25.0	MR	3	39.5	MS	3
S32	28.2	MR	4	45.4	MS	4
H21	29.6	MR	5	47.7	MS	5
S74	31.9	MS	6	49.9	MS	6
S33	32.3	MS	7	50.4	MS	7
DW01	33.0	MS	8	51.7	MS	8
S11	33.0	MS	9	52.7	MS	9
H15	33.7	MS	10	54.0	MS	10
S67	37.7	MS	11	56.7	MS	11

Continued on next page

Table C.9: Table C.9 (continued).

Accession	SCN-only			SCN + water deficit		
	FI	Class	Rank	FI	Class	Rank
H05	38.7	MS	12	62.2	S	12
H14	42.1	MS	13	63.3	S	13
S100	43.5	MS	14	63.4	S	14
SW03	43.7	MS	15	66.6	S	15
DW02	43.8	MS	16	66.7	S	16
S14	44.7	MS	17	76.4	S	17
S05	45.2	MS	18	77.2	S	18
S76	49.0	MS	19	78.5	S	19

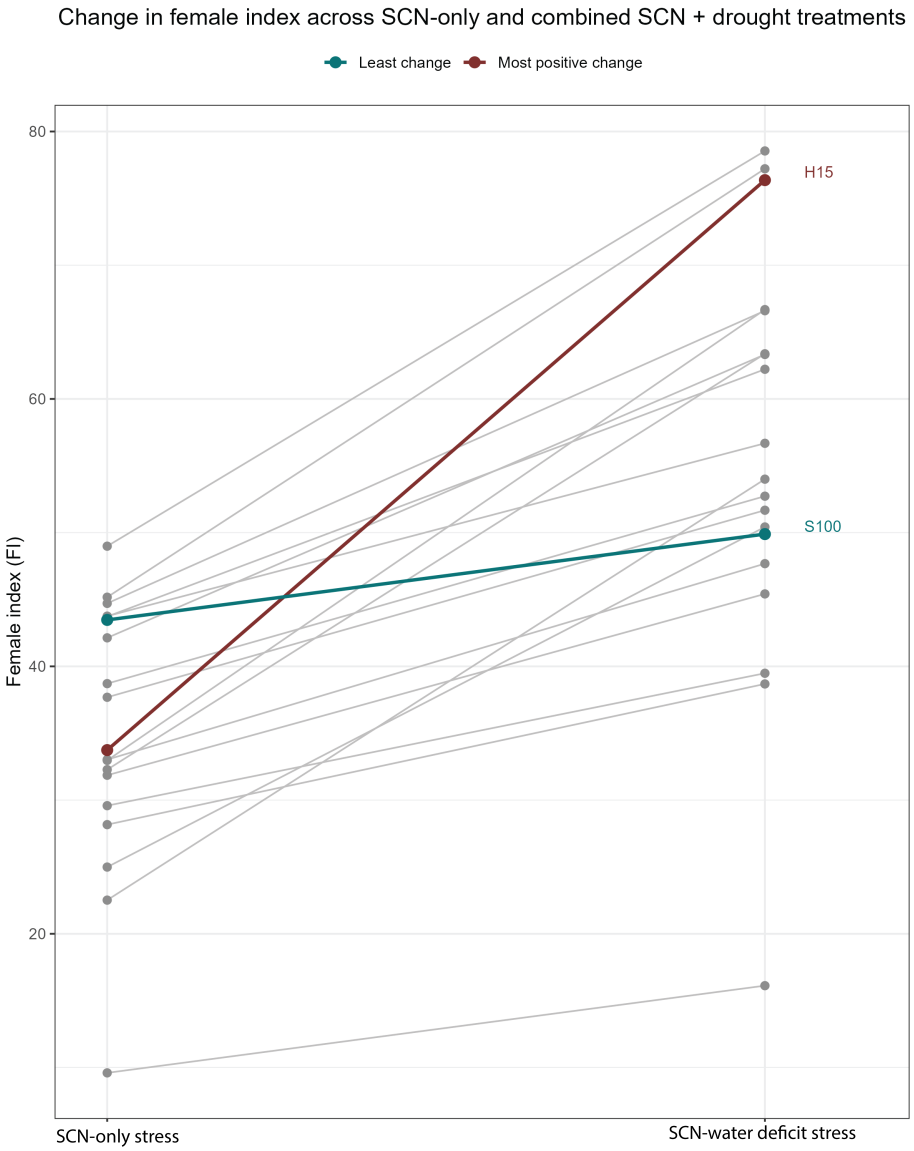

Figure C.1: Change in Female index (FI) values of wild soybean genotypes between SCN-only and combined SCN-water deficit treatments. Each line connects FI values calculated from mean cyst counts for genotypes under different stress environments. Most genotypes exhibited modest increases in FI under SCN-water deficit conditions. Highlighted accessions illustrate representative response patterns: the accession with the largest increase in FI (red) and the genotype with the smallest change in FI (teal). No accessions exhibited lower FI in SCN-drought treatment than in SCN-only treatment.

Table C.10: Shapiro–Wilk normality test results and skewness estimates for *Glycine soja* biomass traits under SCN-only and combined SCN and water deficit treatments. Biomass traits assessed included root mass, shoot mass, total biomass, and root:shoot ratio. Reported values include the Shapiro–Wilk test statistic (W), corresponding p-values, and skewness.

Treatment	Biomass metric	W	p-value	Skewness
SCN-only				
	Root mass	0.982	0.967	−0.015
	Shoot mass	0.912	0.081	0.982
	Total biomass	0.954	0.466	0.551
	Root:shoot ratio	0.976	0.887	0.374
SCN + water deficit				
	Root mass	0.959	0.556	−0.284
	Shoot mass	0.905	0.707	1.116
	Total biomass	0.967	0.060	0.274
	Root:shoot ratio	0.960	0.581	0.476

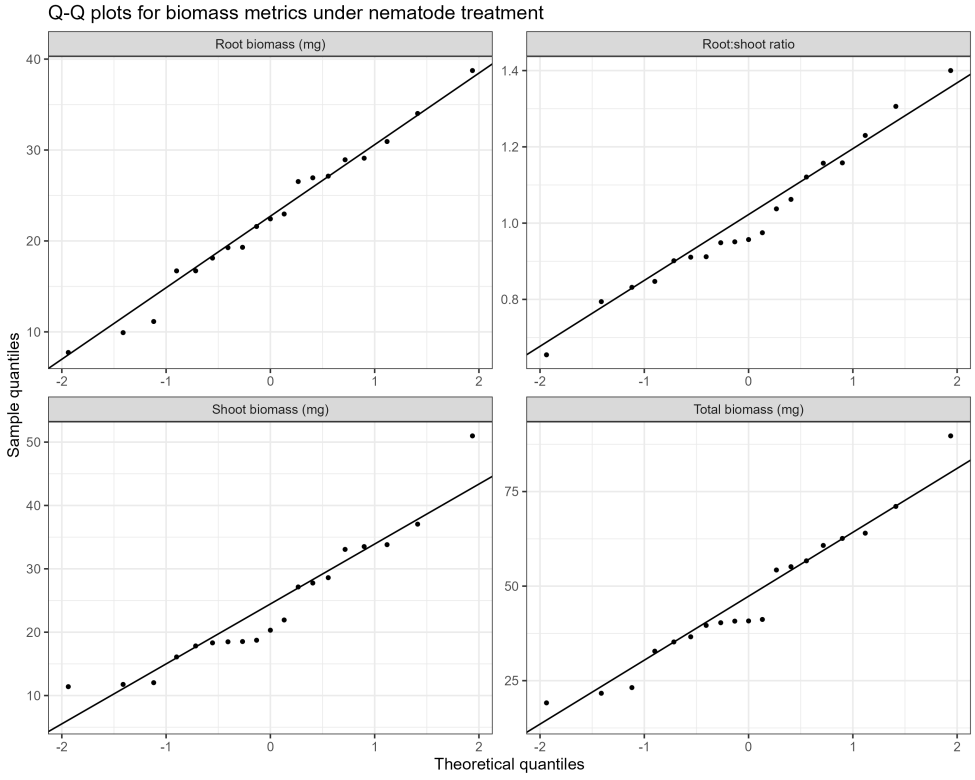

Figure C.2: Q-Q plot for four biomass metrics (root mass, shoot mass, total mass, and root to shoot ratio) for *Glycine soja* accessions when exposed to soybean cyst nematode stress. .

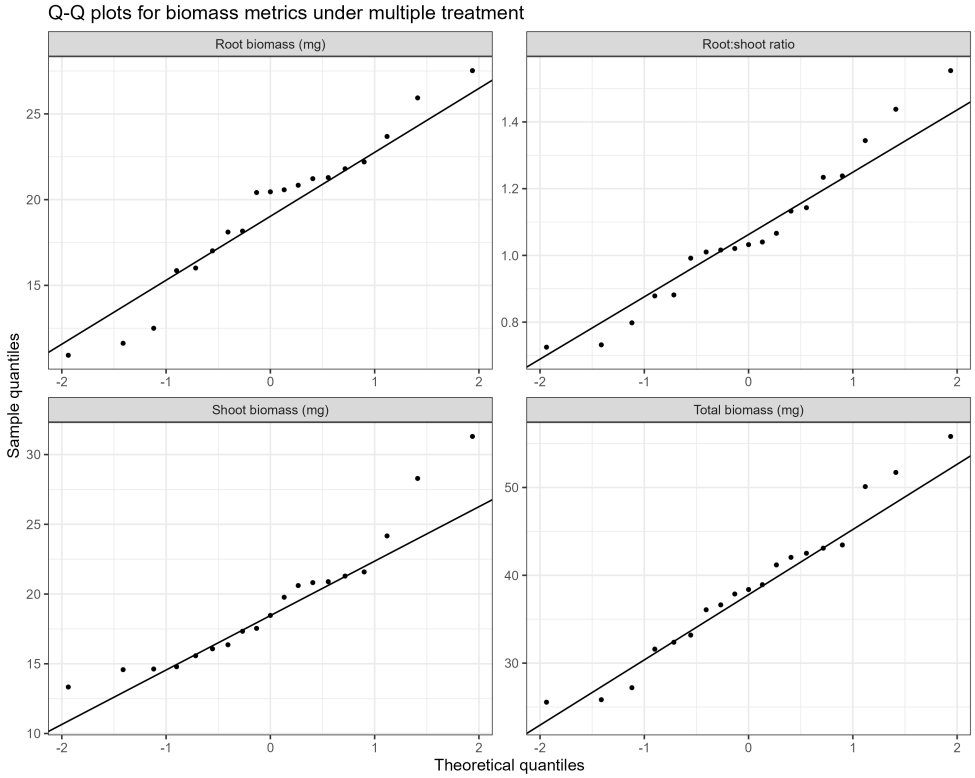

Figure C.3: Q-Q plot for four biomass metrics (root mass, shoot mass, total mass, and root to shoot ratio) for *Glycine soja* accessions when exposed to combined soybean cyst nematode stress and water deficit

Table C.11: Spearman rank correlations between biomass traits and three indicators of soybean cyst nematode (SCN) reproduction (cyst count, model-adjusted cyst count, and Female Index). Biomass traits were compared to identify which variable most consistently reflected plant performance under SCN-only and combined SCN and water deficit stress. The mean absolute correlation coefficient ($|\rho|$) was used to summarize overall association strength across response variables.

Treatment	**Metric**	**Cyst count**		**Model-adjusted cysts**		**Female Index**		**Mean $\lvert\rho\rvert$**
		ρ	p	ρ	p	ρ	p	
SCN-only stress								
	Total biomass	0.425	0.071	0.437	0.063	0.425	0.071	0.429
	Root mass	0.388	0.102	0.411	0.082	0.388	0.102	0.395
	Root:shoot ratio	0.389	0.100	0.323	0.177	0.389	0.100	0.367
	Shoot mass	0.305	0.203	0.309	0.198	0.305	0.203	0.306
SCN + water deficit stress								
	Total biomass	−0.268	0.265	−0.361	0.129	−0.268	0.265	0.299

Continued on next page

Table C.11: Table C.11 (continued).

Treatment	Metric	Cyst count		Model-adjusted cysts		Female Index		Mean $\lvert\rho\rvert$
		ρ	p	ρ	p	ρ	p	
	Root mass	−0.254	0.292	−0.242	0.317	−0.254	0.292	0.250
	Shoot mass	−0.132	0.590	−0.293	0.223	−0.132	0.590	0.185
	Root:shoot ratio	−0.118	0.631	−0.123	0.616	−0.118	0.631	0.119

Table C.12: Summary statistics for end-of-experiment physiological and phenotypic traits. Reported values include number of observations (n), mean ± standard deviation (SD), median, and skewness for each trait.

Trait	n	Mean ± SD	Median	Skewness
Cyst count	382	167.100	155.000	2.2063
ARI1	795	0.009	0.003	12.1530
Chlorophyll a:b ratio	790	0.656	0.654	5.0780
CCI	790	4.278	3.829	0.7833
Chlorophyll a	793	7.838	8.450	−0.9016
Chlorophyll b	789	12.052	12.577	−0.5428
Chlorophyll total	792	19.921	21.080	−0.7376
CNDVI	796	0.158	0.154	0.2259
CRI1	792	0.029	0.025	10.4512
Root mass (mg)	796	46.116	28.400	2.9199
Shoot mass (mg)	796	56.713	32.400	3.3135
FRI	781	0.502	0.480	0.5150
Greenness index	796	1.927	2.009	−0.5905
Health index	784	−15.047	−14.787	0.0556
Leaf count	789	1.861	2.000	0.6212
NDVI	795	0.510	0.560	−1.2080
PRI	788	−0.027	−0.025	−0.5912
PSRI	751	0.012	−0.011	2.5675
Root:shoot ratio	796	0.933	0.878	1.3207
Shoot height (cm)	790	6.705	4.800	2.8154
SPAD	766	13.591	13.861	0.0978
Total biomass (mg)	796	102.830	59.800	2.9795
WBI	795	0.992	0.994	−5.2237
Female index (FI)	382	49.537	43.757	1.1101
log(cyst + 1)	382	2.124	2.193	−2.2859
Chlorophyll fluorescence (y_{II})	796	0.437	0.496	−0.8183

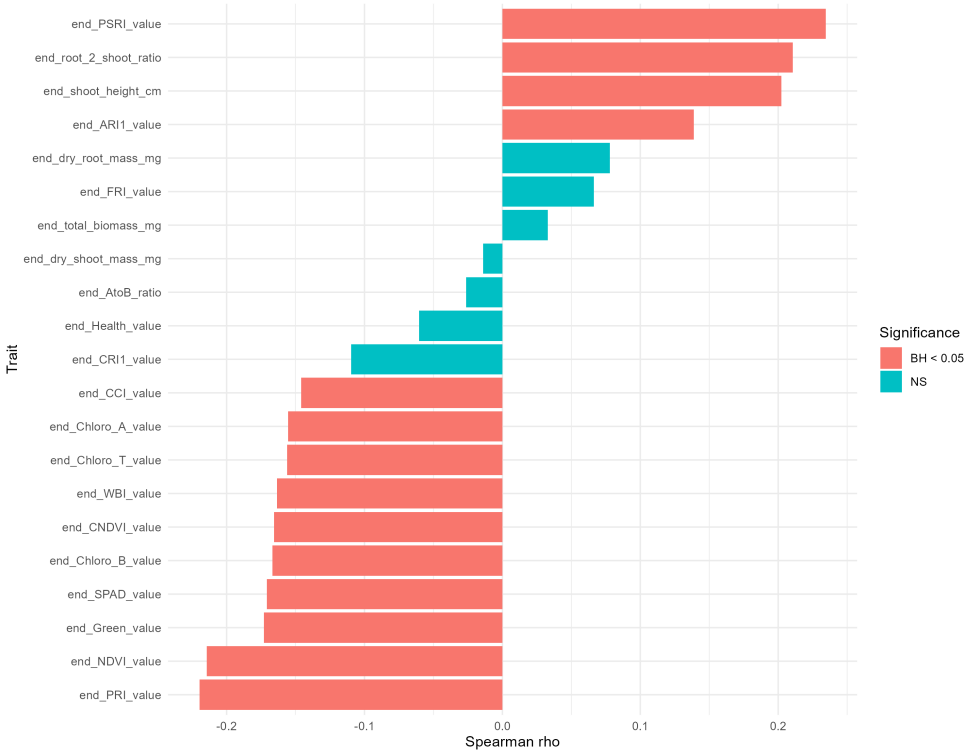

Figure C.4: Ranked Spearman correlation between log-transformed SCN cyst counts and end-point physiological and phenotypic traits of *G. soja* accessions. Correlation coefficients are shown for each trait and ranked by effect magnitude. Significance was evaluated using Bejamaini-Hochberg (BH) correction, with traits meeting adjusted p < 0.05 highlighted separately from non-significant (NS) traits.

Table C.13: Spearman rank correlations between end-of-experiment plant traits and log-transformed cyst counts (log(cyst + 1)) for *Glycine soja* accessions. Sample size (n) indicates the number of observations used for each correlation. P-values were adjusted using the Benjamini–Hochberg method.

Trait	n	ρ	p-**value**	**Adj.** p-**value**
PSRI	304	0.2345	3.63×10^{-5}	0.0005
PRI	331	−0.2197	0.0001	0.0005
NDVI	336	−0.2145	0.0001	0.0005
Root:shoot ratio	337	0.2107	0.0001	0.0005
Shoot height (cm)	337	0.2023	0.0002	0.0008
Greenness index	337	−0.1730	0.0014	0.0050
CNDVI	337	−0.1656	0.0023	0.0055
Chlorophyll b	331	−0.1669	0.0023	0.0055
SPAD	312	−0.1707	0.0025	0.0055

Continued on next page

Table C.13: Table C.13 (continued).

Trait	n	ρ	p-value	Adj. p-value
WBI	337	−0.1635	0.0026	0.0055
Chlorophyll total	333	−0.1562	0.0043	0.0077
Chlorophyll a	335	−0.1553	0.0044	0.0077
CCI	336	−0.1460	0.0074	0.0119
ARI1	337	0.1389	0.0107	0.0161
CRI1	333	−0.1098	0.0454	0.0635
Root mass (mg)	337	0.0779	0.1535	0.2015
FRI	326	0.0664	0.2321	0.2868
Health index	329	−0.0605	0.2742	0.3199
Total biomass (mg)	337	0.0330	0.5460	0.6035
Chlorophyll a:b ratio	332	−0.0264	0.6323	0.6639
Shoot mass (mg)	337	−0.0139	0.7989	0.7989

Table C.14: Pairwise Spearman rank correlations among end-of-experiment traits measured in *Glycine soja* accessions infected with soybean cyst nematode. Strong correlations between trait pairs were defined as $|\rho| \geq 0.80$. Reported values include sample size (n), Spearman correlation coefficient (ρ), and corresponding p-values.

Trait 1	Trait 2	n	ρ	p-value
Chlorophyll b	Chlorophyll total	329	0.9873	1.59×10^{-236}
Chlorophyll a	Chlorophyll total	333	0.9801	1.65×10^{-234}
SPAD	CCI	311	0.9484	3.46×10^{-156}
Root mass	Total biomass	337	0.9412	6.12×10^{-160}
Shoot mass	Total biomass	337	0.9412	6.45×10^{-160}
Chlorophyll a	Chlorophyll b	331	0.9398	2.01×10^{-155}
NDVI	Greenness index	336	0.8855	3.25×10^{-113}
NDVI	CNDVI	336	0.8654	3.02×10^{-102}
CCI	Chlorophyll a	334	0.8416	8.00×10^{-91}
CCI	Chlorophyll total	332	0.8330	8.04×10^{-87}
SPAD	Chlorophyll a	312	0.8207	2.44×10^{-77}
SPAD	Chlorophyll total	312	0.8125	1.27×10^{-74}
CCI	Chlorophyll b	330	0.8070	5.11×10^{-77}

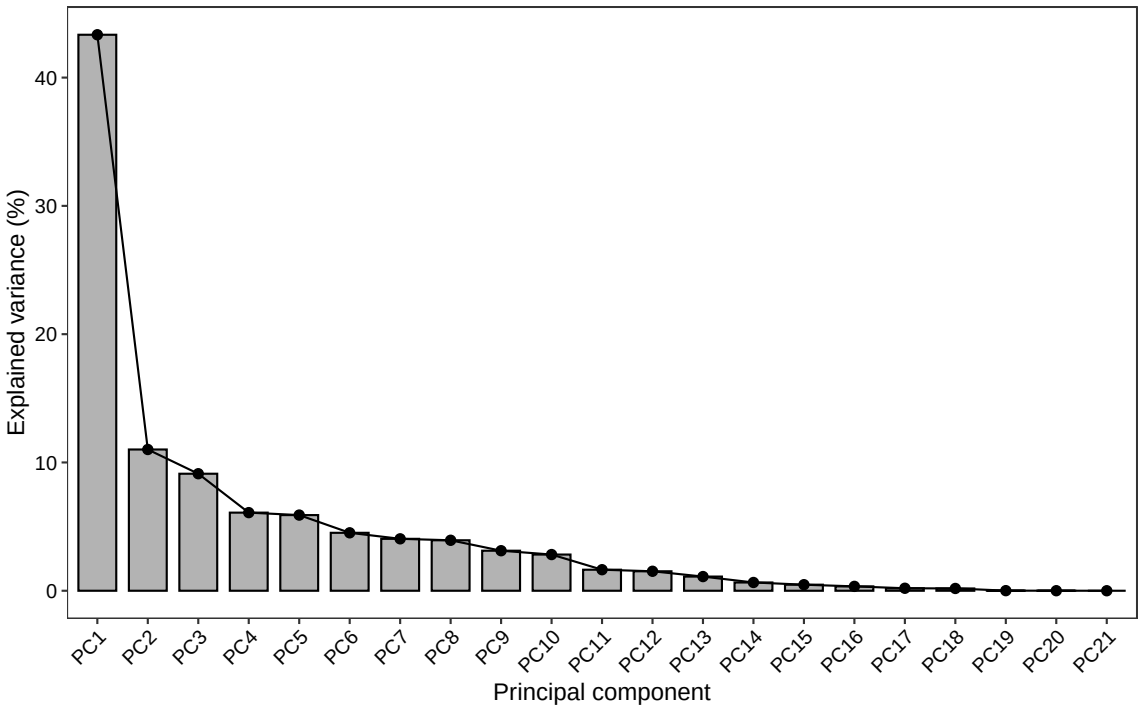

Figure C.5: Scree plot showing allocation of principal components explaining the variance of wild soybean traits when plants are infected with SCN. PCA analysis included all traits measured, including biomass traits.

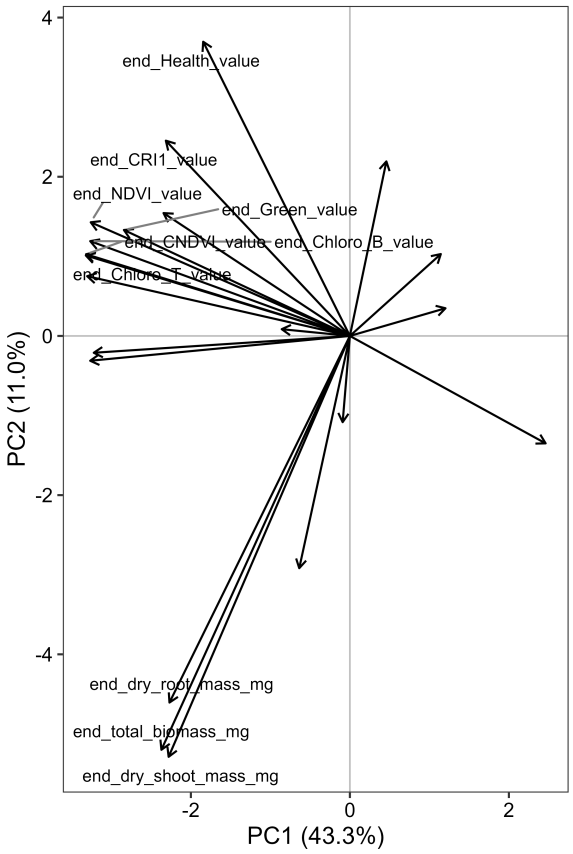

Figure C.6: PCA loading plot of wild soybean traits, including biomass traits, when infected with SCN. PC1 and PC2 explained 54.3% of variance. Biomass traits (root mass, shoot mass, and total mass) clustered together, while chlorophyll measurements and other greenness related traits also clustered together.

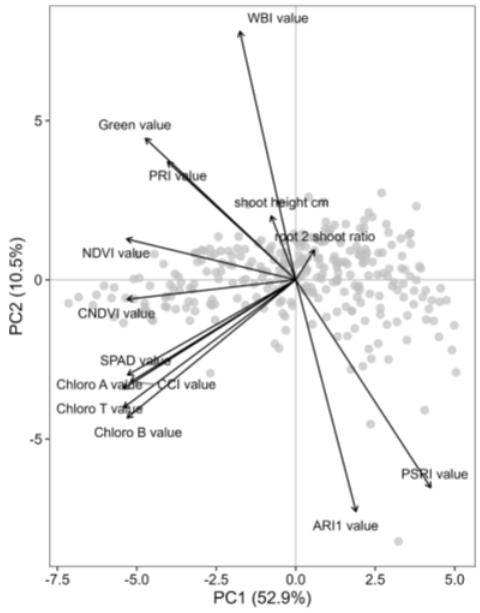

Figure C.7: PCA biplot for wild soybean plant traits found to be significantly correlated to SCN reproduction after Benjamini-Hochberg (BH) correction. Chlorophyll-related traits, including chlorophyll A, chlorophyll B, and total Chlorophyll (Chloro T), and CCI clustered together, traits associated with plant stress pigments, including anthocyanin reflectance index (ARI1) and PSRI clustered together.